MECHANISM OF ELECTRON IMPACT INDUCED DECOMPOSITION OF MONOSUBSTITUTED 1,2-DIPHENYLETHANE-1,2-DIONES

By

RONALD KEM MITCHUM

Bachelor of Science

Southwestern State College

Weatherford, Oklahoma

1968

Submitted to the Faculty of the Graduate College
of the Oklahoma State University
in partial fulfillment of the requirements
for the Degree of
DOCTOR OF PHILOSOPHY
July 1973

MECHANISM OF ELECTRON IMPACT INDUCED DECOMPOSITION OF MONOSUBSTITUTED 1,2-DIPHENYLETHANE-1,2-DIONES

Thesis Approved:

Stuart E. Scheppele
Thesis Adviser

J. Paul Fleschner

E. E. Evans

Calvin G. Reames, Jr.

N. M. Durham
Dean of the Graduate College

ACKNOWLEDGEMENTS

I am deeply indebted to Dr. Stuart E. Scheppele for his guidance, patience, encouragement and friendship throughout the course of graduate study. I thank Dr. O. C. Dermer for his comments on the final thesis draft. I also thank Mr. Keith Kinneburg for without his sincere dedication this thesis would not have been possible.

My appreciation is also extended for financial support of this project to Oklahoma State University Chemistry Department in the form of teaching assistantships and a NSF traineeship. I also wish to thank the Continental Oil Company for partial support.

To my wife Jane and son Scott, I would like to express my deepest gratitude for their understanding, encouragement, and many sacrifices.

TABLE OF CONTENTS

LIST OF TABLES

LIST OF TABLES (Continued)

LIST OF FIGURES

LIST OF FIGURES (Continued)

LIST OF FIGURES (Continued)

LIST OF FIGURES (Continued)

LIST OF FIGURES (Continued)

LIST OF FIGURES (Continued)

CHAPTER I

INTRODUCTION

The description of the mass spectra of polyatomic molecules in terms of competitive and successive decompositions from molecular ions was developed by Rosenstock, Wahrhaftig, and Eyring.[1] This statistical or quasi-equilibrium theory assumes that ionization by electron impact is a vertical (Franck-Condon) process yielding molecular ions which initially have a finite amount of electronic, vibrational, and/or rotational excitation energy. The time for decomposition of these molecular ions is assumed to be long compared to the time required for the nonradiative randomization of the excess energy over the accessible states. This mechanism requires a sufficient number of crossings of the hypersurfaces for these states. Since in the low-pressure limit the mean free path for collision is large compared to the ion source dimensions, intermolecular randomization of the excess energy is of no consequence. When a sufficient amount of energy is localized in the vibrational modes of a critical bond, decomposition will occur either by simple bond rupture or skeletal reorganization prior to bond cleavage. Thus, the observed mass spectrum is composed of stable molecular ions, fragment ions, and

metastable ions. For the unimolecular decomposition described by Equation 1,

$$BC^+ \xrightarrow{k} B^+ + C \qquad (1)$$

the rate of formation of product ion, B^+, is given by Equation 2.

$$d\,[B^+]\,/dt = k\,[BC^+] \qquad (2)$$

The rate constant k is given by Equation 3,

$$k = \int_0^\infty k(E)\;P(E)\;dE \qquad (3)$$

where k(E) is the rate constant for decomposition and P(E) is the probability of BC^+ possessing internal energy between E and E+dE. Thus calculation of the mass spectrum requires knowledge of both k(E) and P(E).

One approach to the calculation of the mass spectrum consists of (a) calculation of k(E), (b) construction of a breakdown graph from the k(E) values, the appropriate kinetic expressions describing the decomposition and the ion source residence time and (c) folding (b) into P(E) whose functional form has been either arbitrarily assumed or determined experimentally. This method has been used successfully to calculate the mass spectrum of simple and complex polyatomic molecules, e.g., propane[2] and phenanthrene[3], respectively. An alternative approach[4] consists of the experimental or numerical acquistion of the appropriate derivative of the ionization efficiency

curves for electron or photon impact. A normalized set of these derivative curves can be used (a) to construct a breakdown graph which is compared with the calculated one or (b) to estimate P(E) which in conjunction with the theoretical breakdown graph is used to predict the mass spectrum. Application of the theory requires the explicit calculation of k(E), which is given in the simplest form by Equation 4, where ν is the frequency factor, ε the activation energy, and s the number of internal degrees of freedom. Regardless of the functional form chosen for P(E) the rate constants obtained using Equation 4 have been found to give poor agreement between calculated and experimental mass spectra over a wide range of ionizing energy.[4,6]

$$k(E) = \nu \{(E - \varepsilon)/E\}^{s-1} \qquad (4)$$

The principal reason for the inadequacies of Equation 4 is the use of the classical approximation in enumerating the states of a collection of harmonic oscillators. An improved rate expression given by Vestal, Wahrhaftig, and Johnston[7] uses a good continuous approximation to the exact quantum mechanical density of states. The application of this VWJ modification to complex polyatomic molecules is mathematically complex. However for propane the breakdown graph using the k(E) values calculated by the VWJ equation and the experimental one are in good agreement.[2] An alternative approach has been to assume a P(E) function similar to the one deduced experimentally for propane and then to vary the number of effective oscillators in Equation 4 so as to

obtain reasonable agreement between calculated and observed mass spectra.[8] Since the energy distribution functions for complex systems are essentially unknown, the real significance of this method is open to question.

The following constitute techniques which can be used to experimentally estimate P(E). Morrison[9] showed that if the ionization probability for the excitation of a molecule in its ground state to a single electronic level of the ion is equal to a polynomial of degree j (a Heavyside function), the (j + 1) derivative of the ionization efficiency gives the energy distribution of the ionizing beam, with its maximum value at $V=E_c$, where E_c is the vertical ionization potential, and the amplitude is proportional to the transition probability. The value of j depends upon the threshold law for ionization, which for electrons is a linear[9,10,11] (j = 1) and for photons a step function[12] (j = 0) of the energy. Thus, P(E) may be determined experimentally from the appropriate derivative of the total ionization as a function of the excess energy, E. P(E) so determined is applicable to the prediction of the spectra produced by electrons or photons having energy in excess of the IP + E_{max}, where E_{max} is the maximum internal energy. For beam energies less than IP + E_{max}, P(E) must be multiplied by the function (V - E_{max}), where V is the electron energy. Using this technique, Chupka and Kaminsky[5] have determined P(E) for propane and n-butane and discussed the results within the framework of the Lennard-Jones and Hall[13] treatment of orbital energies in these

molecules. The first derivatives of the photon-impact total-ionization-efficiency curves for propylamine, propanol, and methyl ethyl ketone were obtained and used to investigate the variation of ion intensities as a function of photon energy.[4] Berkowitz and co-workers[14] determined P(E) for methane, ethane, propane, and butane directly by determining the intensity of the electrons ejected from the molecules when irradiated with 21.21 eV photons (helium resonance line). McLafferty et al.[15] estimated the P(E) functions of several mono-ring substituted 1,2-diphenylethanes by summing the photoelectron spectra of toluene and the corresponding substituted toluene[16,17] and convoluting this with the calculated thermal energy distribution of 1,2-diphenylethane. For example the P(E) of 1-(4-nitrophenyl)-2-phenylethane was constructed by summing the photoelectron spectra of toluene and 4-nitrotoluene followed by convolution with the calculated thermal energy distribution. Meisels et al.[18] calculated an energy loss function derived from the Bethe-Born treatment of collisions. P(E) values evaluated in this manner for methane, ethane, and ethylene when folded into the respective breakdown graphs yield mass spectra in good agreement with those reported from analytical mass spectrometers. Lindholm and Pettersson[19] estimate P(E) values applicable to the most intense ions in the mass spectrum of ethane by using the experimental ion intensities and the breakdown curves determined by charge transfer. The P(E) function for a polyatomic molecule may be approximated from the mass spectra and a knowledge of the ionization and appearance

potentials.[20a] This method consists of a plot of the relative ion intensities versus the ionization and appearance potentials and subsequent convolution of the resultant vertical lines with a step function of 1 to 2 eV in width. For ethane the P(E) function so obtained is in reasonable agreement with the function obtained from the photoelectron spectrum.[20b] To circumvent the experimental difficulties, wide usage has been made of empirical P(E) functions.[21] Since knowledge of P(E) is necessary for the application of quasi-equilibrium theory it is surprising that very little attention has been devoted to the determination of P(E) for complex organic molecules.[3,15]

Morrison's differential method should provide (a) reasonable estimates of P(E) and (b) if the results are interpreted with caution, accurate ionization and/or appearance potentials for atoms,[9b,22] simple polyatomic molecules,[22] and generally reasonable estimates of these values for complex polyatomic systems.[3] In many instances the technique yields values of IP and AP in excellent agreement with those values obtained by non-electron impact methods, e.g., photoionization. However for some polyatomic systems ionization and appearance potentials cannot be accurately determined using this technique.[22] For vertical or adiabatic ionization occurring from a state of the neutral molecule to a state of the ion, the second derivative of the ionization efficiency (SDIE) curve constitutes a reversed Maxwellian energy distribution, whose width at half height is proportional to the electron energy spread. For monoatomic species which do not have closely

spaced electronic or autoionizing states the shape of the SDIE curve is taken to be the distribution of energies in the electron beam. However for large polyatomic molecules the SDIE curve will represent the effect of convolting the electron energy spread with the curve representing the transition probabilities to closely spaced vibrational, rotational and/or electronic states.[23] Other methods of measuring ionization and appearance potentials can be divided into three major groups: (a) linear extrapolation,[24] (b) vanishing current,[25] and (c) logarithmic techniques.[26] These methods may grossly overestimate ionization and appearance potentials owing to the population of closely spaced states in excess of the lowest ionic state.

Considerable attention has been devoted to the elucidation of the effect of substituents upon competitive and successive decompositions of aromatic molecular ions. Bursey and McLafferty[27] have attempted to relate the rate of decomposition of meta- and para- substituted aromatic molecular ions to the aromatic substituent constants derived from solution kinetics. It is found that a correlation does exist if the system is carefully chosen.[28]

In general, when a molecular ion M decomposes to a fragment ion A, the rate of change of concentration of A in the ion source is given by Equation 5, where the second term on the right includes terms for all decomposition modes of A, and the third includes terms for loss of A due to instrumental factors. Upon application of the steady state approximation ($d A/dt = 0$), Equation 5 reduces to Equation 6. When A is formed

from a series of precursors, k in general will show a dependance upon the precursor.

$$\frac{d[A]}{dt} = k_1 [M] - \Sigma k_2 [A] - \Sigma k_3 [A] \quad (5)$$

$$[A] / [M] = \frac{k_1}{\Sigma k_i + \Sigma k_j} \quad (6)$$

If A is formed with the same energy distribution from each molecular ion,[29] $\Sigma k_i + \Sigma k_j$ will be independent of the mode of formation of A. Defining $Z = [A] / [M]$ and $Z_o = [A]_o / [M]_o$, where A is formed from the molecular ion M of a standard, equation 7 allows the comparison of Z values from different precursors with that of a standard.

$$\frac{Z}{Z_o} = \frac{[A] / [M]}{[A]_o / [M]_o} = \frac{k_1}{k_o} \quad (7)$$

The Z/Z_o ratio is then correlated with the σ constants of the Hammett equation,[30] Equation 8, by equating k_1/k_o to Z/Z_o.

$$\log (Z/Z_o) = \sigma (\sigma^+) \quad (8)$$

Williams et al.[31] pointed out that factors which affect ionic abundances are (a) the effect of substitution upon the activation energy, (b) competitive fragmentation from the molecular ion, (c) secondary decomposition of product ions and (d) internal energy of the molecular ion. McLafferty and co-workers[15] agree that any effect on product ion formation should result from the effect of substitution upon P(E) and also the rate constants k(E) for all processes.

Clearly, knowledge of the variation of P(E) with substitution is essential to the understanding of competitive and successive decomposition. This thesis is primarily concerned with the determination and investigation of substituent effects on the two competitive decompositions of the C-1--C-2 bond ($[R - R']^{\ddagger} \rightarrow R^+ + R^{\cdot}$ vs $R'^+ + R^{\cdot}$) of a series of meta- and para- substituted benzils. The effect of molecular temperature on the P(E) function has been qualitatively investigated. The investigation was conducted using the following series of compounds: 1-(4-methylphenyl)-2-phenylethane-1,2-dione (I), 1-(4-methoxyphenyl)-2-phenylethane-1,2-dione (II), 1-(3-trifluoromethylphenyl)-2-phenylethane-1,2-dione (III), 1,2-diphenylethane-1,2-dione (IV), and 1-(phenyl-d_5)-2-phenylethane-1,2-dione (V).

CHAPTER II

RESULTS AND DISCUSSION

The 70 eV mass spectra of I at ion source temperatures of 230° and 310°, and of II and III at ion source temperatures of 250° and 310°, are reproduced in Figures 1-3. The spectra have been corrected for naturally occurring ^{13}C, ^{2}H, ^{17}O, and ^{18}O. ^{32} It is seen that the dominant fragmentation is cleavage of the C-1--C-2 bond. The mass spectra of I and II are characterized by five ions while the mass spectrum of III is characterized by six ions at 70 eV, as shown in Tables I-III. These ions account for approximately one hundred per cent of the total ion current produced from I, II, and III at electron energies below 20 eV.

Figure 4 represents the basic fragmentation pattern for the molecular ions of I, II, and III, neglecting trivial fragmentations which are not common to all three or which do not contribute appreciably to the total ion current. Figures 5-7 represent detailed fragmentation pathways for the molecular ions of I, II, and III (Ia, IIa, and IIIa). Cleavage of the central C-1--C-2 bond in Ia produces both m/e 105 (Ib) and m/e 119 (Ic); these ions carry off 54.0 and 58.5 per cent of the ion current at 310° and 230° respectively (Note: an m/e value, when used as a substantive, is to be understood as referring to the ion having that value.). Loss of carbon monoxide from Ib and Ic yield ions as m/e 77 (Id) and m/e 91 (Ie). In terms of total ion current these ions undergo trivial fragmentations with loss of acetylene forming ions corresponding in mass to

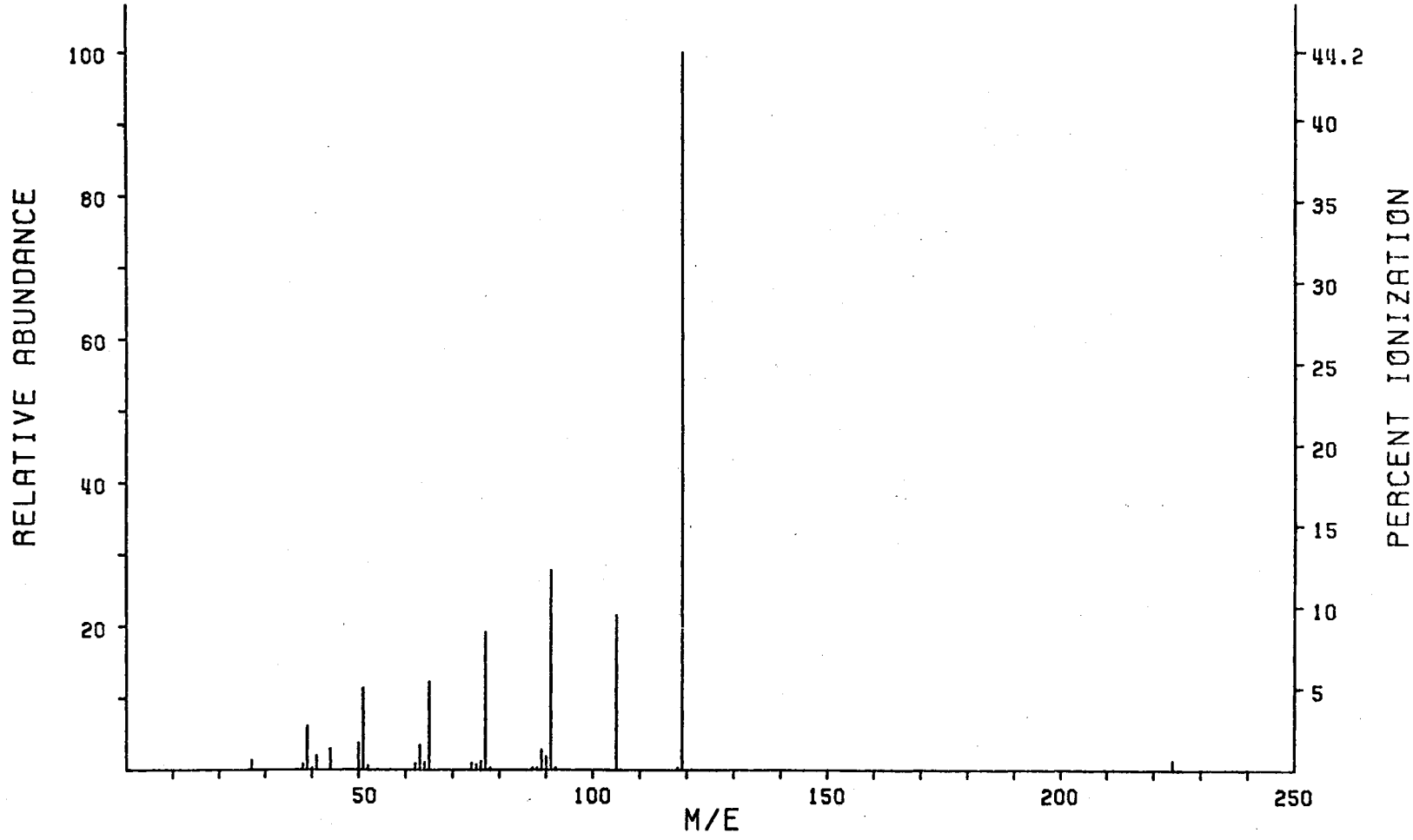

Figure 1a. 70 eV Mass Spectrum of I, 310° Ion Source Temperature

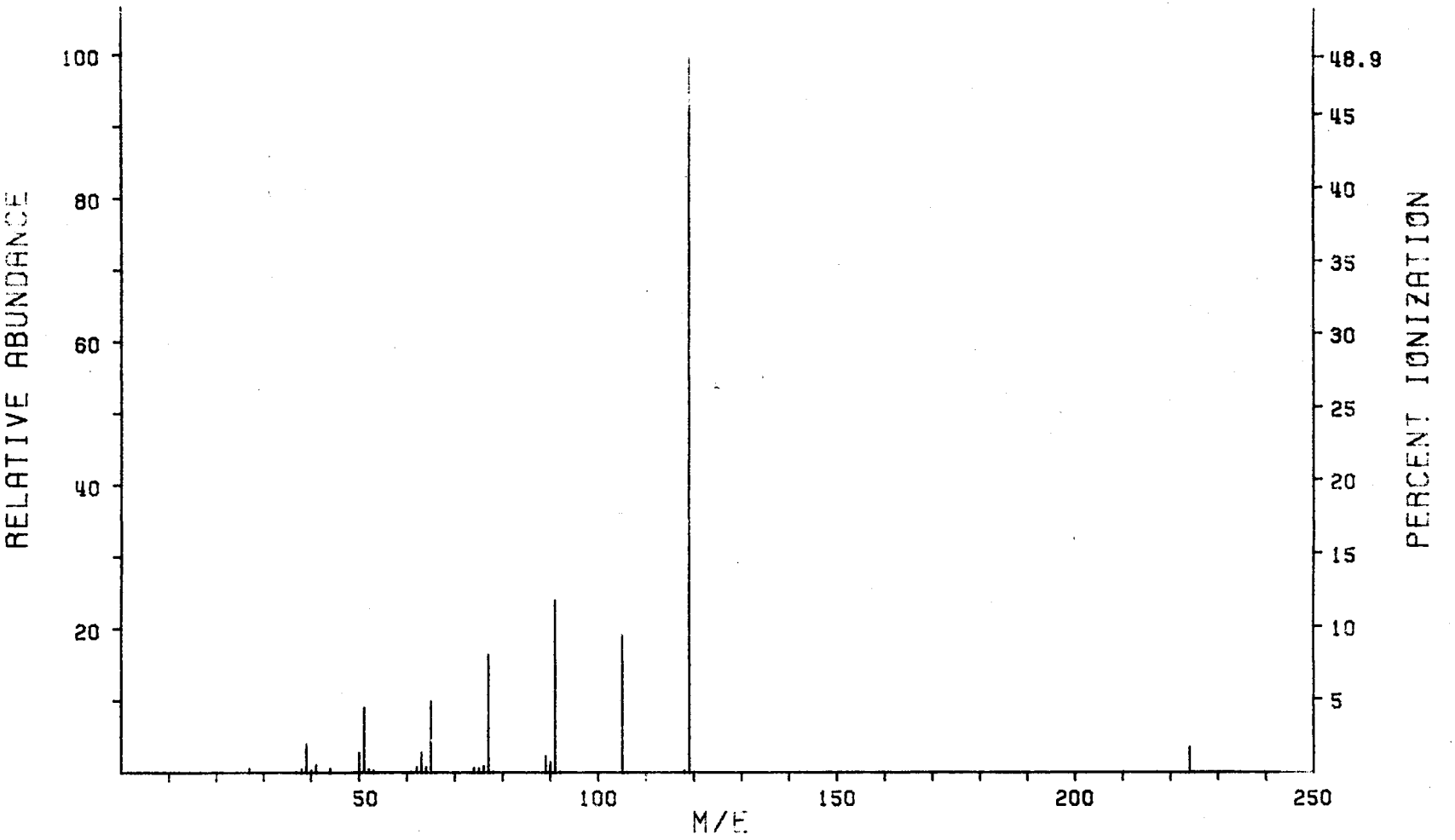

Figure 1b. 70 eV Mass Spectrum of I, 230° Ion Source Temperature

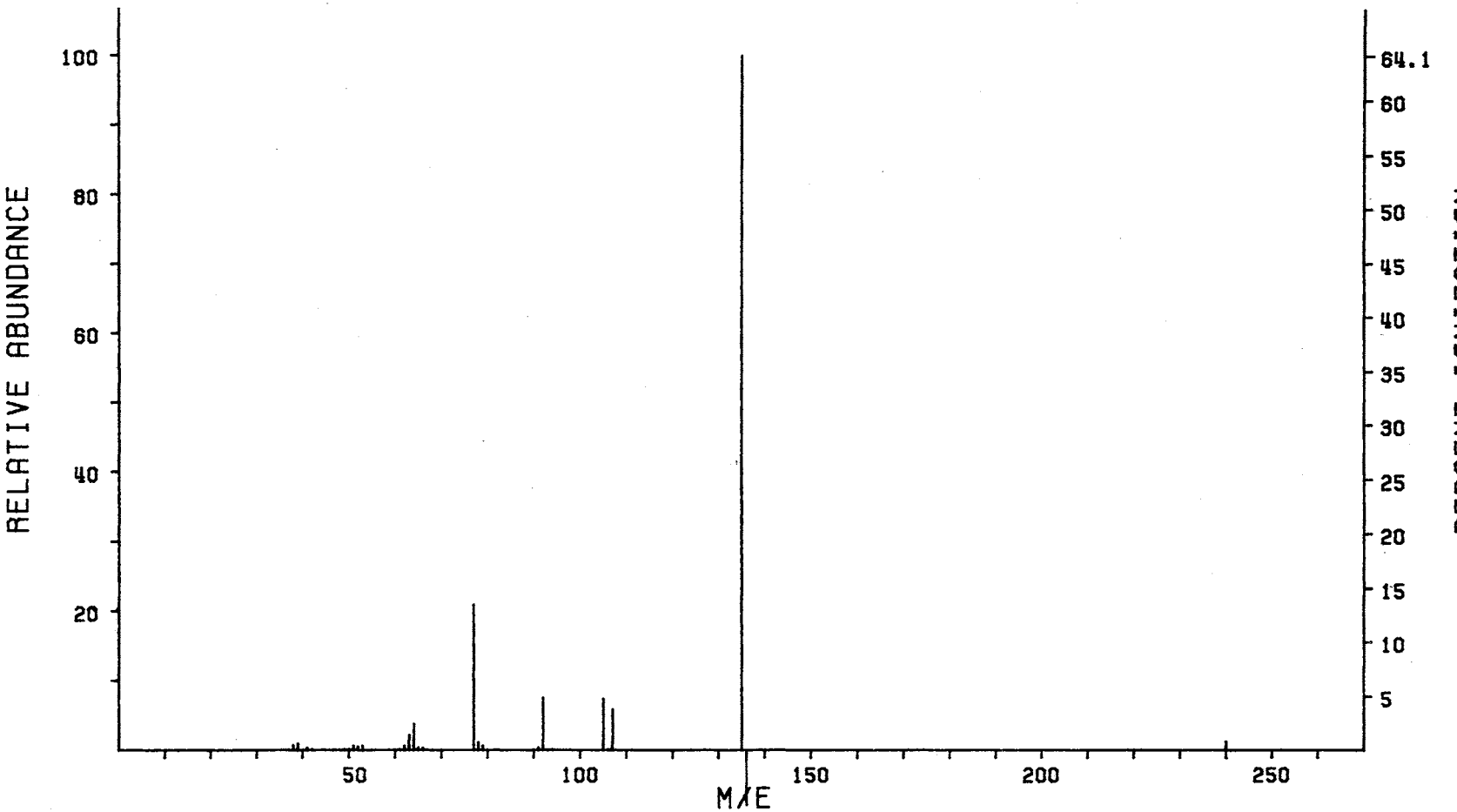

Figure 2a. 70 eV Mass Spectrum of II, 250° Ion Source Temperature

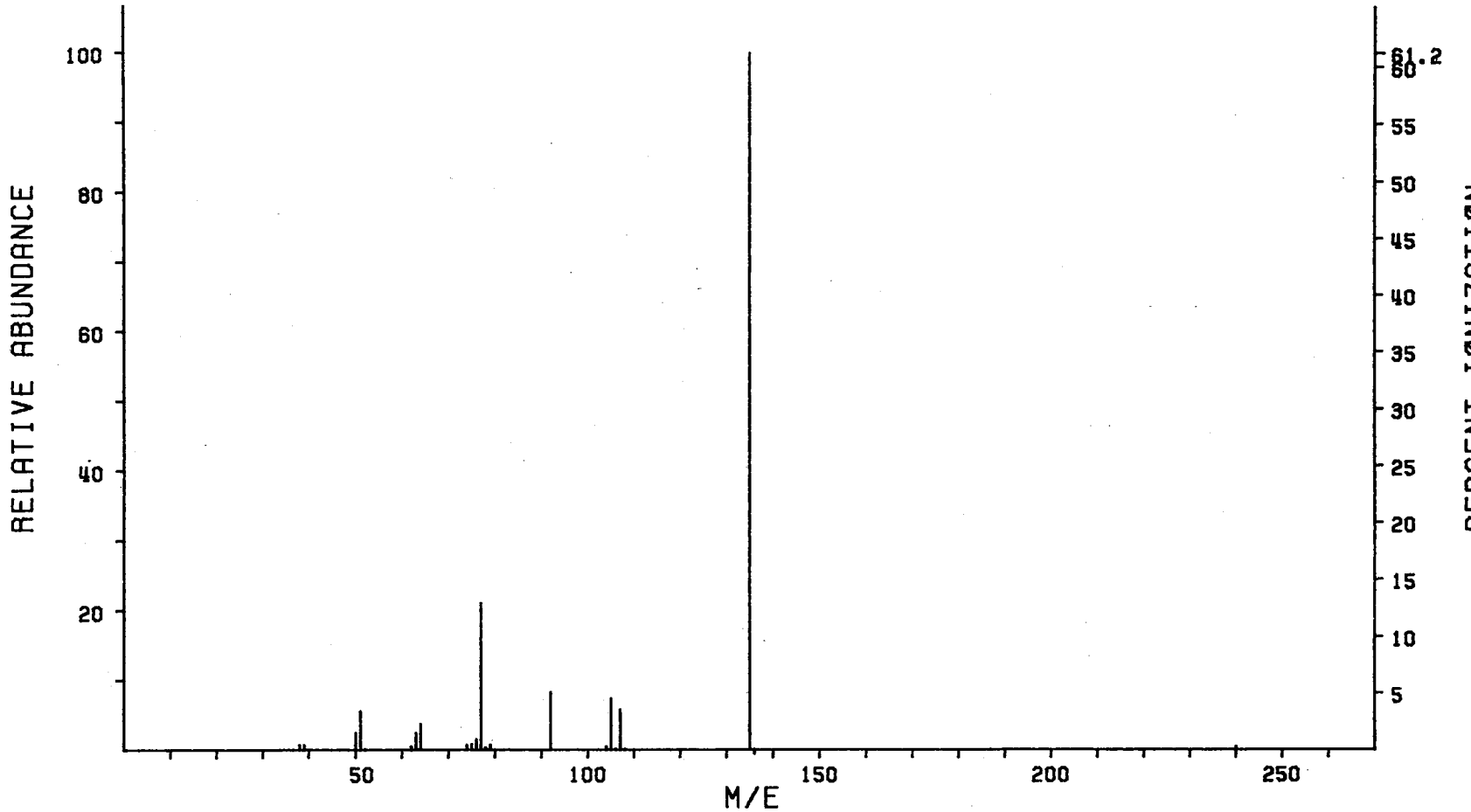

Figure 2b. 70 eV Mass Spectrum of II, 310° Ion Source Temperature

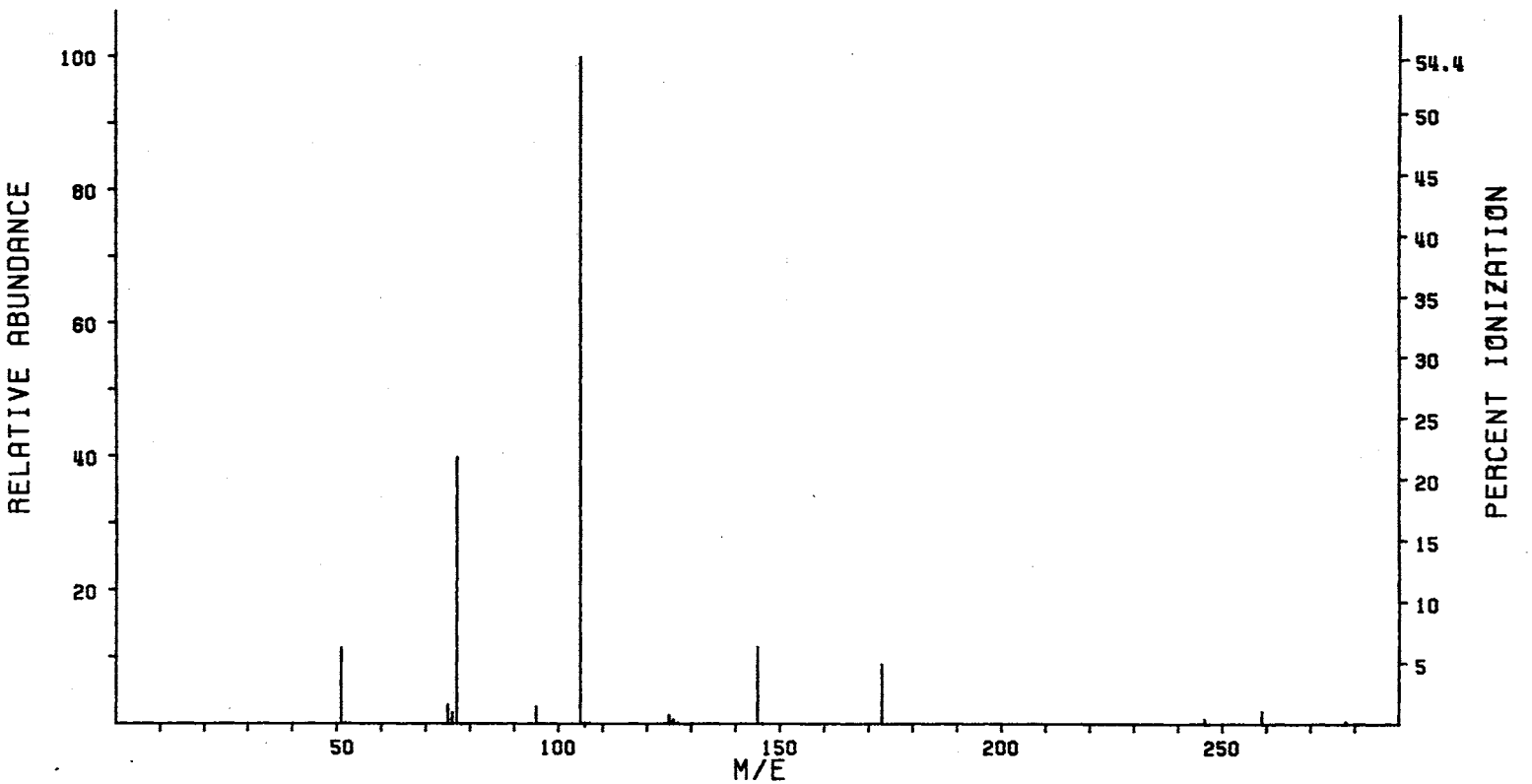

Figure 3a. 70 eV Mass Spectrum of III, 310° Ion Source Temperature

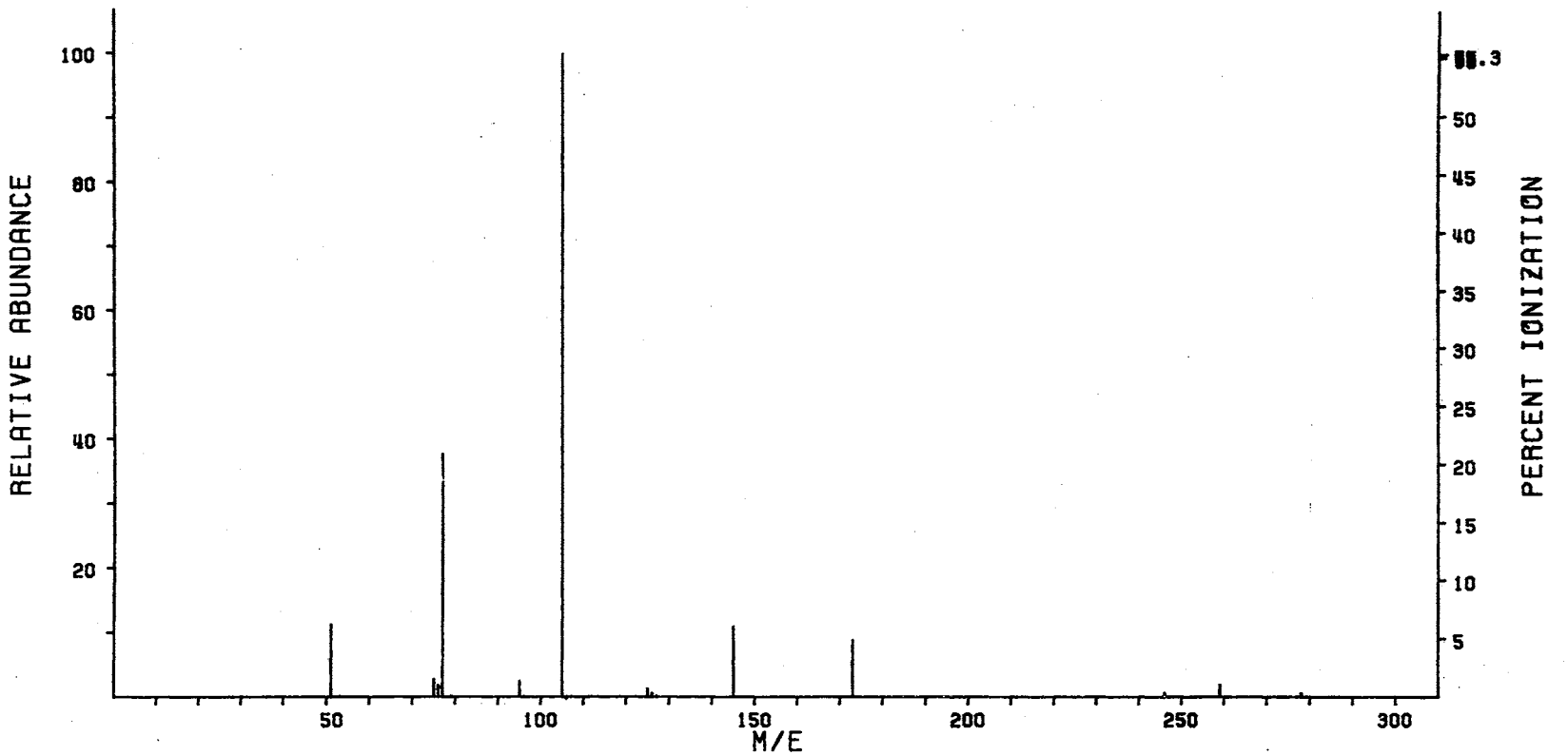

Figure 3b. 70 eV Mass Spectrum of III, 250° Ion Source Temperature

TABLE I

PERCENT IONIZATION IN THE MASS SPECTRA OF I
AS A FUNCTION OF ELECTRON ENERGY
AND SOURCE TEMPERATURE

Ion m/e	Percent Ionization[a] 230° Beam energy 15 eV	20 eV	70 eV	310° Beam energy 15 eV	20 eV	70 eV
51	0.0	0.0	4.4	0.0	0.0	5.0
65	0.0	0.5	5.0	0.0	0.5	5.8
77	0.4	2.4	7.9	0.3	2.7	8.6
91	1.7	9.2	11.7	2.7	11.0	12.4
105	7.9	10.6	9.4	8.8	11.8	9.5
119	84.3	73.1	49.1	86.5	72.5	44.5
224	4.3	3.1	1.8	1.7	1.2	0.6
Total %	98.6	98.9	89.3	100.0	99.7	86.4

[a]Energy calibrated

TABLE II

PERCENT IONIZATION IN THE MASS SPECTRA OF II
AS A FUNCTION OF ELECTRON ENERGY
AND SOURCE TEMPERATURE

Ion m/e	Percent Ionization[a] 250° Beam energy 16 eV	21 eV	70 eV	310° Beam energy 16 eV	21 eV	70 eV
51	0.0	0.0	3.2	0.0	0.1	3.4
77	0.1	4.0	13.4	0.5	5.5	12.9
92	0.0	0.7	4.8	0.0	1.3	5.1
105	1.5	3.3	4.7	1.4	3.5	4.5
107	0.9	4.3	3.8	1.8	5.2	3.5
135	95.5	85.7	61.1	95.8	83.7	61.2
240	1.7	1.2	0.8	0.5	0.3	0.2
Total %	99.7	99.2	91.8	100.0	99.6	90.8

[a]Energy calibrated

TABLE III

PERCENT IONIZATION IN THE MASS SPECTRA OF III
AS A FUNCTION OF ELECTRON ENERGY
AND SOURCE TEMPERATURE

Ion m/e	Percent Ionization[a] 250° Beam energy 16 eV	21 eV	70 eV	310° Beam energy 16 eV	21 eV	70 eV
51	0.0	0.1	6.2	0.1	0.1	6.1
77	0.8	11.1	20.8	0.9	9.8	21.7
95	0.1	0.0	1.3	0.1	0.0	1.4
105	95.1	81.4	55.3	95.4	83.1	54.4
145	0.1	1.4	6.0	0.1	1.1	6.2
173	2.1	4.4	4.8	1.6	4.1	4.8
259	0.0	0.0	1.0	0.1	0.4	1.0
278	0.4	0.2	0.3	0.7	0.5	0.1
Total %	98.6	98.6	95.7	99.0	99.1	95.7

[a]Energy calibrated

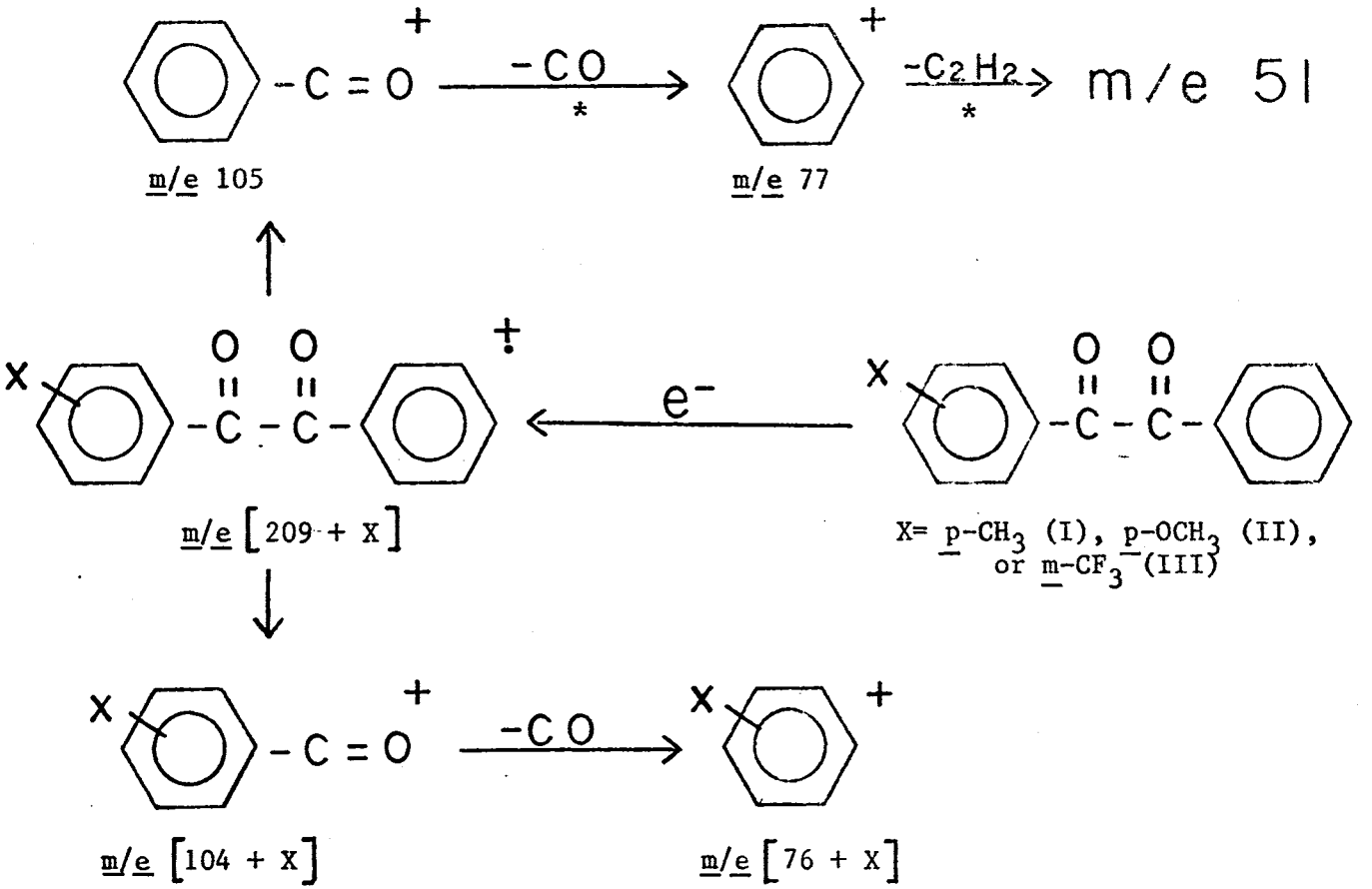

Figure 4. General fragmentation mechanism for I - V

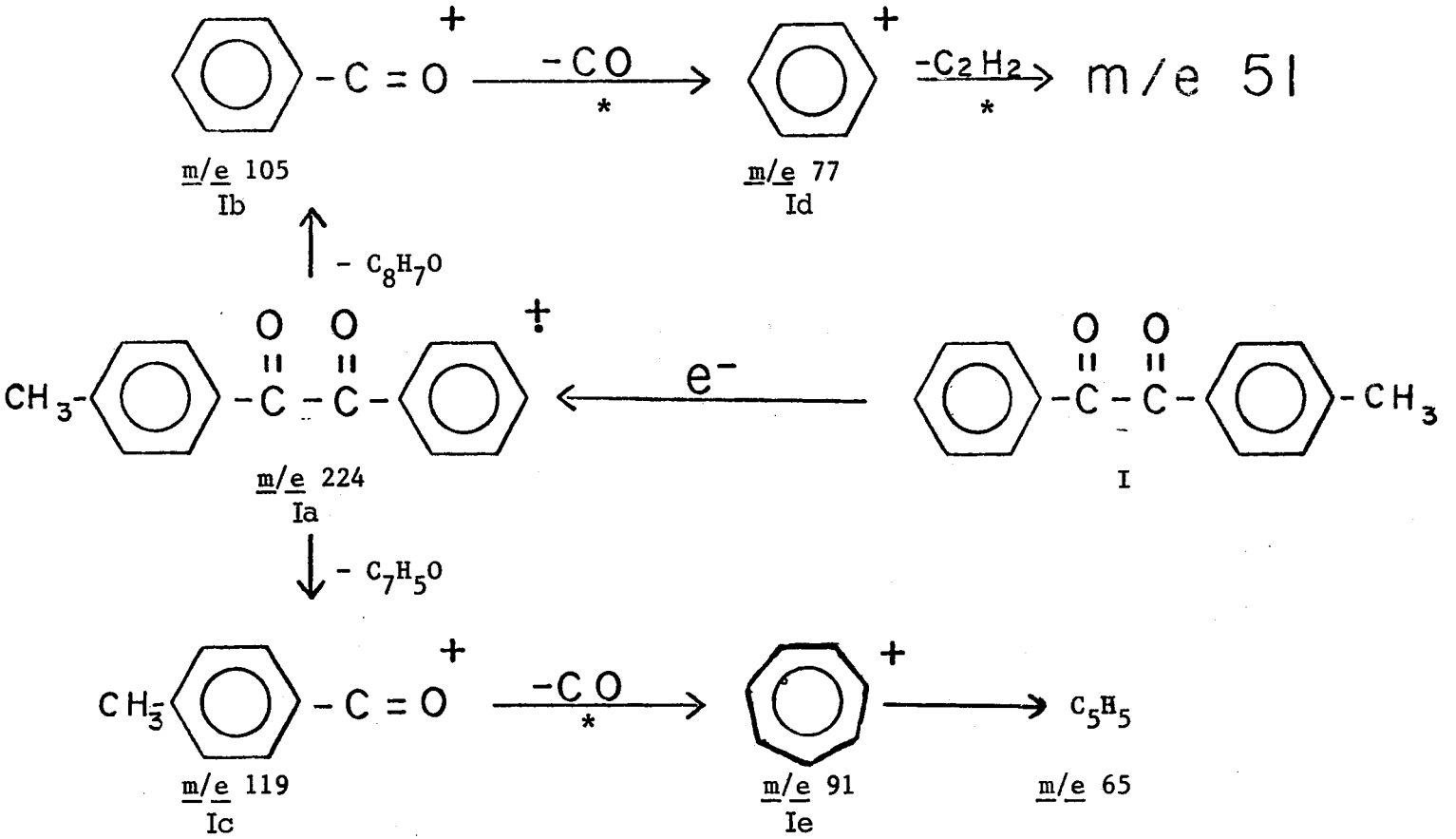

Figure 5. Detailed fragmentation mechanism for I

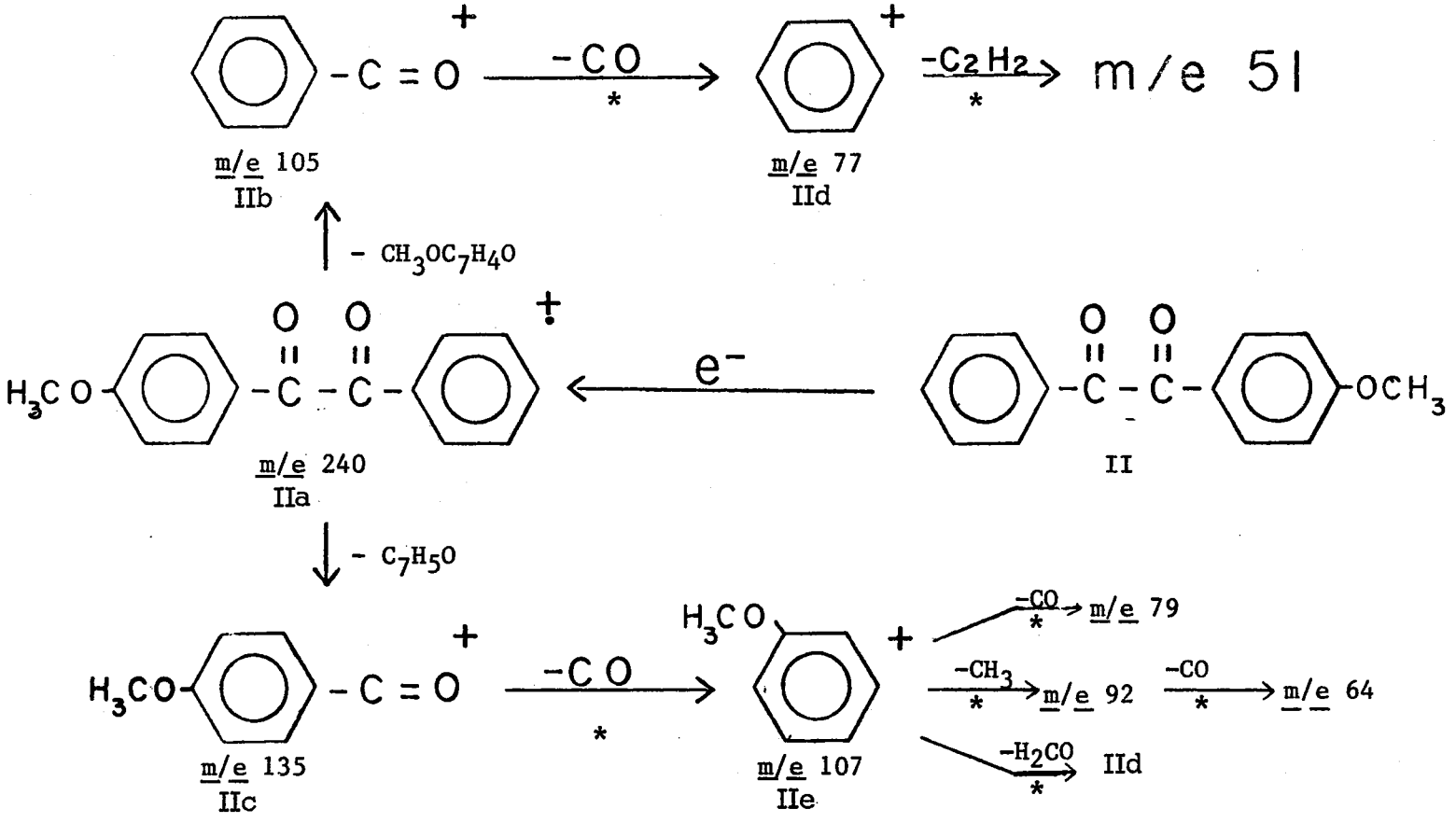

Figure 6. Detailed fragmentation mechanism for II

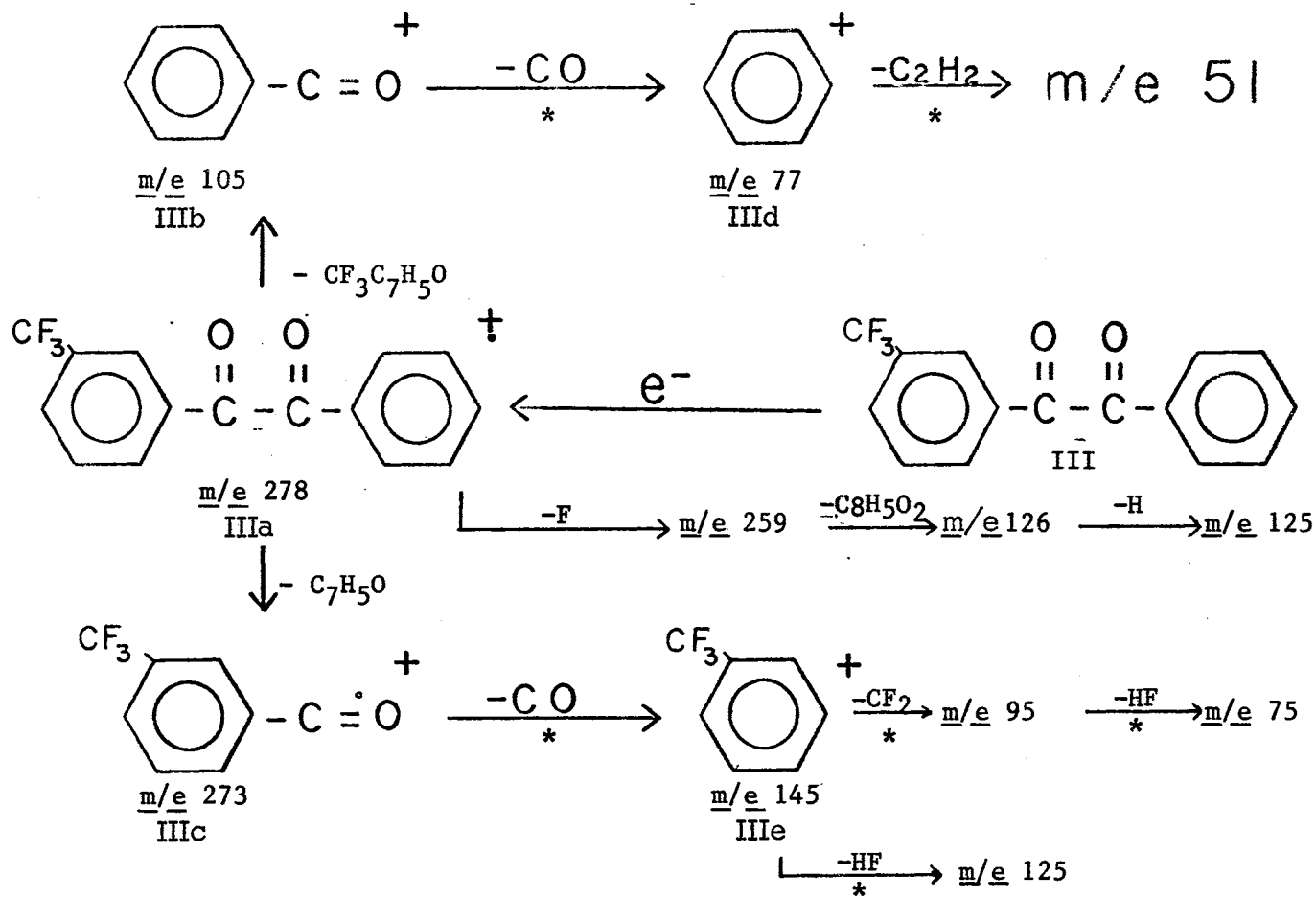

Figure 7. Detailed fragmentation mechanism for III

m/e 51 and m/e 65. Loss of acetylene from Id and Ie is found to be a high-energy process accounting for 10.8 per cent of the ion current at 310° and 9.4 per cent at 230°, in the 70 eV spectra, but only 0.5 per cent of the ion current at 20 eV in both the 310° and 230° spectra. Because of the high energy requirements for the formation of m/e 51 and m/e 65 these fragments were not investigated. Metastable ions were observed at (a) m/e 56.47 and 69.59 for loss of carbon monoxide from Ib and Ic respectively, and (b) at 33.78 and 46.43 for loss of C_2H_2 from Id and Ie respectively. No metastable ions were observed for the fragmentations of Ia to Ib or to Ic. These processes may not be discounted for the following reasons. Metastable ions were observed for the loss of carbon monoxide from ions corresponding to Ib and Ic which can only be formed reasonably from central carbon carbon bond cleavage of Ia. Metastable ions will only be observed for those ions decomposing with a rate which is consistent with decomposition in the first field-free region.[33]

The detailed fragmentation pathways of IIa are depicted in Figure 6. The scheme adheres to the general fragmentation pattern shown in Figure 4. Cleavage of the C-1--C-2 bond in IIa produces ions at m/e 105 (IIb) and m/e and m/e 135 (IIc). In the 21 eV mass spectrum these ions account for 88.9 per cent at 310° and ninety per cent at 250°. In the 70 eV spectrum at both ion source temperatures sixty-five per cent of the ion current is carried off by these two ions. Loss of carbon monoxide from IIb and IIc produces ions at m/e 77 (IId) and m/e 107 (IIe). Trivial fragmentations of IId and IIe were observed giving rise to ions at

m/e 51 and m/e 92 and 79 respectively. At a source temperature of 250° these processes account for only 0.9 per cent of the total ion current at 21 eV and 8.3 per cent of total ion current at 70 eV. Table IV gives the metastable peaks which were observed in the mass spectrum of II. A metastable peak was observed for the loss of the elements of formaldehyde from IIe giving an ion at m/e 77 (IId). Consequently, formation of IId occurs via fragmentation of IIb and IIe. The ions at m/e 51, 64, 79, and 92 were not investigated in this study and represent high-energy processes which carry off a negligible percentage of the ion current at electron energies less than 20 eV.

Unimolecular decomposition of the molecular ion of III(IIIa) under electron impact proceeds in a similar manner to that of Ia and IIa as shown previously in Figure 4. Figure 7 indicates cleavage of the C-1--C-2 bond in IIIa produces ions at m/e 105 (IIIb) and m/e 273 (IIIc) corresponding to the benzoyl and 3-trifluoromethylbenzoyl ions respectively. Table V gives the metastable ions which were observed in the mass spectrum of III. It is important to note that the metastable ions appearing at 107.66 and 107.76, corresponding to formation of IIIc from IIIa and of m/e 125 from IIIe respectively, could not be resolved with the instrumental arrangement used. Loss of carbon monoxide is common to IIIb and IIIc and yields ions at m/e 77 (IIId) and m/e 145 (IIIe). The loss of the elements of acetylene from IIId produces an ion at m/e 51. The major fragment observed for the decomposition of IIIe is m/e 95. A minor process results in the production of m/e 125 from IIIe via the loss

TABLE IV

METASTABLE IONS OBSERVED IN THE MASS SPECTRUM OF II

Parent	Daughter	Metastable Peak
IIb	IId	56.47
IIc	IIe	84.81
IId	m/e 51	33.78
IIe	m/e 92	79.10
IIe	m/e 79	58.33
IIe	IId	55.41
m/e 92	m/e 64	44.52

TABLE V

METASTABLE IONS OBSERVED IN THE MASS SPECTRUM OF III

Parent	Daughter	Metastable Peak
IIIb	IIId	56.47
IIIc	IIIe	121.53
IIId	m/e 51	33.78
IIIe	m/e 125	107.76[a]
IIIe	m/e 95	62.24[b]
m/e 126	m/e 125	124.01
m/e 95	m/e 75	59.21

[a] This metastable ion was observed to be a broad peak.

[b] This metastable ion was of very low intensity extending over several mass units.

of hydrogen fluoride. Loss of hydrogen fluoride from m/e 95 produces an ion at m/e 75. At 70 eV m/e 51, 75, 95, and 125 account for 9.7 per cent of the total ion current while at 20 eV these ions only account for approximately 0.1 per cent of the ion current. Loss of atomic fluorine from m/e 278 (IIIa) produces an ion at m/e 259 (IIIf). Although this ion supplies only 1.0 per cent of the ion current at 70 eV it was investigated since it is a primary fragmentation process. Further fragmentation of IIIf produces secondary and tertiary daughter ions at m/e 126 and m/e 125. Third- and fourth- generation daughter ions were not included in this study.

The detailed fragmentation patterns for IV and V depicted in figures 8a and 9a adhere to the general fragmentation pattern in Figure 4 and to that proposed by others.[29,34,35] The 70 eV spectra for IV and V are reproduced in Figures 8b and 9b. The pertinent metastable ions observed in the spectrum of IV are shown in Table VI. Metastable ions for the transitions m/e 210 (IVa) to m/e 105 (IVb) or to m/e 77 (IVc) were not observed. Analogous to IVa similar metastable ions were observed in the mass spectrum of V, as shown in Table VI.

The mass spectra of I, II, III, IV, and V all exhibit ions corresponding to loss of molecular oxygen from the parent molecule. Although these ions may conceivably be formed from the unimolecular loss of molecular oxygen from Ia, IIa, IIIa, IVa, and Va this process seems unlikely for the following reason. The $M-O_2$ ions from II and III show a marked dependence upon filament area. For example when the area of

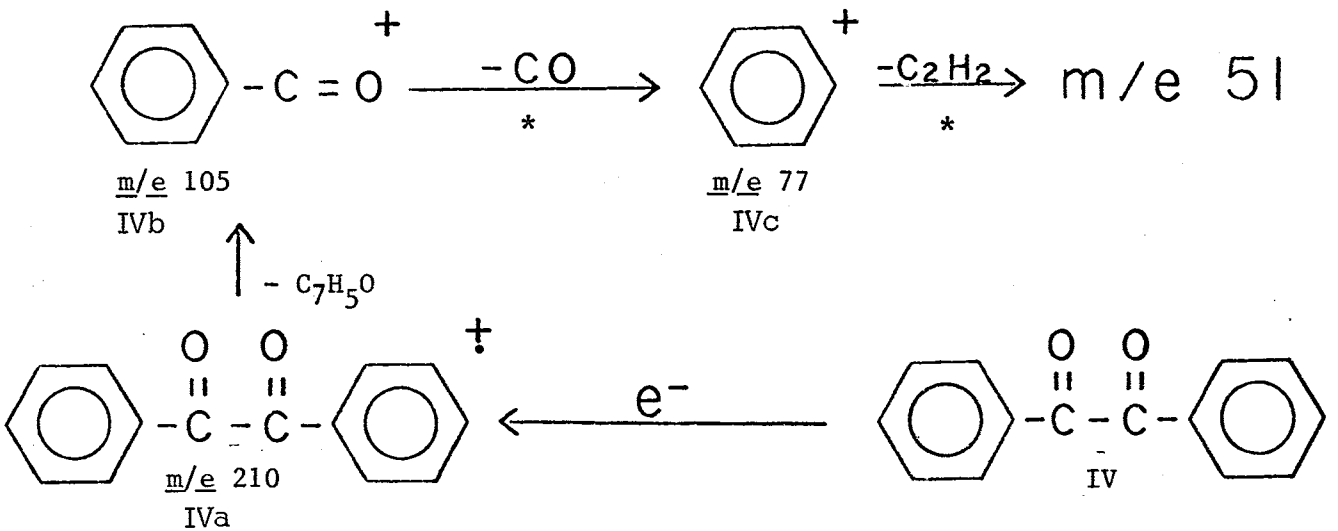

Figure 8a. Detailed fragmentation mechanism for IV

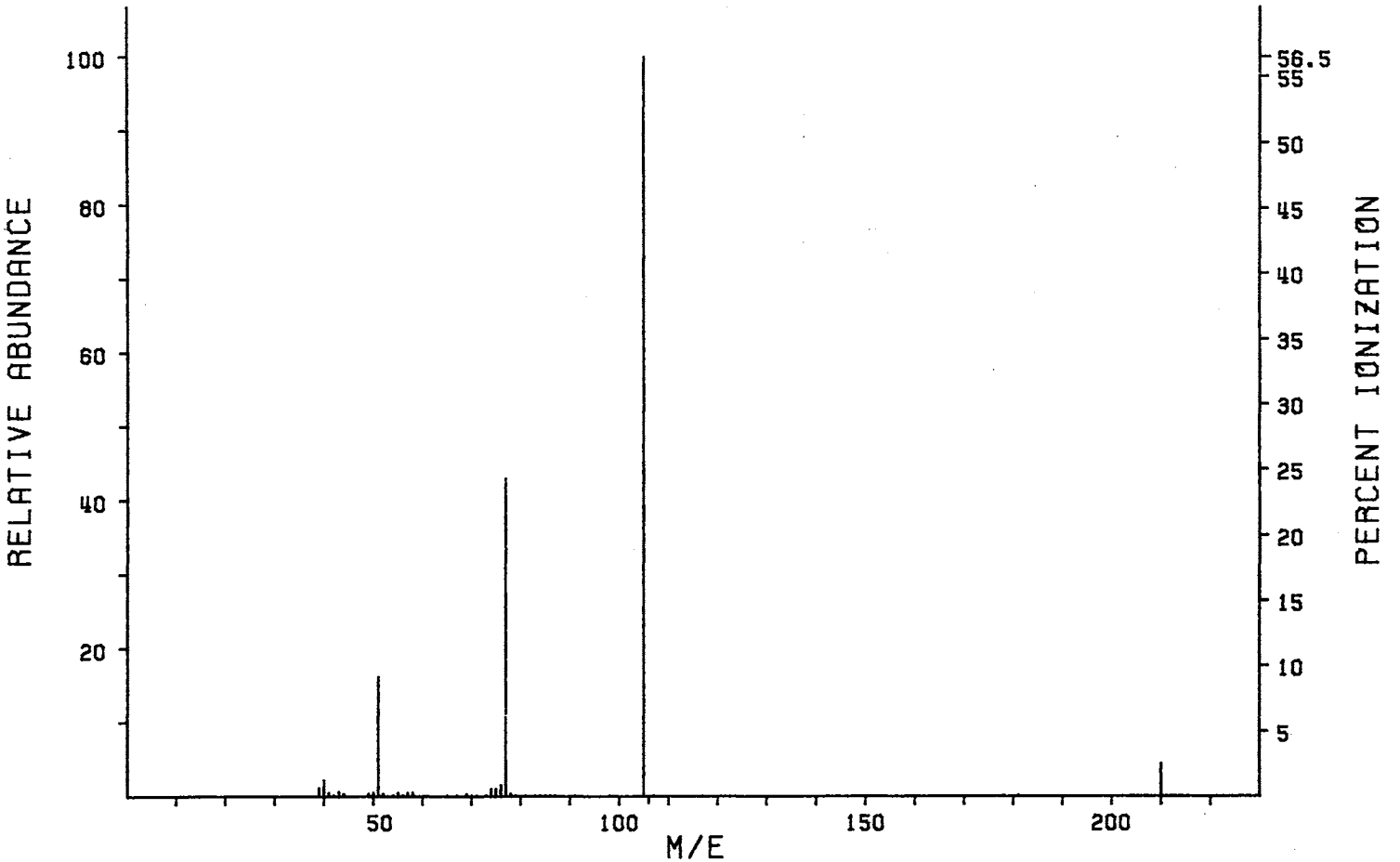

Figure 8b. 70 eV Mass Spectrum of IV, 250° Ion Source Temperature

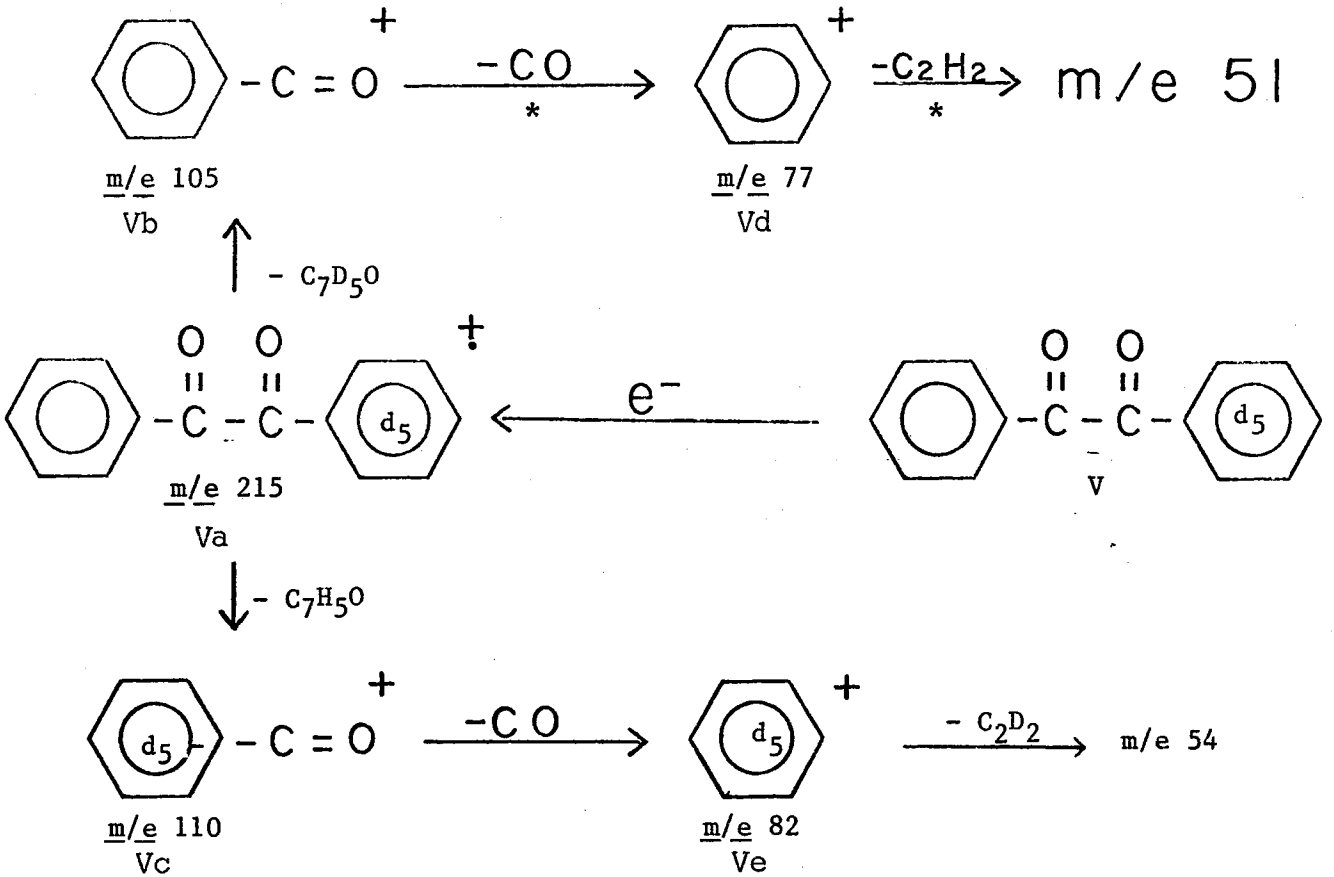

Figure 9a. Detailed fragmentation mechanism for V

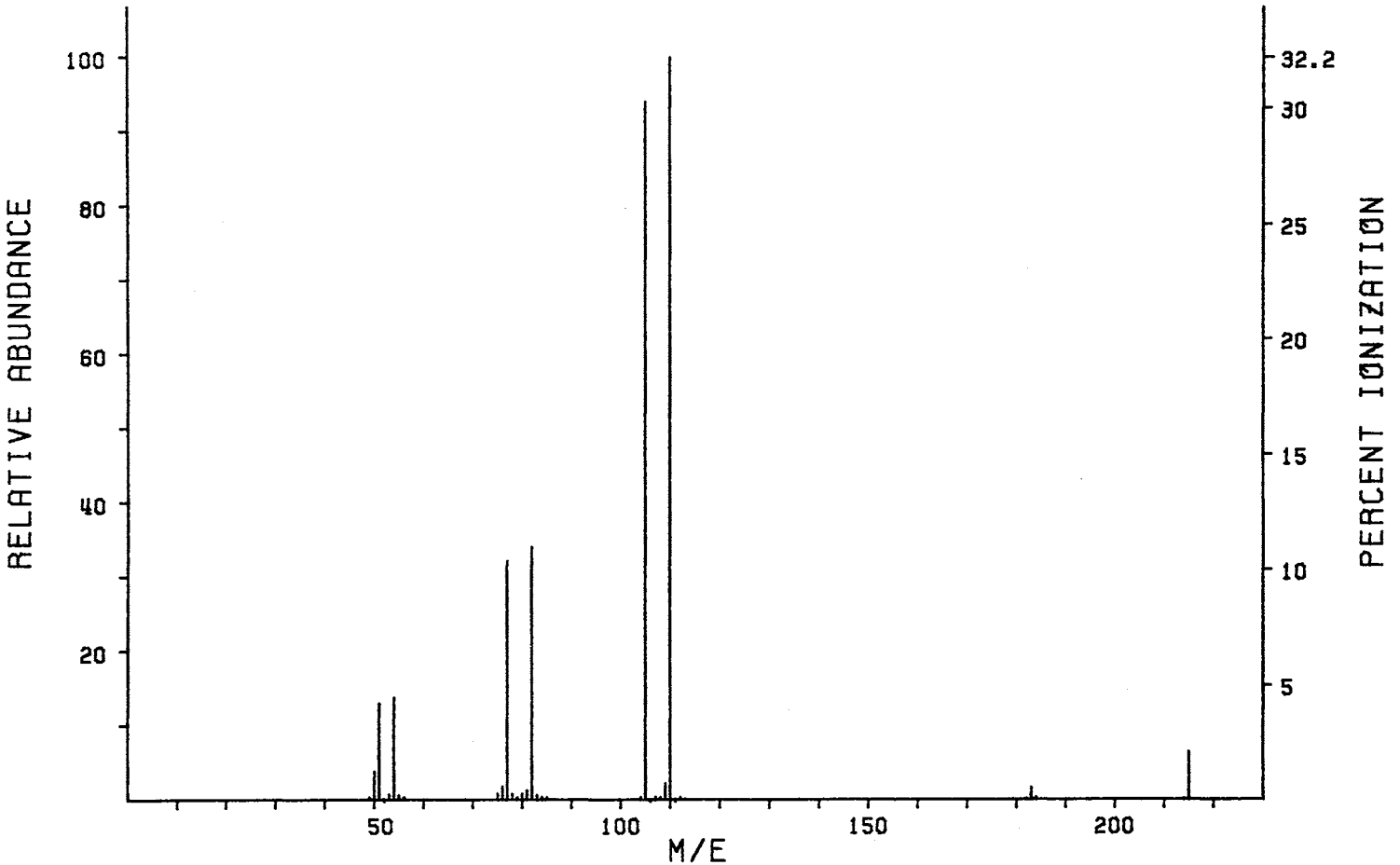

Figure 9b. 70 eV Mass Spectrum of V, 250° Ion Source Temperature

TABLE VI

METASTABLE IONS OBSERVED IN THE MASS SPECTRUM OF IV AND V

Parent	Daughter	Metastable Peak[a]
IVb	IVc	56.47
IVc	m/e 51	33.78
Vb	Vd	56.47
Vc	Ve	61.13
Vd	m/e 51	33.78
Ve	m/e 54	35.56

[a]At an ion source temperature of 250°.

the filament is defined by a 0.03-inch rhenium ribbon, the $M-O_2$ ions in the spectra of II and III are on the average 7.2 times as abundant as those observed with a filament of 0.02 inches in width. This intensity dependence upon filament area is not consistent with electron-impact-induced phenomena but provides evidence for the hot filament pyrolysis of II and III with loss of molecular oxygen prior to electron impact. Loss of O_2 from IVa has not previously been observed.[34,35]

Skeletal rearrangement processes of the type $ABC^+ \rightarrow AC^+ + B$ in the mass spectrum of IV have been reported by Bowie et al.[35] and are envisioned to proceed by the following route.

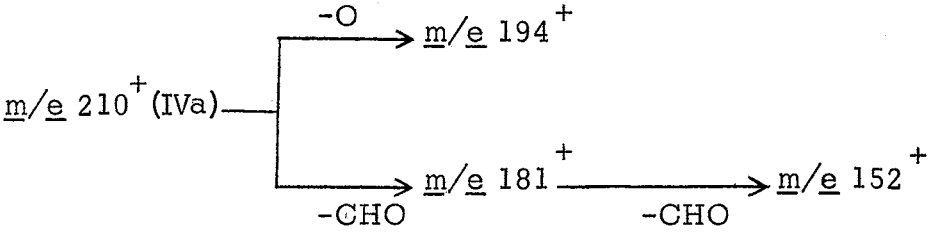

(9)

We observed ions at m/e 151 and 152 exhibiting relative abundances of 0.2 and 0.4 at 70 eV. However, no evidence could be found for loss of atomic oxygen from IVa. The corresponding skeletal rearrangement processes for Ia, IIa and IIIa were observed to be minor, typically on the order of 0.1 per cent of the base peak. On the basis of these data and the results of others,[34,35] the principal features in the mass spectra of I, II, III, IV, and V are accounted for by the schemes in figures 4-7, 8a, and 9a.

The first differential ionization efficiency (FDIE), based on (dI/dE) data for ions Ia-Ie, IIa-IIe, IIIa-IIIf, IVa-IVc, and Va-Ve are reproduced in Appendix A. These average sets of experimental dI/dE values were obtained by changing the electron energy by steps of $0.1 \pm .002$ eV and recording six to twenty dI/dE values at each 0.1 eV interval. The FDIE curves obtained after smoothing the averaged experimental dI/dE values exhibited broad maxima, each remaining at a constant value, within the limits of error, for approximately 3 eV. For purposes of numerical differentiation the average of these values was taken as the maximum in the FDIE curve. Figures 10 and 11 give representative twice numerically smoothed dI/dE curves (FDIE) of Ia and Ib, except at the maxima, which are normalized to the most intense ion in the set with its maximum value equal to 100.

The shot noise contribution to the standard deviation ($\underline{\sigma}$) in dI/dE and the effects of the dI/dE sample size, the lock-in-amplifier time constant, the integration time, and the sampling rate on the experimental $\underline{\sigma}$ have been considered analytically. The $\underline{\sigma}$ for all the dI/dE data in this study are estimated as those obtained from shot noise calculations. The dI/dE points tabulated in Appendix A represent the numerical average of a small number of experimental values. Owing to the lock-in-amplifier (LIA) time constant and the relatively small sampling interval successive dI/dE values along the curve will not be statistically independent. An attempt was made experimentally to estimate the standard deviation of dI/dE for Ia-Ie, at an ion source temperature of 310°,

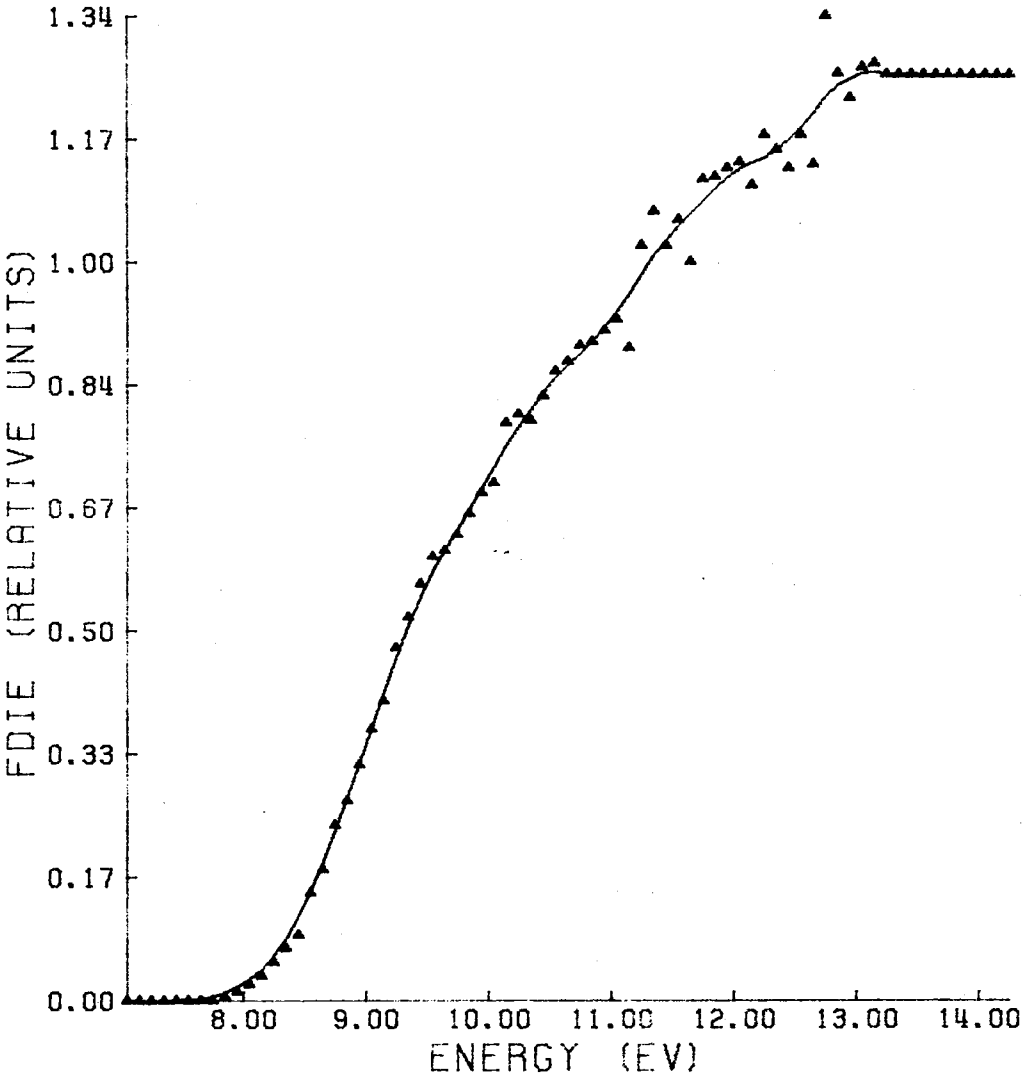

Figure 10. FDIE curve of Ia, 310° Ion Source Temperature

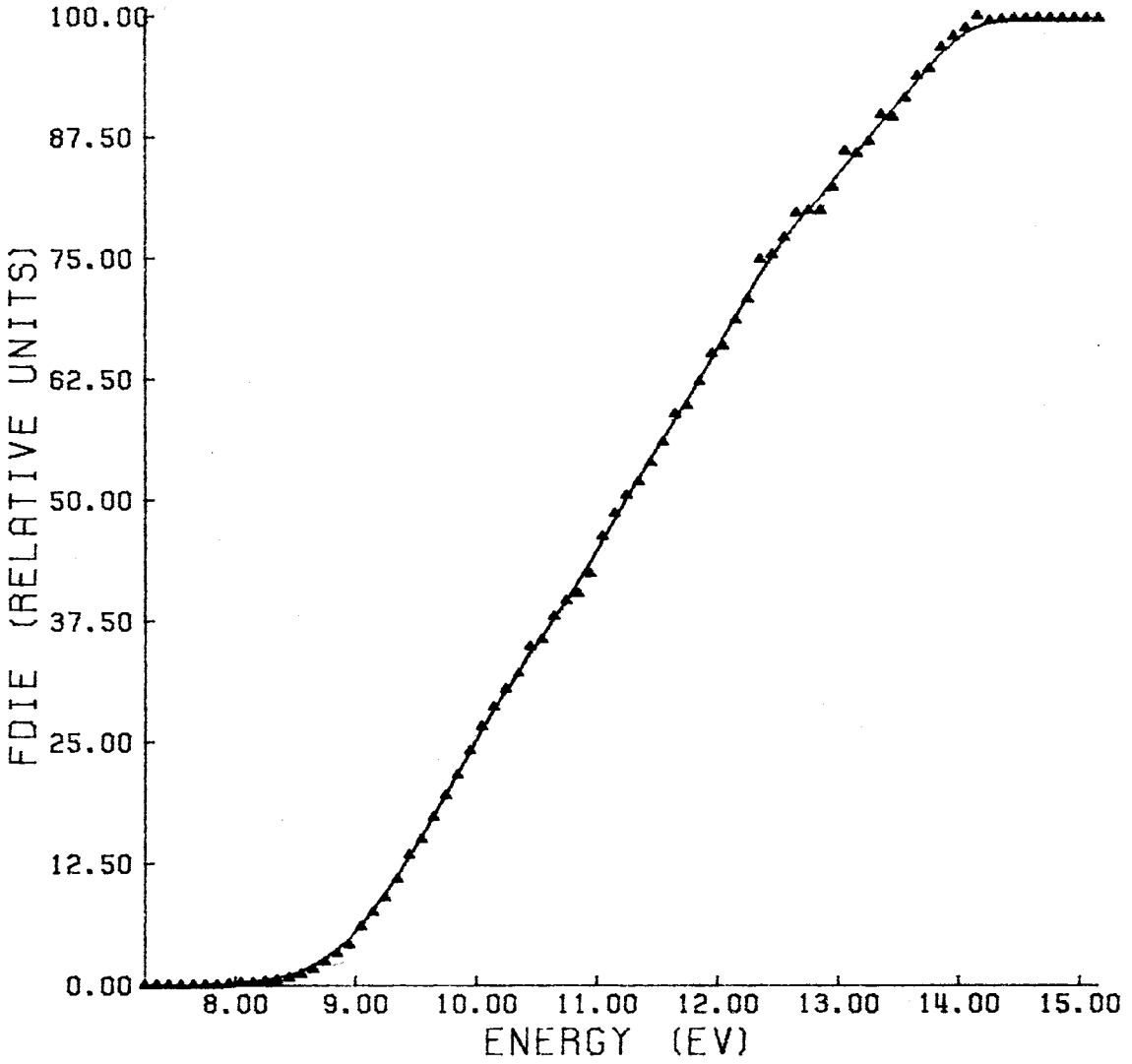

Figure 11. FDIE Curve of Ic, 310° Ion Source Temperature

as a function of the electron energy. A large sampling of points was taken at three values of the electron voltage for each ion. The experimental conditions such as sample pressure, LIA parameters, and integration time were brought into coincidence with the experimental parameters used to obtain the dI/dE data for Ia-Ie. The calculation of $\underline{\sigma}$ was carried out by obtaining the experimental $\underline{\sigma}$ of an increasing number of dI/dE values until constancy of $\underline{\sigma}$ was attained. Clearly, calculation of $\underline{\sigma}$ from a limited number of dependent dI/dE values will tend to underestimate the true standard deviation. This is shown graphically in Figure 12, for Ia. For Ia-Ie a sufficient number of dI/dE values were taken to give a $\underline{\sigma}$ which approached a more or less constant value. The experimental estimates of $\underline{\sigma}_{true}$ ($\underline{\sigma}_{exp}$) so obtained for Ia through Ie are given in Table VII. The mathematical treatment of the shot noise[36] predicts that $\underline{\sigma}_{shot\ noise}$ ($\underline{\sigma}_{sn}$) should vary as the one-half power of the absolute ion intensity. Calculation of $\underline{\sigma}_{sn}$ for Ia-Ie (see Appendix B) at each value of the electron voltage in Table VII is plotted in Figure 13 as the solid lines. The points in Figure 13 represent the values of the $\underline{\sigma}_{exp}$ determined at the various electron voltages versus the absolute ion intensity. Although some random scatter in the experimental points about the appropriate calculated curves is observed, the fact that for a given ion $\underline{\sigma}_{exp}$ and $\underline{\sigma}_{sn}$ differ by a factor of two or less indicates that shot noise contribution to the deviations observed in the dI/dE values is the major source of error. The agreement between $\underline{\sigma}_{exp}$ and $\underline{\sigma}_{sn}$ as a function of the absolute ion intensity indicates that a valid estimate of

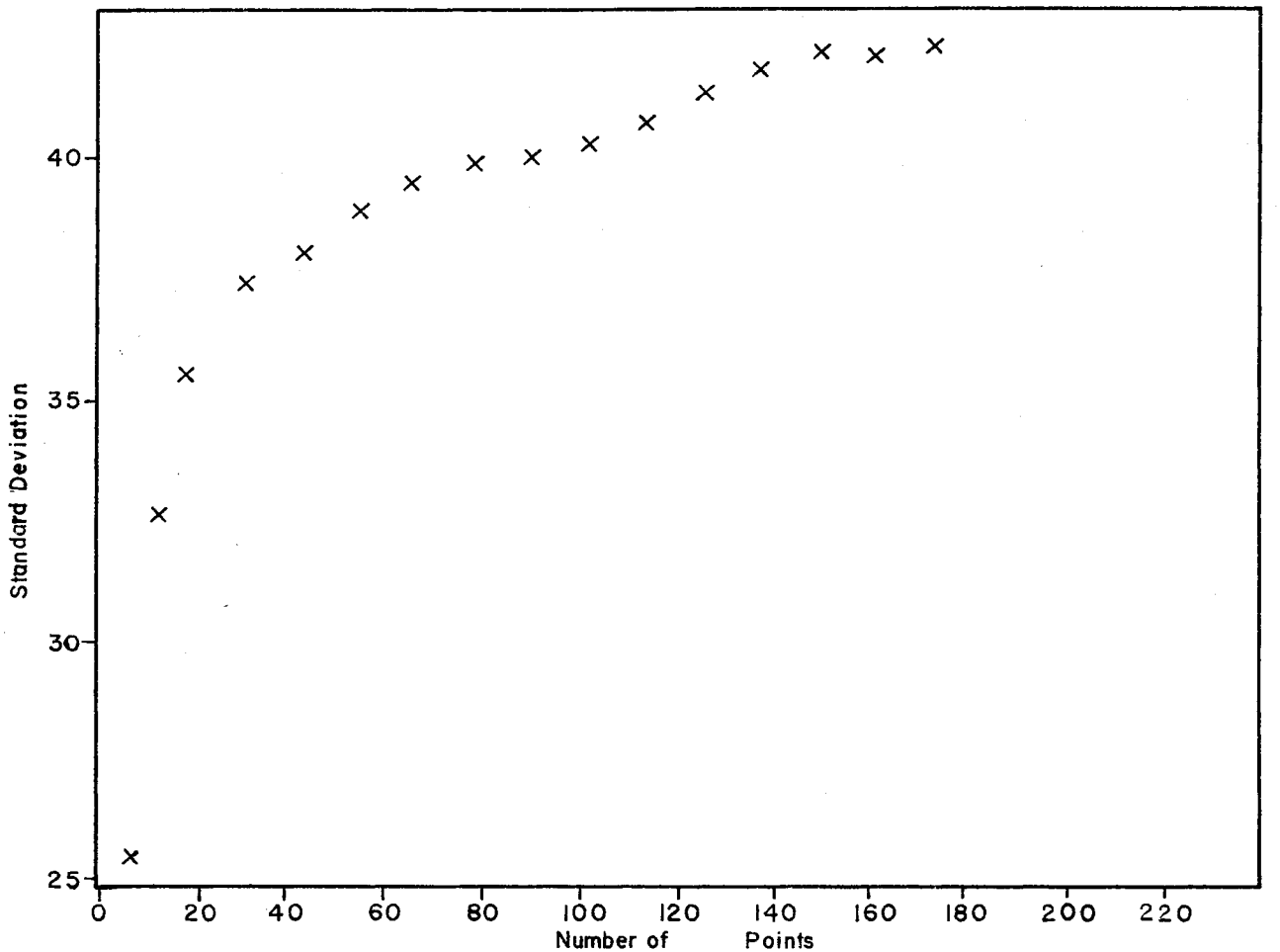

Figure 12. Variation of σ_{exp} for Ia as a Function of Number of dI/dE Points Taken

TABLE VII

EXPERIMENTAL PERCENT STANDARD DEVIATIONS
IN THE FDIE AS A FUNCTION
OF ELECTRON ENERGY

Ion	eV[a]	Percent of dI/dE[b] values
Ia	8.65	5.68
	11.25	3.21
	12.85	3.52
Ib	9.85	5.00
	12.05	1.96
	16.55	2.11
Ic	9.55	1.00
	11.55	1.18
	13.55	0.617
Id	14.05	2.84
	17.05	2.59
	19.55	1.51
Ie	13.05	3.78
	15.05	1.61
	18.05	1.69

[a]Energy calibrated

[b]For each ion the lock-in-amplifier time constant (sec.), integration time (sec.), number of points taken to estimate $\underline{\sigma}$, and the multiplier gain are: Ia: 100, 1, 180, 1.20×10^4; Ib: 30, 1, 60, 1.35×10^4; Ic: 30, 1, 60, 1.31×10^4; Id: 30, 10, 60, 1.50×10^4; Ie 30, 1, 60, 1.37×10^4. The sampling interval was 11 seconds.

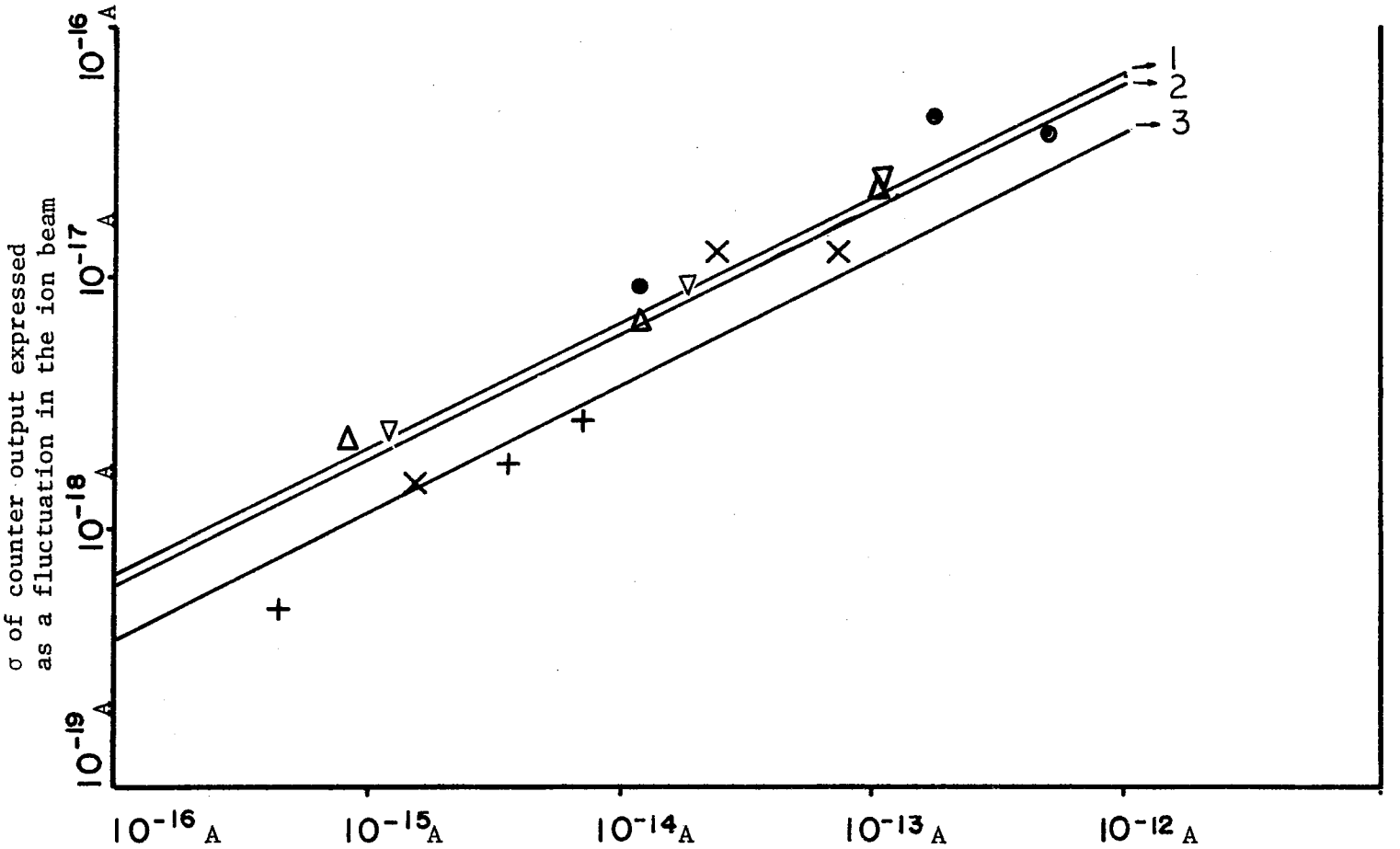

Figure 13. Comparison of calculated (lines) and experimental (points) σ
Line 1 is the calculated σ for Ib (⊙), Ic (Δ), and Ie (▽)
Line 2 is the calculated σ for Id (X)
Line 3 is the calculated σ for Ia (+)

the deviation in dI/dE can be made from a shot noise calculation of $\pm\sigma_{sn}$. The standard deviations ($\pm\sigma_{sn}$) associated with the experimental dI/dE values at three values of the electron voltage for the dI/dE data in Appendix A are tabulated in Appendix B.

The xenon-132 molecular ion peak was used to calibrate the energy axis. The second differential ionization efficiency (SDIE) curve for xenon was obtained by the numerical differentiation of the experimental dI/dE values. To determine the uniqueness of the calibration the dI/dE curve of argon was measured and numerically differentiated. A comparison of the maxima in the second derivative curves of xenon and argon yielded an ionization potential difference of 3.60 eV. The argon-xenon ionization potential difference calculated from the respective literature values of 15.77 eV and 12.15 eV[37] yields a difference of 3.62 eV, which is in good agreement with the experimental difference. A representative xenon SDIE curve is reproduced in Figure 14. The xenon SDIE curve exhibited a second maximum at 12.80 $\pm$ 0.06 eV which results from the 6_d autoionizing state.[38] The full width at half maximum (FWHM) of the xenon SDIE curve was found to be dependent upon the filament dimensions. The FWHM values from the xenon SDIE curves used to calibrate the energy axis for ions Ia-Ie, IIa-IIe, IIIa-IIIf, IVa-IVc, and Va-Ve at two values of the source temperature are shown in Table VIII.

The FDIE curves in Figures 10 and 11 were numerically differentiated to obtain the d^2I/dE^2 values. The per cent standard deviations associated with the d^2I/dE^2 values at three eV values and the method

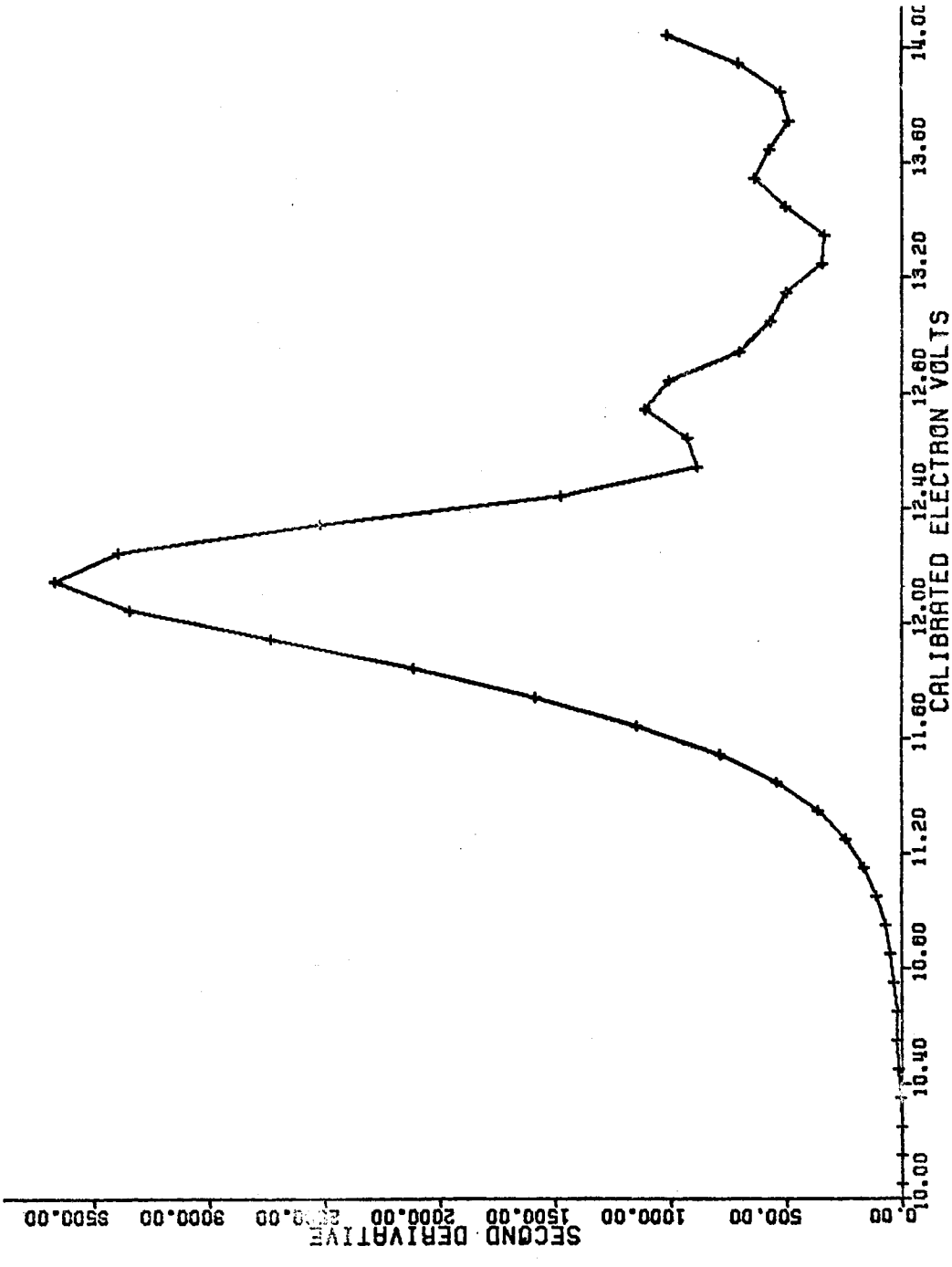

Figure 14. SDIE Xenon m/e 132

TABLE VIII

FWHM ENERGIES FOR XENON SDIE CURVES USED TO CALIBRATE ENERGY AXIS

Ion(s)	12.15 eV Minus Experimental I.P., eV	FWHM, eV	Filament Width, Inches
Ia-Id[a]	+1.05	0.70	0.03
Ie[a]	+1.20	0.50	0.02
Ia, Ic, Id[b]	+0.75	0.58	0.02
Ib[b]	+1.20	0.50	0.02
Ie[b]	+0.75	0.60	0.02
IIa-IIe[c]	+1.05	0.72	0.02
IIa-IIe[a]	+1.05	0.74	0.03
IIIa-IIIf[c]	+1.10	0.84	0.03
IIIa-IIIf[a]	+1.05	0.65	0.03
IVa-IVc[c]	+0.75	0.74	0.03
Va-Ve[c]	+1.20	0.70	0.03

[a]Ion source temperature 310°.

[b]Ion source temperature 230°.

[c]Ion source temperature 250°.

of calculation are given in Appendix B. The factors which influence the deviation in dI/dE, such as absolute ion intensity, also affect the accuracy with which d^2I/dE^2 may be determined. The deviation in d^2I/dE^2 at low values of the ion intensity depends mainly on the accuracy with which the increment size may be determined and at high values of the ion intensity, this contribution is minimal compared to the shot noise contribution. The SDIE curves correspond to the line drawn through the points obtained from a single smoothing of these d^2I/dE^2 values.

Four separate measurements of dI/dE for the ions resulting from the decomposition of Ia at 310° yields qualitative support to the calculated deviations. Deviations in the SDIE curves which are in excess of the predicted values may be explained in part by the differences in width at half height of the electron energy distribution. At low values of the electron voltage an increase (decrease) in the electron energy distribution will manifest itself in an increase (decrease) in an SDIE curve near threshold. Dual determinations of the FDIE curves for ions Ia-Ie at an ion source temperature of 230° were made. The SDIE curves of IIa-IIe, IIIa-IIIf, IVa-IVc, and Va-Ve represent a single determination.

The ionization potentials for the molecular ions of I, II, III, IV, and V are tabulated in Table IX along with the respective FWHM values. The ionization potentials of I, II, and III apparently depend upon the amount of thermal energy present in the molecule prior to ionization. The experimental ionization potential of I at an ion source temperature of 310° and the corresponding value at 230° are 9.05 ± 0.10 and 9.30 ± 0.15

eV respectively. The FWHM values were computed from the low-energy tail of the SDIE curves and correspond to twice the half width at half height. The FWHM values could not be determined from the full width at half height because of the non-Maxwellian shape of the SDIE curves. The FWHM values of 1.34 eV and 1.37 eV for Ia (Figure 15) at source temperatures of 310° and 230° are approximately twice the magnitude which would be predicted from the FWHM values of the corresponding xenon SDIE curves (Table IX). The experimental ionization potentials of II at source temperatures of 310° and 250° are 8.35 eV and 8.55 eV. The FWHM values of these SDIE curves (Figure 16) are 0.74 eV and 0.72 eV, corresponding to source temperatures of 310° and 250° respectively. These values of the FWHM are in good agreement with the corresponding ones for xenon. The SDIE curves for IIIa (Figure 17) give ionization potentials of 9.5 eV at a source temperature of 310° and 9.5 eV at a source temperature of 250°. The FWHM values of these SDIE curves are 1.40 eV and 1.62 eV at the high and low source temperatures respectively. The FWHM values for IIIa is approximately twice that which would be predicted from the corresponding xenon SDIE curves. The ionization potentials of IV and V were experimentally determined to be 8.86 $\pm$ 0.15 eV and 9.20 eV respectively. The FWHM values of the SDIE curves of IVa and Va (Figures 18-19) were determined to be 1.10 eV and 1.30 eV for Va. These values for the ionization potential of I, III, IV, and V may not represent the ionization potential corresponding to a vertical transition to the lowest ionic state of the ion for the following reason. The

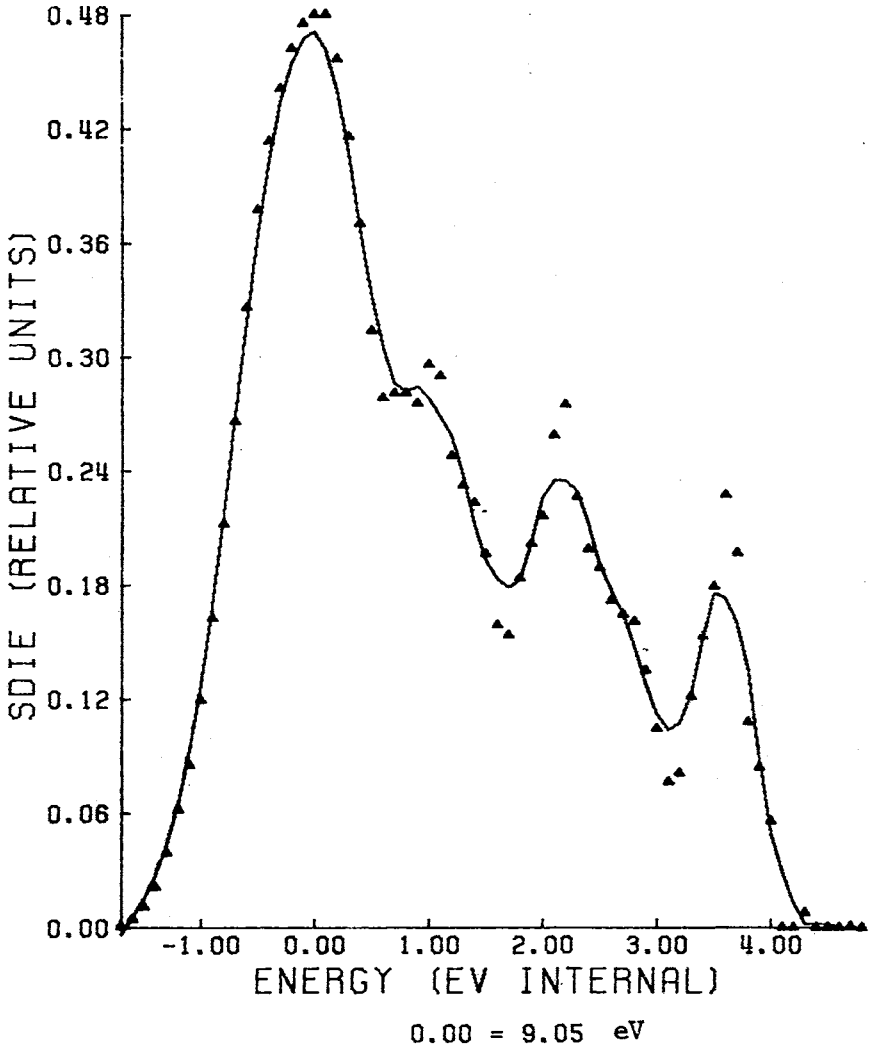

Figure 15a. SDIE Curve of Ia, 310° Ion Source Temperature

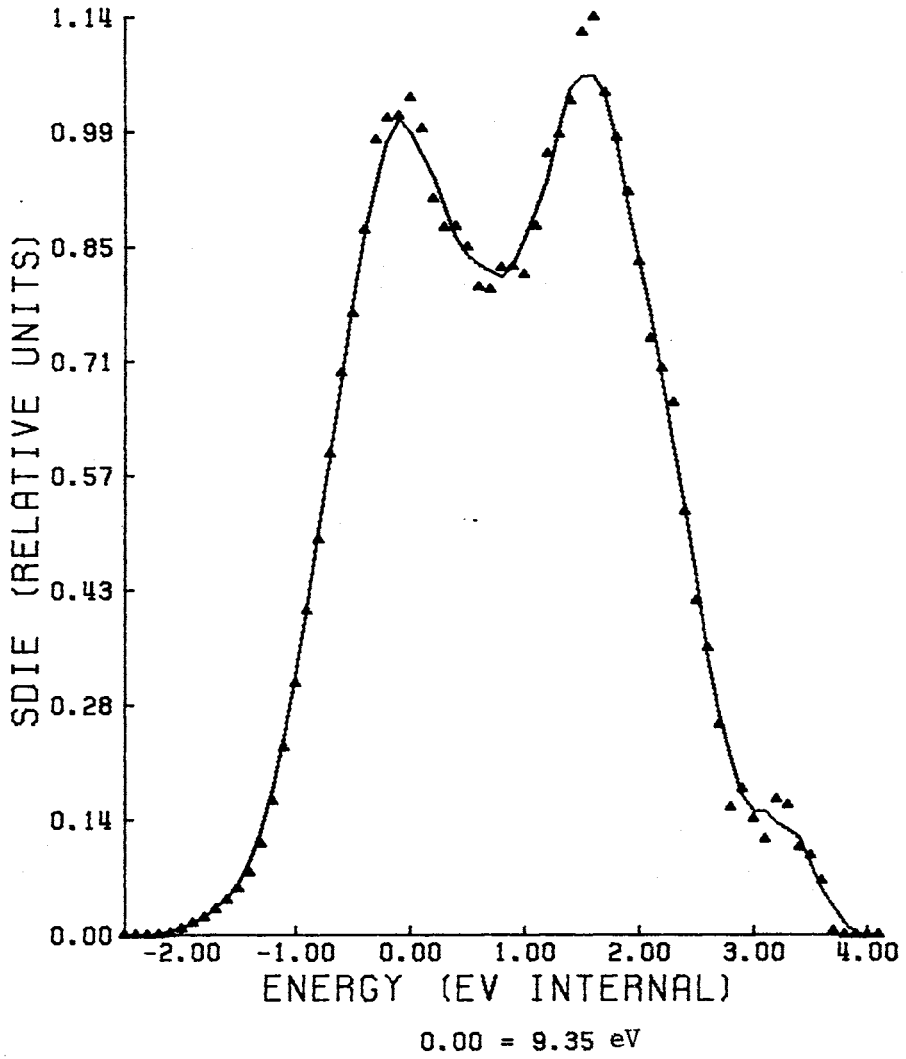

Figure 15b. SDIE Curve of Ia, 230° Ion Source Temperature

TABLE IX

IONIZATION POTENTIALS AND FWHM
FOR MOLECULAR IONS

Molecular Ion	Ion Source Temp., °C	Experimental I.P., eV	FWHM	FWHM Energy for Xenon, eV
Ia	310	9.05 ± 0.10	1.34	0.64
	230	9.30 ± 0.15	1.37	0.54
IIa	310	8.35	0.72	0.74
	250	8.55	0.62	0.72
IIIa	310	9.5	1.40	0.65
	250	9.5	1.62	0.84
IVa	250	8.86 ± 0.15	1.10	0.74
Va	250	9.20	1.30	0.70

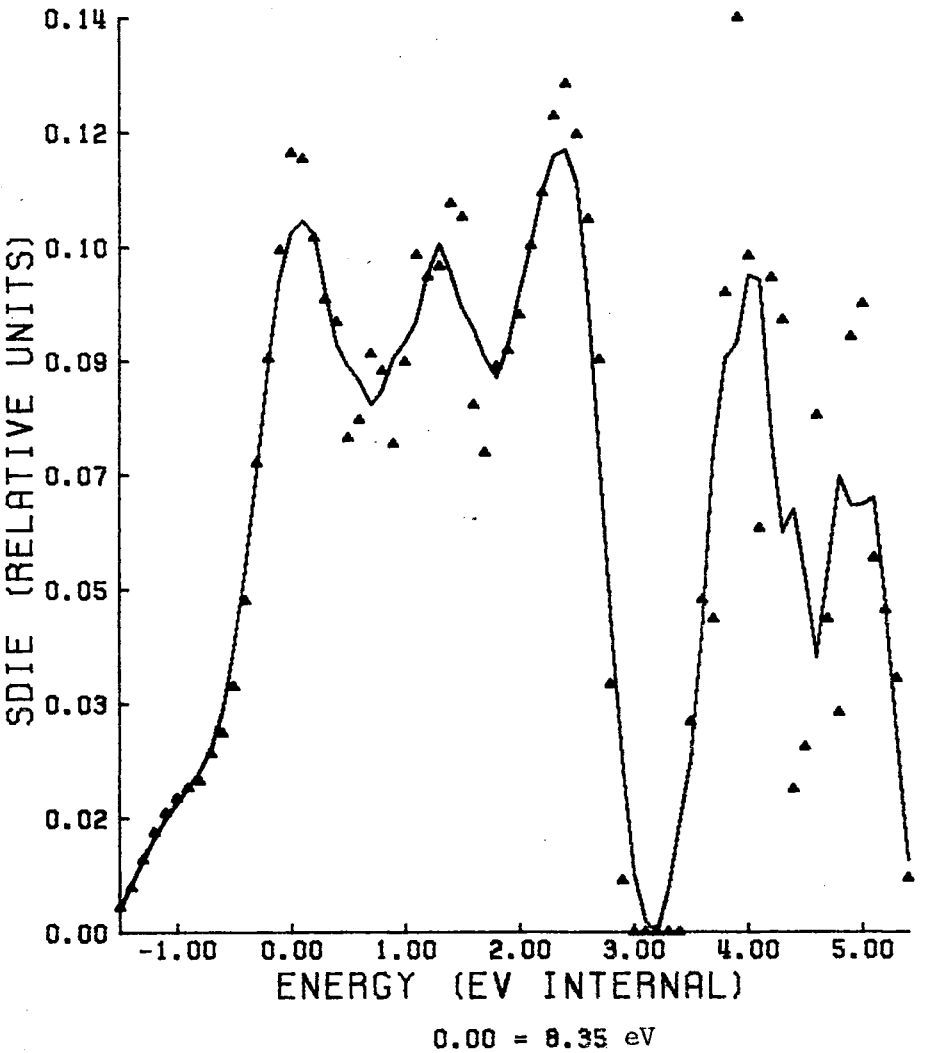

Figure 16a. SDIE Curve for IIa, 310° Ion Source Temperature

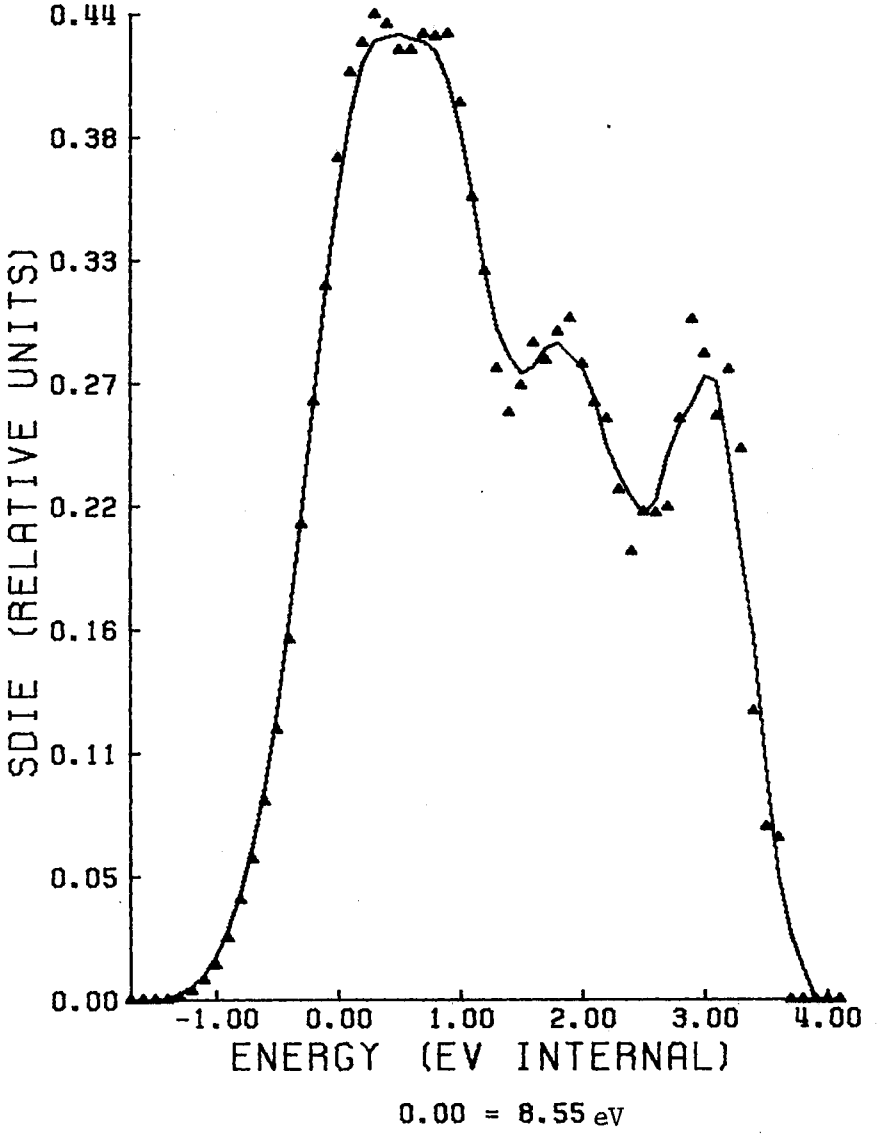

Figure 16b. SDIE Curve of IIa, 250° Ion Source Temperature

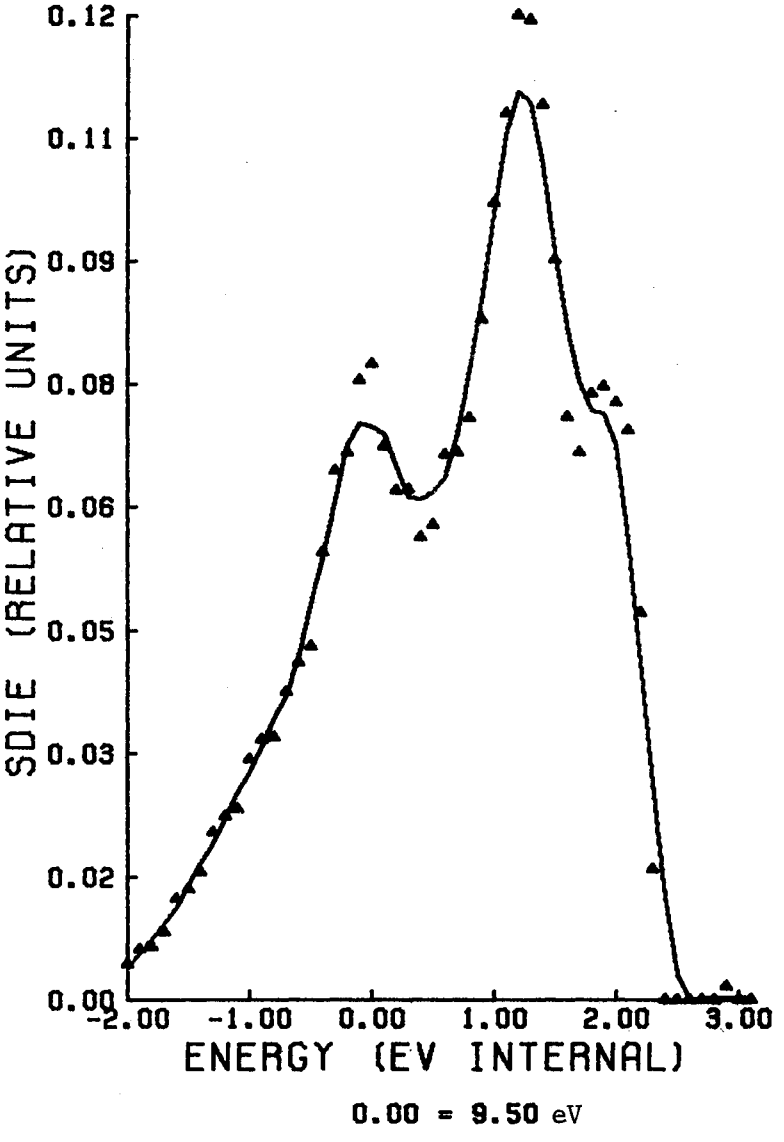

Figure 17a. SDIE Curve of IIIa, 310° Ion Source Temperature

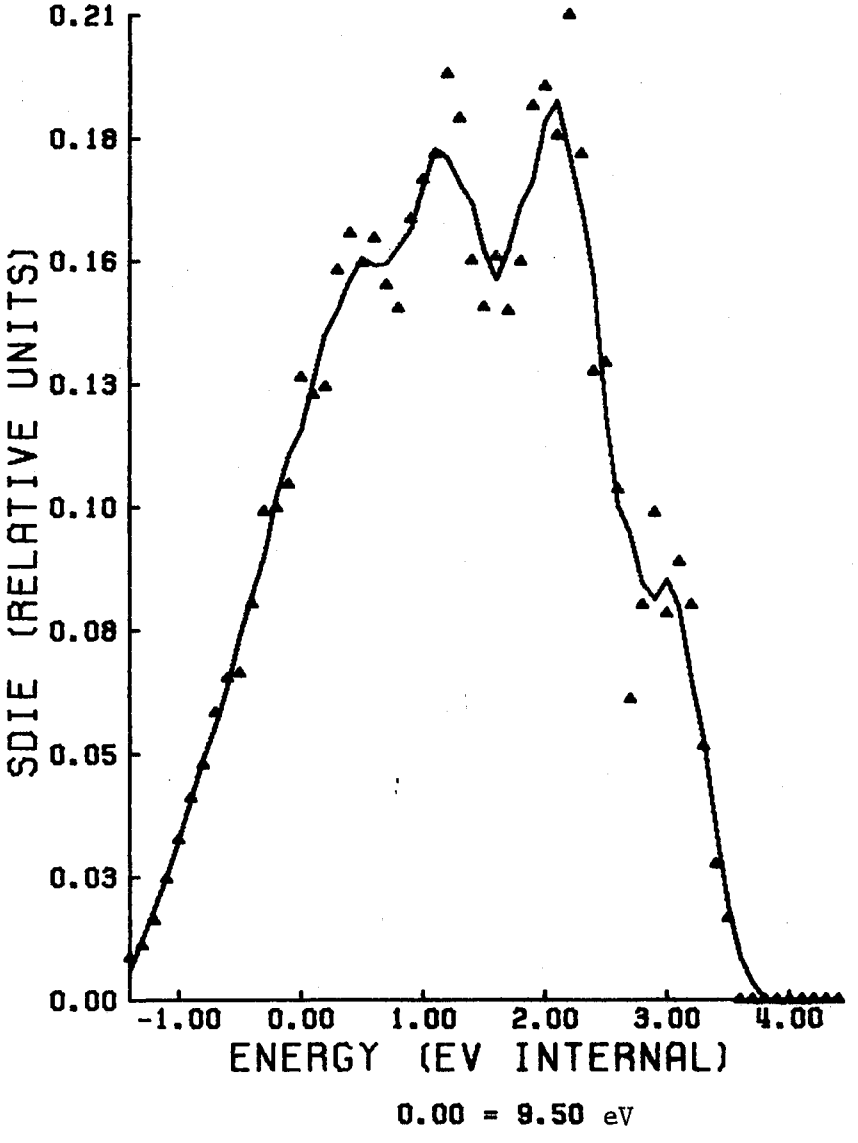

Figure 17b. SDIE Curve of IIIa, 250° Ion Source Temperature

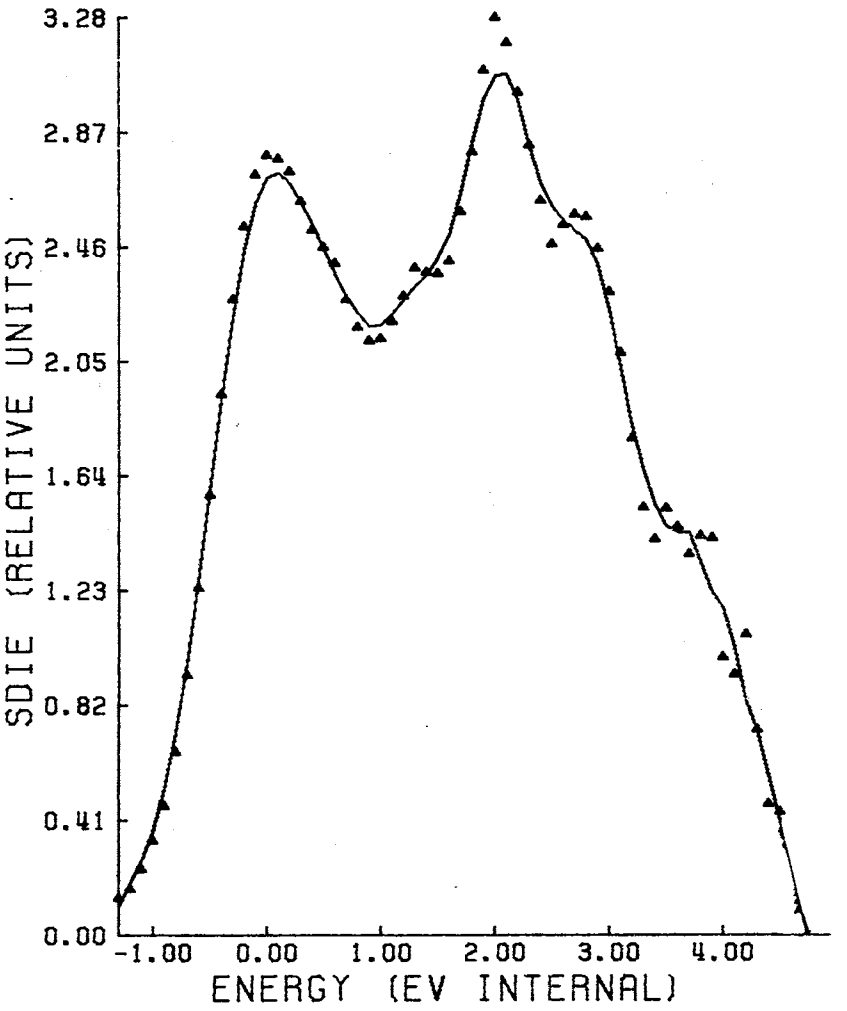

Figure 18. SDIE Curve, 0.00 = 8.75 eV, of IVa, 250°

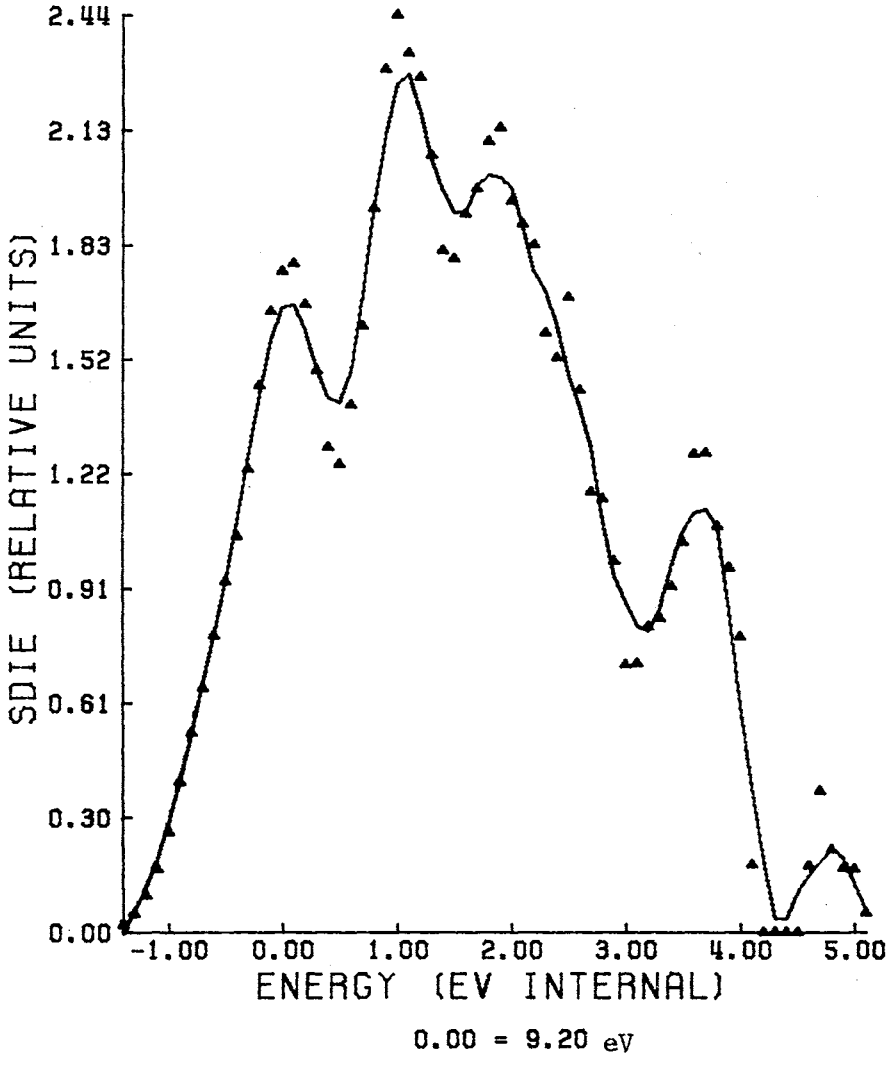

Figure 19. SDIE Curve of Va, 250° Ion Source Temperature

FWHM values of the SDIE curves of Ia, IIIa, IVa, and Va, when compared with the corresponding ones from xenon SDIE curves are found to exceed the xenon Maxwellian half-height width by approximately a factor of two. This observation is consistent with populations of vibrational levels in excess of those found in the lowest ionic states, resulting in ionization potentials corresponding to the most probable transitions. The FWHM values of the SDIE curves of IIa at both temperatures are in good agreement with those of the xenon SDIE curves, indicating that the population of the lowest ionic state may be the most probable. The calculated values for the ionization potentials (Appendix C), 8.61 ± 0.17 eV and 8.83 ± 0.61 eV for I and III respectively, when compared with the experimental values at 310 °of 9.05 ± 0.10 eV for I and 9.5 eV for III, give reasonable agreement. The calculated value of 8.10 ± 0.11 eV for the ionization potential of II is in good agreement with the experimental value at 310° of 8.35 eV. The experimental ionization potential of 8.86 ± 0.15 eV for IV is in good agreement with the literature value of 8.78 eV.[34] Although no literature value for the ionization potential of V is given, deuterium substitution should have a negligible effect on the ionization potential. The experimental value of the ionization potential of 9.2 eV for V is not in agreement with the literature value of 8.78 eV for the ionization potential of IV.

Although the ionization potential data obtained for II and III represent single determinations, the data in Table IX indicate that these potentials of I, II, and III decrease with increasing source temperature.

The ionization potentials of I, II, III, IV, and V are of considerable interest. The configuration of benzil in both the solid and liquid phase at room temperature has been investigated by a number of workers[39a-e] using such techniques as UV, PMR, and phosphorescence. These studies lend to a skew (VI) configuration for IV rather than a coplanar trans (VII) configuration. The trans configuration is preferred over the skew when there is extensive ortho substitution on the benzil moiety,[39b] even though the rings are skewed out of the plane defined by the OCCO linkage.

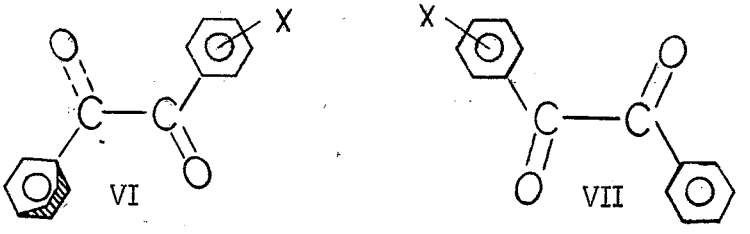

VI VII (10)

X = H, P-CH_3, P-OCH_3, and M-CF_3

The electronic interaction between the benzoyl groups of I, II, III, IV, and V should vary with the angle of rotation (Ø) of the two carbonyl groups. In accord with the skew structure, IV and some of its corresponding derivatives exhibit absorption spectra which resemble those of benzaldehyde and its corresponding derivatives. This result would require that Ø must not be that angle which gives maximum interaction. For Ø equal to 90° the carbonyl interaction in VI should be minimal. In this skew conformation the lowest ionization potentials of I, II, III, IV, and V should correspond to the ionization potentials of their corresponding benzaldehyde and substituted benzaldehydes. Table X gives these

TABLE X

IONIZATION POTENTIALS OF SUBSTITUTED BENZILS AND BENZALDEHYDES

Substituent	Source Temp., °C	Parent Moiety: Benzil I.P., eV	Parent Moiety: Benzaldehyde I.P., eV
H	250°	8.86	9.51[42]-9.80[40]
	310°	8.75	
p-CH_3	230°	9.30	9.33[41]
	310°	9.05	
p-OCH_3	230°	8.55	8.60[41]
	310°	8.35	
m-CF_3	230°	9.5	not available
	310°	9.5	

values. The S-trans configuration of VII and its molecular ions would allow interaction of the π-orbitals of the adjacent carbonyl groups and this conjugation would allow aromatic π-orbital interaction. For planar ethane-1,2-dione and near planar butane-2,3-dione in the S-trans configuration the π-orbital interaction is reflected in the $n \rightarrow \pi^*$ transitions in the ultraviolet spectra.[39a] This conjugation also produces a depression in the ionization potential of ethane-1,2-dione (9.48 eV[41]) and butane-1,2-dione (9.25 eV[42]) compared to formaldehyde (10.78 eV[42]) and acetone (9.69 eV[42]). These results indicate that the energy on the potential energy hypersurface for benzil and substituted benzil as well as on the ground state of the corresponding molecular ions will be a function of ϕ. Although the high-temperature ultraviolet spectra of benzil and substituted benzils have not been reported, the average sample temperature prior to electron impact, i.e., 150° -310°, should be sufficient to affect the rotamer distribution; the marked temperature dependence of the ultraviolet spectrum of oxalyl chloride has been discussed in such terms. The ionization potentials for I, II, and IV compared to the ones for benzaldehyde and its p-methyl and p-methoxy derivatives are qualitatively consistent with vertical transitions occurring from the planar conformation. Although the temperature prior to ionization is unknown, the samples will have achieved thermal equilibrium prior to introduction into the ion source. The most probable thermal distribution of molecules will lie between the values of the temperature of the thermally equilibrated molecules prior to entrance into the ion source and the ion source

temperature. Thus the most probable thermal distribution will be dependent upon ion source temperature only if the temperature of the thermally equilibrated molecules prior to ion source entrance remains at a constant value. The relative temperature dependence of the ionization potentials of I, II, III, and IV (Table IX) are qualitatively in agreement with different weighting factors for the band envelopes which describe the transition probabilities and/or with vertical transitions from different rotamer distributions. The ionization potentials corresponding to the higher temperature distribution are consistent with increased conjugation resulting in an ionization potential depression. Since the observed SDIE curves for Ia, IIIa, and IVa would correspond to vertical transitions from various conformations, this offers a plausible explanation for the doubling of the FWHM values of the SDIE curves of Ia, IIIa, and IVa over those of the xenon SDIE curve. The SDIE curve of IIa yields a FWHM value which is in good agreement with the one for the xenon SDIE curve.

The effect of ion source temperature on photoionization efficiency curves and their first derivatives has been investigated. [6,44] The effect of thermal energy upon the dissociation of the parent ions of some alkanes is found to contribute almost fully toward the dissociation. This contribution is observed to produce a shift in the first derivative of the photoionization efficiency curves toward lower energies.[44] It is difficult to make quantitative measurements of the effect ion source temperature has upon the SDIE curves of fragment ions produced from polyatomic molecules. The energy distribution of the electron beam would tend to mask

any thermal effect unless this effect was large. Although the energy distribution of the electron beam may be deconvoluted out of the SDIE curve it is analytically difficult to do so.[45,46] Fragment ions may not have discrete maxima in the SDIE curves but consist of broad maxima,[23] so that a quantitative comparison of the thermal shift of either the half heights or the maxima cannot be made. Fragment ions produced via decomposition of the molecular ions of I, II, and III yield some evidence for the effectiveness of thermal energy in producing dissociation. Increasing the ion source temperature resulted in some broadening in the SDIE curves for most fragment ions resulting from dissociation of Ia, IIa, and IIIa. No apparent broadening was observed in the SDIE curves of Ie, IIIc, and IIIf. Although the above results represent only qualitative evidence for a temperature effect upon the SDIE curves of fragment ions formed via electron impact, it is consistent with the photon impact results obtained for simple hydrocarbons.[6a,44]

Rather than attempting to define exact values of the appearance potentials, the following thermodynamic discussion is directed toward elucidating the details of the lowest energy process. The calculated thermodynamic quantities for the mechanism in Figures 4 - 7, 8a, and 9a listed in Table XI were calculated (Appendix C) from heats of formation of ions, neutral radicals, and neutral molecules.

Concerted rupture of the C-1--C-2 and C_6H_5--C-1 or the XC_6H_4--C-2 bonds in Ia, IIa, IIIa, IVa, and Va (Equations 11 and 12)

TABLE XI

CALCULATED IONIZATION AND APPEARANCE POTENTIALS FOR SUBSTITUTED BENZILS

Ion	m/e	I.P.(A.P.), eV R = p-CH_3	m/e	I.P.(A.P.), eV R = p-OCH_3	m/e	I.P.(A.P.), eV R = m-CF_3
m^+	224	8.61 ± 0.17	240	8.10 ± 0.11	278	8.83 ± 0.61
$m^+ - C_7H_5O$	119	9.73 0.10	135	9.22 0.14	173	9.96 0.60
$m^+ - RC_7H_4O$	105	10.02 0.17	105	10.05 0.18	105	9.77 0.75
$RC_7H_4O^+ - CO$	91	11.37 0.52	107	13.14 0.35	145	13.87 0.88
		10.37 0.47				
$C_7H_5O^+ - CO$	77	13.95 0.66	77	13.96 0.66	77	13.68 0.98

represent an alternative to the one-bond-rupture mechanism given in Figure 4, vide supra, for formation of $C_6H_5^+$ and $XC_6H_4^+$.

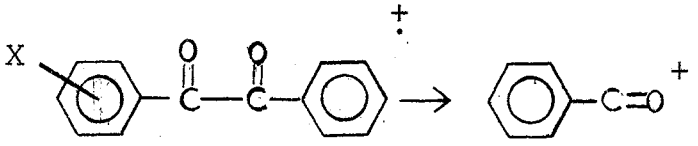

$$+ \; CO + XC_6H_4 \qquad (11)$$

X = H, p-CH_3, p-OCH_3, m-CF_3

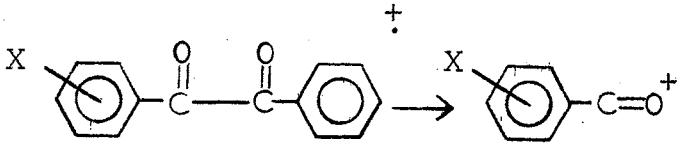

$$+ \; CO + C_6H_5 \qquad (12)$$

X = H, p-CH_3, p-OCH_3, m-CF_3

Table XII tabulates the calculated appearance potentials for the one- and two-bond-rupture mechanisms. Figures 20a-b, 21a-b, and 22a-b are the SDIE curves for Ib, IIb, IIIb and IVb at two values of the ion source temperature. Figures 23 and 24 are the SDIE curves for IVb and Vb at one source temperature. These curves rise slowly with increasing internal energy of the molecular ion and, hence, the appearance potentials are not well defined. Points of inflection occur in all the m/e 105 SDIE curves below the first local maxima. The first local maxima in these curves cannot reasonably be the appearance potentials since the estimated width at half height is from 4-6 eV.

The SDIE curves for Ic, IIc, and IIIc at two values and Vc at one value of the ion source temperature are given in Figures 25a-b, 26a-b, 27a-b and 28a. The first local maxima in Figures 25a-b for Ic may

TABLE XII

CALCULATED APPEARANCE POTENTIALS FOR Ib, Ic, IIb, IIc, IIIb, AND IIIc CORRESPONDING TO ONE AND TWO-BOND RUPTURE

Ion	One-Bond-Rupture A.P., eV	Two-Bond-Rupture A.P., eV
Ib	10.02 ± 0.17	10.86 ± 0.22
Ic	9.73 ± 0.18	10.58 ± 0.23
IIb	10.05 ± 0.18	10.89 ± 0.23
IIc	9.22 ± 0.14	10.07 ± 0.20
IIIb	9.77 ± 0.75	10.61 ± 0.76
IIIc	9.96 ± 0.60	10.80 ± 0.63

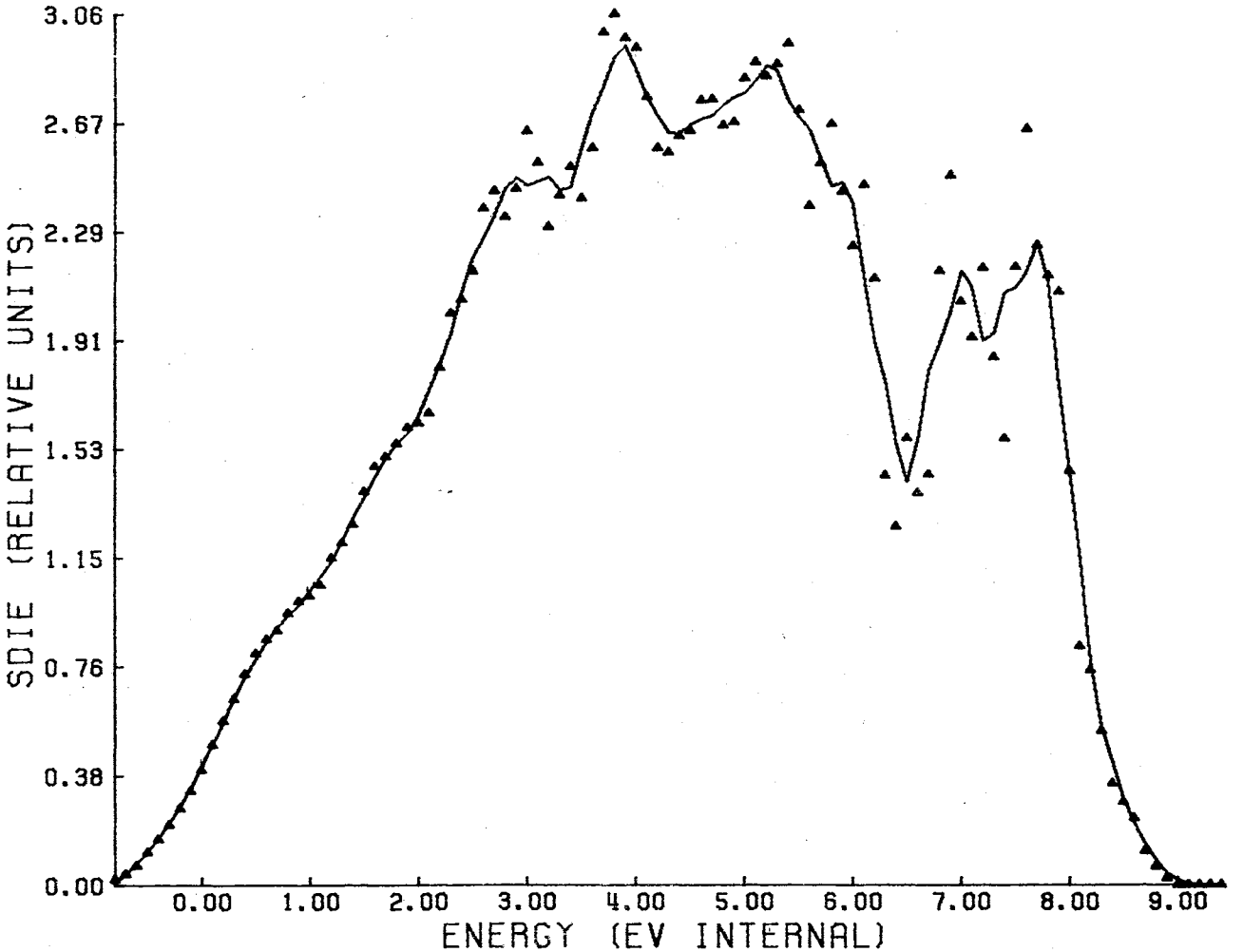

Figure 20a. SDIE Curve of Ib, 0.00 = 9.05 eV, 310° Ion Source Temperature

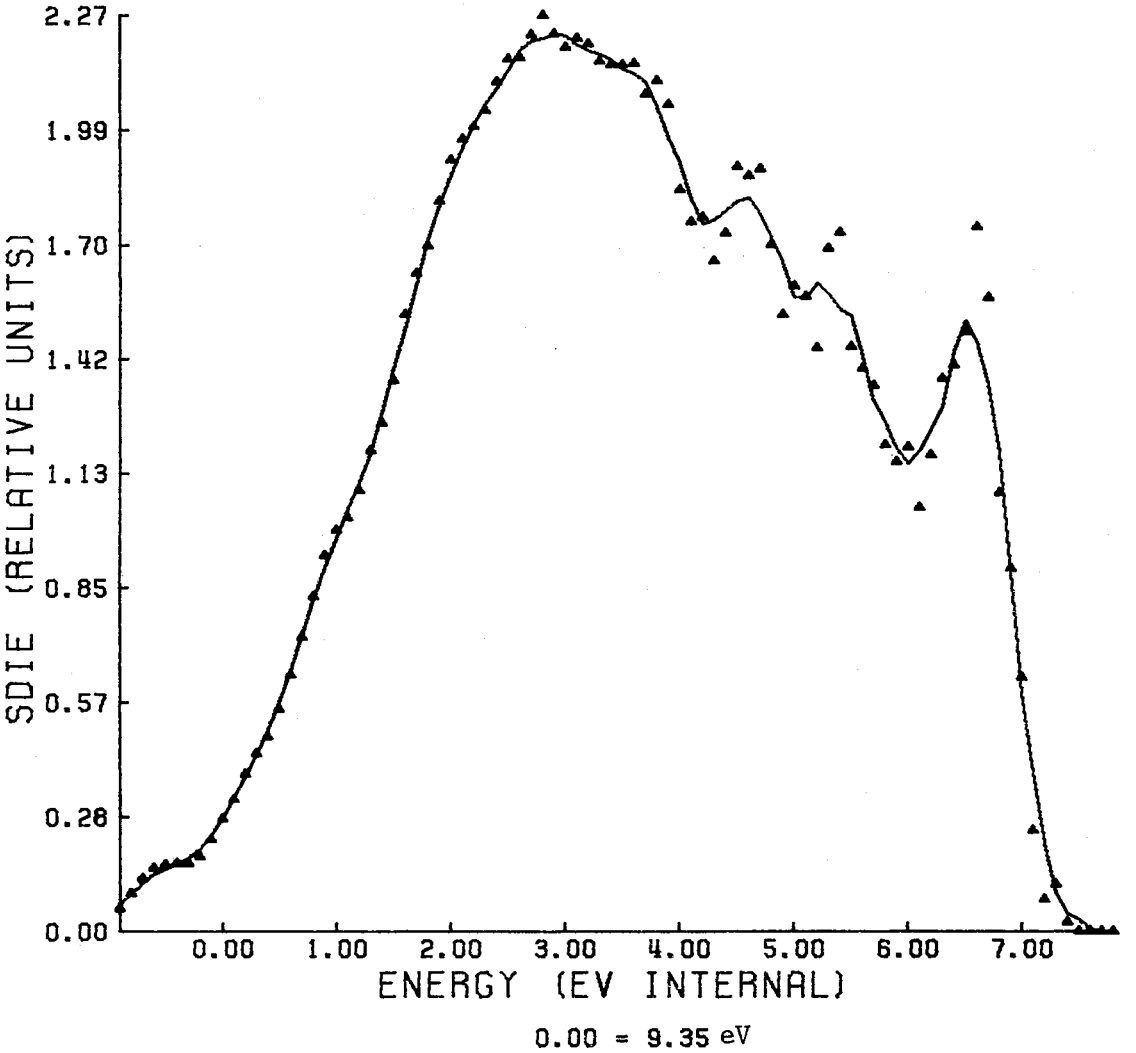

Figure 20b. SDIE Curve of Ib, 230° Ion Source Temperature

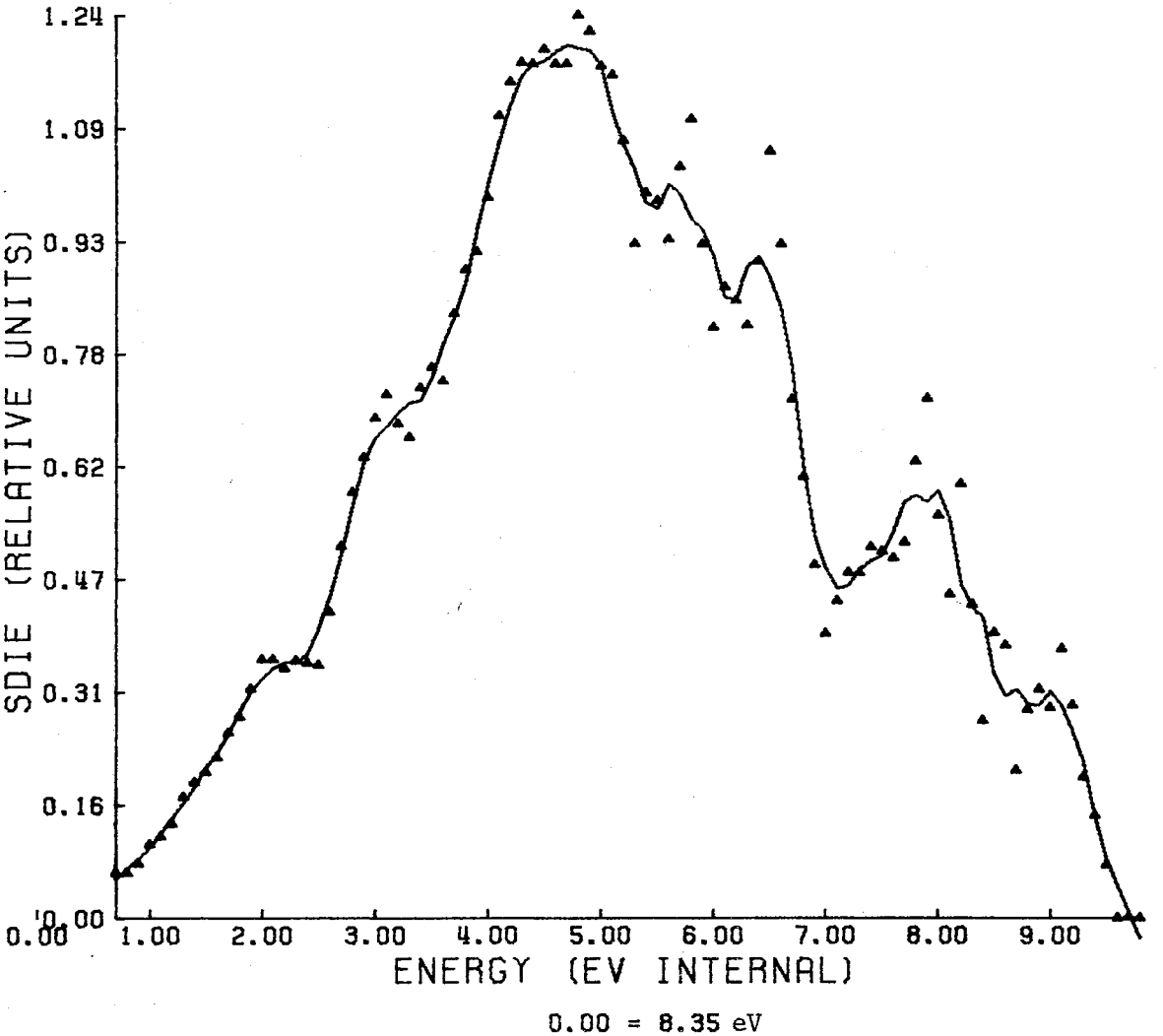

Figure 21a. SDIE Curve of IIb, 310° Ion Source Temperature

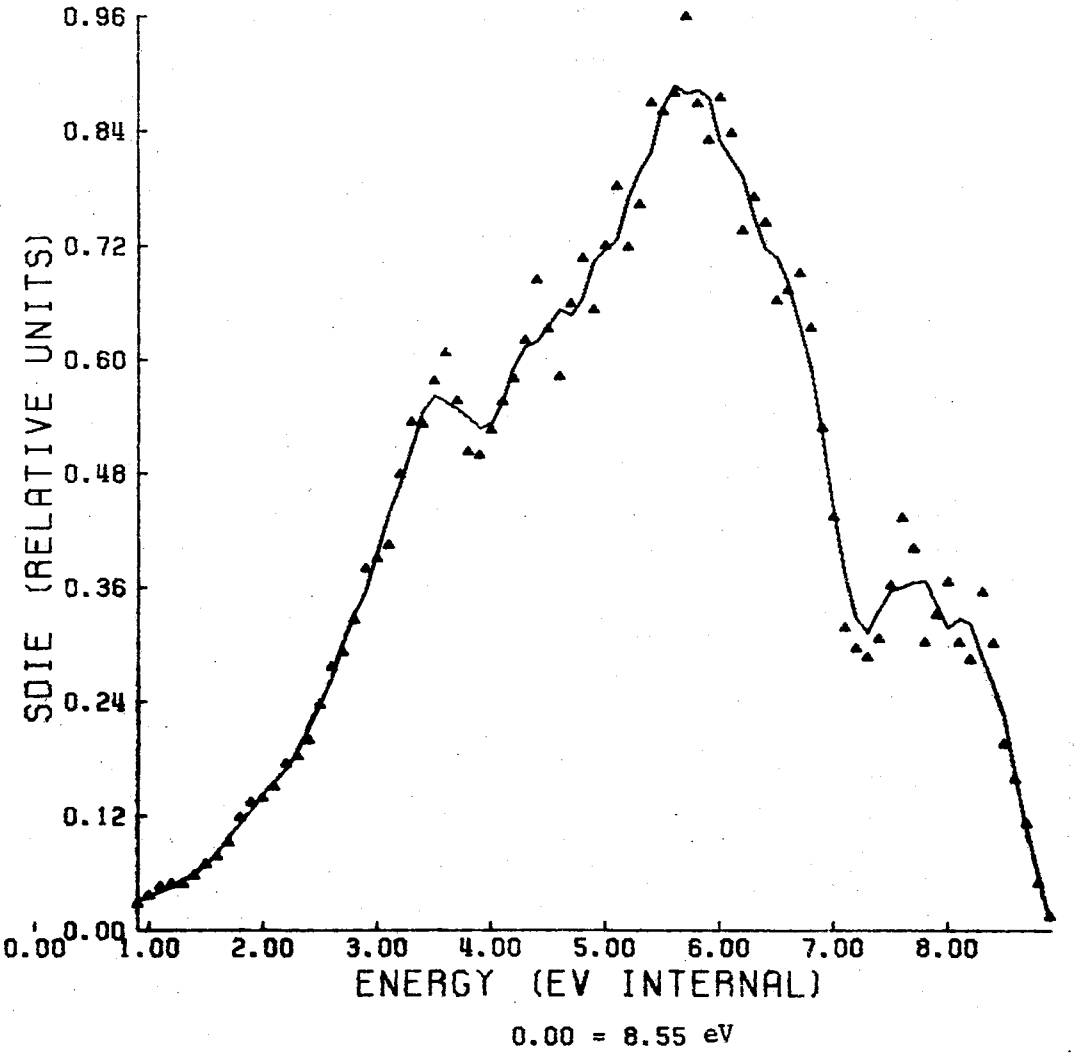

Figure 21b. SDIE Curve of IIb, 250° Ion Source Temperature

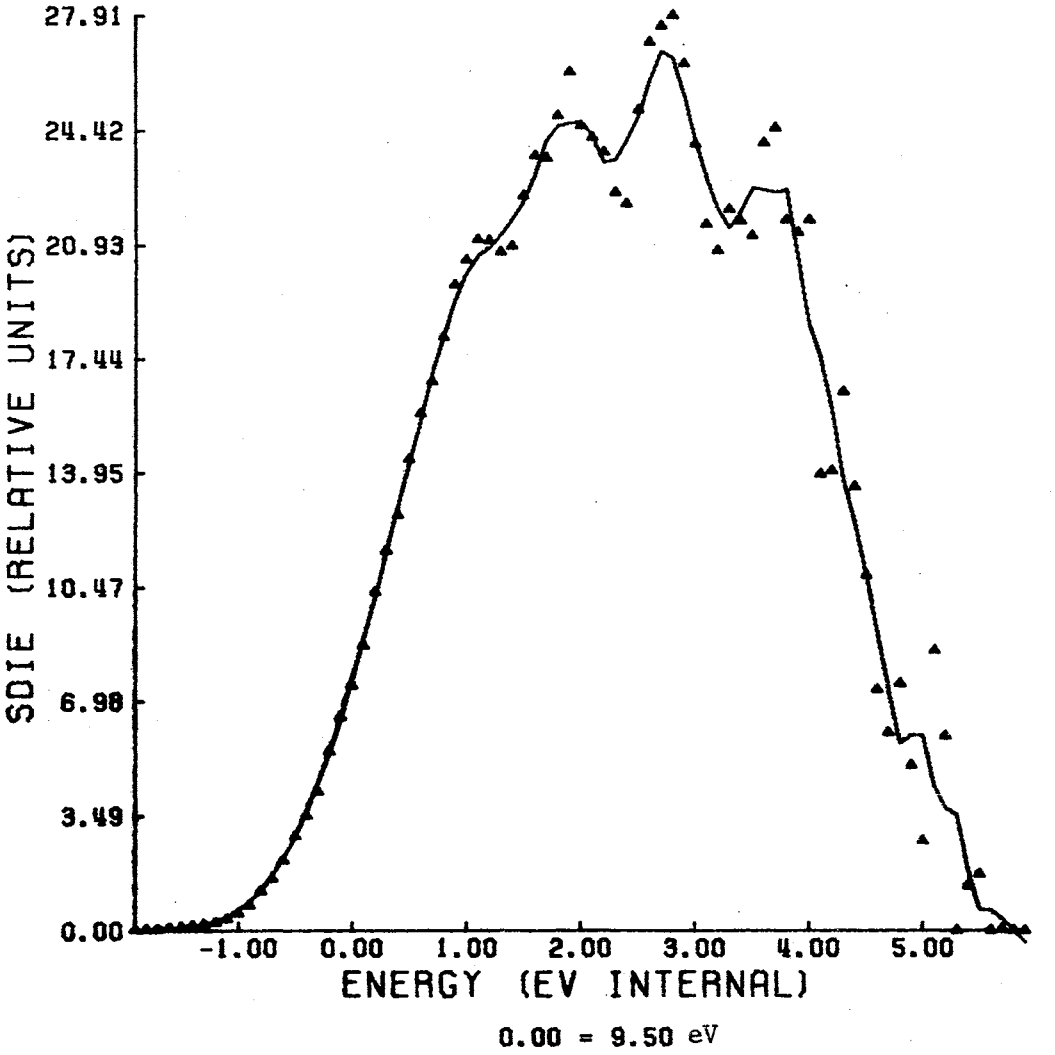

Figure 22a. SDIE Curve of IIIb, 310° Ion Source Temperature

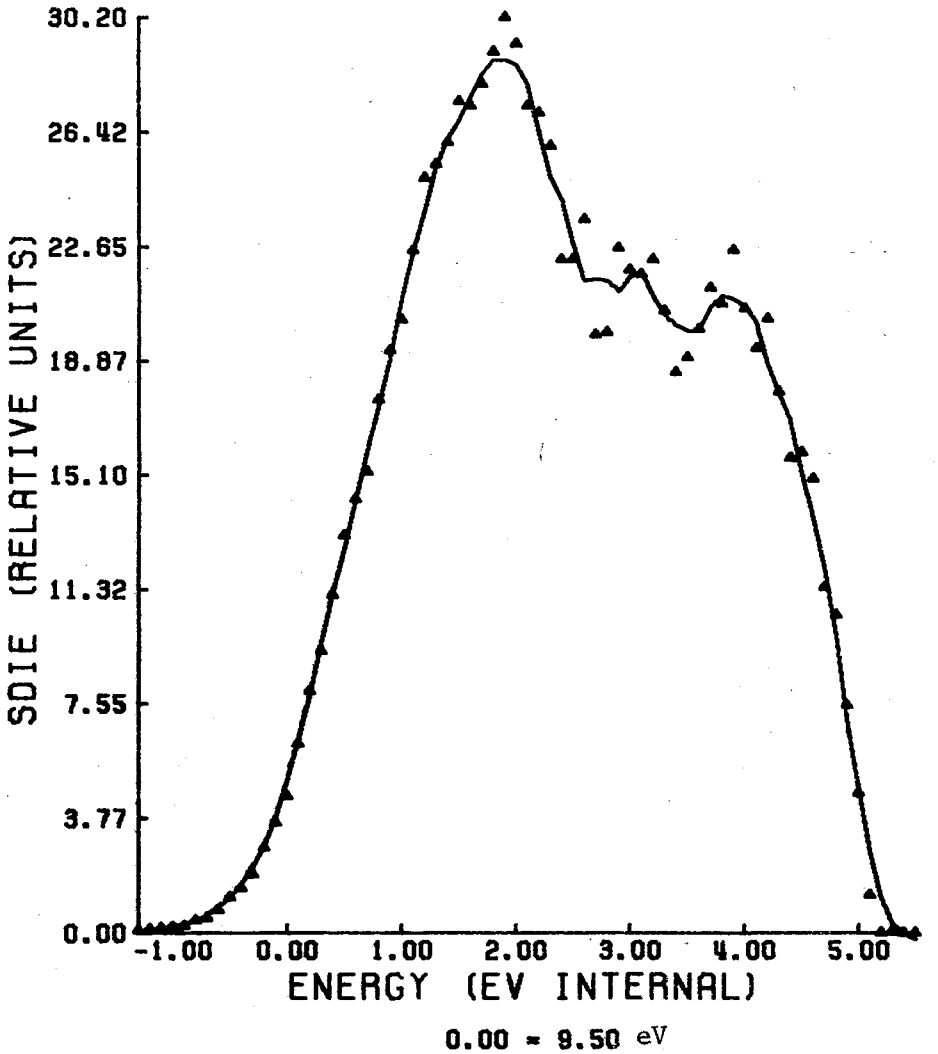

Figure 22b. SDIE Curve of IIIb, 250° Ion Source Temperature

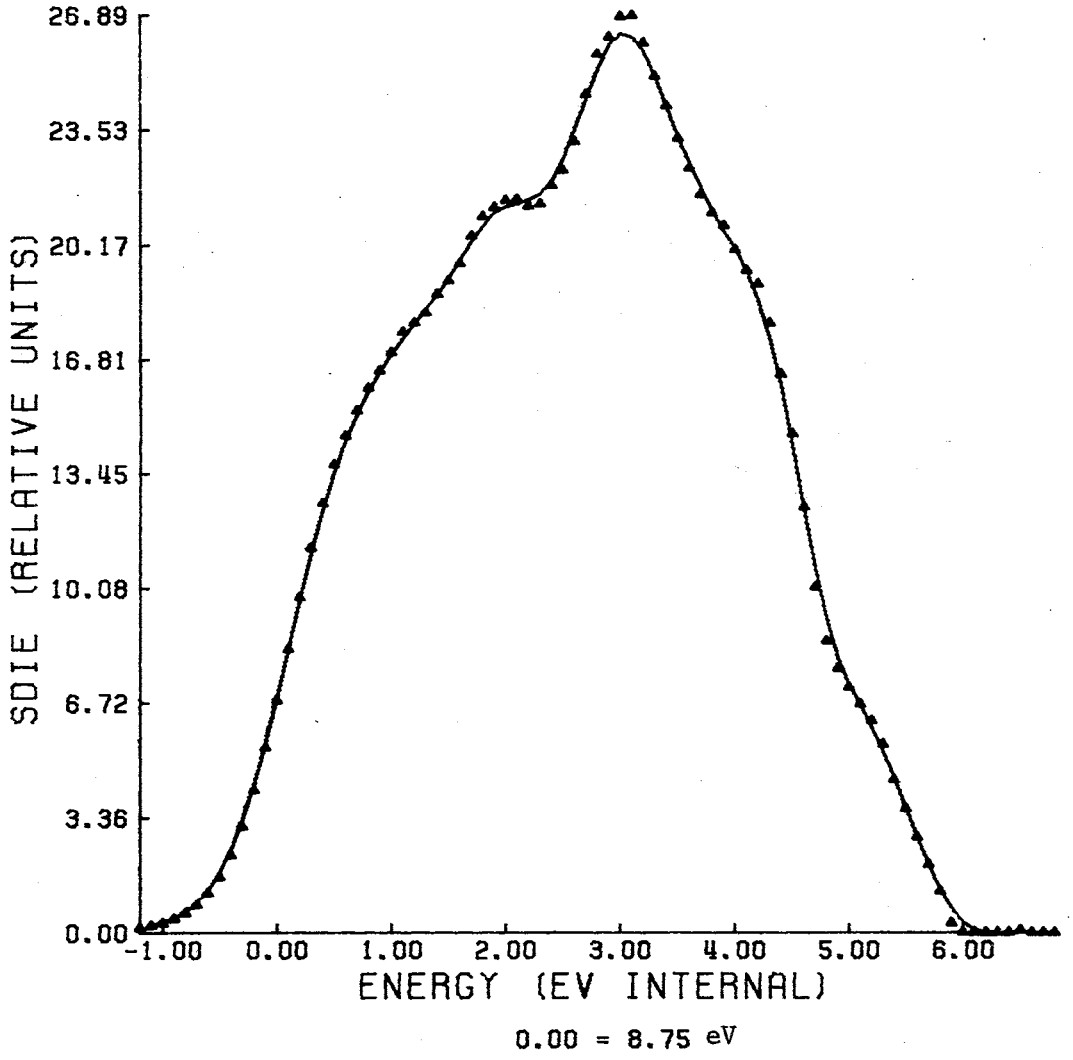

Figure 23. SDIE Curve of IVb, 250° Ion Source Temperature

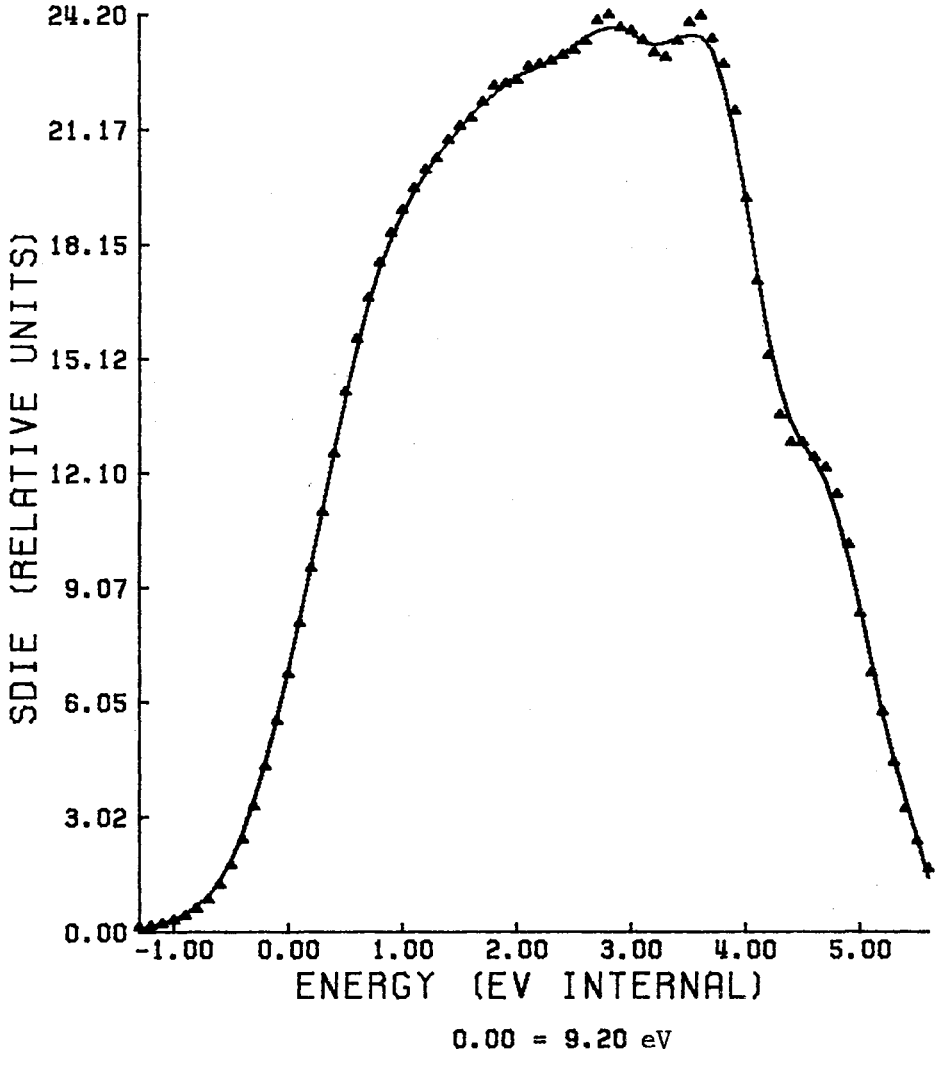

Figure 24. SDIE Curve of Vb, 250° Ion Source Temperature

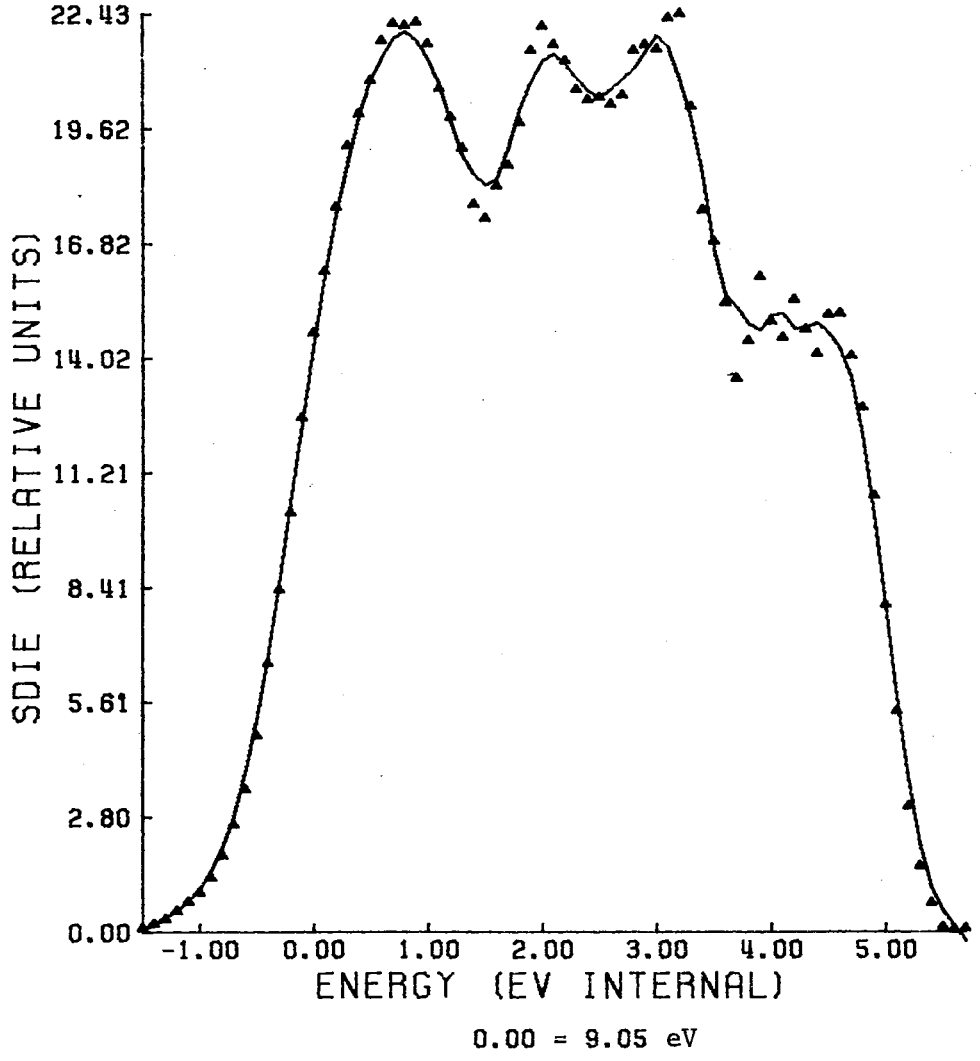

Figure 25a. SDIE Curve of Ic, 310° Ion Source Temperature

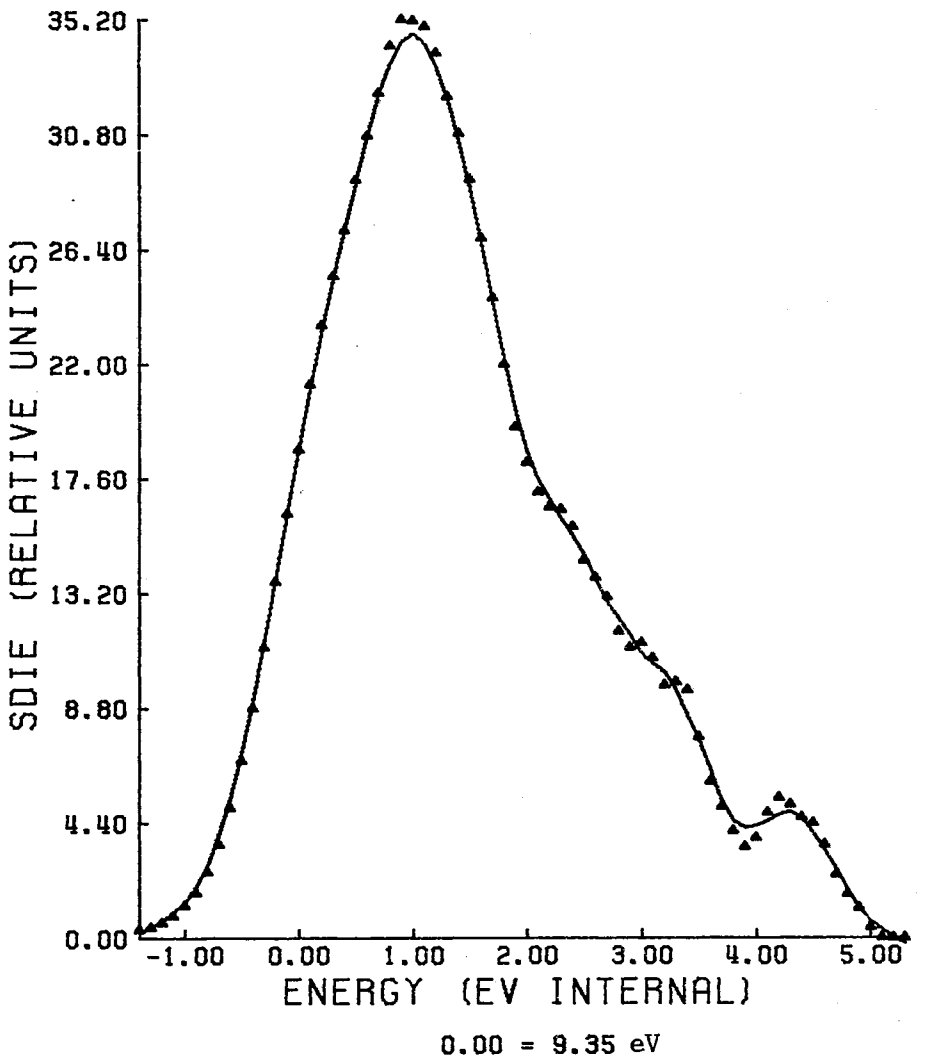

Figure 25b. SDIE Curve of Ic, 230° Ion Source Temperature

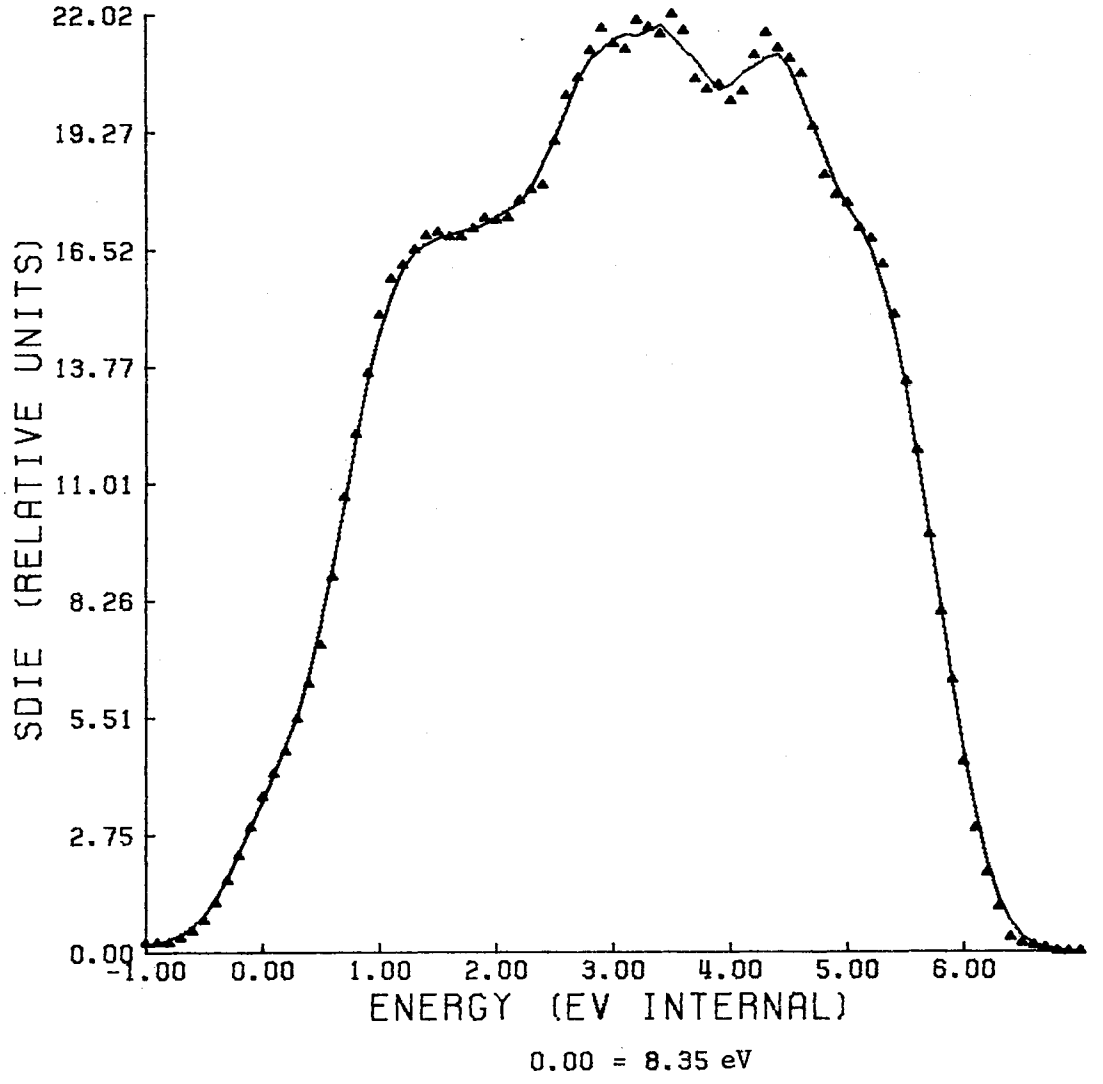

Figure 26a. SDIE Curve of IIc, 310° Ion Source Temperature

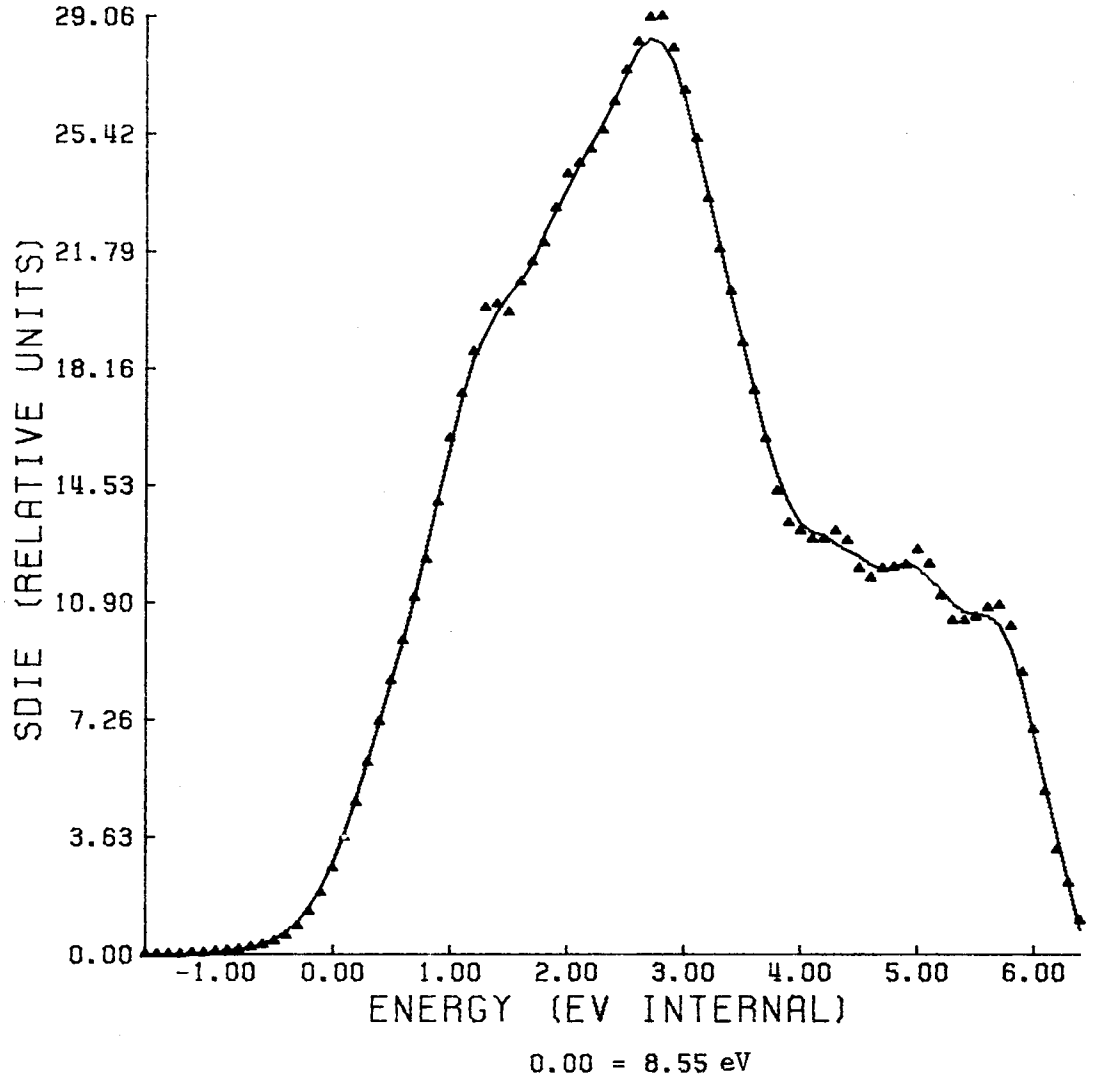

Figure 26b. SDIE Curve of IIc, 250° Ion Source Temperature

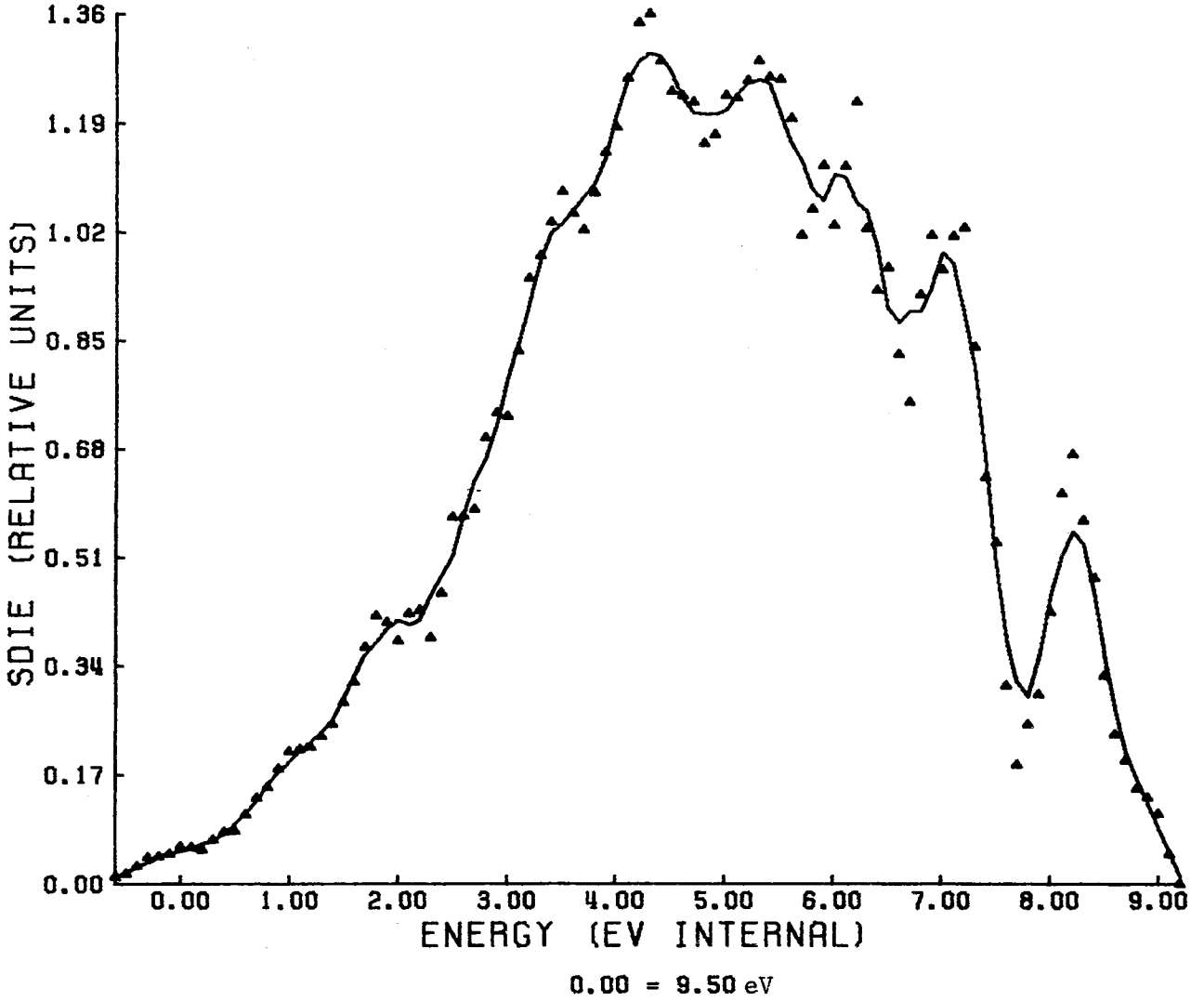

Figure 27a. SDIE Curve of IIIc, 310° Ion Source Temperature

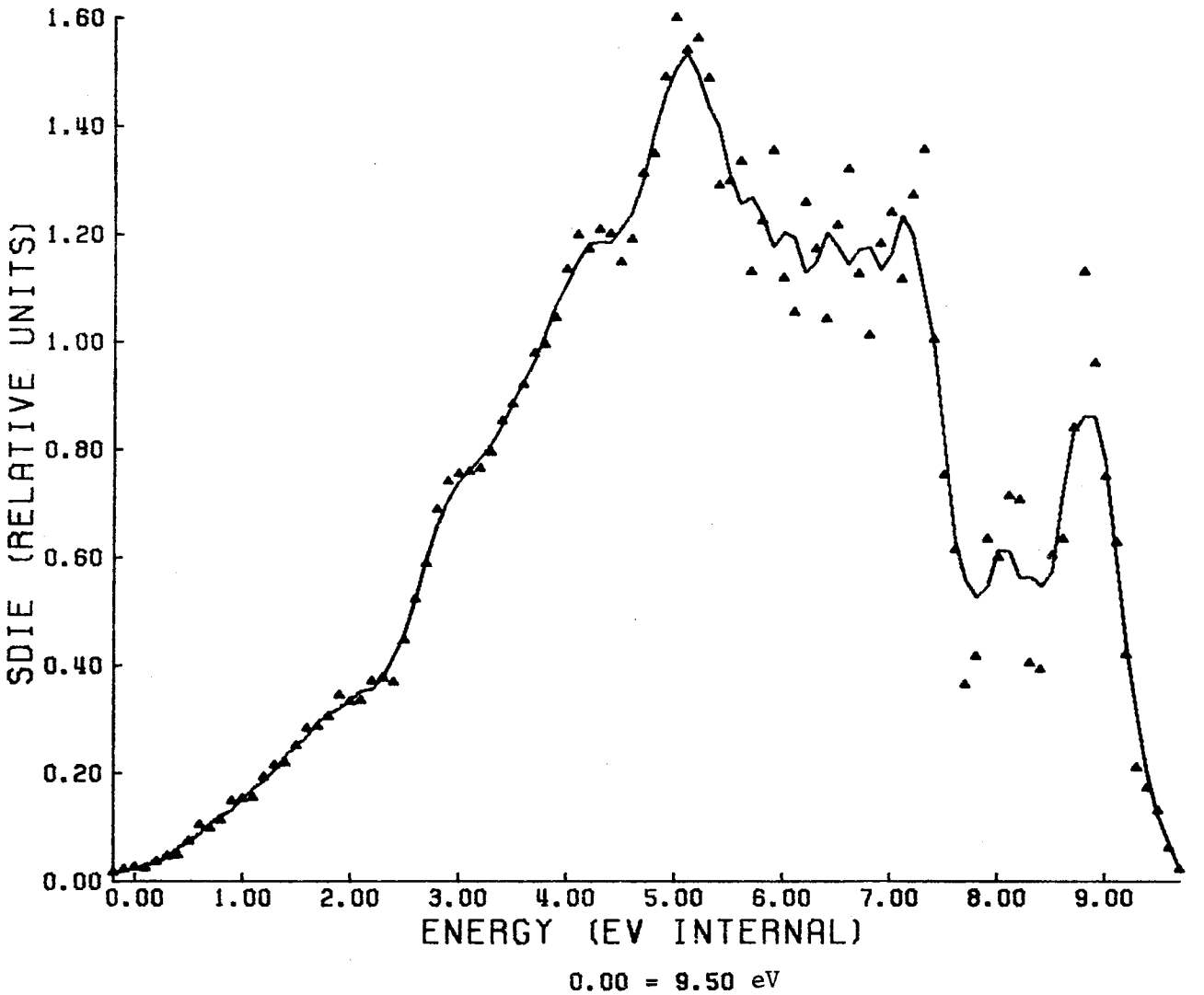

Figure 27b. SDIE Curve of IIIc, 250° Ion Source Temperature

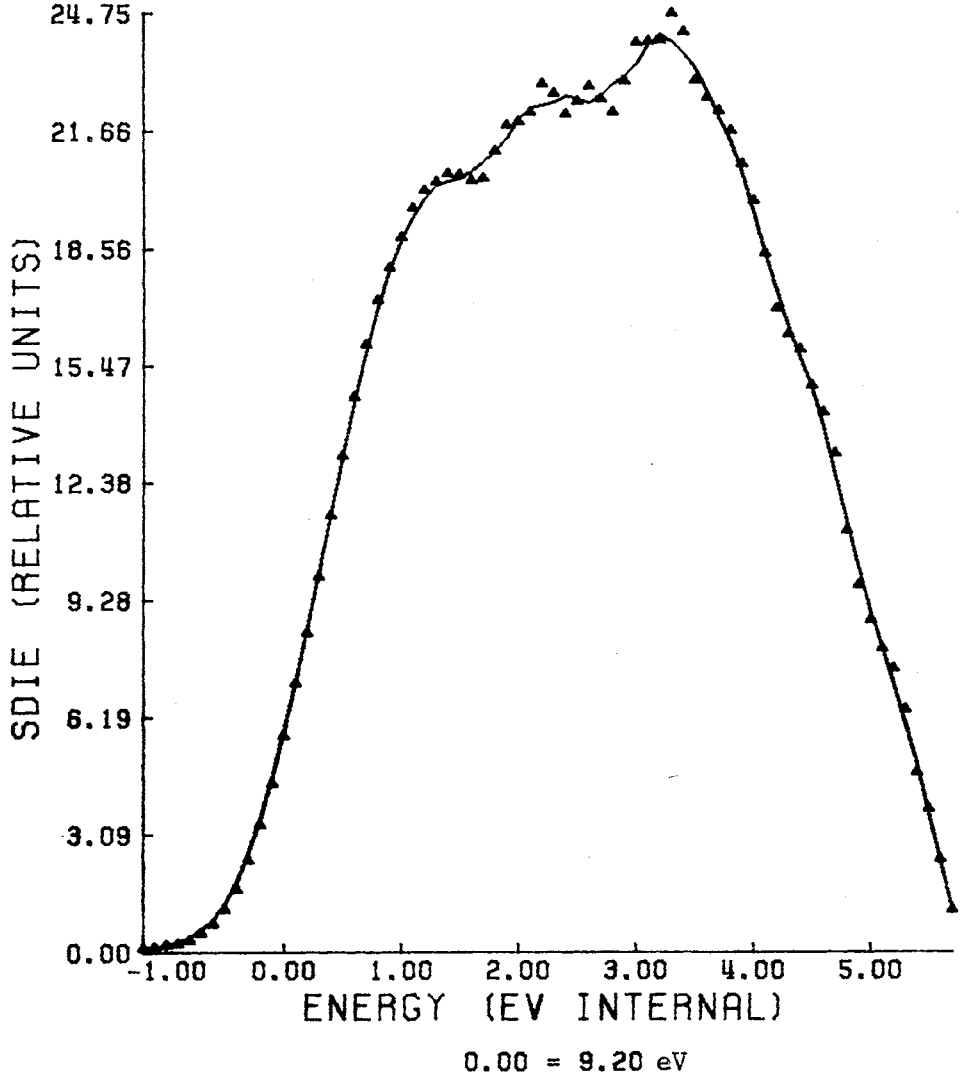

Figure 28a. SDIE Curve of Vc, 250° Ion Source Temperature

reasonably represent the appearance potential. At source temperatures of 230° and 310° values of 10.15 and 9.84 respectively are obtained. The SDIE curves of IIc and IIIc have points of inflection prior to the first local maximum. The SDIE curve of Vc has no inflection point prior to the first maximum at 10.6 eV.

The appearance potential data for the benzoyl and substituted benzoyl ions seem at least in part consistent with the central C-1--C-2 bond cleavage mechanism in Figure 4. For the SDIE curves for which an appearance potential could not be assigned there were points of inflection below the first local maxima which are in the range of the calculated appearance potentials for one-bond rupture. The results obtained by Franklin[34] for IVb by a similar analysis offer further support for a one-bond-rupture mechanism.

The SDIE curves for IIIf (m/e 259) corresponding to loss of fluorine atom from IIIa are presented in Figures 28b-c. At both ion source temperatures of 310° and 250° there is a maximum centered at 12.65 - 12.85 eV. Under these conditions a second maximum is located at 14.9 - 15.0 eV. It is interesting to note that these maxima are resolved and separated by ca. 2.25 eV.

The SDIE curves of Ie, IIe, and IIIe (Figures 29-31) all exhibit low energy tails and then rise sharply to a maximum. The calculated appearance potentials in Table XII give values of 13.14 eV for IIe and 13.87 eV for IIIe. Calculation of the appearance potential for Ie using $\Delta H(C_7H_7^+)$ from toluene and from the cycloheptratrienyl radical gave

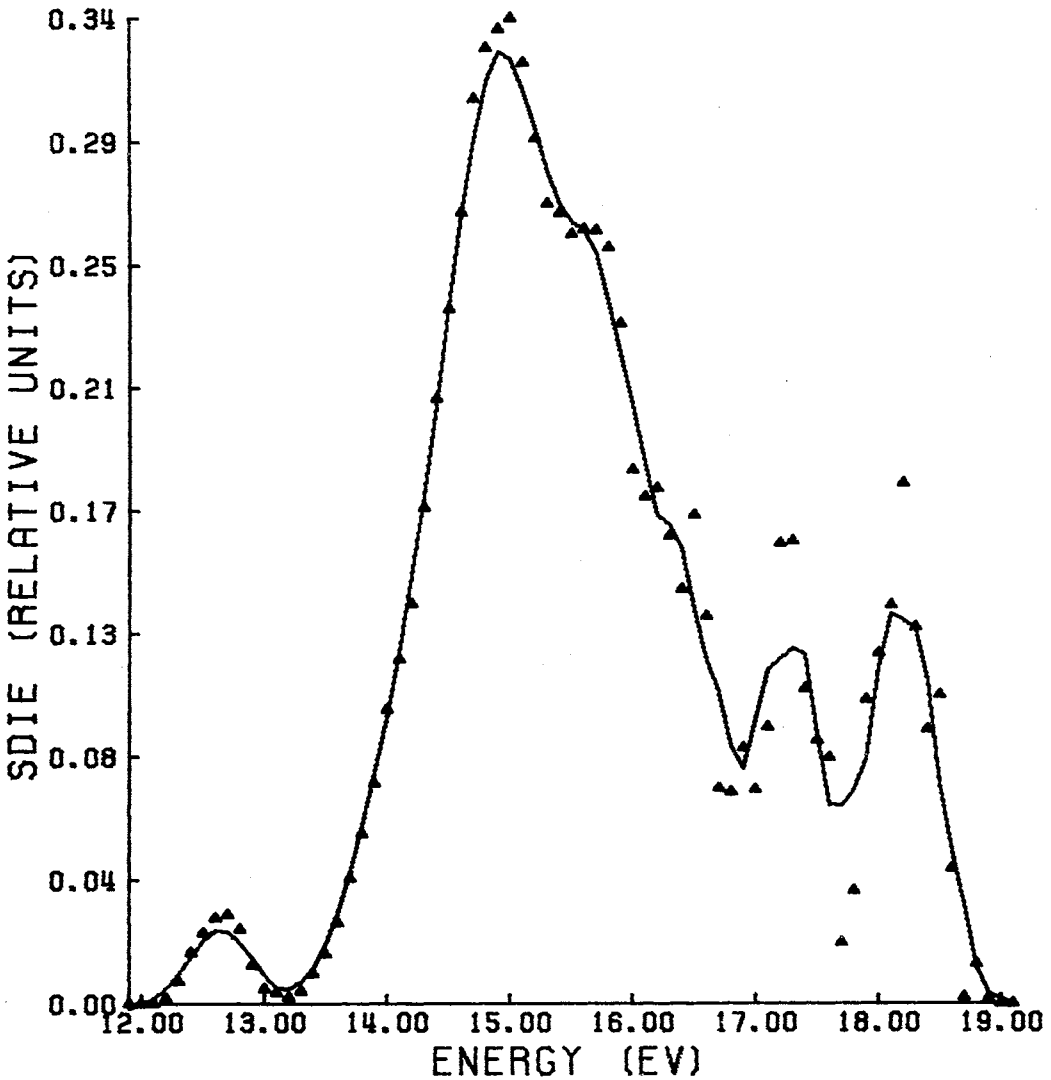

Figure 28b. SDIE Curve of IIIf, 310° Ion Source Temperature

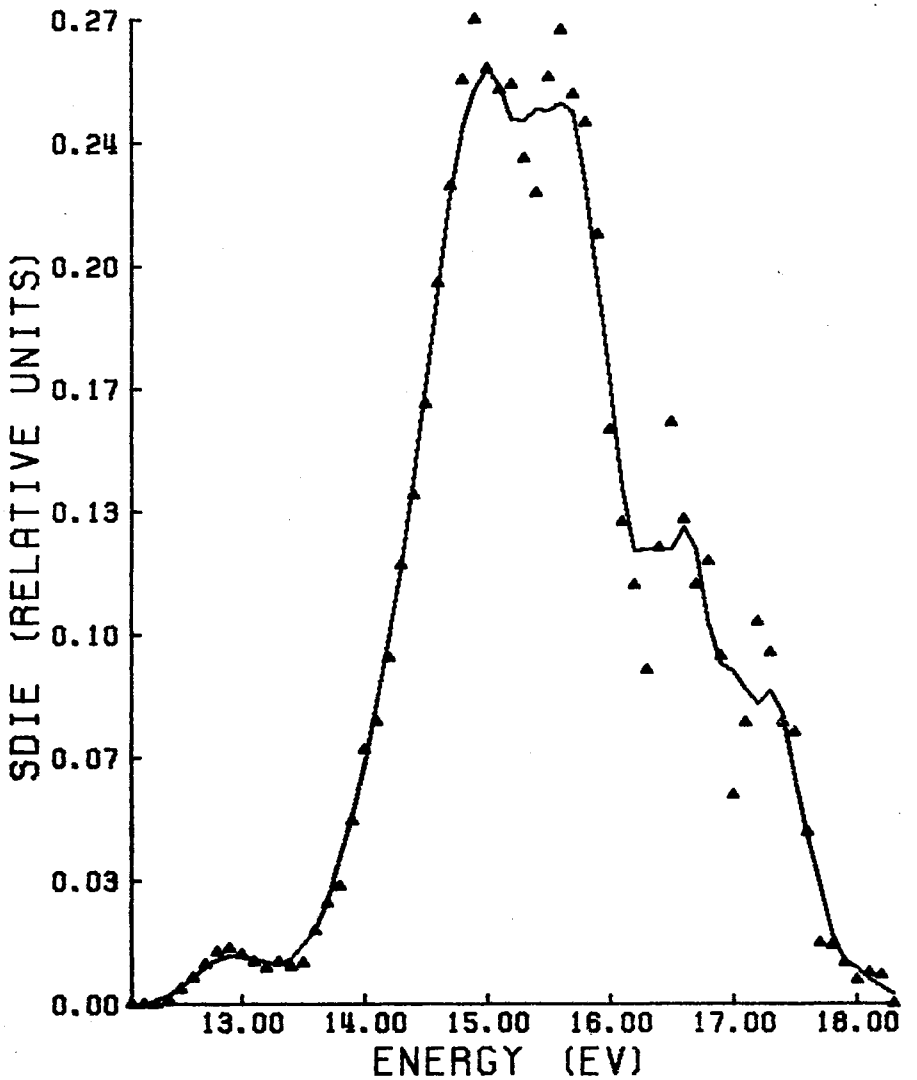

Figure 28c. SDIE Curve of IIIf, 250° Ion Source Temperature

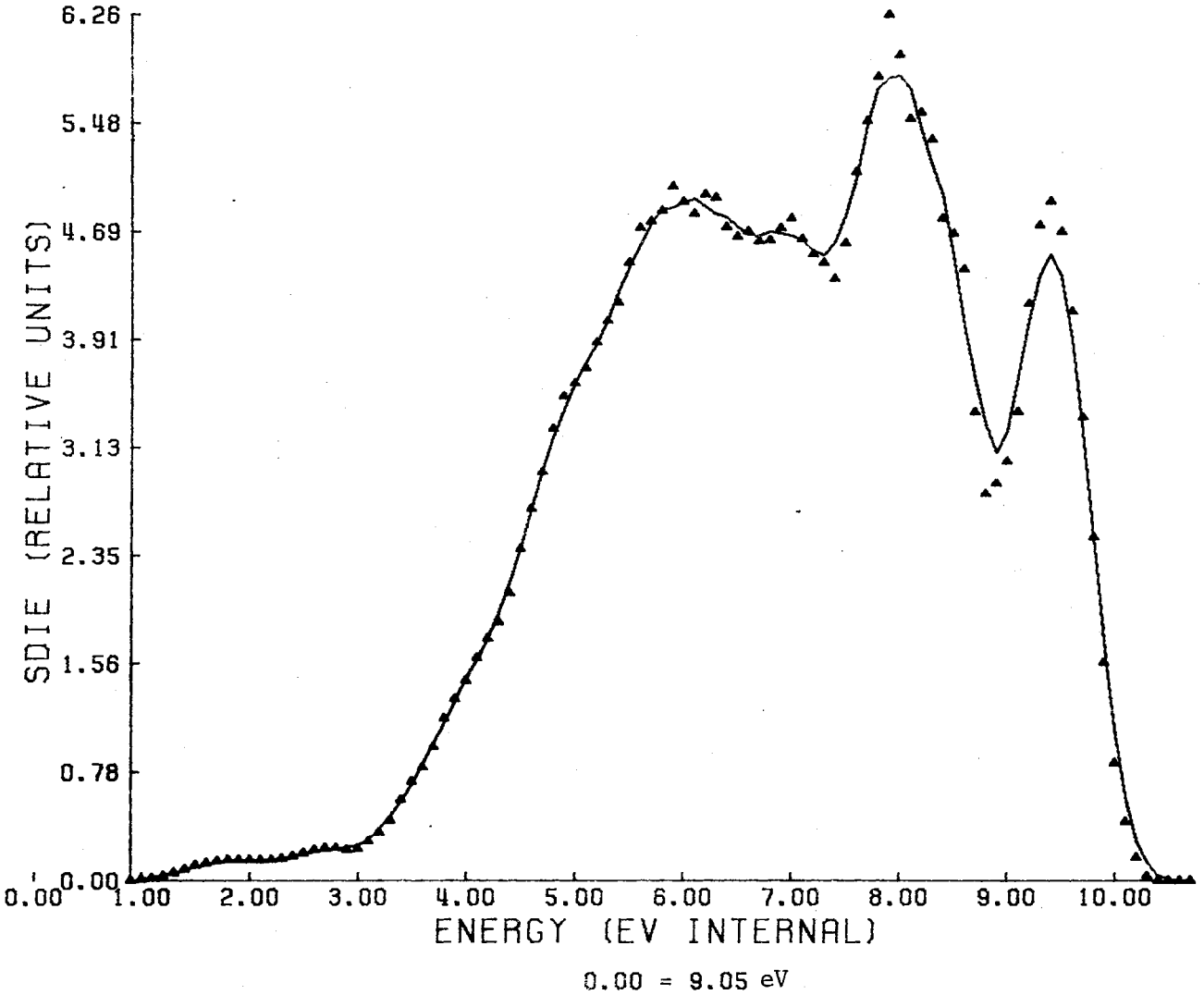

Figure 29a. SDIE Curve of Ie, 310° Ion Source Temperature

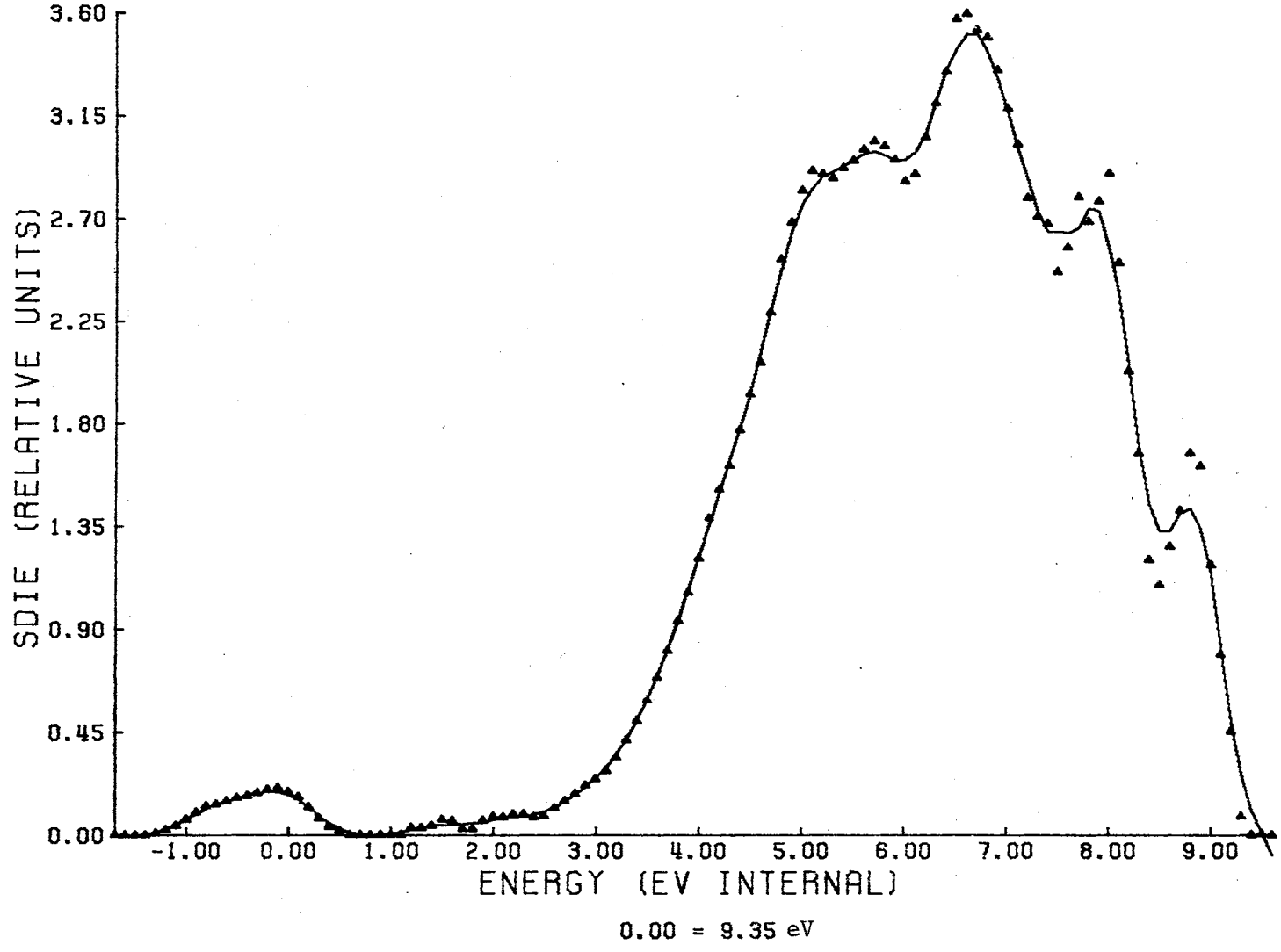

Figure 29b. SDIE Curve of Ie, 230° Ion Source Temperature

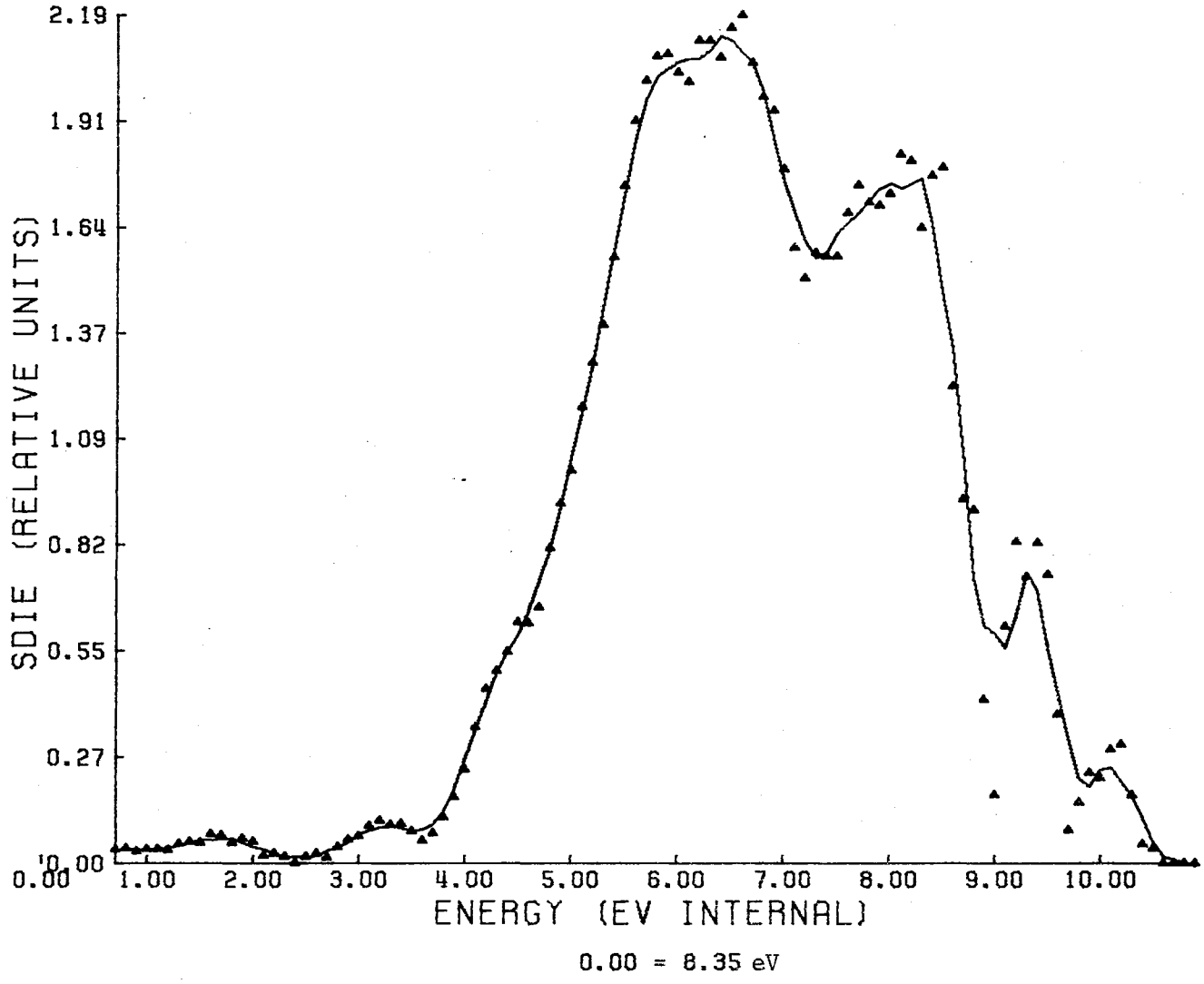

Figure 30a. SDIE Curve of IIe, 310° Ion Source Temperature

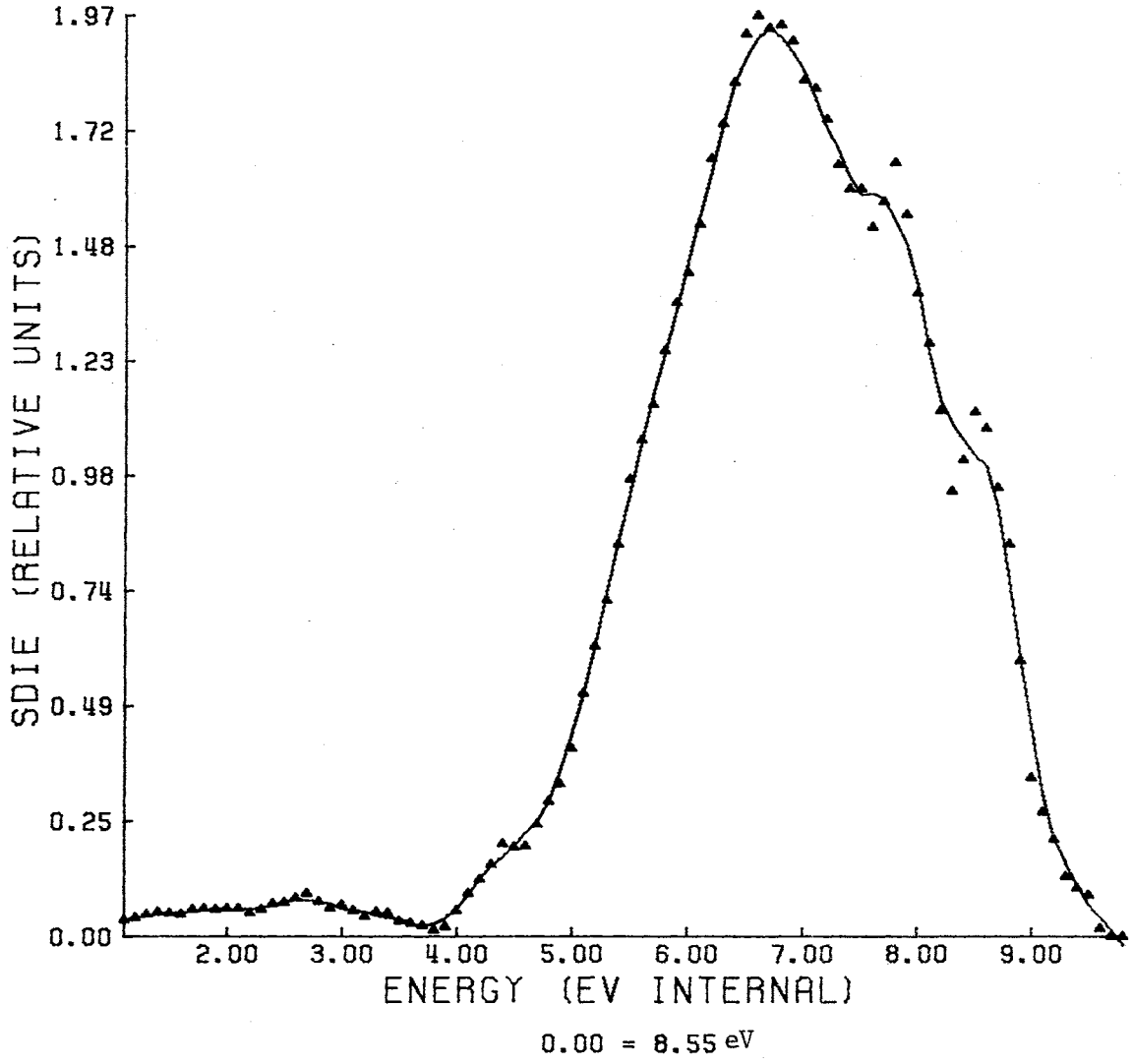

Figure 30b. SDIE Curve of IIe, 250° Ion Source Temperature

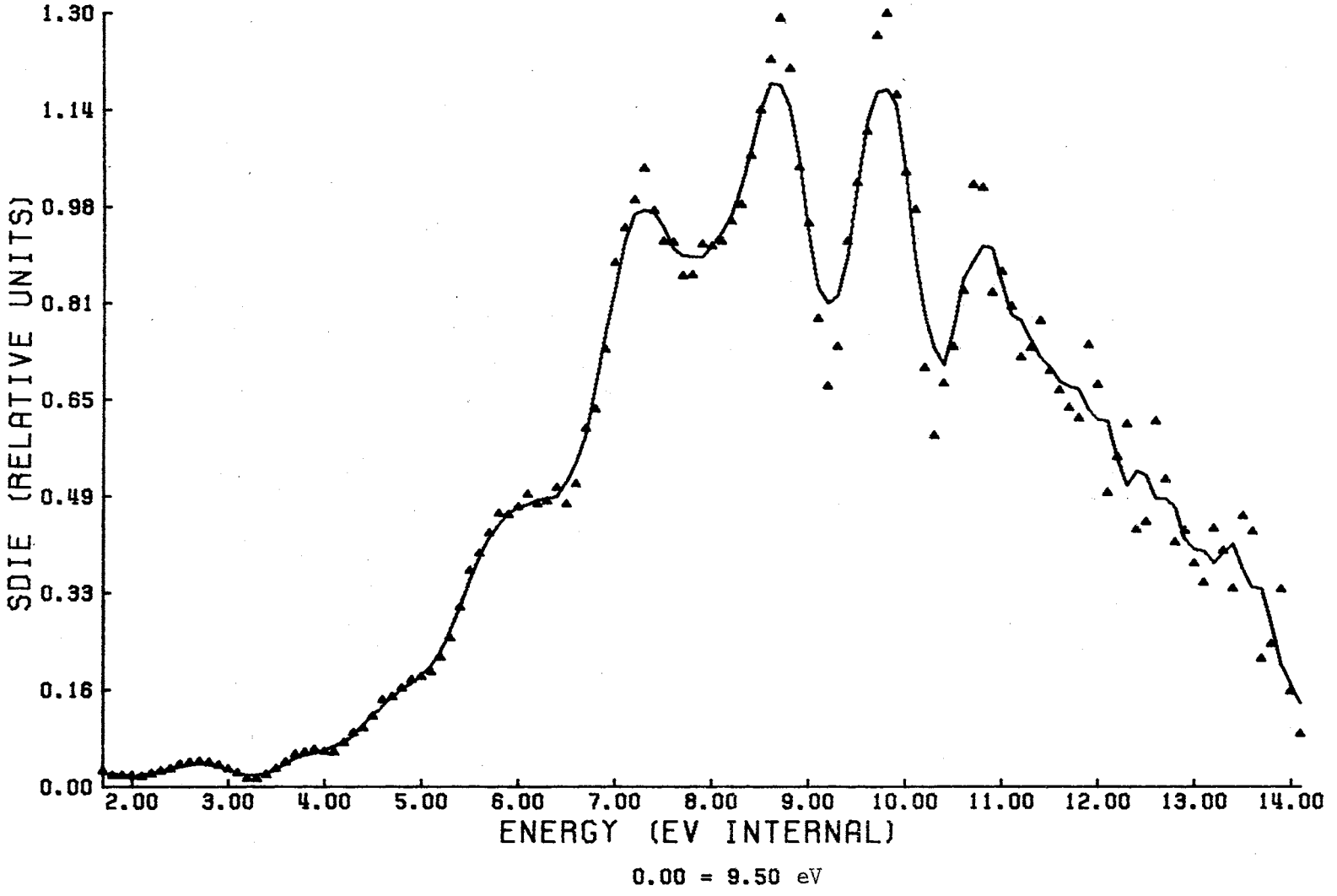

Figure 31a. SDIE Curve of IIIe, 310° Ion Source Temperature

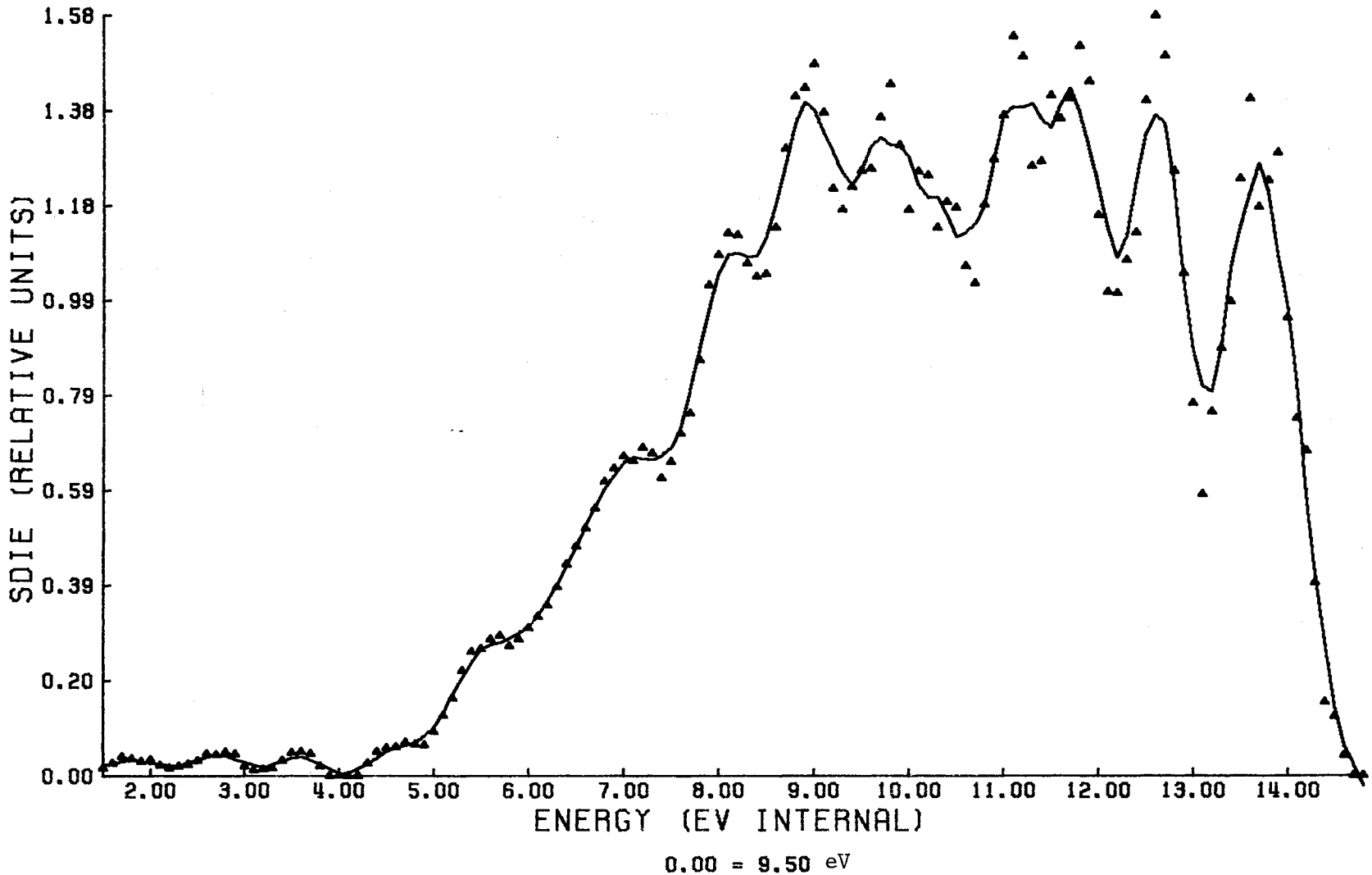

Figure 31b. SDIE Curve of IIIe, 250° Ion Source Temperature

values of 11.37 and 10.37 respectively. The SDIE curve for Ve, (Figure 32) has an inflection point at 15.0 - 15.3 eV, which is in good agreement with the A.P. for m/e 77, from IVb, of 15.12 eV.[34]

Upon decomposition of the molecular ion excess energy present will be distributed between the fragment ions. In the case of the substituted benzil molecular ions undergoing C-1--C-2 bond rupture, the excess energy will be partitioned almost equally between the (substituted) benzoyl radicals and the (substituted) benzoyl ions. In order for the (substituted) benzoyl ions to fragment further, the necessary excess energy must be present in the molecular ion. Therefore, the long tail in the SDIE curves of Ie, IIe, IIIe and Ve are consistent with the suggestion[47] that there are wide statistical fluctuations about the mean value of the excess energy partitioned upon ion decomposition.

The loss of CO from the 4-methylbenzoyl ion, Ic, is of mechanistic interest since it may proceed via two possible mechanisms having different energy requirements. Assuming that the $C_7H_7^+$ ion has the tropylium ion structure[48] the fragmentation reaction requires ring expansion prior to, during, or after loss of CO. Although the heat of formation (ΔH_f) of the 4-methylphenyl cation is unknown, ΔH_f of $C_6H_5^+$ is at least 50 kcal/mole in excess of that for the C_7H_7 cation formed from toluene.[49] The replacement of a para-hydrogen by a methyl should not decrease the ΔH_f of the C_6H_5 cation by more than 15 kcal/mole. Thus the pathway which is most energetically favored would consist of ring expansion prior to or during dissociative loss of CO. Formation of the

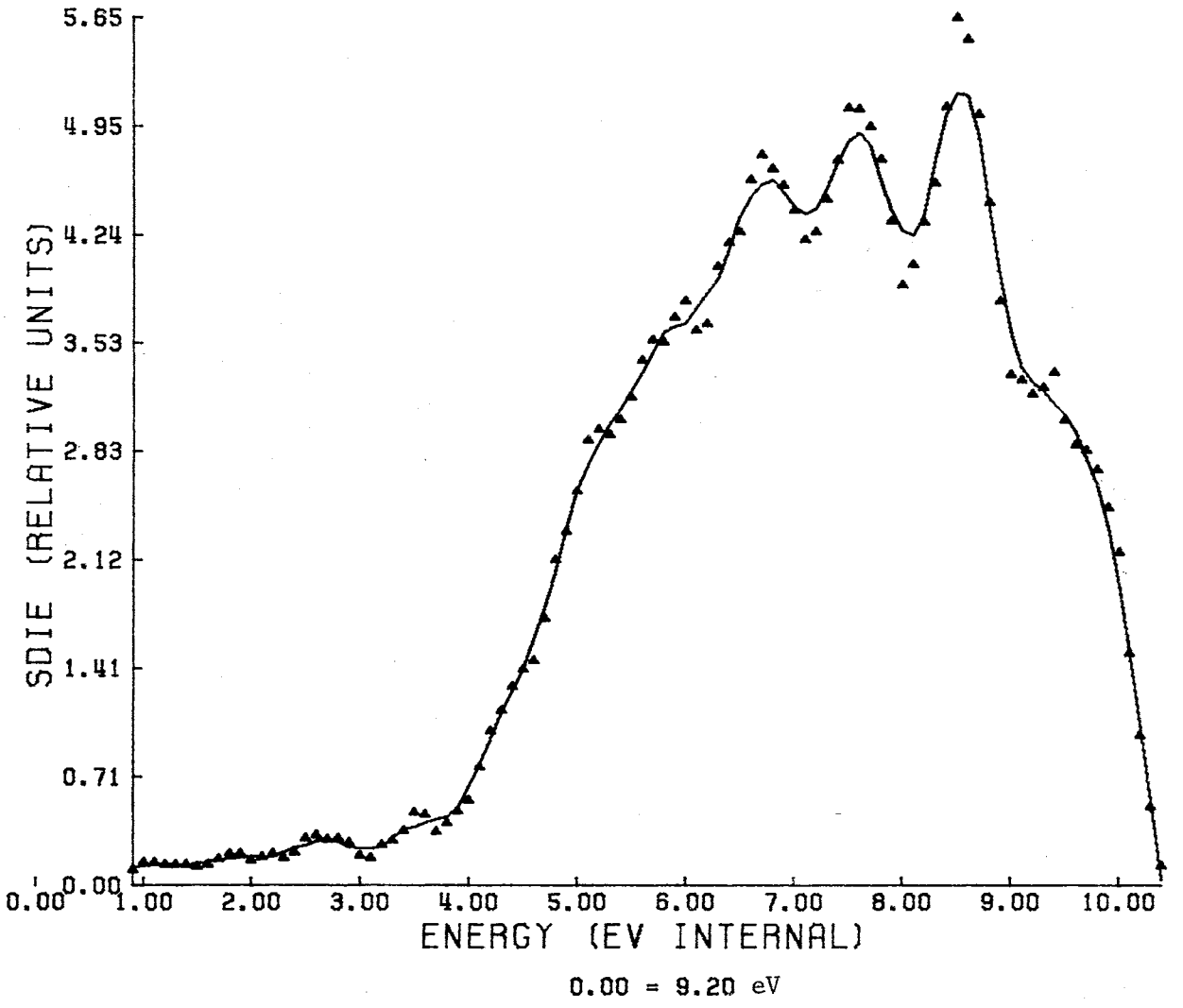

Figure 32. SDIE Curve of Ve, 250° Ion Source Temperature

tropylium ion structure from Ie would require insertion of the exocyclic carbon in the six-membered ring accompanied by the migration of two hydrogens (Equation 13). The energy necessary for the rearrangement to occur must be derived from the excess energy initially present in the molecular ion.

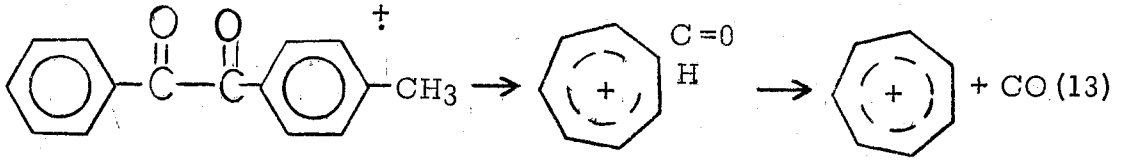

A broad Gaussian metastable ion centered at 69.6 was observed for the formation of Ie. Measurements on the LKB 9000 and on the CEC 21-110-B both show provisional evidence for a broad flat-top peak superimposed on the high mass side of and having only 5-10 per cent of the intensity of the normal metastable ion. The metastable peak was intense enough to permit measurement of the SDIE curve. As seen in Figure 33 the SDIE curve is qualitatively consistent with the SDIE curve obtained for Ie (Figure 29a). The rapid decrease in the SDIE curve at high energy is a direct result of premature termination of the FDIE curve due to excessive noise.

There is some evidence[49] that the structure of IIe is not necessarily that of a p-methoxyphenyl cation but is one that permits stabilization of the incipient charge during the fragmentation. This argument is based upon the deviation of the appearance potential of the p-methoxyphenyl cation, obtained from dissociative ionization of p-chloroanisole, from

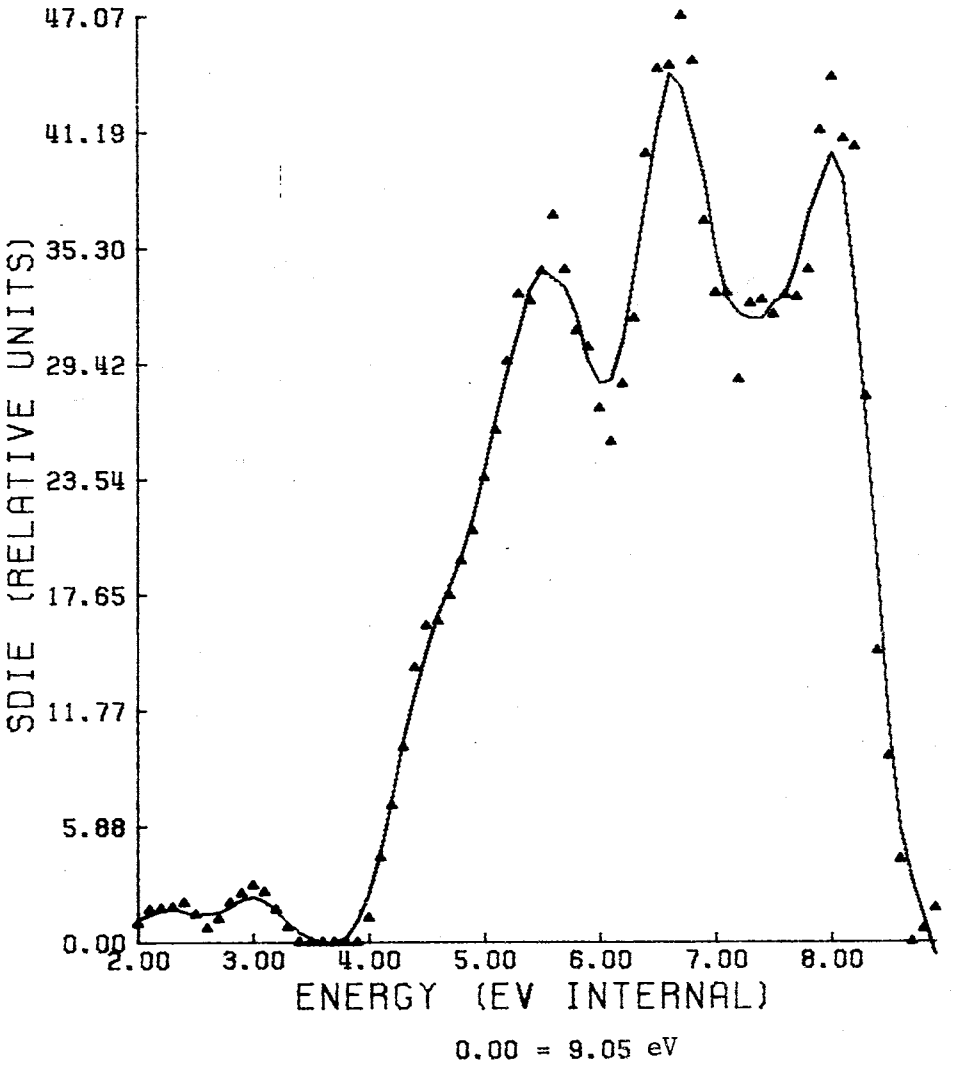

Figure 33. SDIE of Metastable Ic, 310°

the line established by the appearance potentials of other $RC_6H_4^+$ ions when these potentials are plotted versus their substituent constants. From the present data for IIe and IIIe it is not possible to infer the structure of these ions.

Harrison[49] points out that the structure of the C_6H_5 cation formed via loss of CO from the benzoyl ion in the mass spectrum of benzaldehyde and acetophenone may be acyclic. The SDIE curves obtained for Id, IId, IIId, IVc, and Vd resulting from loss of CO from Ib, IIb, IIIb, IVb, and Vb are given in Figures 34-38. Although the SDIE curves show no well defined appearance potential, these curves are not necessarily inconsistent with the calculated A.P. values in Table XI for the following reasons. First, the FWHM values of the first local maxima in the SDIE curves of Id, IId, and IIId all are in the range of two to three eV. Second, there are points of inflection in the SDIE curves of Id, IId, and IIId below the first local maximum. Therefore, these results indicate an appearance potential lower than the first local maximum. The SDIE curves of IVc and Vd (Figures 37 and 38) both show a point of inflection at 14.8 - 15.2 eV and 15.1 - 15.4 eV respectively. These values are in good agreement with the reported A.P. of 15.12 eV.[34]

The maxima in the SDIE curves of Ia (Figure 15), IIa (Figure 16), IIIa (Figure 17), IVa (Figure 18), and Va (Figure 19) are recorded in Table XIII. Autoionizing or long-lived excited states of Ia, IIa, IIIa, IVa, and Va constitute alternative explanations for these maxima. Autoionization could be reflected by the presence of maxima in the SDIE curves of the

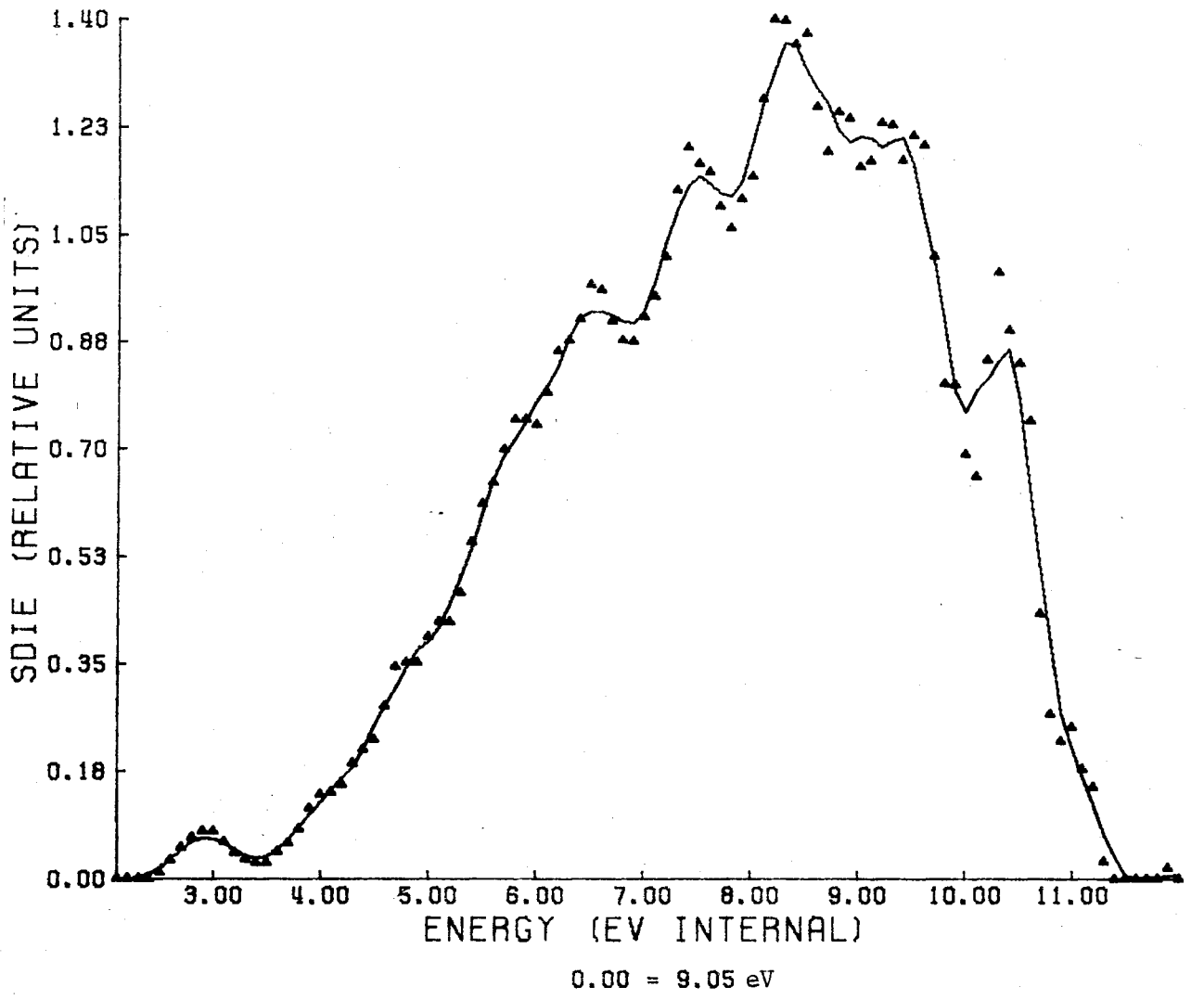

Figure 34a. SDIE Curve of Id, 310° Ion Source Temperature

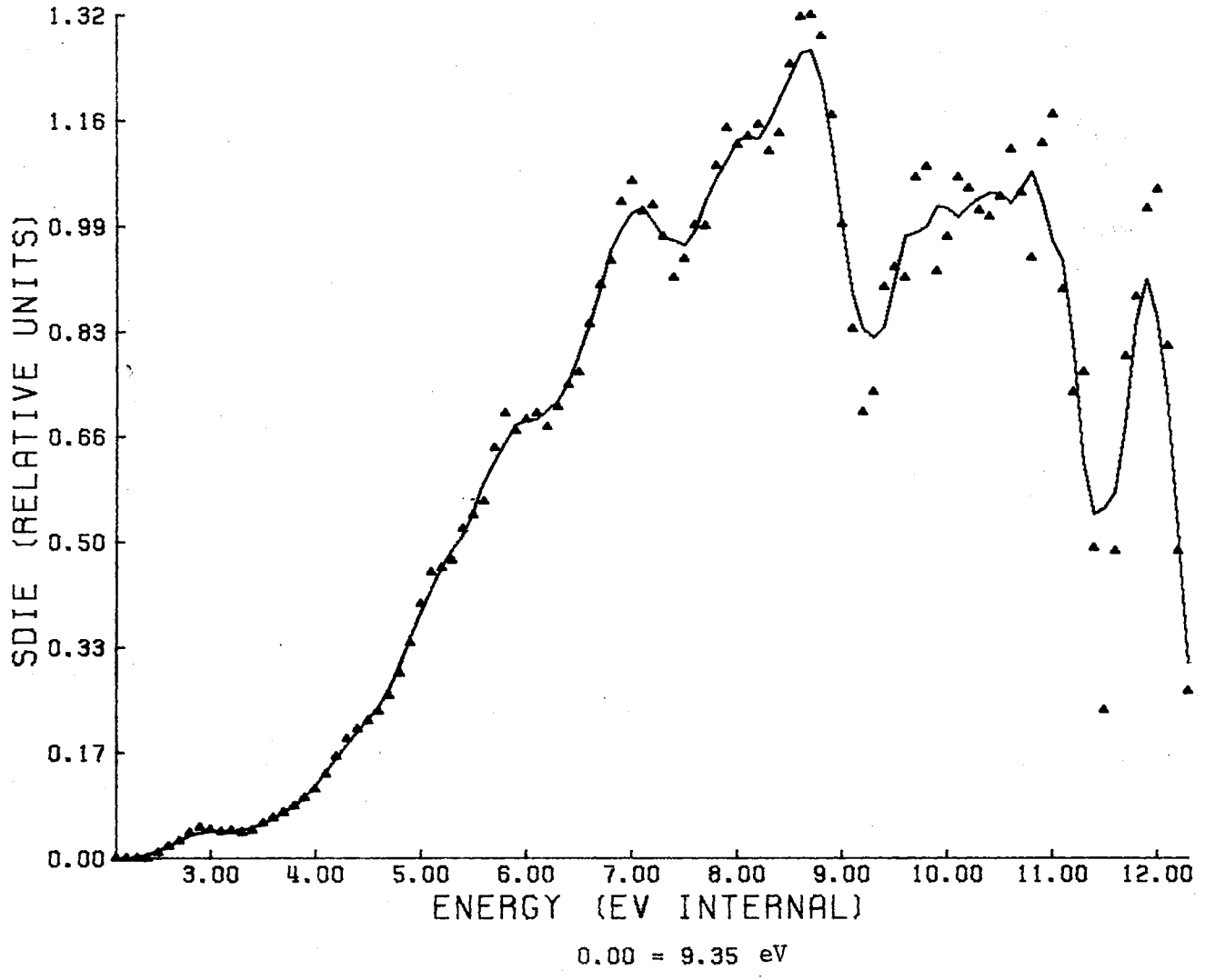

Figure 34b. SDIE Curve of Id, 230° Ion Source Temperature

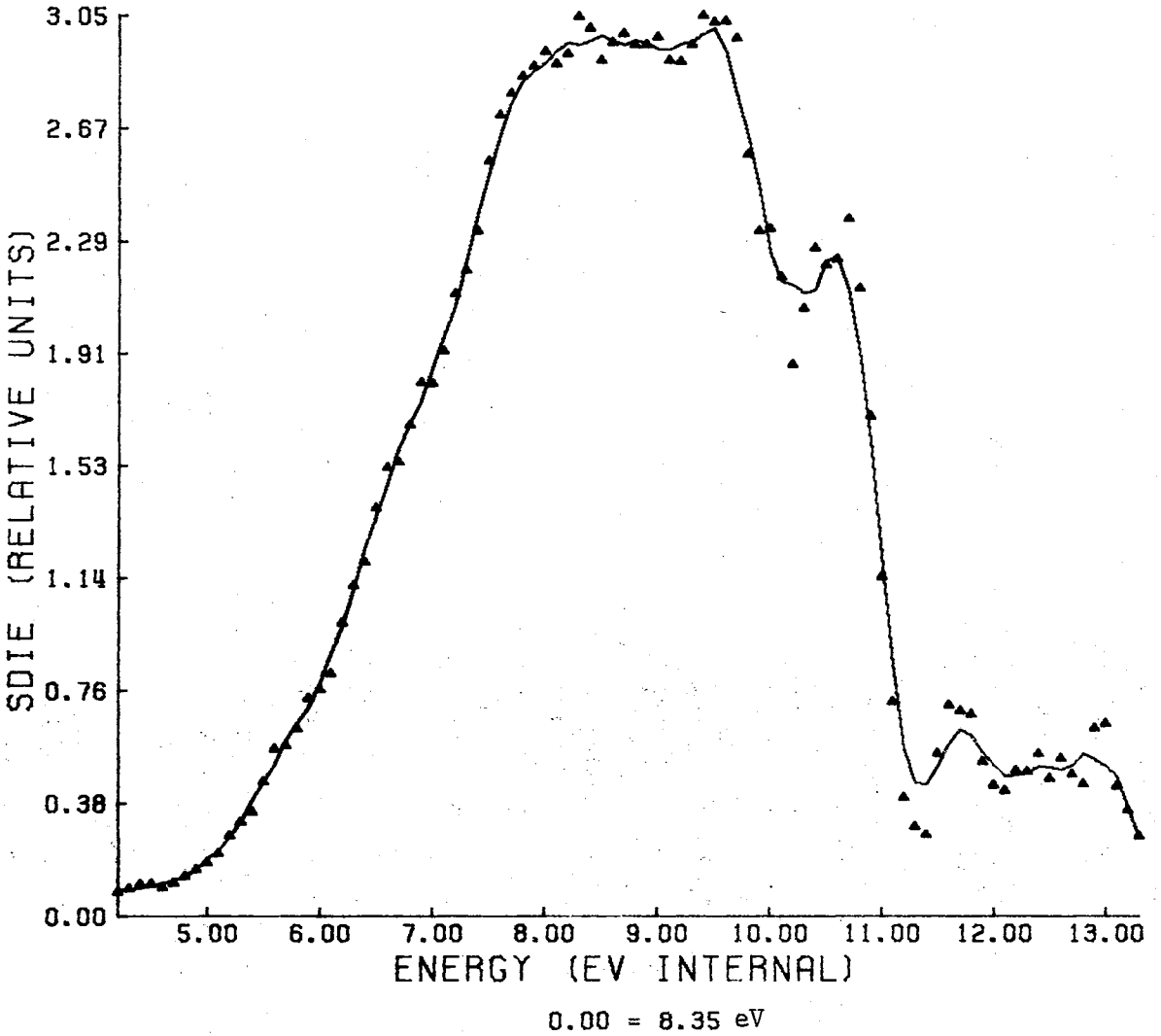

Figure 35a. SDIE Curve of IId, 310° Ion Source Temperature

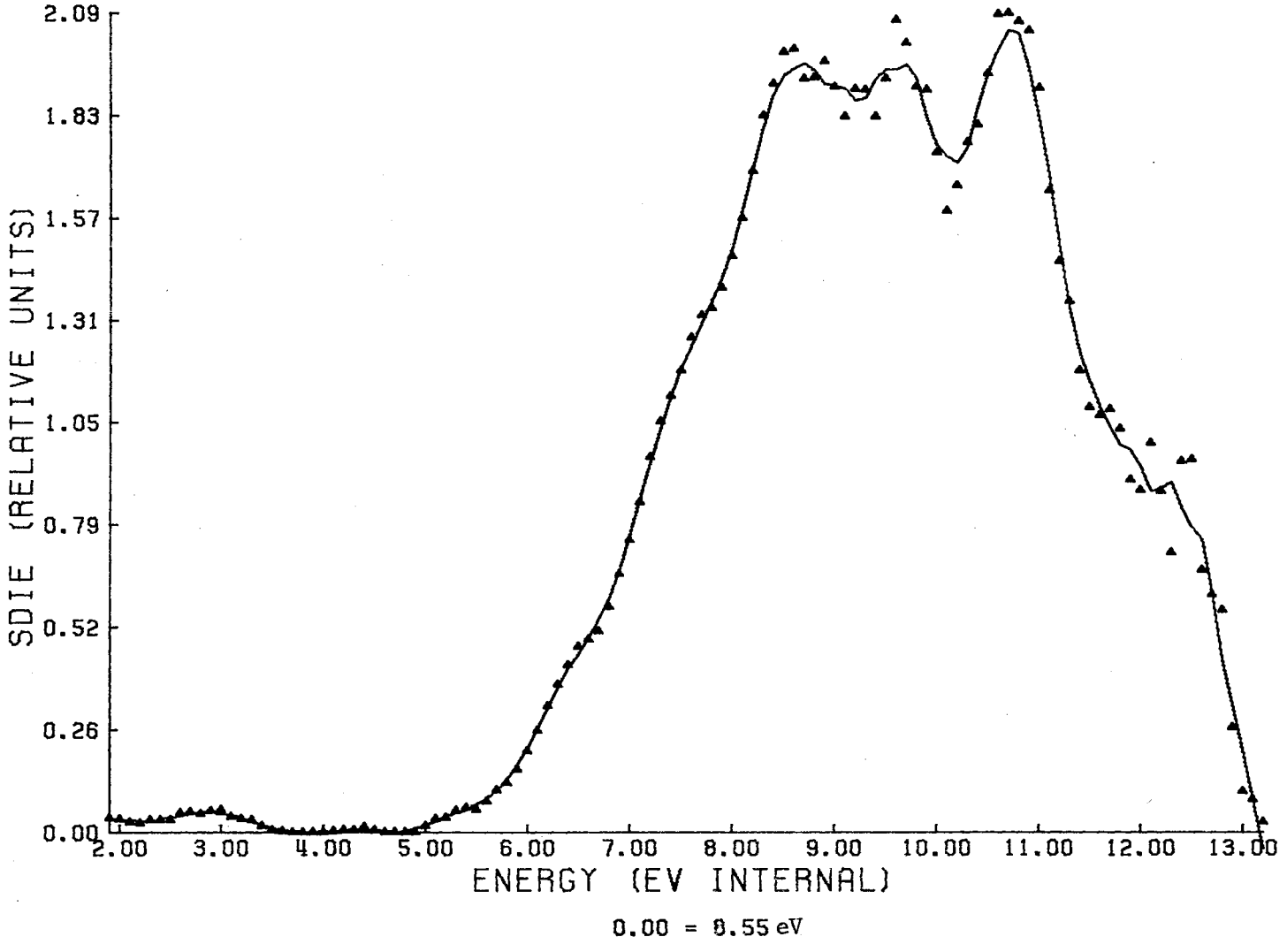

Figure 35b. SDIE Curve of IId, 250° Ion Source Temperature

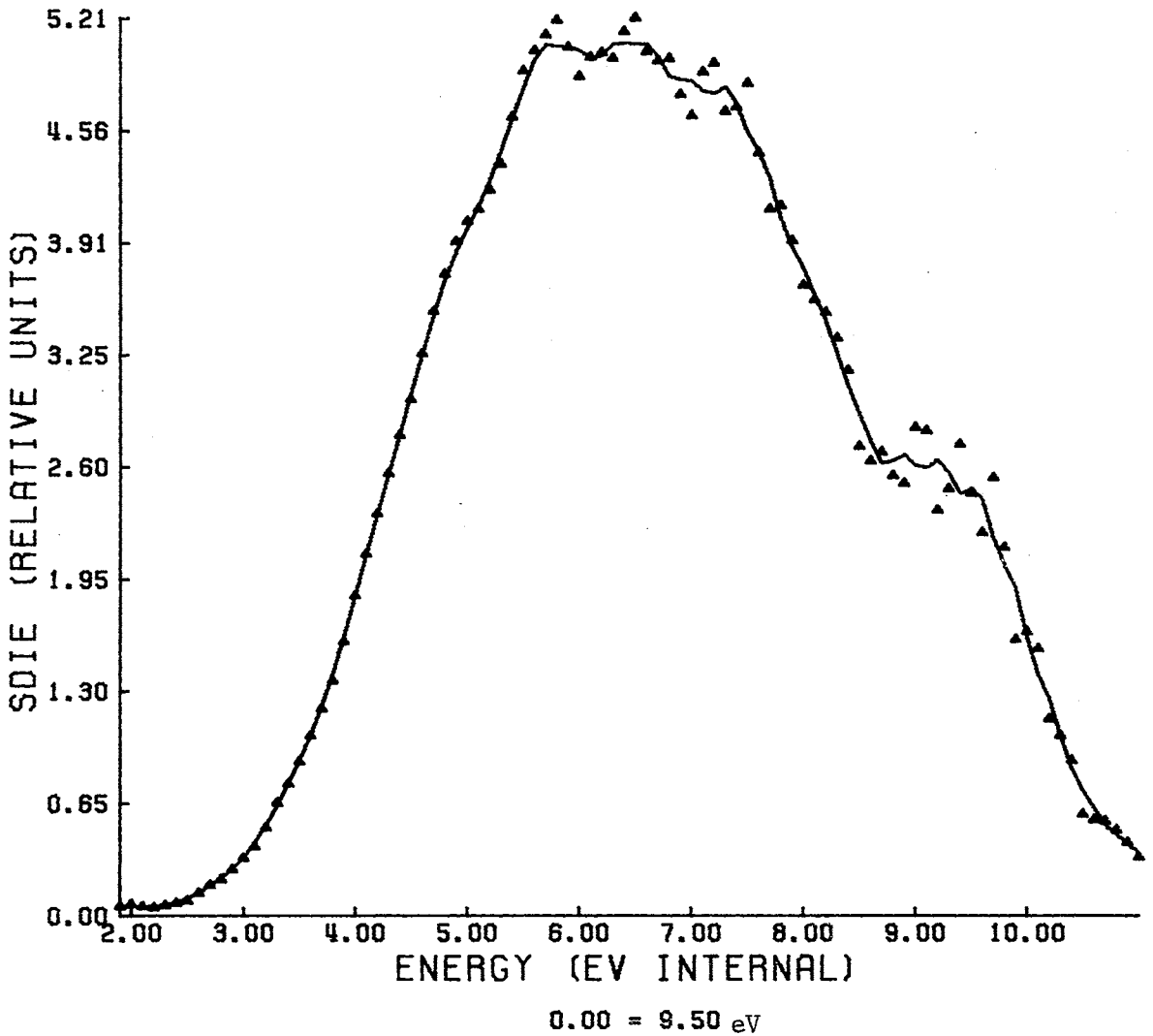

Figure 36a. SDIE Curve of IIId, 310° Ion Source Temperature

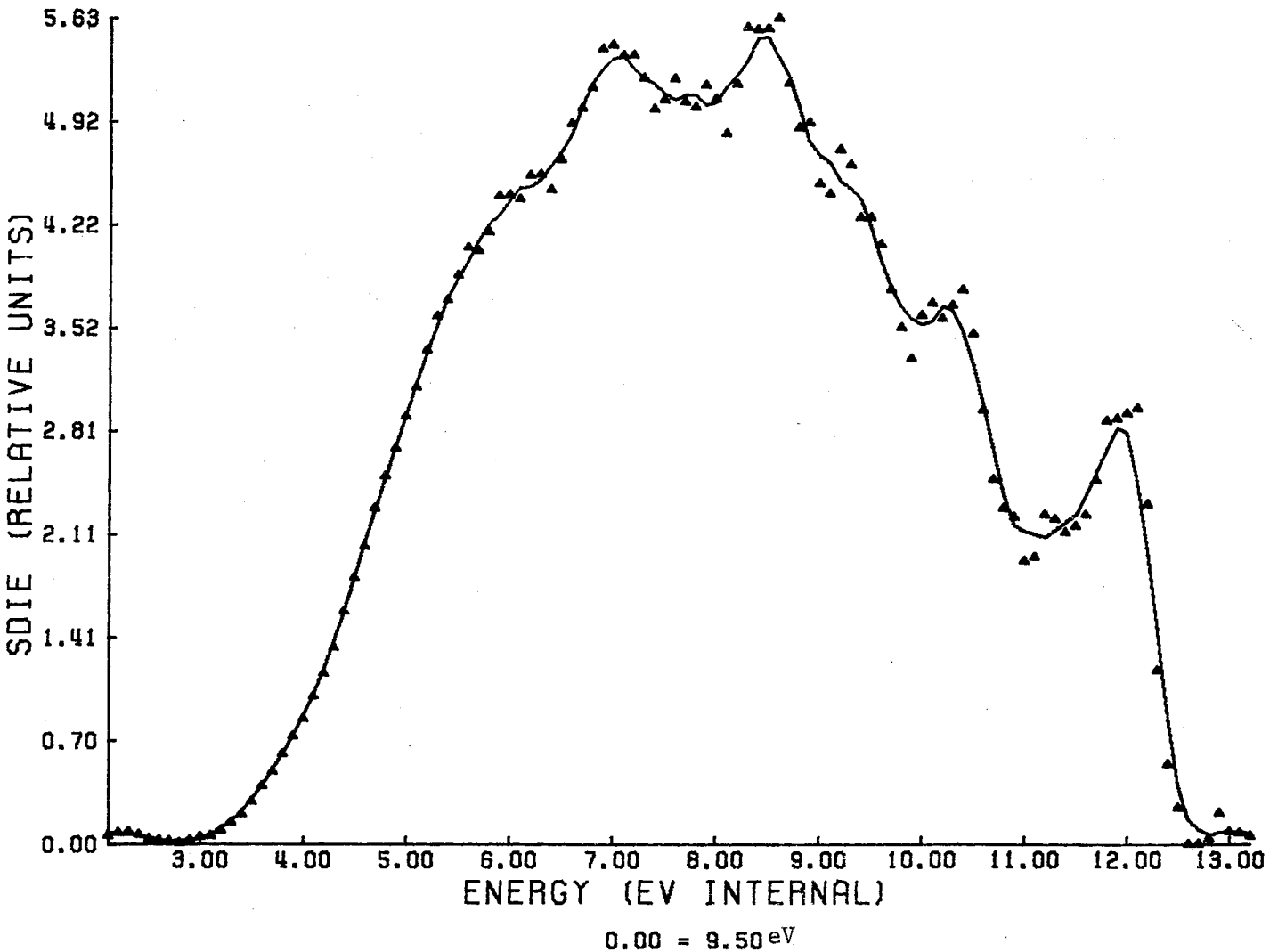

Figure 36b. SDIE Curve of IIId, 250° Ion Source Temperature

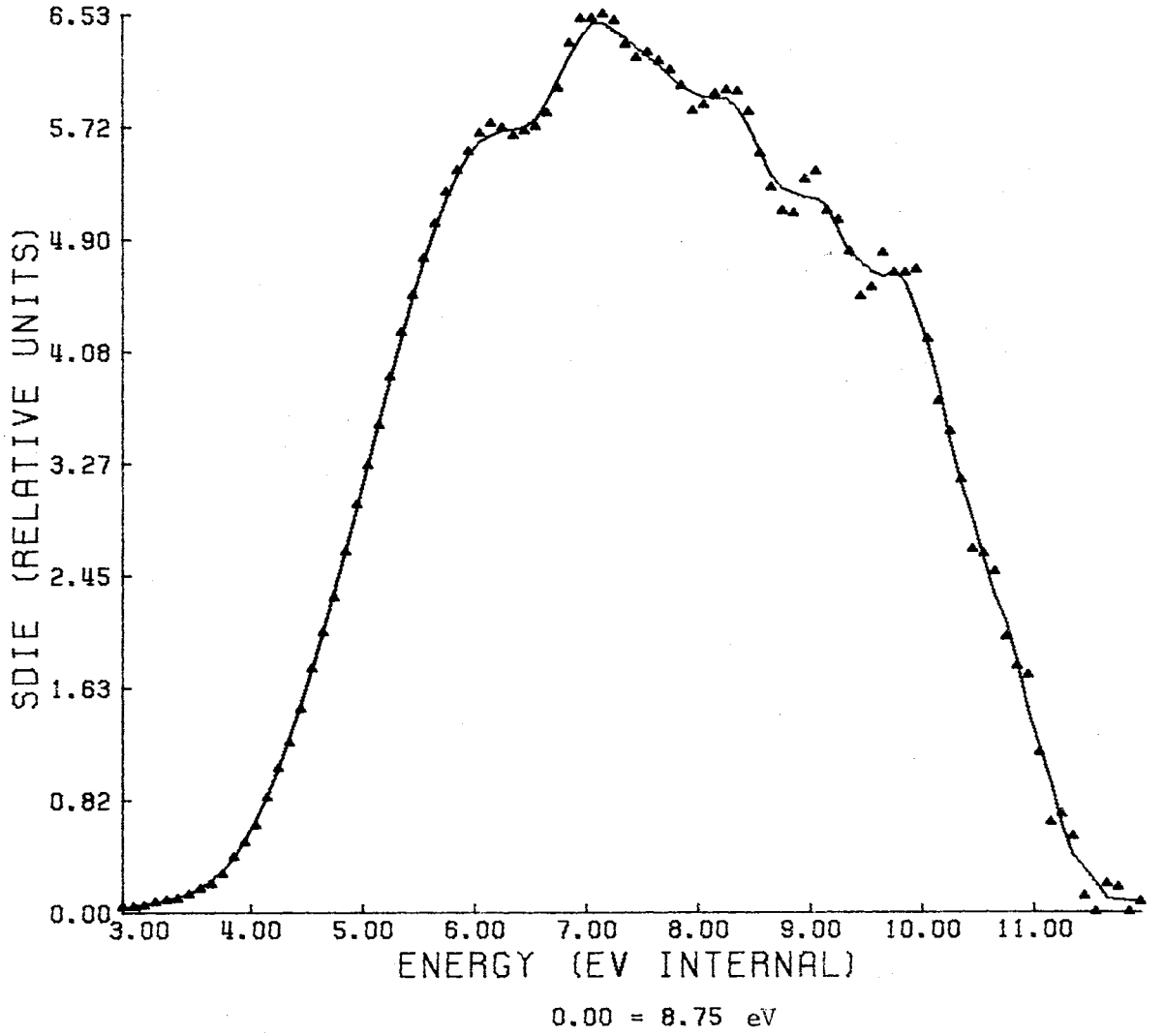

Figure 37. SDIE Curve of IVc, 250° Ion Source Temperature

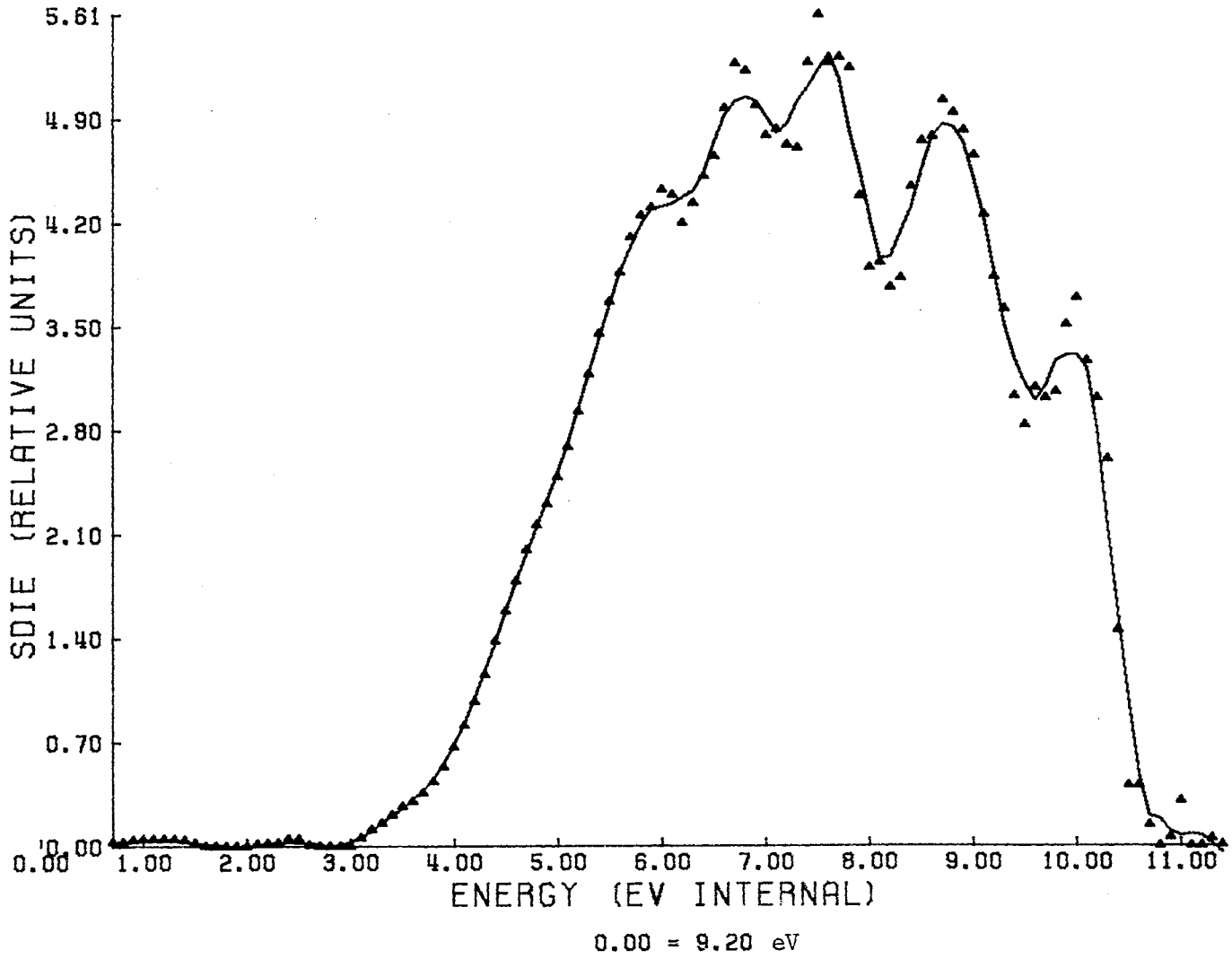

Figure 38. SDIE Curve of Vd, 250° Ion Source Temperature

parent ion and the primary fragment ions at the same electron voltage. The effect of excited and long-lived ionic states on the fragment ion SDIE curves is more difficult to assess for the following reasons. First, since states which permit energy randomization may also be accessible, only a fraction of the molecular ions produced at an electron energy equal to or in excess of the ionization potential of the excited state have to be formed in such a state. Second, limited crossing of the potential energy surfaces would allow the excited ionic molecular ion to undergo competitive fragmentation via partial energy randomization. Third, the molecular ion in excited states should fragment via cleavage of the C-1--C-2 bond upon deposition of sufficient internal energy. The first two phenomena would tend to moderate the rate of decrease (increase) in the fragment ion SDIE curves; the third would lead to a maximum in the SDIE curves for the fragment ions corresponding to the appearance potentials for formation of these ions from the excited molecule ion. Qualitative comparison of the maxima in the SDIE curves of the parent ions (Table XIII) with the maxima in the SDIE curves of the primary daughter ions (Table XIV) produces only tenuous evidence for autoionization. Owing to the uncertainty in these maxima or points of inflection a quantitative comparison is not possible.

The effect of ion source temperature upon the SDIE curves is clearly demonstrated in this study. One of the difficulties in the application of QET theory to fragmentation processes is the determination of the minimum internal energy, E_o , necessary to pass through the

TABLE XIII

THE MAXIMA IN THE SDIE CURVES OF Ia, IIa, IIIa, IVa, AND Va

310° Ia[a]	230°	310° IIa[b]	250°	310° IIIa[b]	250°	IVa[b] 250°	Va[b] 250°
9.05 ± .10							
10.16 ± .11	9.35	8.35	8.85	9.50	9.9	8.75	9.20
		9.75					10.20
11.16 ± .12	10.95	10.75	10.45	10.70	10.70	10.75	11.10
12.72 ± .12	12.55	12.25	11.45	11.40	11.70	11.45	12.80

[a] Based upon four determinations.

[b] Based upon a single determination.

TABLE XIV

THE MAXIMA IN THE SDIE CURVES OF SUBSTITUTED AND UNSUBSTITUTED BENZOYL IONS

Ib		Ic		IIb		IIc		IIIb		IIIc		IVb	Vb	Vc
310°	230°	310°	250°	310°	250°	310°	250°	310°	250°	310°	250°	250°	250°	250°
eV		eV		eV		eV		eV		eV		eV	eV	eV
12.05	12.15	9.85	10.35	10.55	12.15	9.85	9.95	10.6		11.5	11.6	10.75		10.7
12.85	13.95	11.05		11.45	14.25	11.75	11.25	11.4	11.5		12.5	11.85	12.0	11.4
12.45	14.75	12.15		13.05		12.65	12.85	12.3	12.7	13.8	13.8		12.8	12.5
16.05	15.95	13.35	13.55	14.25			13.55	13.2	13.4	14.6	14.5			
16.75				14.85			14.15			15.7				
				16.25	16.15					16.5	16.8			
				17.45						17.7	17.7			
											18.3			

activated complex which ultimately leads to products. An estimate of E_o would be the ionization potential of the neutral molecule minus the appearance potential of the fragment ion but this may well be an overestimate since the internal energy must be above E_o for k(E) to be in the region of $10^5 - 10^6$ sec^{-1}. [4] The excess internal energy is defined as the kinetic shift. Since an increase in the ion source temperature produces molecular ions having higher internal energies than those produced at lower source temperatures, fragment ions will be observed at lower nominal beam energies. A comparison of the daughter ion SDIE curves at two source temperatures should be sufficient to show any partial kinetic shift. Table XV presents the positive internal energy shifts necessary to bring an ion's SDIE curves taken at two ion source temperatures into coincidence. This is accomplished by shifting the energy axis until the first local maximum and/or the low-energy tail are superimposed.

TABLE XV

PARTIAL KINETIC SHIFTS FROM TEMPERATURE DEPENDENCE STUDY

-X	m/e 105	m/e 104 + X	m/e 77	m/e 76 + X
P-CH_3	0.0	0.35	0.0	0.0
P-OCH_3	0.3	0.25	0.8	0.7
m-CF_3	0.2	0.8	0.6	0.8

Since the k(E) for production of a metastable ion is less than k(E) for production of a normal fragment ion, subtraction of the appearance potential of the metastable ion from the appearance potential of the normal ion should give an estimate of E_o.[4] The SDIE curve for the metastable ion m/e 119 → m/e 91 (Figure 33) when compared to the SDIE curve for the normal m/e 91 (Figure 29a) yields no significant difference. This evidence that k(E) for decomposition of m/e 119 may rise very steeply with internal energy, which causes a very small kinetic shift, and E_o for the process is small. This result is also in agreement with the lack of a partial kinetic shift for m/e 91 (see Table XV). The SDIE curves of the molecular ions of I, II, and III were shifted to higher beam energies at the lower ion source temperatures, typically 0.2-0.3 eV. This may be due to thermal broadening of the transition probability curves.[5a,44]

The breakdown graphs for I, II, III and V were constructed from the SDIE values for each ion normalized by their sum (see Equation 14), where n in Equation 14 is equal to the total number of parent and fragment ions, j . Breakdown graphs constructed from Equation 14 with abscissa values equal to the internal energies of the molecular ions are presented in Figures 39-42. The extension of the energy axis to negative values represents the effect of the electron energy distribution and the internal thermal energy of I, II, III, and V.

$$\text{Normalized SDIE(J)} = \text{SDIE(J)} / \sum_{j=1}^{n} \text{SDIE(J)} \qquad (14)$$

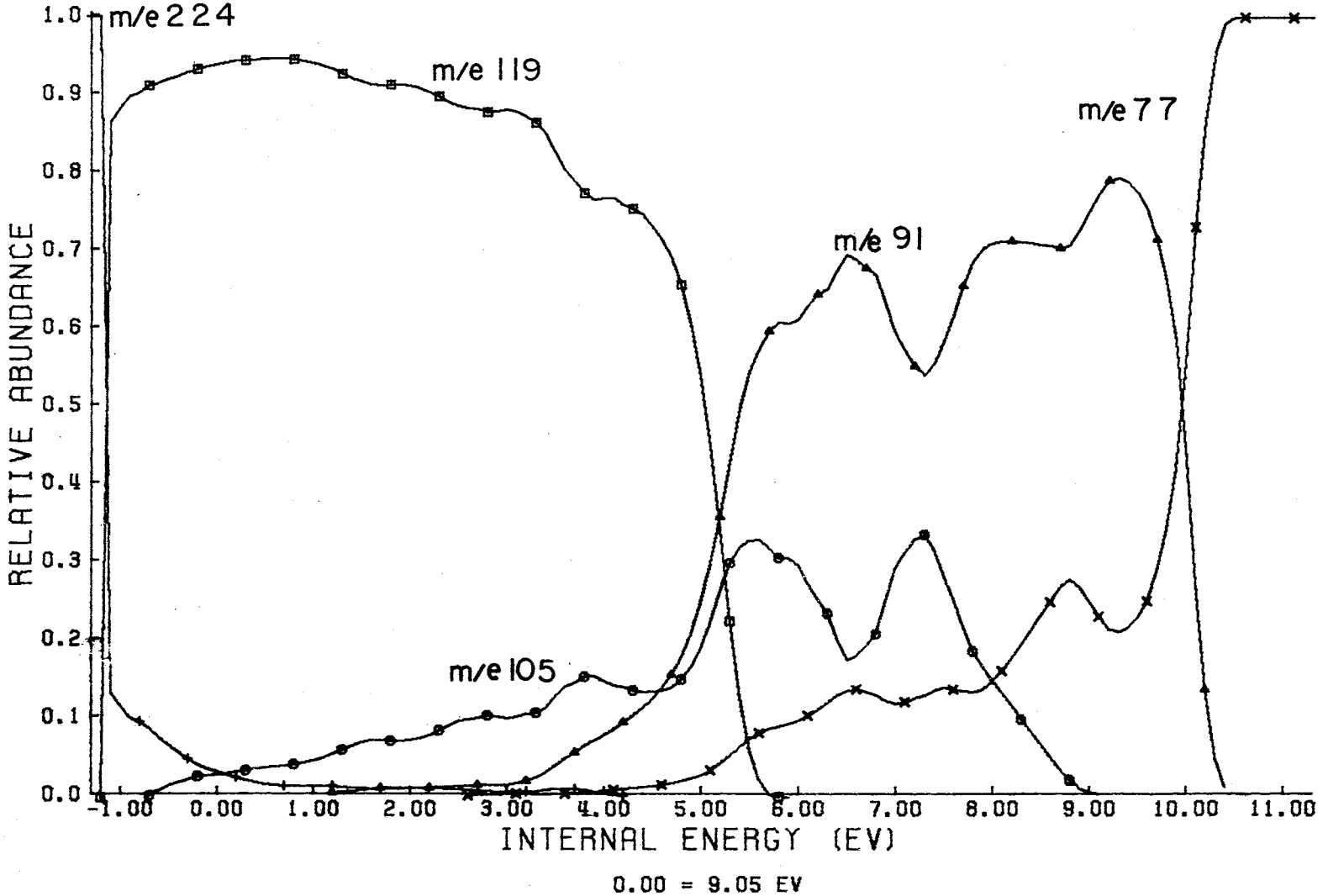

Figure 39a. Breakdown Graph for I, 310°

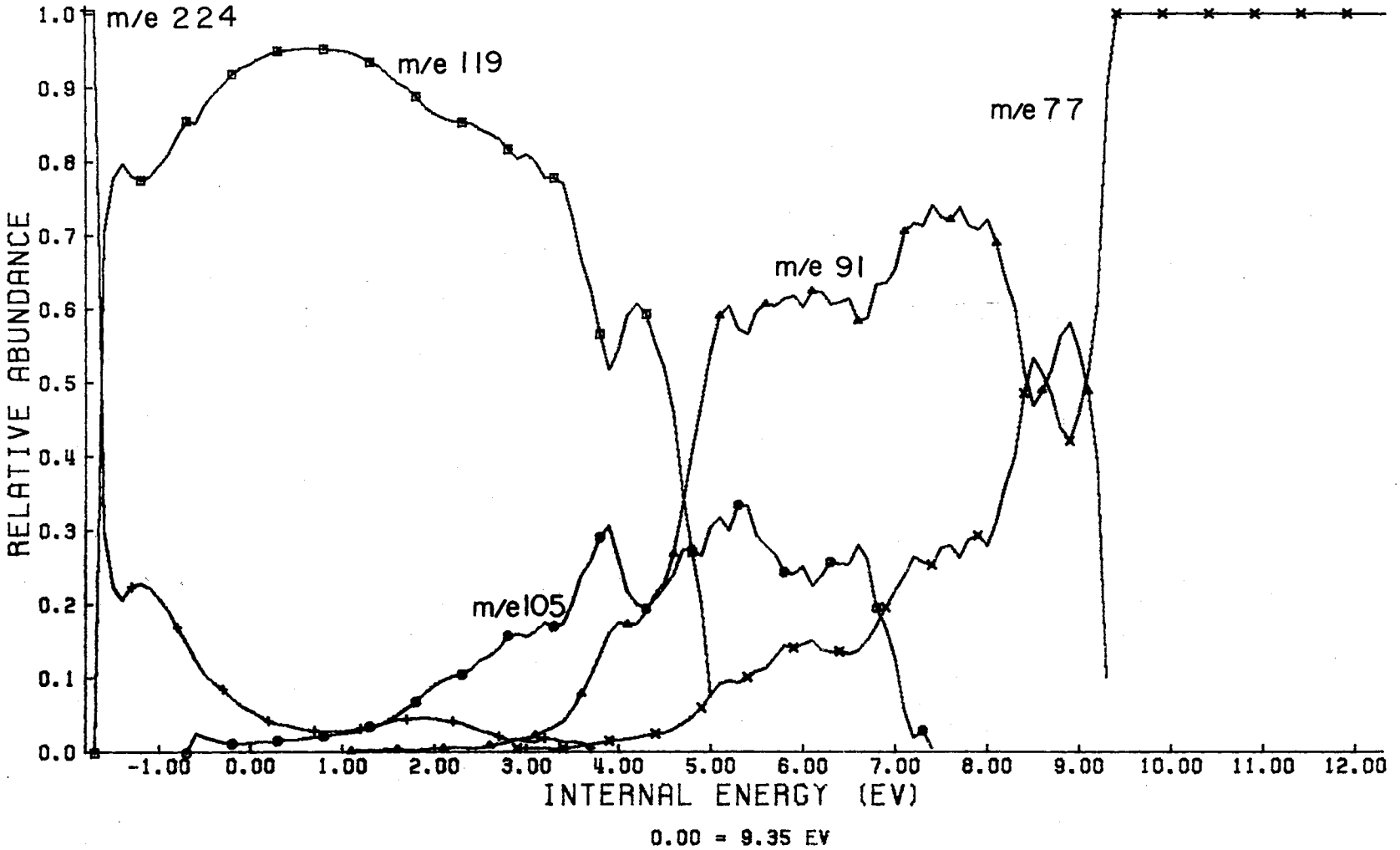

Figure 39b. Breakdown Graph for I, 230°

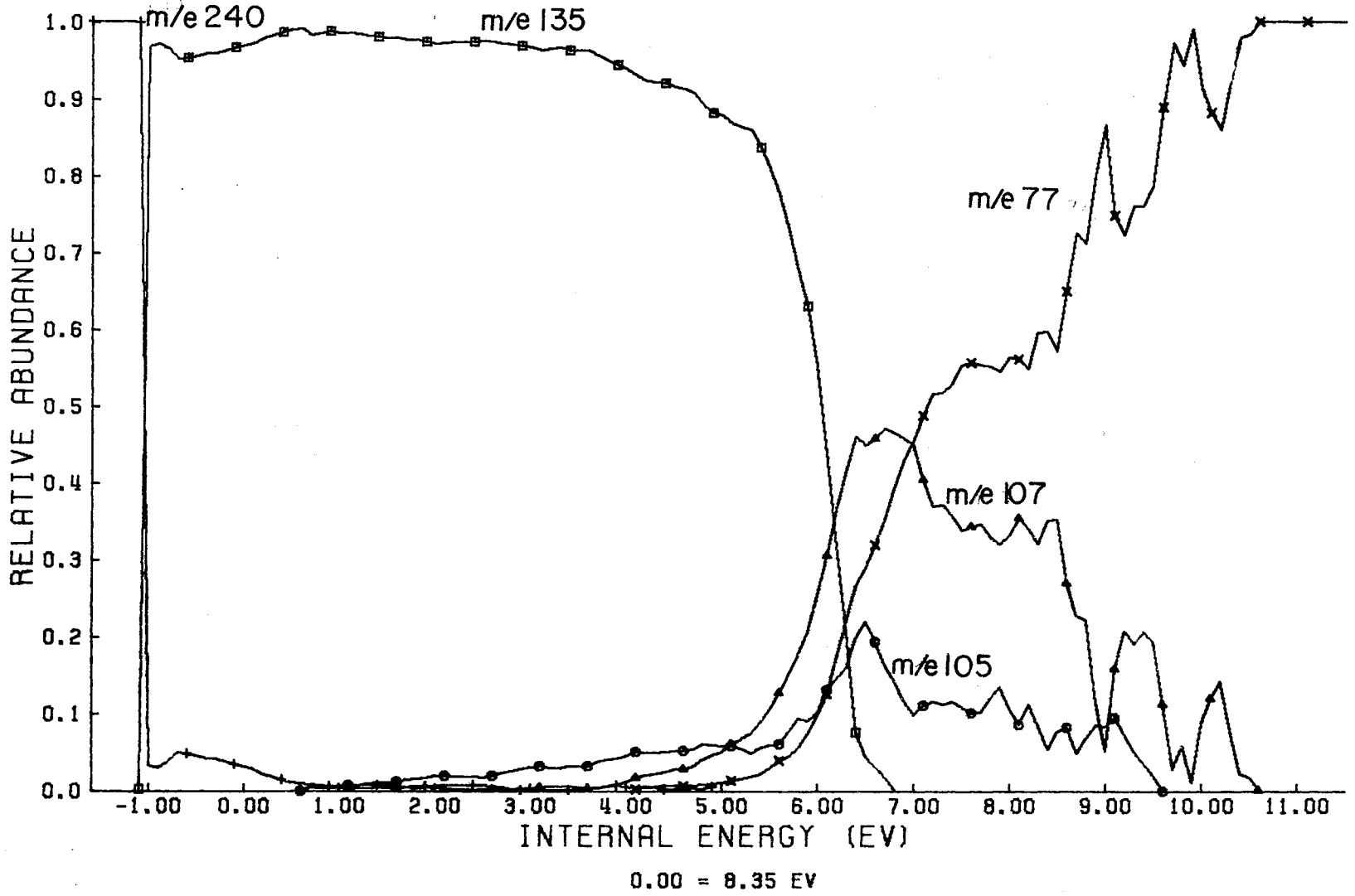

Figure 40a. Breakdown Graph for II, 310°

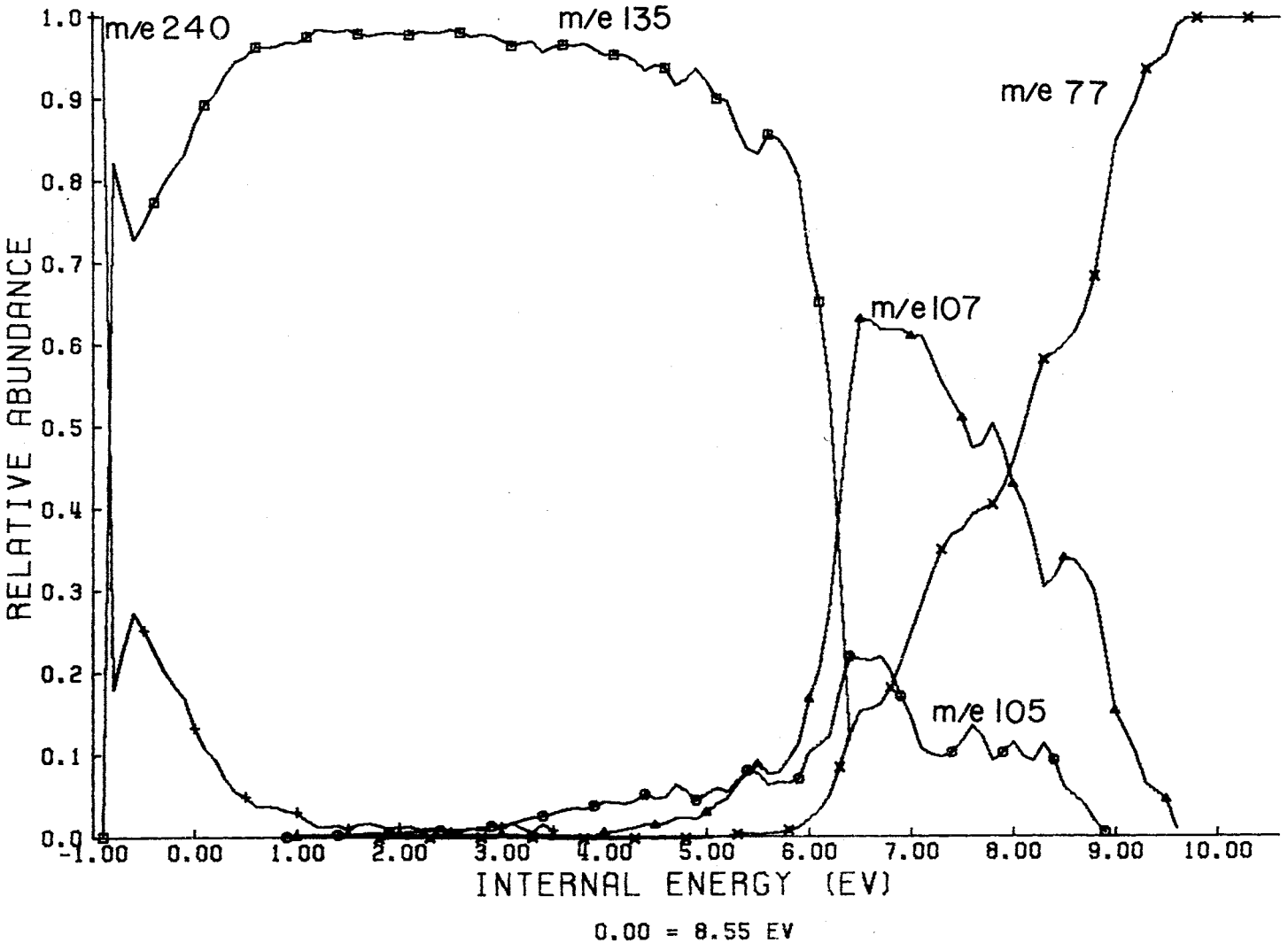

Figure 40b. Breakdown Graph for II, 250°

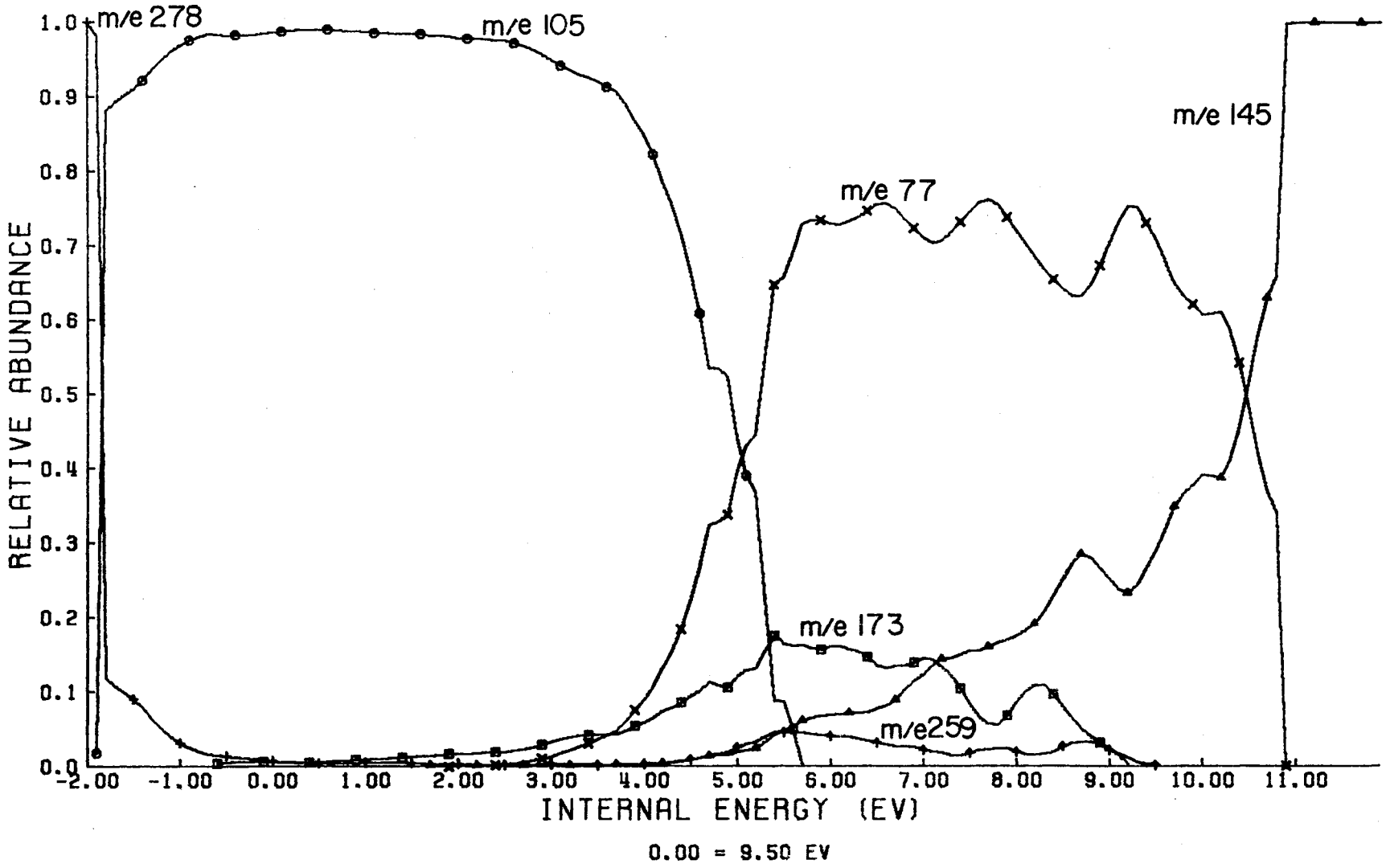

Figure 41a. Breakdown Graph for III, 310°

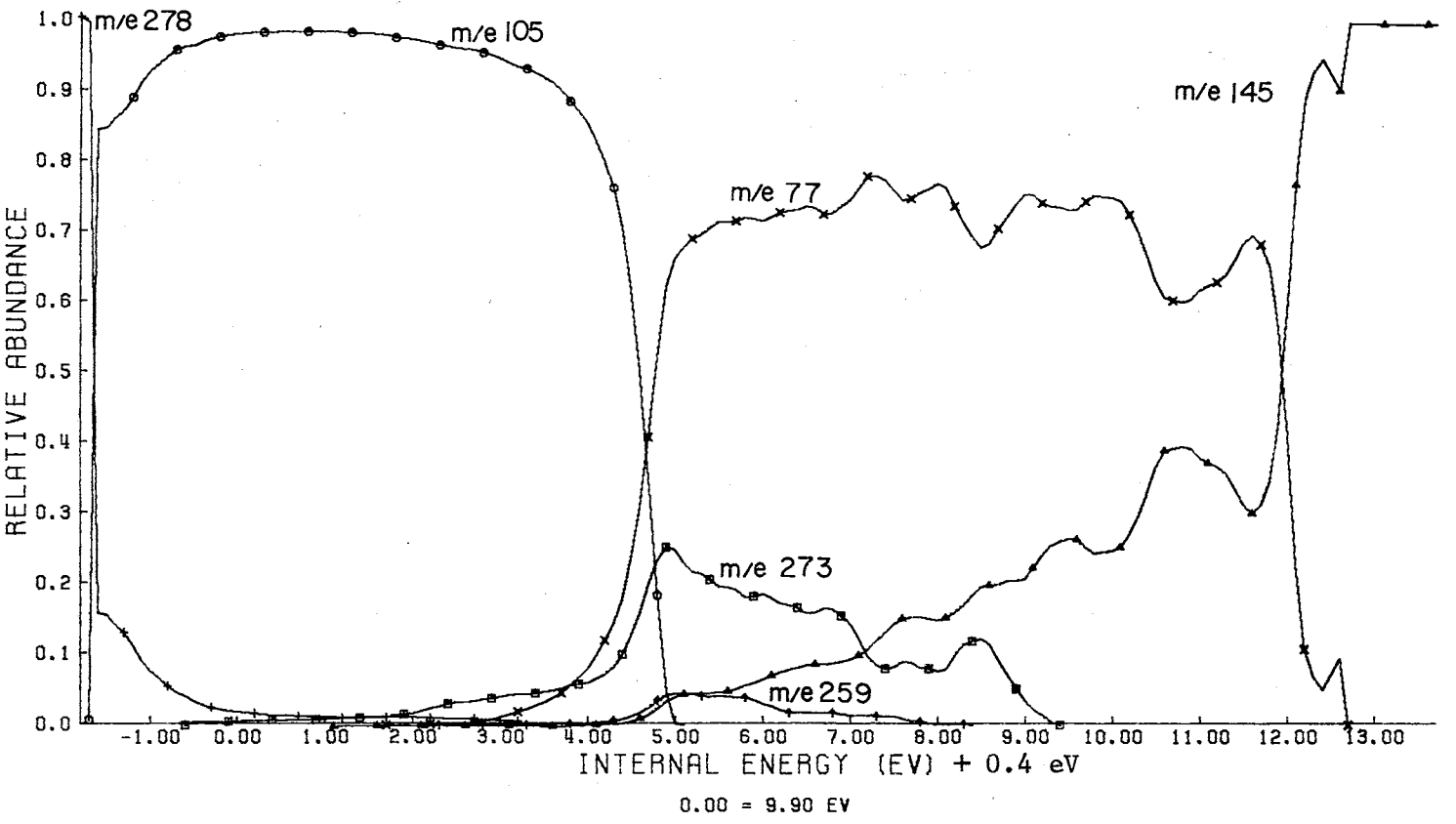

Figure 41b. Breakdown Graph for III, Ion Source Temperature 250°

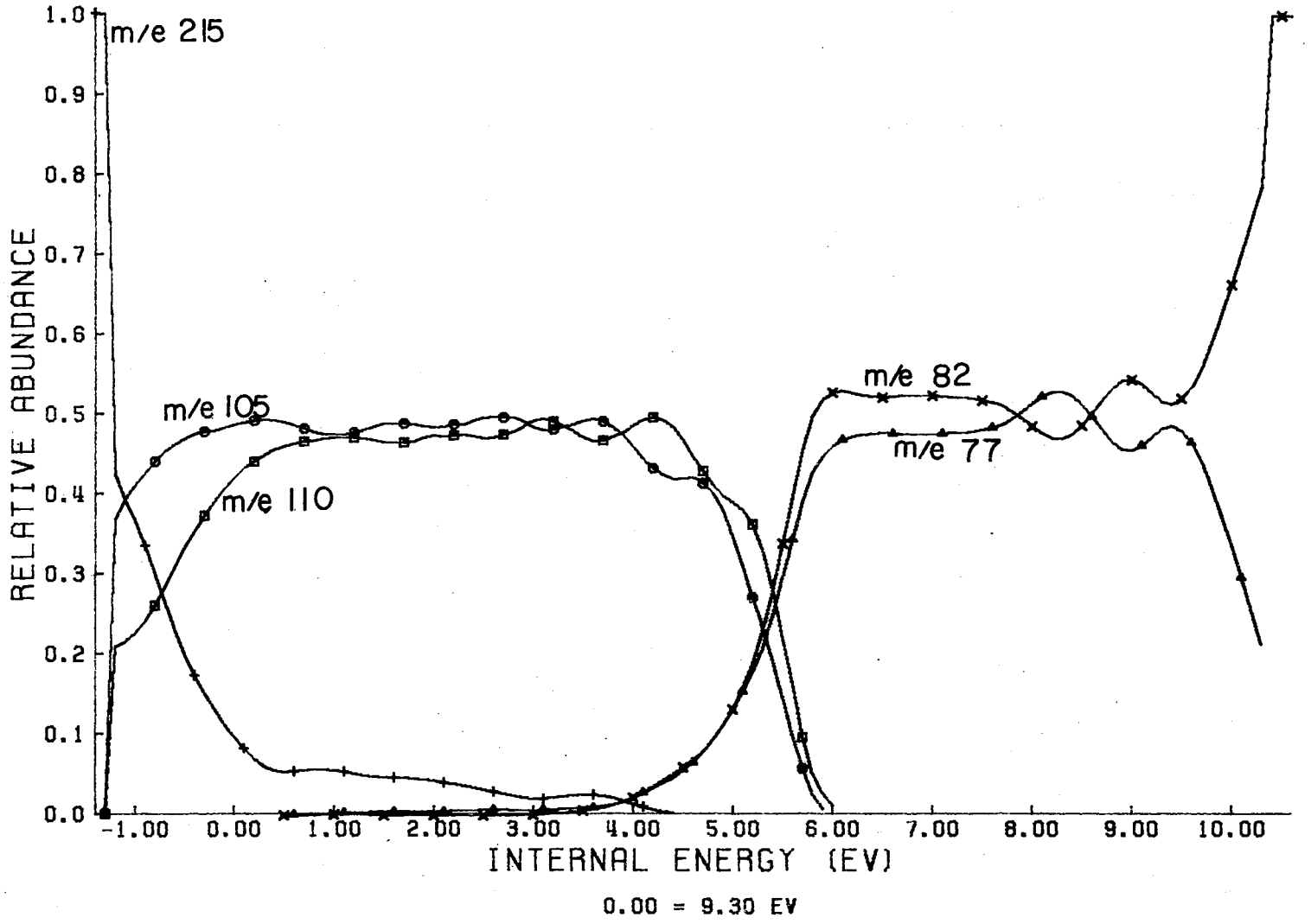

Figure 42. Breaqdown Graph for V, 250°

The ratio of rate constants for the general decomposition given by Equation 15 at the i-th value of the internal energy is given by Equation 16.

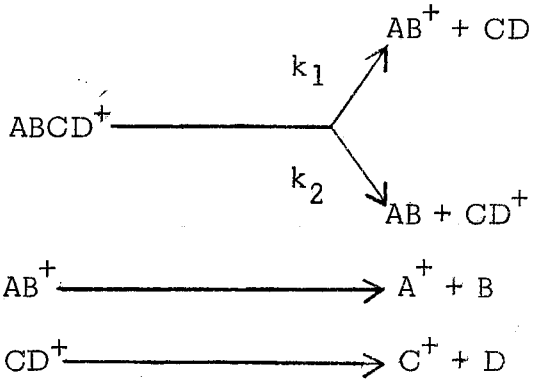

(15)

$$k_1(E_i)/k_2(E_i) = \text{SDIE}(AB^+) + \text{SDIE}(A^+)/\text{SDIE}(CD^+) + \text{SDIE}(C^+) \quad (16)$$

The rate constant ratios for the decomposition of I, II, III, and V were calculated from Equations 17-20 respectively. Figures 43-46 give the rate constant ratio for formation of the ions resulting from central C—C bond rupture of I, II, III, and V as a function of the molecular ion internal

$$\text{(I)} \quad k_1(E)/k_2(E) = (\text{SDIE(Ib)} + \text{SDIE(Id)})/(\text{SDIE(Ic)} + \text{SDIE(Ie)}) \quad (17)$$

$$\text{(II)} \quad k_1(E)/k_2(E) = (\text{SDIE(IIb)} + \text{SDIE(IId)})/(\text{SDIE(IIc)} + \text{SDIE(IIe)}) \quad (18)$$

$$\text{(III)} \quad k_1(E)/k_2(E) = (\text{SDIE(IIIb)} + \text{SDIE(IIId)})/(\text{SDIE(IIIc)} + \text{SDIE(IIIe)}) \quad (19)$$

$$\text{(V)} \quad k_1(E)/k_2(E) = (\text{SDIE(Vb)} + \text{SDIE(Vd)})/(\text{SDIE(Vc)} + \text{SDIE(Ve)}) \quad (20)$$

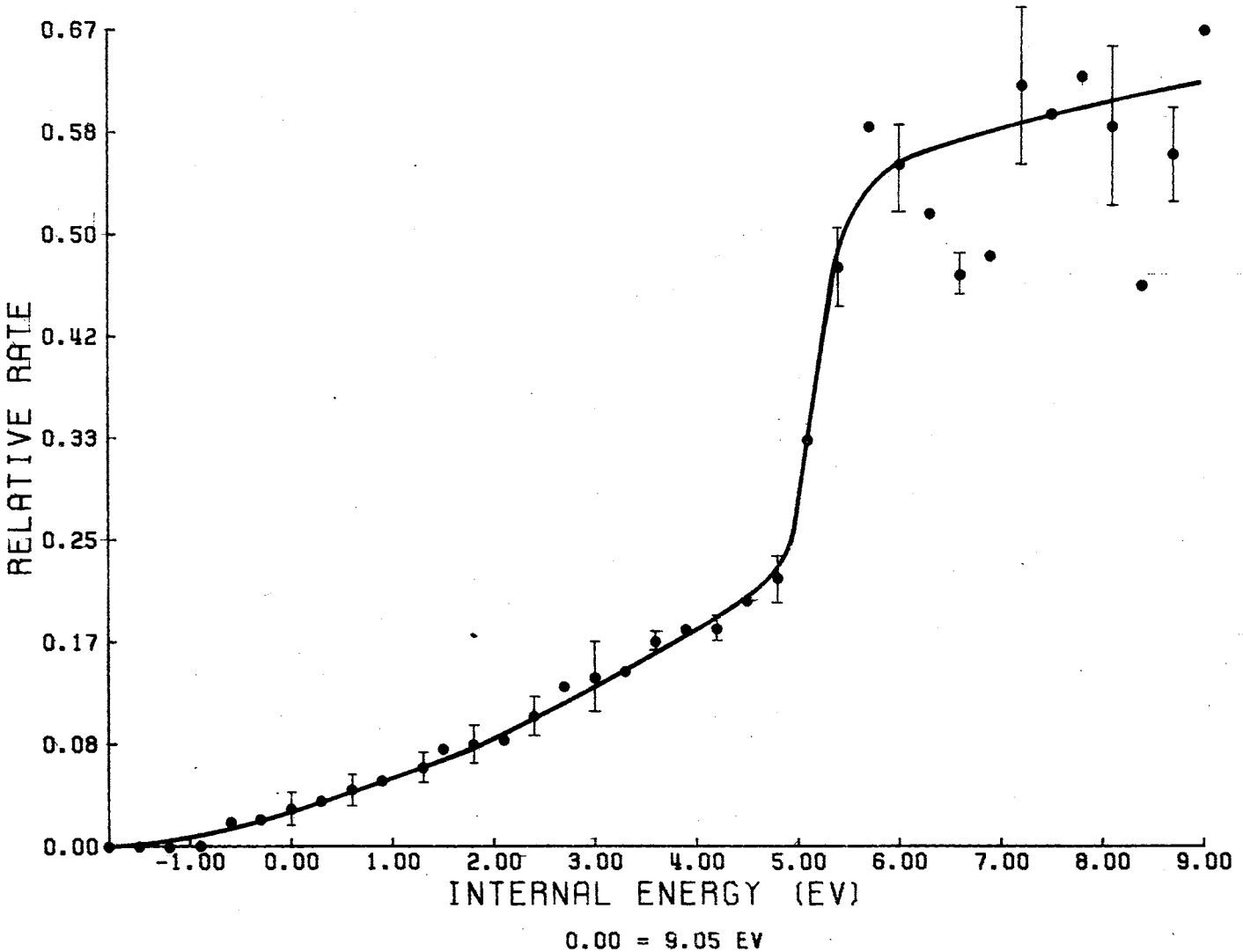

Figure 43a. Relative Rate Constant Plot of I, 310°

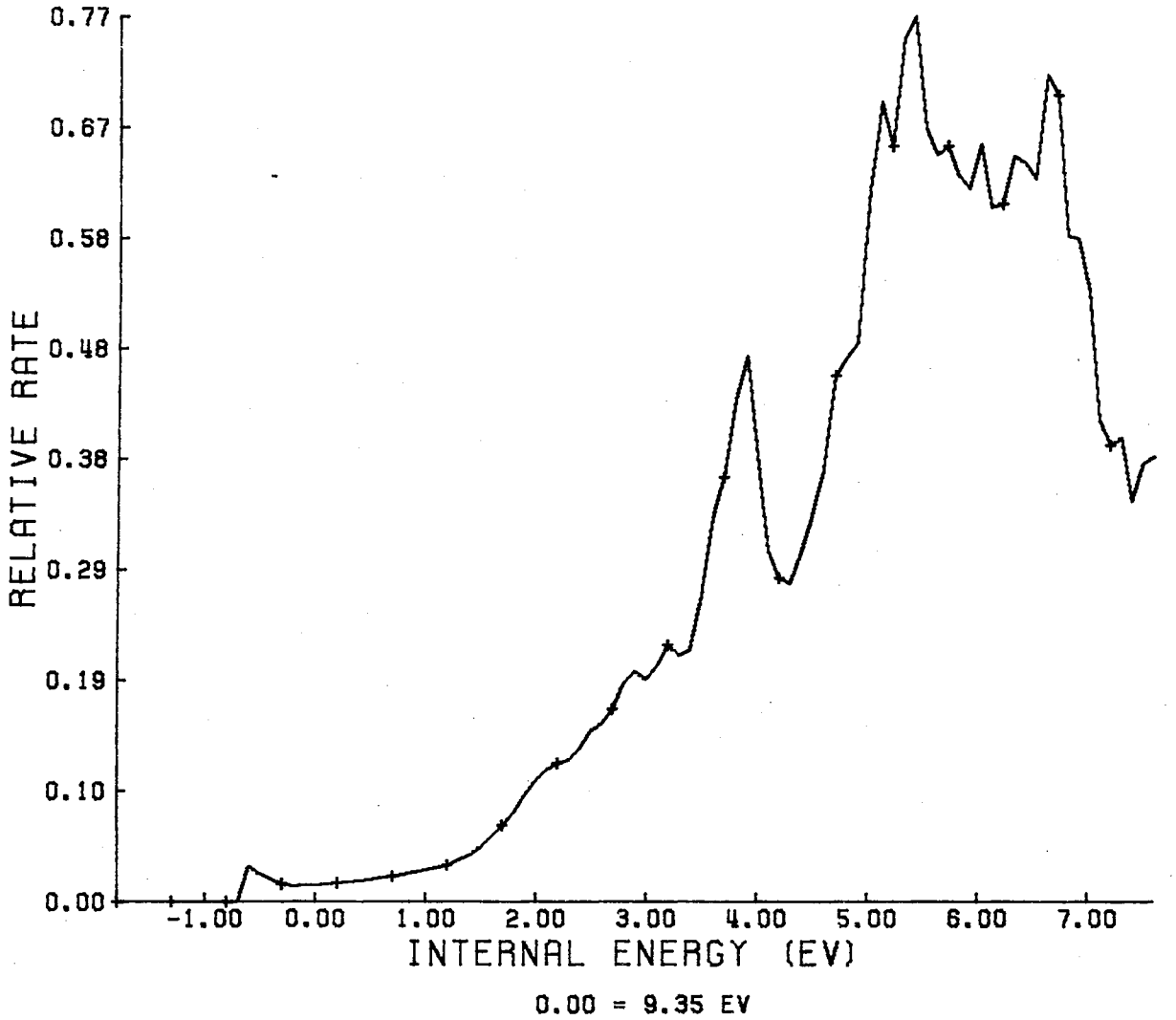

Figure 43b. Relative Rate Constant Plot of I, 230°

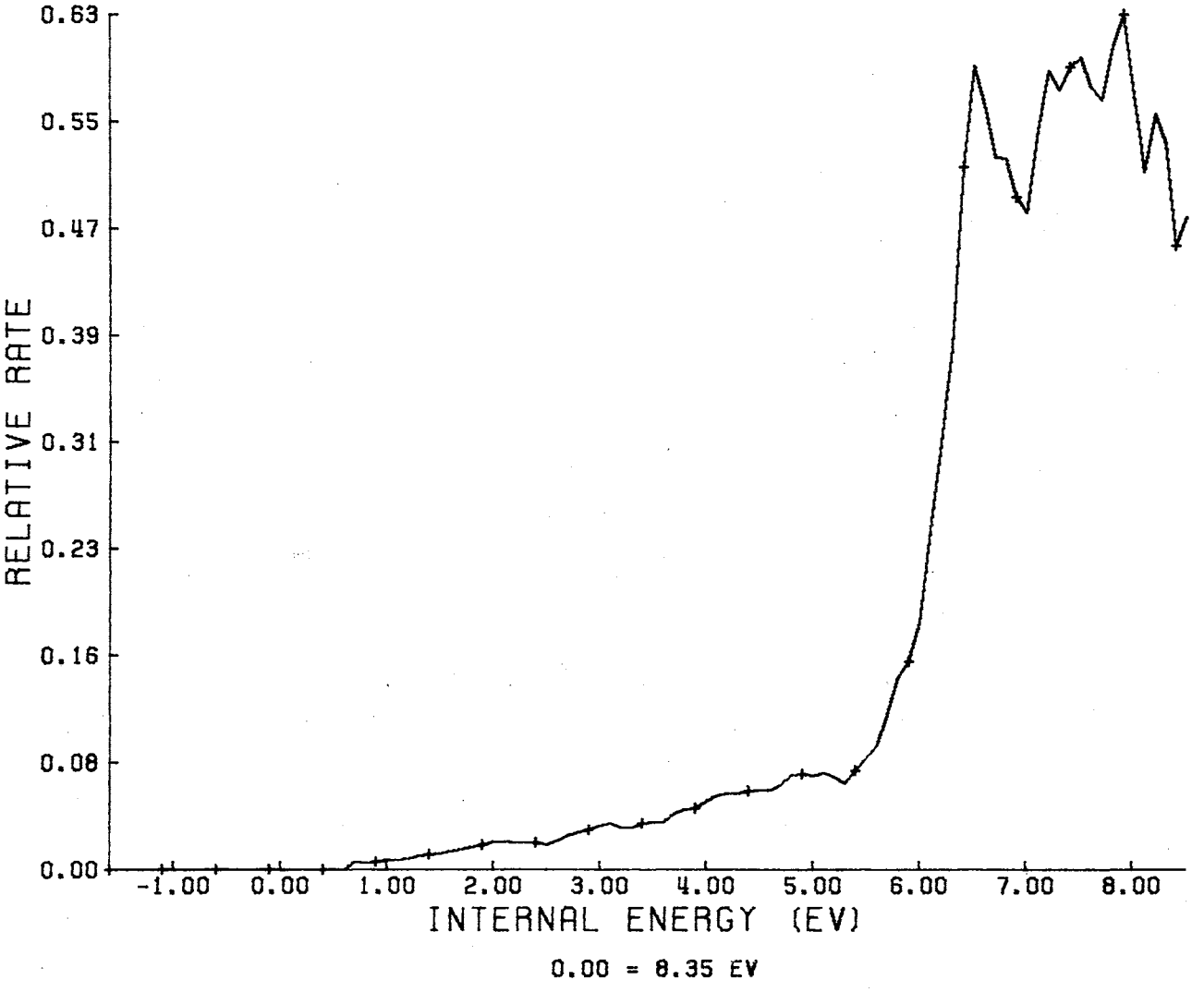

Figure 44a. Relative Rate Constant Plot of II,310[⊖]

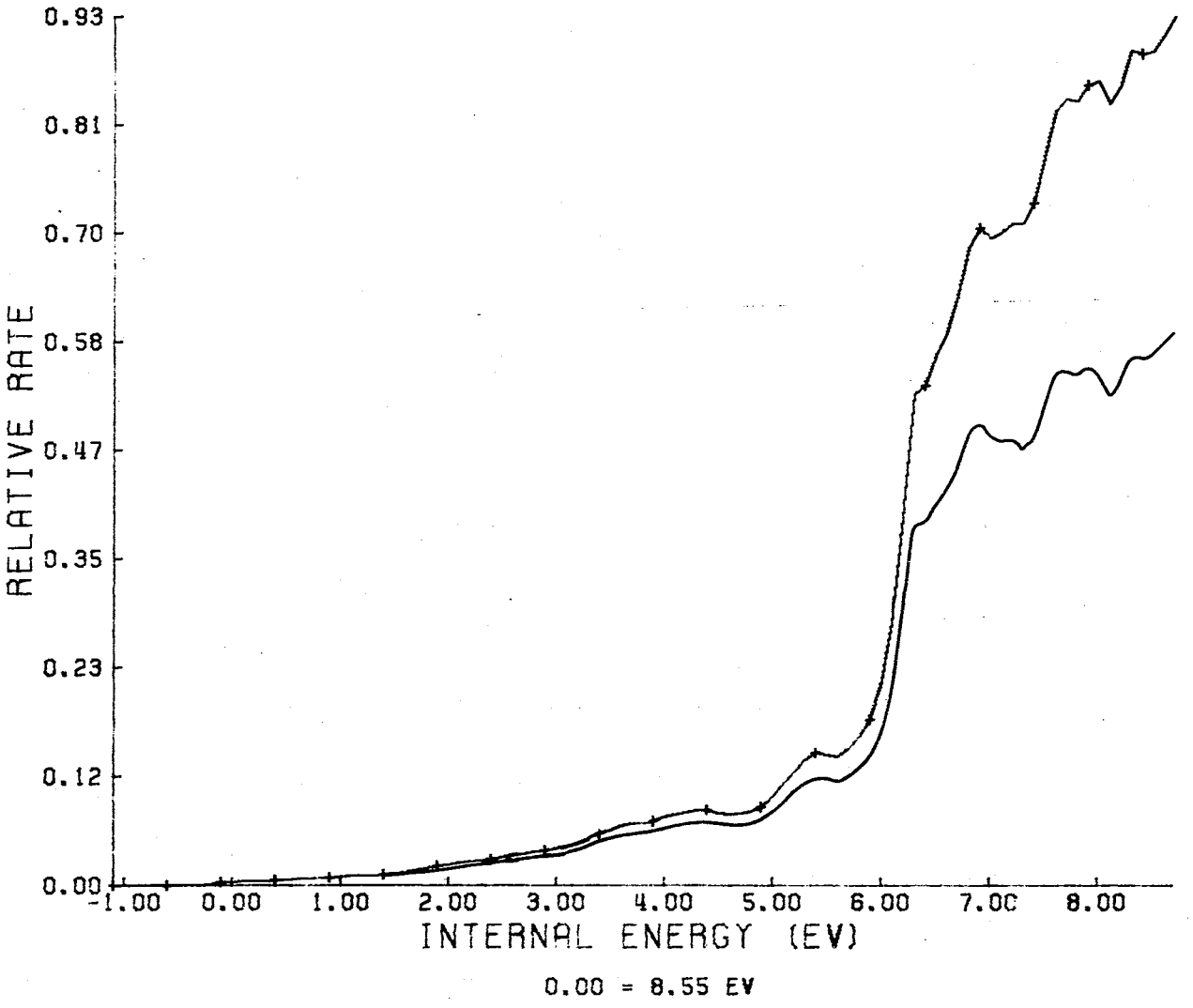

Figure 44b. Relative Rate Constant Plot of II, 250° Ion Source Temperature

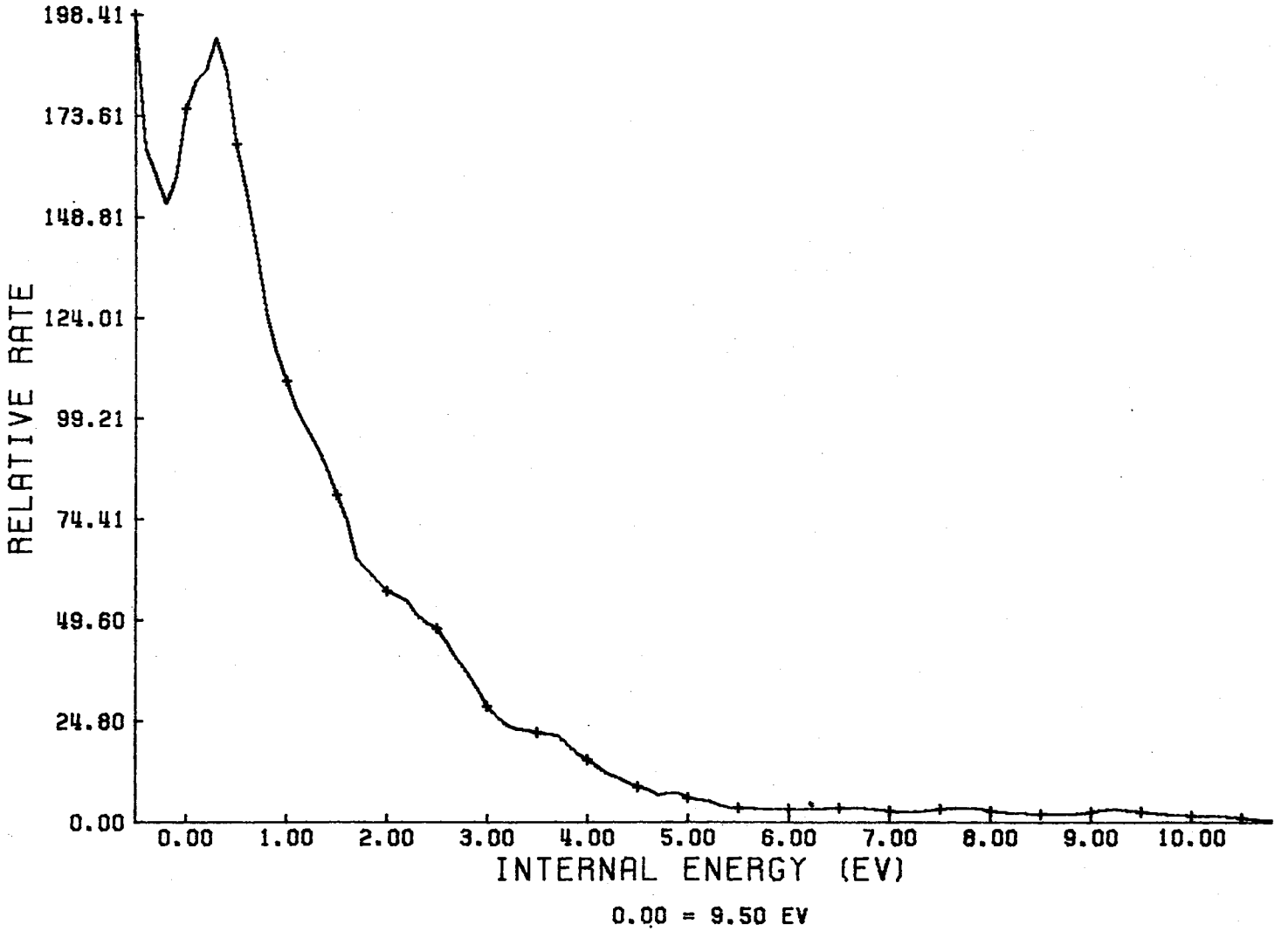

Figure 45a. Relative Rate Constant Plot of II, 310°

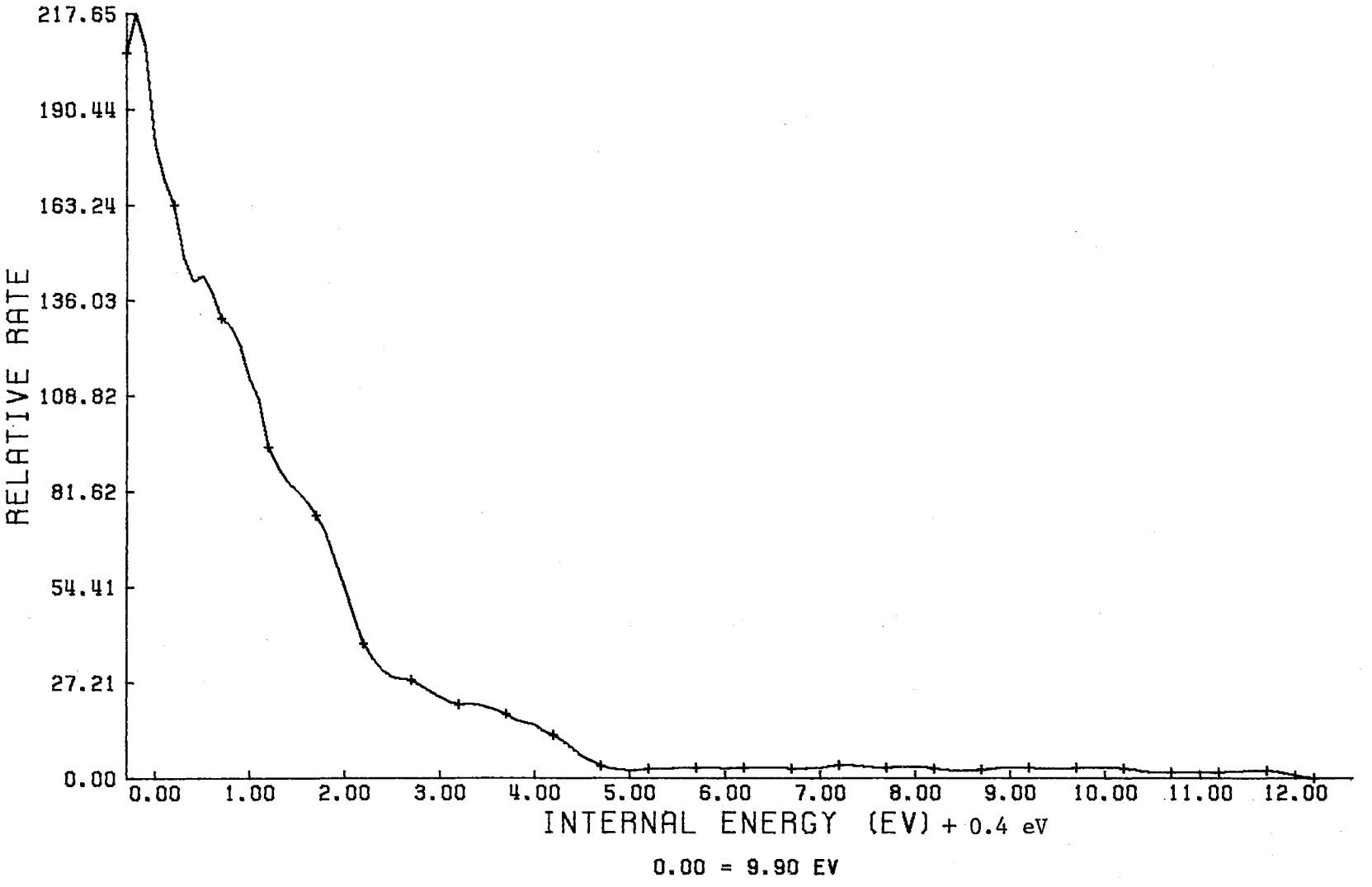

Figure 45b. Relative Rate Constant Plot of III, 250°

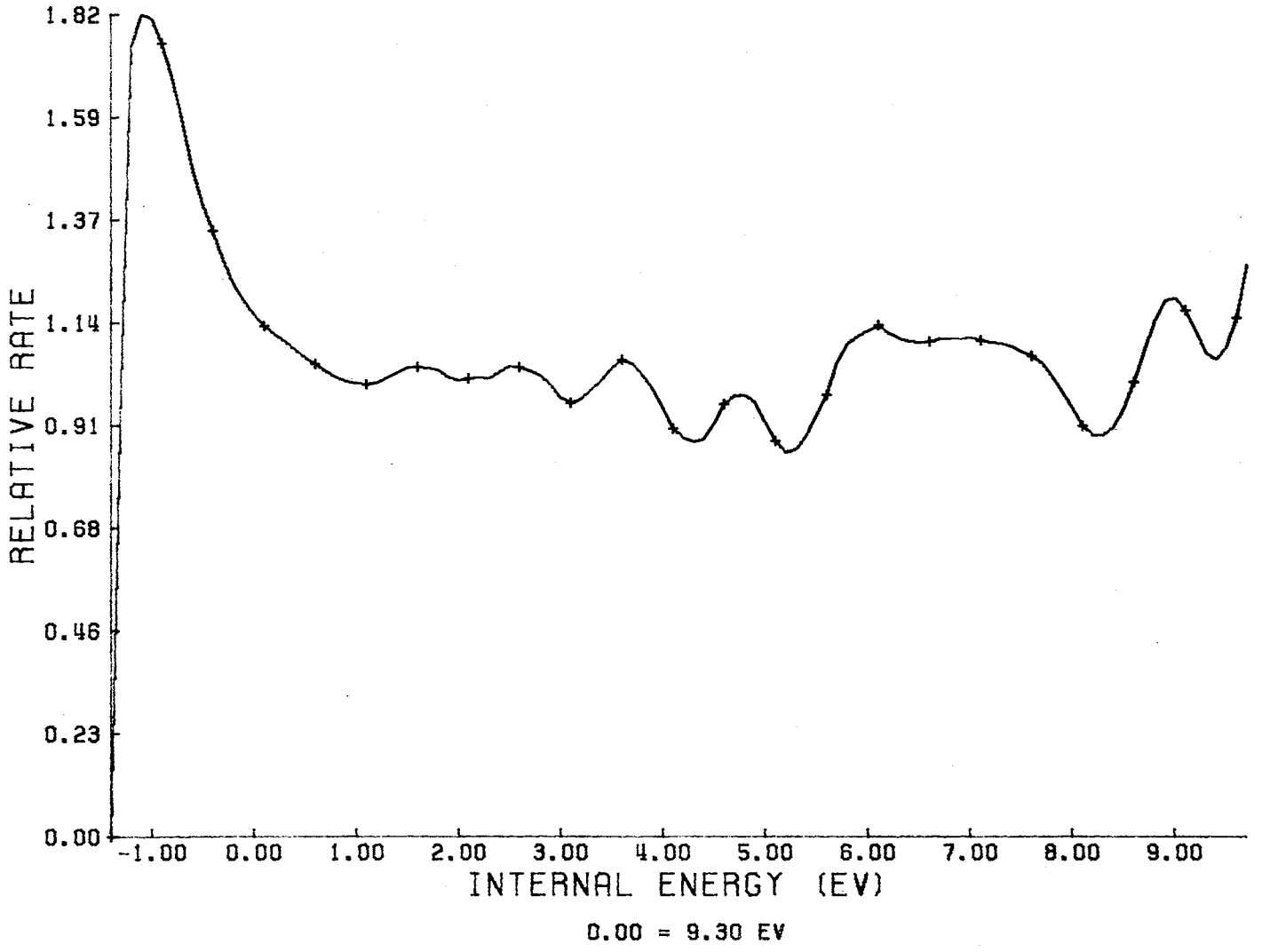

Figure 46. Relative Rate Plot of V,250°

energy. In all cases $k_1(E)$ is the rate constant for formation of the unsubstituted benzoyl moiety and $k_2(E)$ is the rate constant for formation of the substituted benzoyl moiety as a function of internal energy.

At 250° the SDIE curve for IId which derives contributions from both IIb and IIe, vide supra, was corrected for the IIe contribution by determining the SDIE curves for m/e 77 and m/e 82 ions in the mass spectra of 1-phenyl-$\underline{d}_5$-2-(4-methoxyphenyl)ethane-1,2-dione.[50] The SDIE curve for IId at 310° was corrected by assuming that the ratio of the metastable peak intensities for these two processes was equal to the ratio of the SDIE curves.

For I, at a source temperature of 310° the relative rates were calculated for four sets of SDIE curves and the values were then averaged. The smoothed curve drawn through these values is reproduced in Figure 43a. Since the presentation is unaffected by the number of points included, average values are indicated at 0.3 eV intervals for visual clarity. Deviations are shown for points separated by 0.6 eV. In general, the average deviation in any given average relative rate is ca. 10 to 25% of its value.

Figures 43b and 45-46 represent single determinations of the SDIE curves. In Figures 44a and b, both the corrected, vide supra, and uncorrected rate constant ratios are plotted.

The breakdown graphs in Figures 39-42 qualitatively show little structural dependence and are similar to the ones deduced experimentally,[4,5,6a,19] and theoretically[1,2,6d] for hydrocarbons.

From Figure 39 it is clear that the probability of detecting Ia in states corresponding to the maxima in the SDIE curve of Ia is quite low. Typically, stable Ia are collected containing only 0.1 to 0.2 eV of internal energy. A further slight increase in the internal energy produces a marked decrease in the probability of collecting stable Ia. As a result $k_2(E)$ must rise to a value of approximately 10^5 to 10^6 sec^{-1} and produce a corresponding increase in the probability of forming stable Ic. The probability of forming Ib is observed to be a slowly increasing function up to about 4.8 eV of internal energy (see Figure 39).

The breakdown graph for II (Figure 40) is similar to that for I in that only a minimal amount of internal energy is required to produce a rapid decrease in the half life of IIa, i.e., 0.2 to 0.4 eV. The rapid increase in the probability for formation of IIc parallels the decrease in the probability of forming stable IIa. The constant ratio, $k_1(E)/k_2(E)$, is a slowly increasing function up to about 5.8 eV of internal energy (see Figure 44).

The breakdown graph for III (Figure 41) reveals that the probability of forming stable IIIa decreases rapidly at internal energies 0.1 to 0.2 eV above threshold. In contrast to the behavior of Ia and IIa, competitive decompositions of the C-1--C-2 bond of IIIa result in almost complete conversion to the benzoyl ion (m/e 105), as indicated by its relative probability of 0.95 to 0.98 over an internal energy range up to 4 eV. The probability of producing IIIc is a slowly increasing function over this same range of internal energies. The above would produce a rate

constant ratio $k_1(E)/k_2(E)$ which decreases as a function of internal energy (see Figure 45).

For molecular ions of I and II possessing in excess of 5.6 eV (Figure 39a) and 6.4 eV of internal energy the breakdown graphs (Figures 39 and 40) indicate an increased probability of forming Ib and IIb. This increased probability occurring over the energy range from 4.8 to 5.6 for I and 5.4 to 6.4 for II is, as shown in Figures 43 and 44, paralleled by a discontinuous increase in $k_1(E)/k_2(E)$. Above 5.6 eV for Ia the rate attains an average value of 0.55 at a source temperature of 310 and 0.65 at 230°. For IIa above 6.0 eV similar behavior is observed at an ion source temperature of 310°. The average value is 0.50. This behavior is not observed for II at an ion source temperature of 250°. Under these conditions no clear average value is observed but the curve behaves in a nearly exponential manner. For III the energy dependence of the rate constant ratio (see Figure 45) behaves in an exponential manner. The rate constant ratio for competitive fragmentation of the 1-phenyl-$\underline{d}_5$-2-phenylethane-1,2-dione (V) molecular ion (see Figure 46) shows a random variation of ten to twenty per cent from 1 eV to 9 eV of excess energy. This result provides indirect evidence that the behavior of the rate constant ratio of I and possibly II as a function of energy do not represent a systematic error. For V the value of 0.985 for the $k_1(E)/k_2(E)$ ratio is in good agreement with the predicted value of unity. Relative rates were not calculated for internal energies in excess of 8.5 eV because at higher energies the SDIE functions for $\underline{m}/\underline{e}$ 77 and $\underline{m}/\underline{e}$ 76 + X are decreasing to

zero and those for fragment ions m/e 51 and m/e 50 + X have finite values.

Autoionization represents a possible explanation for the behavior of the rate constant ratio in those regions where discontinuities are observed but may not apply for the following reasons. For I and II the region of interest represents ionization produced by electrons possessing in excess of 14.6 eV. Chupka and Kaminsky[5] have commented that for electrons of moderate to high energies autoionization should contribute only a minor amount to the total ionization. Because of the structural similarities of I, II, and V, if autoionization were affecting the rate constant ratio this effect would have been expected for fragmentation of the molecular ion of V.

A rationale for the behavior of the rate constant ratio of I can be made in terms of isolated but not long-lived electronic states in the molecular ion. If the hypersurface for I at 5 eV of internal energy intersects the surface of the 1-cyclohepta-2,4,6-trien-1-yl-2-phenylethane-1,2-dione molecular ions VIII and IX, competition occurs between ring expansion of II to form VIII and IX and randomization of its energy over lower-lying states. Thus at these internal energies some fraction, if not all,

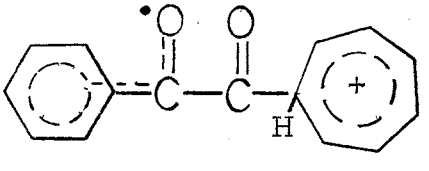

VIII

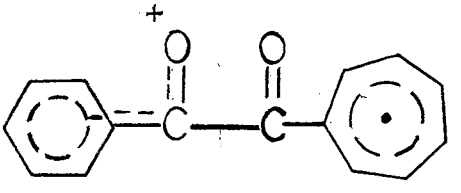

IX

(21)

of primary fragmentations will occur from states corresponding to VIII and IX. Because of charge localization, dissociation of the C-1--C-2 bond in VIII produces only m/e 119 ion, Ic, and in IX only the m/e 105 ion, Ib, with rate constants $k_2(E)$ and $k_1(E)$ respectively (see Equations 22 and 23).

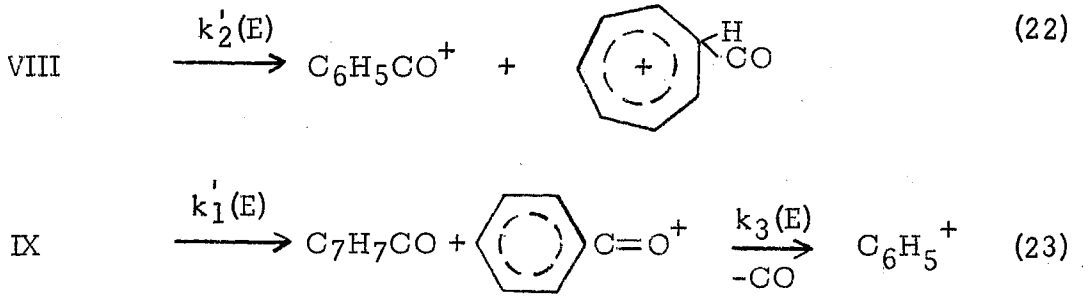

Here m/e 119, Ic, possesses a ring-expanded structure rather than that of a substituted benzoyl ion. As shown above the discontinuity in the relative rate constant ratio for I may indicate a change in mechanism.

The behavior of the relative rate constant ratio plots for II and III are believed to behave in a manner which would be predicted from QET theory. The theory would predict for the lowest energy process an exponential increase (decrease) which is observed (see Figures 44a-b and 45a-b)

Substituent effects on the ionization potential of substituted aromatic rings have been investigated extensively.[4,51-54] The correlation of ionization potential of σ^+ values implies that the description of solution processes in terms of electronic effects of substituents is realized by the simplest processes in which solvent effects have been

removed. The ionization potentials obtained from a) experimental SDIE curves and b) calculated values are plotted versus σ^+ for the substituent in Figure 47. Although a least-squares line could be drawn through the points the values of the slope would have little significance owing to the errors associated with the experiment and conformational factors. However a correlation exists between σ^+ for the substituent and the ionization potential of the molecule.

The rate constant ratios $k_S(E)/k_H(E)$ versus σ values for the substituent at three values of the internal energy are plotted in Figures 48-49. The correlation becomes very poor above 5 eV of internal energy. This behavior may be due in part to the following: a) the errors associated with the SDIE values used to compute the relative rate constant increase with increasing internal energy, and b) the second derivative technique underestimates the P(E) function for higher-energy processes (see discussion of ion intensities and the P(E) function). Rho is found to decrease with increasing internal energy (see Table XVI). A decrease in ρ is expected since as the internal energy of the molecular ions increase the differences in the activation energies for the competitive bond rupture are being overcome. In a recent publication by Munson and Einolf[55] the ratio of intensities of the substituted benzoyl to the unsubstituted benzoyl ions is correlated with the σ constants. From a tablation of experimental and calculated ion intensities, vide post, for I, II, and III these ratios were calculated and compared to the values obtained above. The values for the ratios for I and II at 70 eV are in good agreement with the values

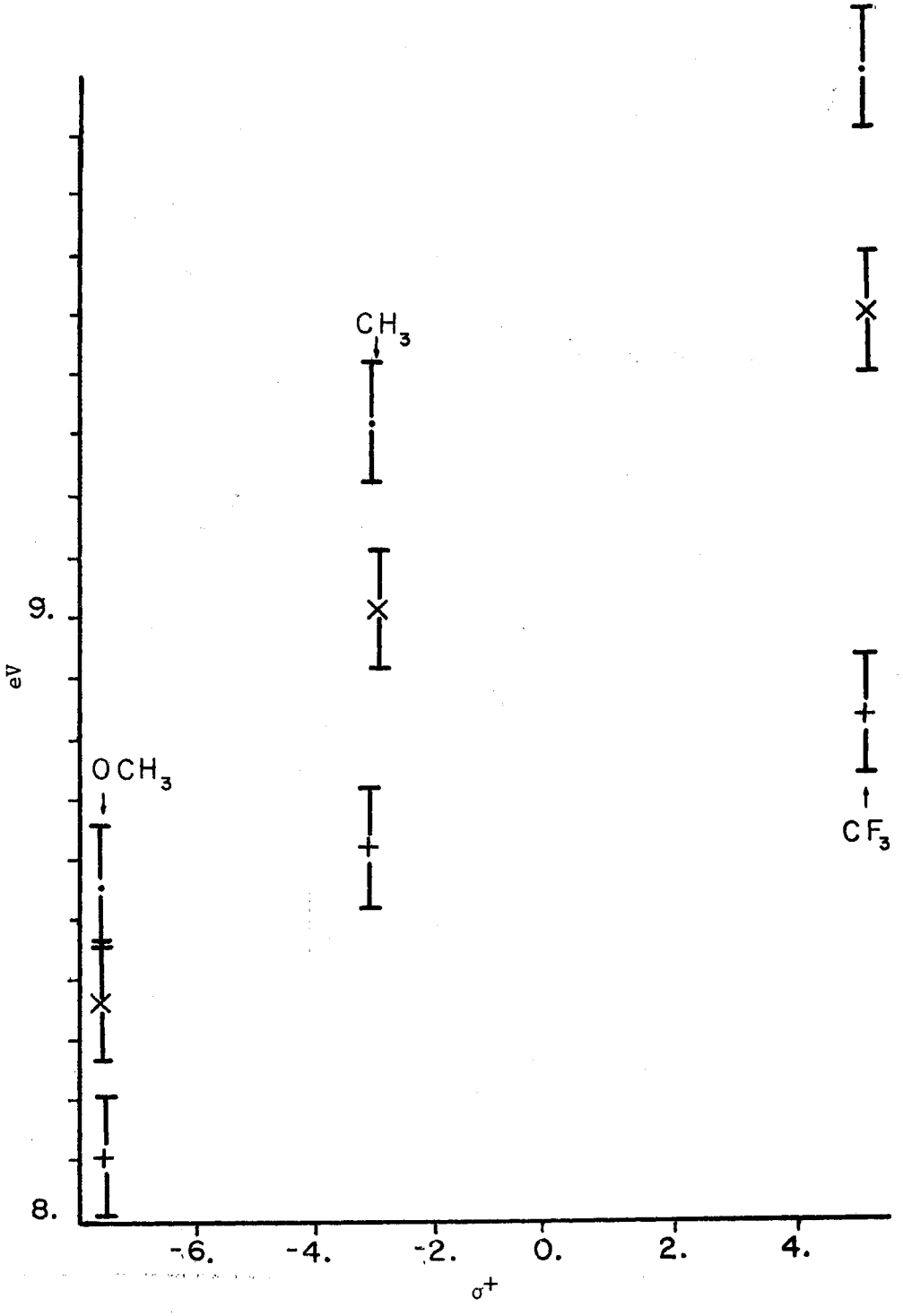

Figure 47. Plot of Ionization Potentials of I, II, III, and IV vs. σ^+

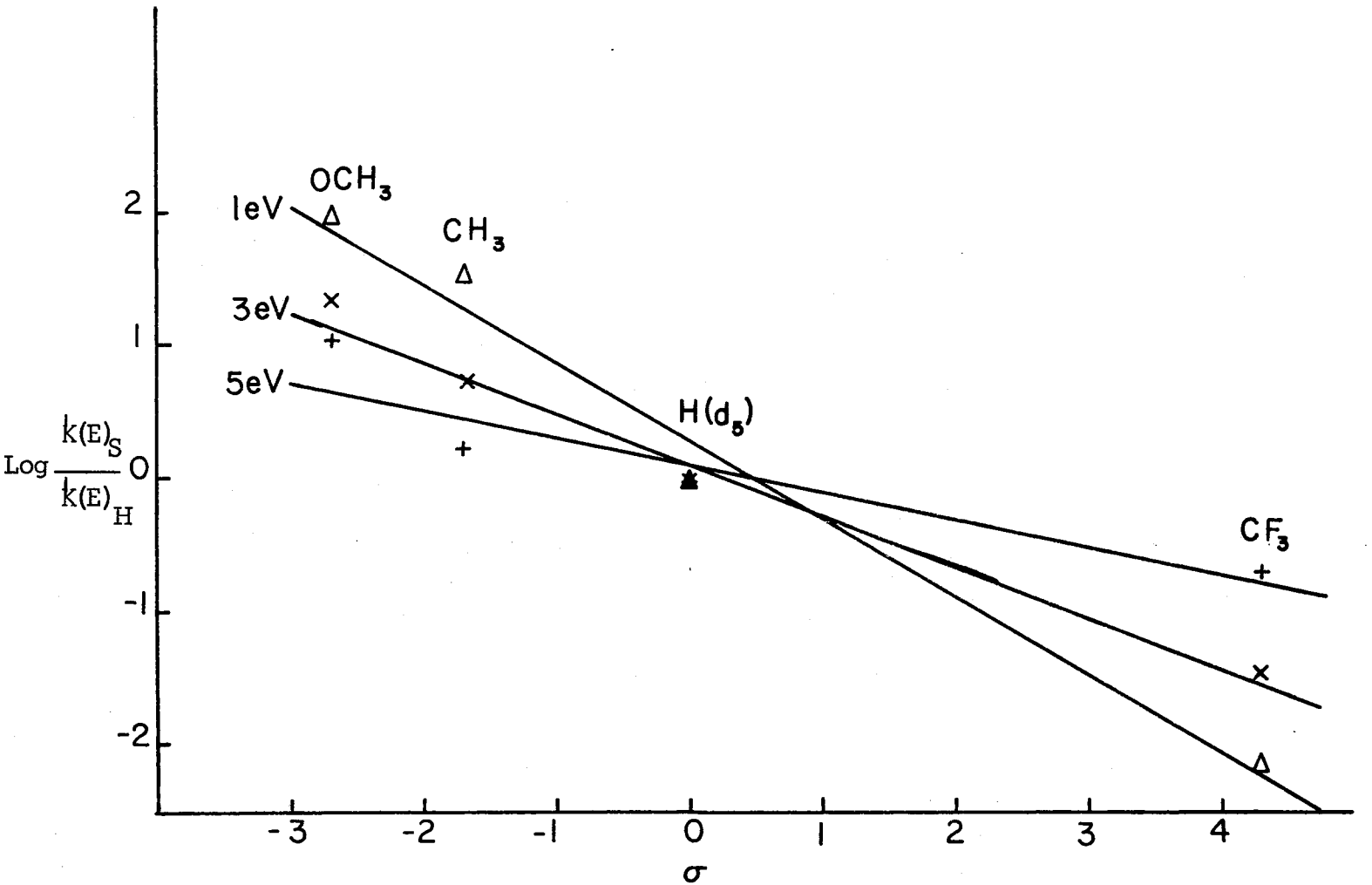

Figure 48. Log $k(E)_S/k(E)_H$ vs. σ at Three Values of the Internal Energy, 250° Ion Source Temperature

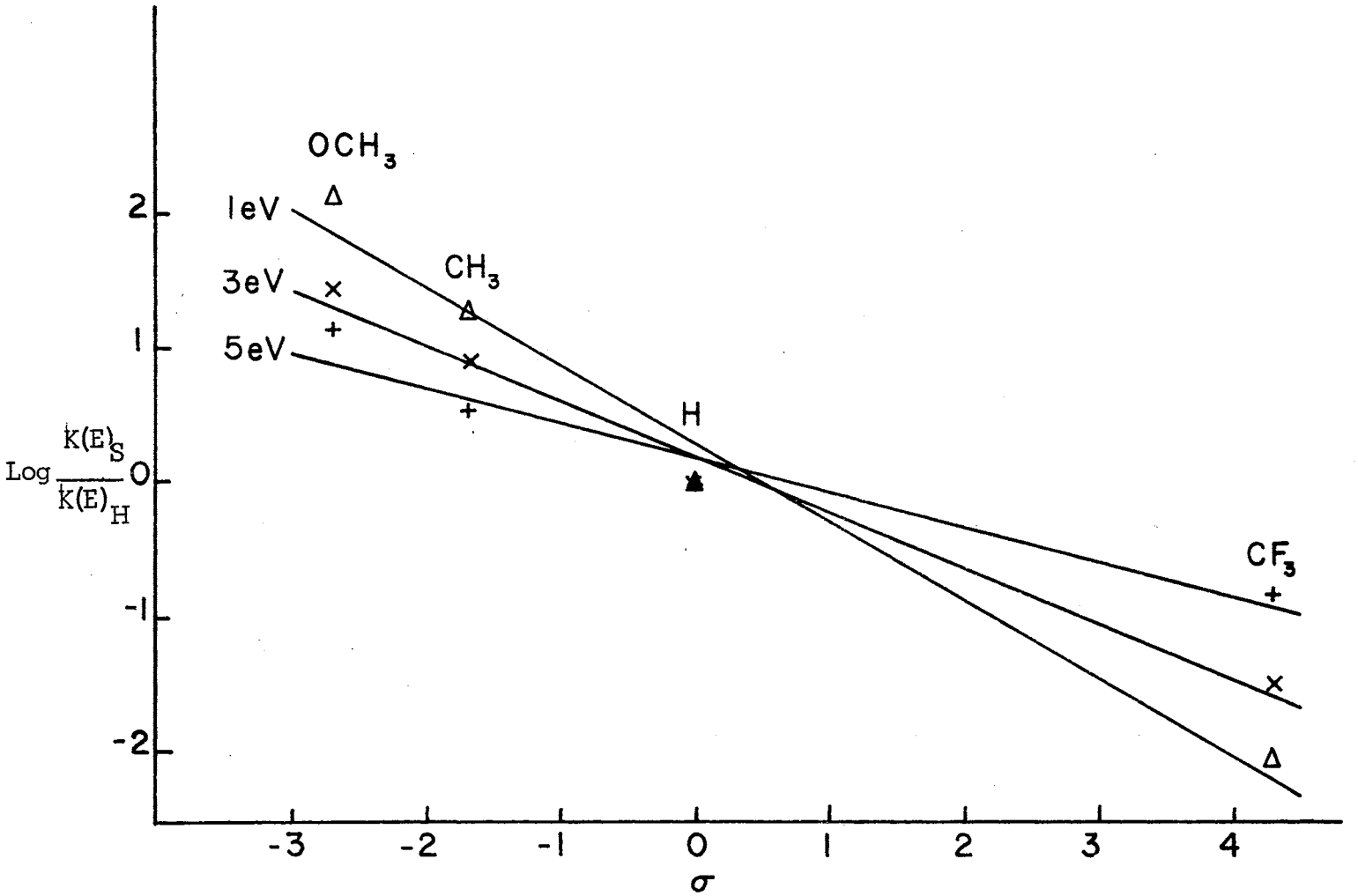

Figure 49. Log $K(E)_S/K(E)_H$ vs. σ at Three Values of the Internal Energy, 310° Ion Source Temperature

TABLE XVI

RELATIONSHIP OF ρ AND INTERNAL ENERGY

I.E., eV	ρ^a	ρ^b
1.	$-6.0 \pm .5$	$-5.9 \pm .6$
3.	$-3.9 \pm .3$	$-4.2 \pm .4$
5.	$-2.1 \pm .5$	$-2.6 \pm .5$

[a]Ion source temperature 230°.

[b]Ion source temperature 310°.

reported by Munson.[55] For II there is a discrepancy of a factor of two at 70 eV and a factor of about seven at 15 eV. For I and II the ratios at 15 eV disagree by a factor of 1.5 for I and 4 for III. The difference in ion ratios at low eV in this work and that of Munson[55] may be due to the energy axis calibration or lack of calibration by the latter. For II the disagreement of ion ratios at 70 eV could be from an ion source temperature effect since Munson operated the source some 200° lower than in this work.

The energy deposition functions,[5,18] P(ED), applicable to the 70 eV mass spectrum of I, II, III, and V are reproduced in Figures 50-53. Even if the second derivative technique yielded the exact P(ED) function the experimental P(ED) functions obtained from this study would be incomplete owing to neglect of processes occurring in excess of 20 - 22 eV. These P(ED) functions encompass wider range of internal energies than

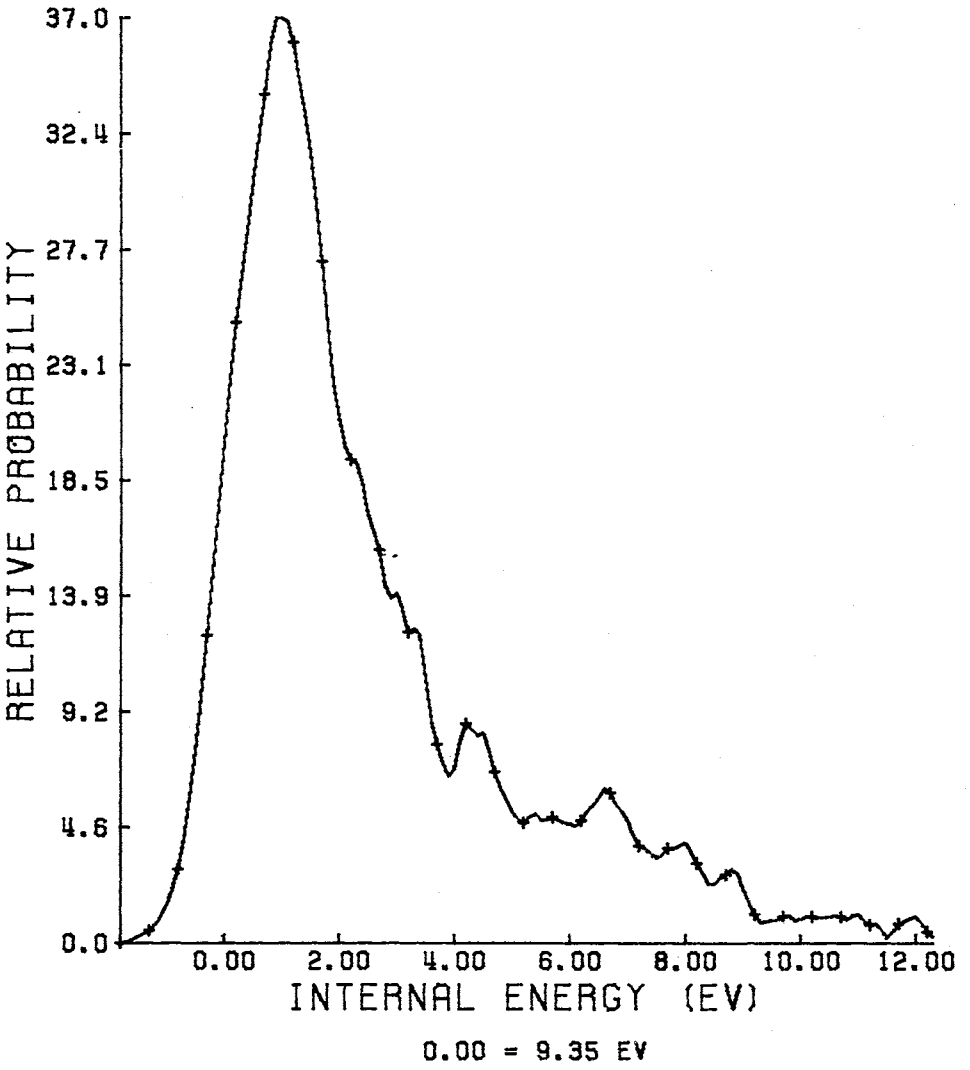

Figure 50a. Energy Deposition Function for Ia, 230° Ion Source Temperature

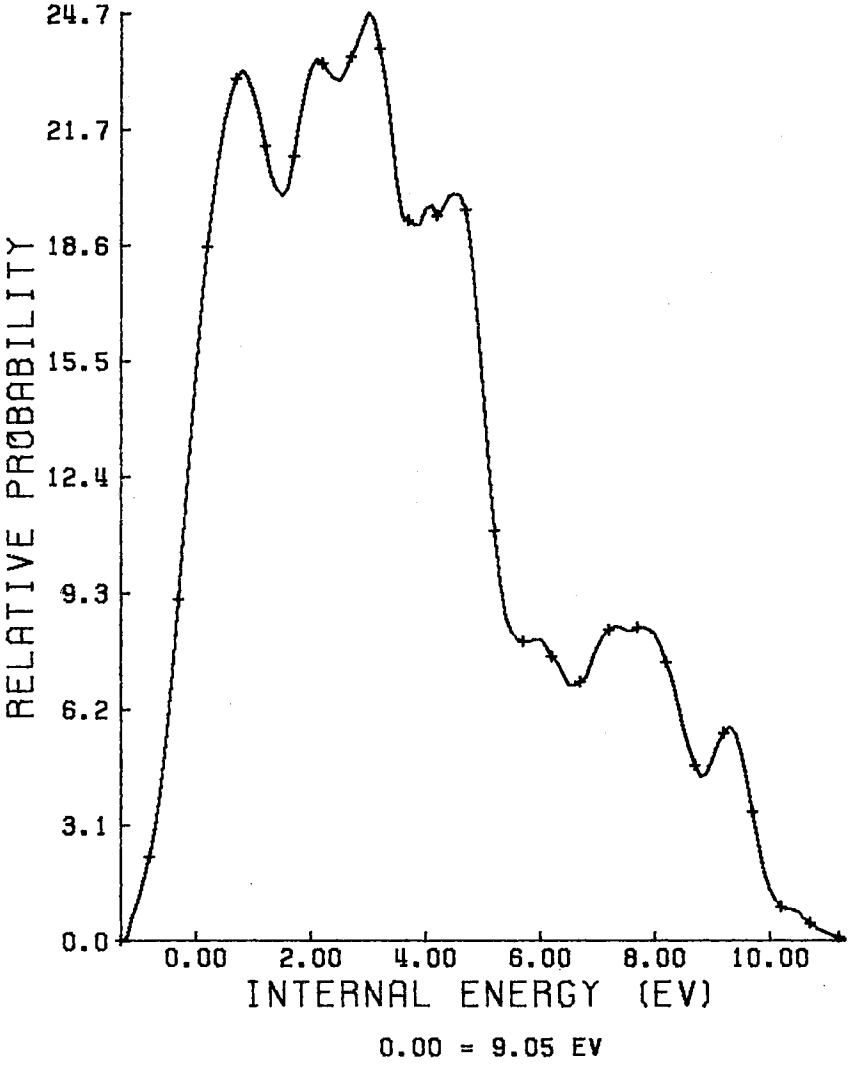

Figure 50b. Energy Deposition Function for Ia, 310° Ion Source Temperature

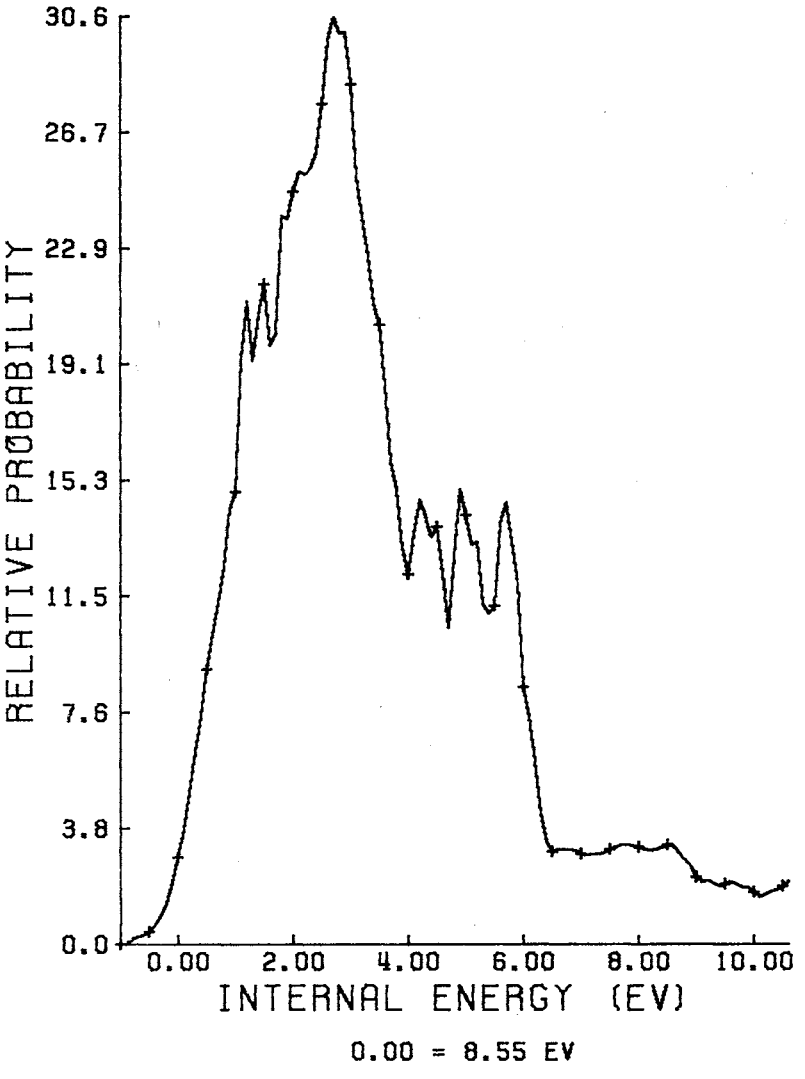

Figure 51a. Energy Deposition Function for IIa, 250° Ion Source Temperature

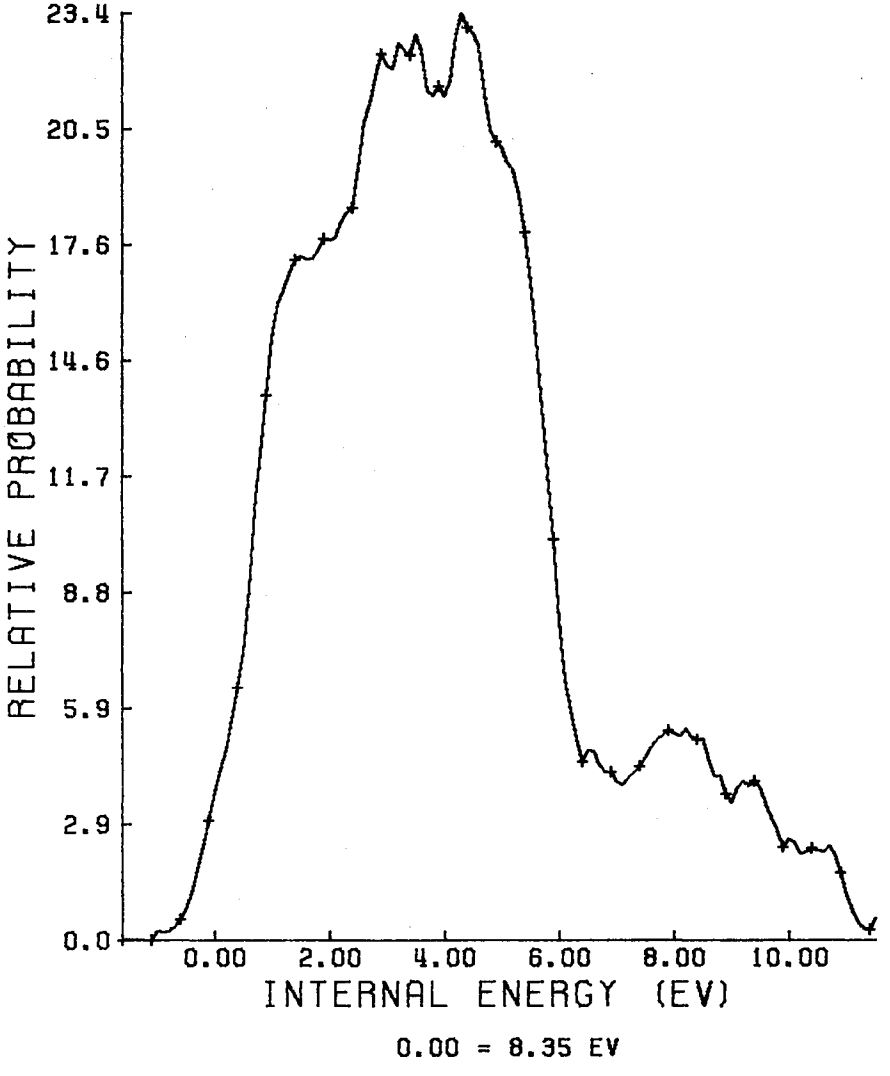

Figure 51b. Energy Deposition Function for IIa, 310° Ion Source Temperature

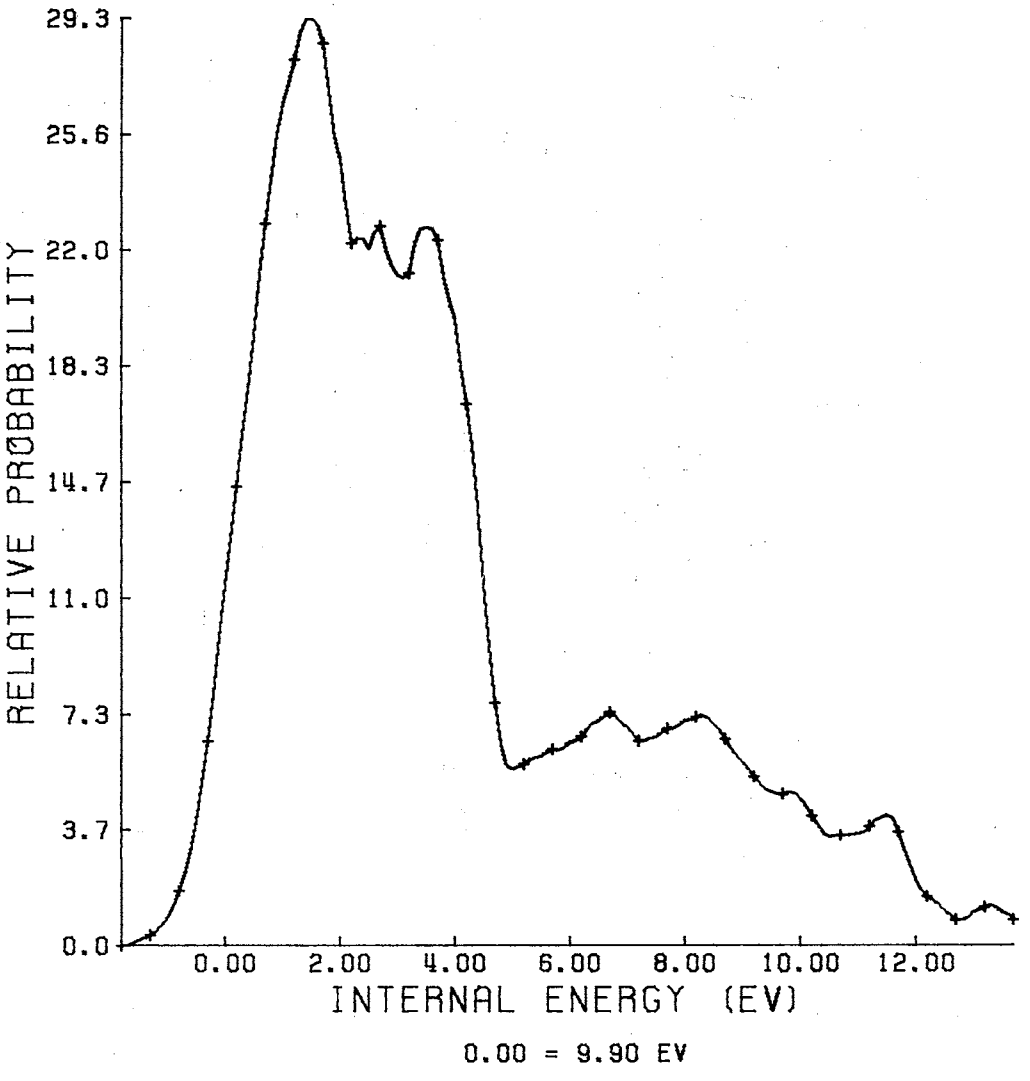

Figure 52a. Energy Deposition Function for IIIa, 250° Ion Source Temperature

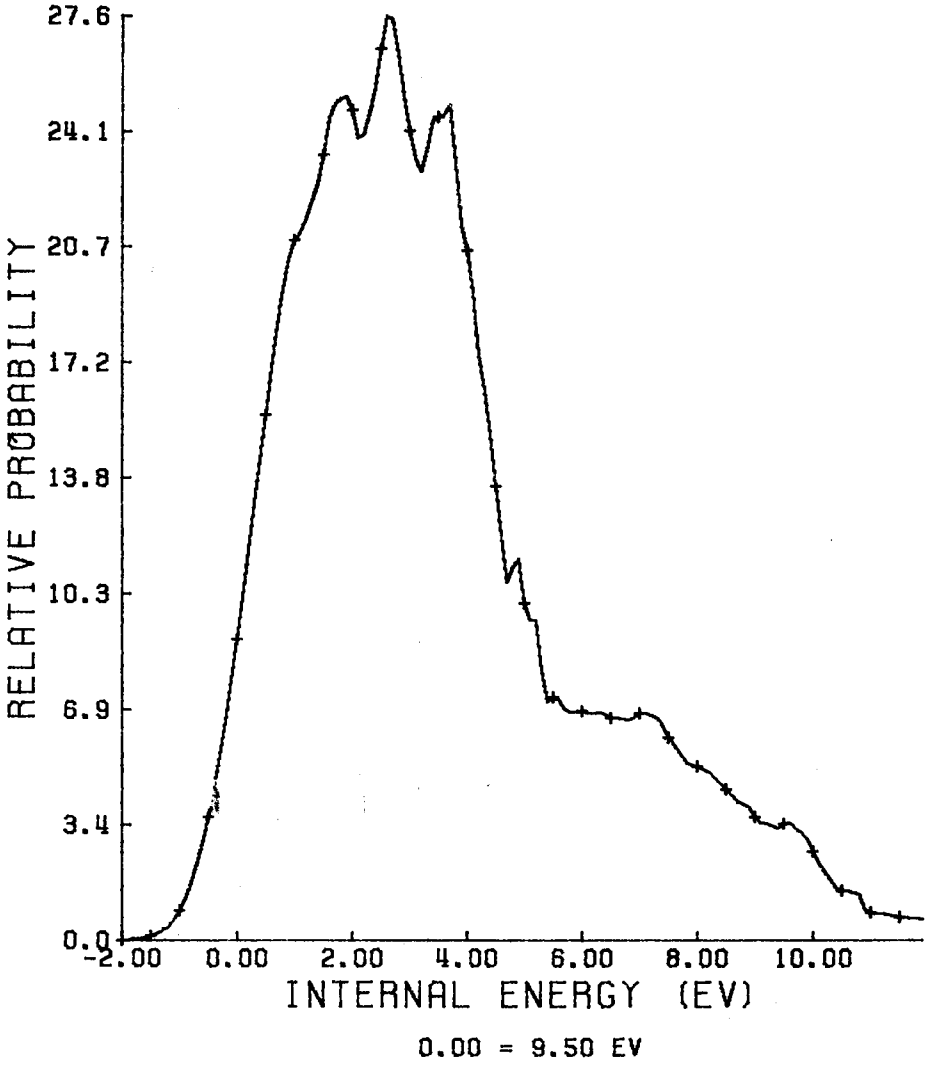

Figure 52b. Energy Deposition Function for IIIa, 310° Ion Source Temperature

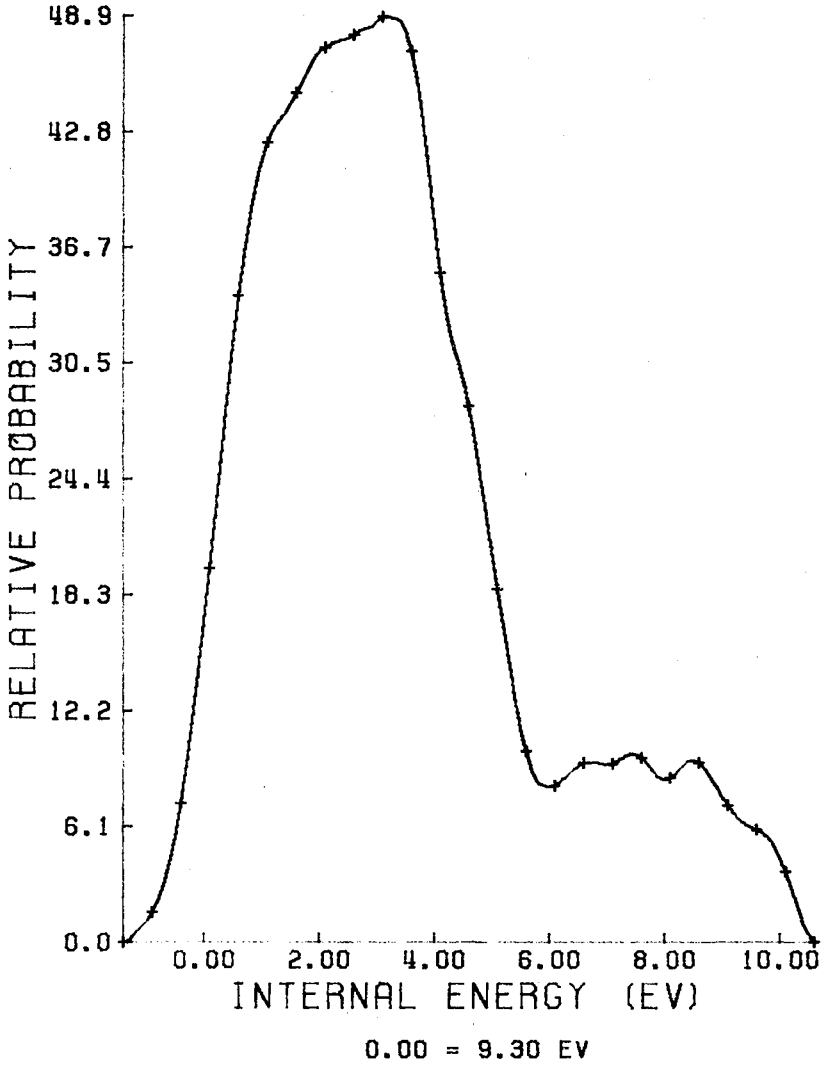

Figure 53. Energy Deposition Function for V, 250° Ion Source Temperature

the ones applicable to propane and butane,[5] but include approximately the same range of internal energies as those for 1,2-diphenylethane.[15] The effect of lowering molecular energy upon the P(ED) function is to cause a decrease in the probability of producing molecular ions with high values of the internal energy. For comparison the total area under the P(ED) curves (Figures 50-53) are two values of the ion source temperature are tabulated in Table XVII. As predicted[44] the total electronic transition probability (which is proportional to the area under the P(ED) curve) does not appear to show a great dependence upon vibrational and rotational

TABLE XVII

TOTAL AREA UNDER THE P(E) CURVES, FIGURES 39-42, FOR I, II, AND III AS A FUNCTION OF TEMPERATURE

Compound	Relative Area[a] 250°	Relative Area[a] 310°	Ratio $A_{250^{\circ}}/A_{310^{\circ}}$
I	138.6[b]	149.8	0.93
II	119.8	127.3	0.94
III	148.7	137.5	1.08

[a]Sum of the integrated SDIE curves.

[b]Ion source temperature of 230°.

excitation. It is evident from the data (Figures 50-53) that an increase in molecular temperature results in a broadening of P(ED). The present data

suggest that there are many closely spaced low-lying electronic states of the ion and the band envelopes describing their formation overlap enough to cancel any broadening near threshold. However, at higher internal energies this is not the case, the net result being an increase in the cross section at higher internal energies.

Tables XVIII-XX present calculated and experimental ion intensities as a function of ion source temperature and calibrated electron energy scale. Normalization of the intensities to the base peak was performed. For simplicity of comparison, if the base peak could not be calculated from the dI/dE data the next largest peak which could be calculated was normalized to a value of 100. In some instances the FDIE curve was extrapolated linearly past its maximum value in order to integrate up to the desired eV. The values so obtained are labeled as approximations. Because of the threshold law, calculation of the intensity of a given ion produced by low-eV electrons requires a double integration of the SDIE curve or a single integration of the FDIE curve. The integrations were performed using Simpson's rule. As seen in Tables XVIII-XX, good agreement is obtained between calculated and experimental low-eV ion intensities. Thus the experimental data (see Appendix A), correspond essentially to the first derivative of the ionization efficiency.

The experimental ion intensities of the 70 eV spectra for I, II, and III and those obtained from a single integration of the SDIE curves are found to be in reasonable agreement. In all cases the largest discrepancy occurs for those ions whose SDIE curve extends to high energies or which

TABLE XVIII

EXPERIMENTAL AND CALCULATED ION INTENSITIES FOR I

Source Temperature 310° C

m/e Ion	70 eV Exp.	70 eV Calc.	18 eV Exp.	18 eV Calc.	15 eV Exp.	15 eV Calc.	10 eV Exp.	10 eV Calc.
224	1.3	1.3					4.3	4.2
119	100.0	100.0			100.0	100.0	100.0	100.0
105	20.2	16.8	100.0	100.0	9.0	8.1	3.2	5.1
91	26.3	25.8		71.0	2.7	2.2		
77	15.7	5.9		10.7	0.3	0.2		

Source Temperature 230° C

m/e Ion	70 eV Exp.	70 eV Calc.	20 eV Exp.	20 eV Calc.	15 eV Exp.	15 eV Calc.
224	3.67	3.58				
119	100.0	100.0			100.0	≃100.0[a]
105	19.1	12.1	100.0	≃ 100.0[a]	9.4	6.1
91	23.8	15.4			2.1	1.6
77	16.1	7.5	22.6	19.8	0.5	0.1

[a]Extrapolated

TABLE XIX

EXPERIMENTAL AND CALCULATED ION INTENSITIES FOR II

Source Temperature 310° C						
Ion m/e	70 eV Exp.	70 eV Calc.	21 eV Exp.	21 eV Calc.	16 eV Exp.	16 eV Calc.
240	0.4	0.5				
135	100.0	100.0			100.0	≃ 100.0[a]
107	5.7	8.1	94.8	≃ 81.8[a]	1.8	2.0
105	7.4	5.4	64.3	≃ 69.8[a]	1.4	2.1
77	21.1	13.4	100.0	100.0	0.5	0.7

Source Temperature 250° C						
Ion m/e	70 eV Exp.	70 eV Calc.	21 eV Exp.	21 eV Calc.	16 eV Exp.	16 eV Calc.
240	1.2	1.3				
135	100.0	100.0			100.0	100.0
107	5.9	5.8	100.0	≃ 100.0[a]	1.0	1.3
105	7.4	3.5	76.8	≃ 77.4[a]	1.6	1.7
77	20.9	9.4	94.0	98.3	0.1	0.4

[a]Extrapolated

TABLE XX

EXPERIMENTAL AND CALCULATED ION INTENSITIES FOR III

Ion m/e	70 eV Exp.	70 eV Calc.	20 eV Exp.	20 eV Calc.	15 eV Exp.	15 eV Calc.
Source temperature 310° C						
278	0.3	0.3				
173	8.9	6.3	39.6	41.1	2.2	2.2
145	11.4	6.5	12.8	11.0	0.1	0.1
105	100.0	100.0			100.0	100.0
77	39.8	24.4	100.0	100.0	0.8	1.8
Source Temperature 250° C						
278	0.5	0.6				
173	8.7	7.2	41.4	53.2	1.7	2.0
145	10.9	9.1	11.3	12.0	0.1	0.1
105	100.0	100.0			100.0	100.0
77	37.5	31.6	100.0	100.0	0.9	0.9

are formed by high energy pathways. The low value for the calculated intensities of these ions does not represent experimental error since Simpson's rule integration of FDIE up to its experimental maximum recovers the experimental ion intensity. The observed discrepancy for ions produced by 70 eV electrons between the calculated and experimental ion intensities is indicative of a nonlinear threshold law for formation.

This research shows that ionization potentials of complex organic molecules can be experimentally determined with reasonable precision using the second differential technique. These values may be an upper limit due to the electron beam spread, which would mask lower maxima in the SDIE curves. The agreement is reasonable between the experimental and calculated ionization potentials for I-III but in all cases the experimental ionization potential is higher than the calculated value. For the molecules in this study we were unable to obtain meaningful appearance potentials for ions produced from the high energy primary pathway and for second generation fragment ions in general. The factors which affect the SDIE curve of fragment ions, i.e., beam energy spread and closely spaced ionic states, result in broad curves with no well defined maximum corresponding to the appearance potential. In this work the inability to assess appearance potentials casts serious doubt upon other methods using ionization efficiency curves as their basis. The calculation of the appearance potentials for the primary and secondary daughter ions of Ia, IIa, and IIIa from tabulated heats of formation and/or reasonable estimates of these values gave appearance potentials which were in coincidence with the

low-energy tail of the SDIE curves. This indicates these calculated values are not gross underestimates of the appearance potentials. Correlation of the experimental or calculated ionization potentials with σ^+ was found which indicates that near threshold there is a relationship between electronic effects and the amount of energy necessary to produce ionization. The correlation of the relative rate constant ratios with σ values is found to be dependent upon ion internal energy. Rho for the correlation is negative and decreases as a function of energy. This phenonmenon may be rationalized in terms of the activation energies for the competitive cleavage. The energy deposition functions obtained by the second derivative technique are a good approximation for all ions except Id and IId as indicated from calculated ion intensities. The effect of a temperature increase upon production of higher-energy molecular ions is demonstrated by the increased probability of the P(ED) function at higher energies.

Suggestions for further work include a) the synthesis and analysis of other monosubstituted benzils in order to gain confidence in the Hammett correlations obtained in this study, b) further investigation of the effect of rotational and vibrational energy upon the energy deposition function, and c) a radical change (see Figure 54) in the method of obtaining the first derivative of the ionization. This method would allow rapid scanning of a given energy range using a voltage ramp generator and a multichannel analyzer for signal collection. The rapid scan of the voltage would eliminate effects such as sample pressure drift and instrumental instability.

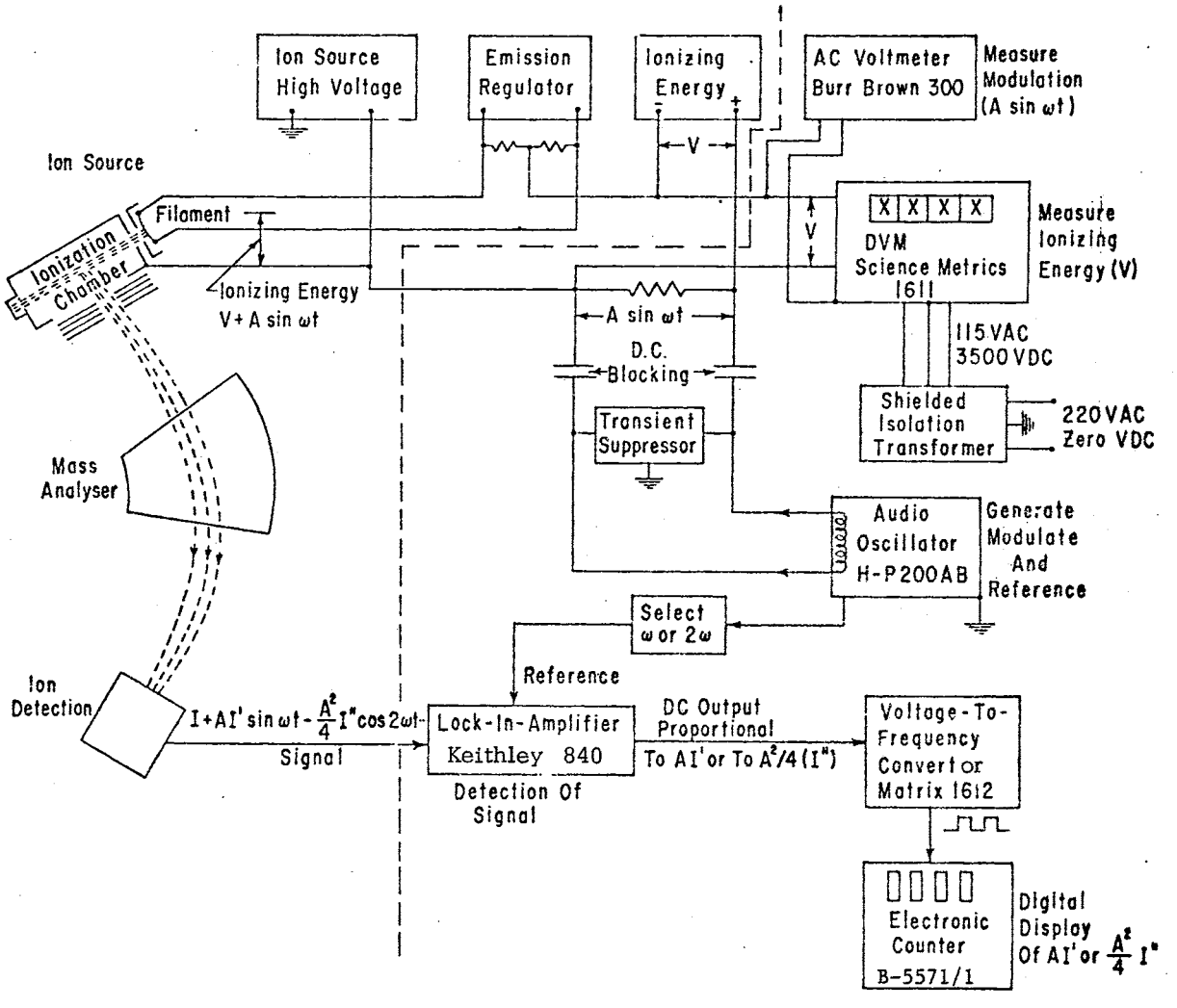

Figure 54. Instrument Arrangement for Acquisition of dI/dE Values

For purposes of data handling this system would be readily adaptable to either a mini-computer or a remote computer terminal.

CHAPTER III

EXPERIMENTAL

Synthesis of 1-(4-Methylphenyl)-2-phenylethane-1,2-dione (I)

Bis(4-methylphenyl)cadmium was prepared by first treating 32.8 g (1.35 moles) of magnesium turnings suspended in ether with 226.7 g (1.33 moles) of 4-bromotoluene, dissolved in anhydrous ether, followed by addition of 123.7 g (0.675 mole) of anhydrous cadmium chloride. The ether was distilled out of the reaction flask and an equivalent amount of anhydrous benzene was added. Phenylacetyl chloride[56] (193.1 g, 0.125 mole) was added dropwise and the reaction mixture was then hydrolyzed by addition of cold fifteen per cent sulfuric acid. The organic layer was separated, washed with water, neutralized (5% Na_2CO_3), dried ($MgSO_4$), filtered and concentrated. Recrystallization from ethanol gave 38.7 g (0.184 mole) of p-tolyl benzyl ketone. The product was dissolved in glacial acetic acid, selenium dioxide[57] (20.4 g, 0.184 mole) added, and the suspension refluxed for three hours. The elemental selenium was removed by filtration and the filtrate extracted with ether. The ether extracts were neutralized (5% Na_2CO_3), washed with water, dried ($MgSO_4$), filtered and concentrated. A solution of the yellow oil in ethanol was refluxed for two hours with 50 ml. of hydrochloric acid (20%) and 2.0 g

decolorizing charcoal and then filtered. Ether was added and the aqueous layer separated and extracted with ether. The combined ether portions were neutralized (5% Na_2CO_{30}), washed with water, dried ($MgSO_4$), filtered, and concentrated, giving 33.5 g of crude I. Distillation gave I as the major fraction (b.p. 132.5° - 133.5° @ 0.27 mm) which crystallized from n-pentane at 0°. Five subsequent recrystallizations gave 32.5 g (11.9%) of I, m.p. 28.8° - 29.0° (lit. 31°).[58]

Synthesis of 1-(4-Methoxyphenyl)-2-phenylethane-1,2-dione (II)

P-anixyl benzyl ketone (4.5 g, .02 mole, Aldrich Chemical Co.) was added to a suspension of selenium dioxide[57] (5.5 g, .05 mole) in 50 ml. of anhydrous dioxane and the mixture refluxed for three hours. The selenium (1.4 g, .017 mole) was removed by filtration. After addition of 200 ml. water the filtrate was refluxed (18 hours) with decolorizing charcoal (20.0 g) and then extracted with ether three times. The combined ether extracts were neutralized (5% Na_2CO_3), dried ($MgSO_4$), and concentrated under reduced pressure, yielding a yellow oil which crystallized from carbon tetrachloride and gave after four recrystallizations 1.69 g (35%) of II, m.p. 62.0° - 62.7° (lit. 61° - 62°).[59]

Synthesis of 1-(3-Trifluoromethylphenyl)-2-phenylethane-1,2-dione (III)

Meta-bromobenzotrifluoride[60] (25.7 g, 0.114 mole) was added dropwise to a suspension of magnesium turnings (3.1 g, 0.125 mole) in

anhydrous ether. The resultant solution was added dropwise to an anhydrous ether solution of phenylacetaldehyde (12.7 g, 0.114 mole) over a period of one hour. The reaction mixture was hydrolyzed with a saturated rochelle salt solution, the ethereal layer was separated, and the aqueous layer was extracted with ether. The combined ether extracts were neutralized (5% Na_2CO_3), dried ($MgSO_4$), filtered, and concentrated under reduced pressure. Oxidation[61] of the crude product with selenium dioxide (8.4 g, 0.076 mole) as before gave a viscous oil which gave upon distillation 2.5 g of a yellow oil, b.p. 125° - 170° @ 0.75 mm. The crude product after treatment with decolorizing charcoal (see preparation of I) gave a yellow oil (1.4 g) which consisted of 65.8% of III by GLC analysis (0.25 inches x 20 feet, 5% SE-30 on 100/120 Chromosorb-W @ 230°). The neat oil crystallized after standing for several weeks. Recrystallization from carbon tetrachloride yielded III, m.p. 65.2° - 66.0° (lit. 65°).[62]

Synthesis of 1-(Phenyl-$\underline{d}_5$)-2-phenylethane-1,2-dione (V)

Oxidation[61] of 1-(phenyl-$\underline{d}_5$)-2-phenylethanol (2.0 g, 0.01 mole), vide post, followed by treatment of the crude product with selenium dioxide (1.11 g, 0.01 mole), gave V (1.65 g, 77.5%). Recrystallization three times from carbon tetrachloride yielded V melting at 93.8° - 94.1° (lit. 94° - 95°).[63]

Instrumentation

The mass spectra of I, II, III, IV, and V and the first derivative of the ionization efficiency curves for the various ions were determined using the LKB 9000 mass spectrometer. Xenon was introduced into the ion source via the direct probe as modified for gas analysis. To maintain uniform sample pressure all compounds were introduced into the ion source via the gas chromatograph inlet and separator systems. The relevant ion source parameters and inlet conditions for I - V are given in Appendix A. The trap current was maintained constant at 20 μA and the electron shield was at zero potential with respect to the filament. Except for spectra recorded at 70 eV both spectra and dI/dE data were obtained with the extraction plates near the block potential. To optimize peak shape and ion intensity the source slit was 0.1 mm and the collector slit 9.75 - 0.9 mm depending upon the compound being analyzed. First derivative data were obtained by modifying[38] the LKB 9000 (see Figure 55) to allow modulation of the ionizing voltage. The modulation frequency and voltage were 595 *Hz* (generated from a H-P 200B Audio Oscillator) and 0.075 V peak to peak (measured on a Burr Brown 300 AC voltmeter) respectively. The dI/dE data were read from a Beckman Model 5571/1 electronic counter which was driven by the output from a Matrix Model 1612 voltage-to-frequency converter. The electron energy was measured with a Science Metrics 1611 digital voltmeter and was manually increased in 0.100 ± 0.003 eV steps. The lock-in amplifier was a Keithley Model 840.

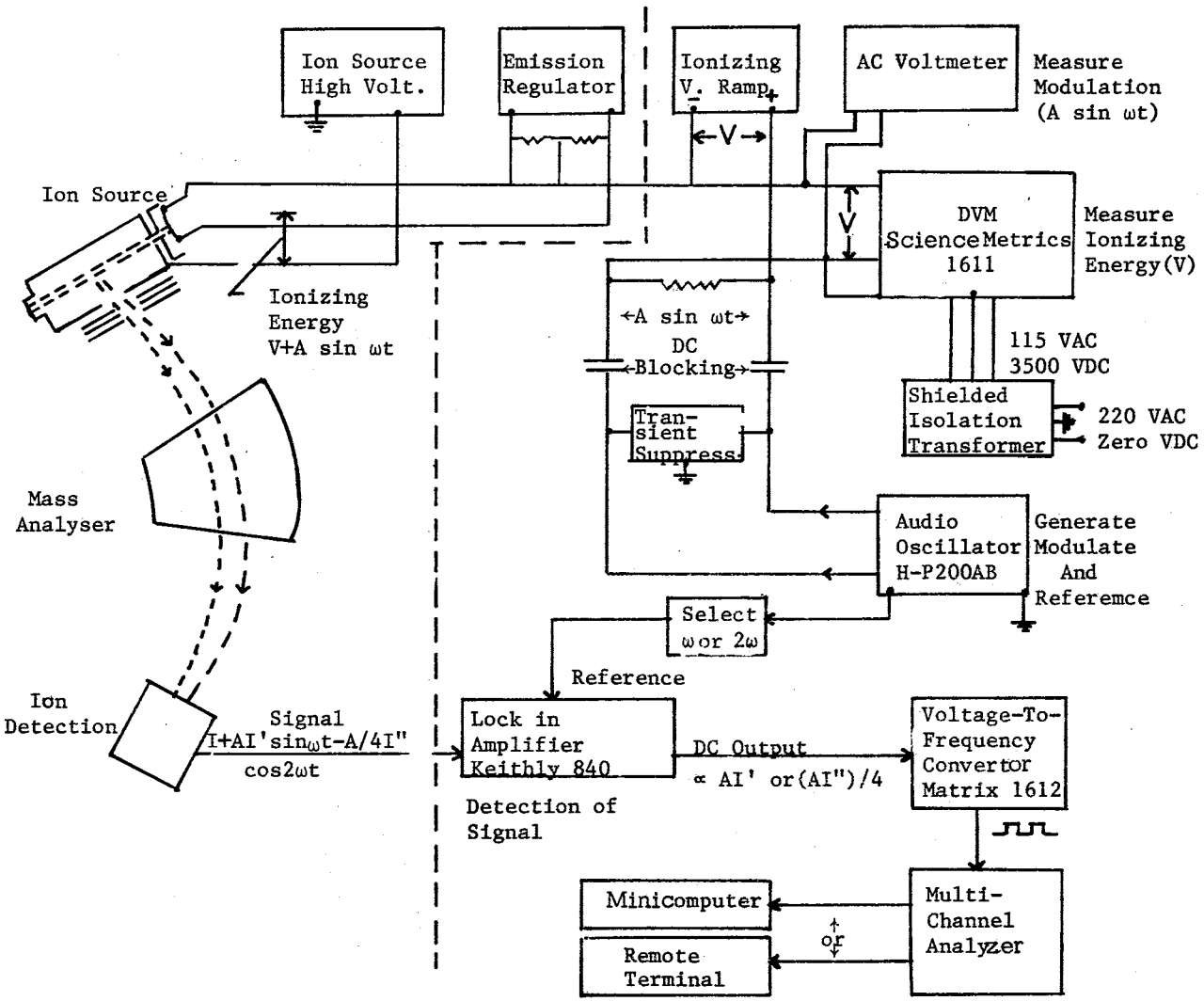

Figure 55. Measurement of Derivatives of Ionization Efficiency

BIBLIOGRAPHY

1. (a) H. M. Rosenstock, M. B. Wallenstein, A. L. Wahrhaftig, and H. Eyring, Proc. Natl. Acad. Sci. U.S., 38, 667(1952); (b) H. M. Rosenstock, A. L. Wahrhaftig, and H. Eyring, J. Chem. Phys., 23, 2200(1955).

2. M. L. Vestal, Ibid., 43, 1356(1965).

3. P. Naunou, Advan. Mass. Spectrom., 4, 551(1968).

4. W. A. Chupka, J. Chem. Phys., 30, 191(1959).

5. W. A. Chupka and M. Kaminsky, Ibid., 35, 1991(1961).

6. (a) B. Steiner, C. F. Grise, and M. G. Inghram, Ibid., 34, 189 (1961); (b) W. A. Chupka and J. Berkowitz, Ibid., 32, 1546 (1960); (c) L. Friedman, F. A. Long, and M. Wolfsberg, Ibid., 26, 714(1957); (d) Ibid., 27, 613(1957).

7. M. Vestal, A. L. Wahrhaftig, and W. H. Johnston, Ibid., 37, 1276(1962).

8. A. N. H. Yoe and D. H. Williams, J. Amer. Chem. Soc., 92, 3984(1970).

9. (a) J. D. Morrison, J. Chem. Phys., 21, 1767(1953); (b) J. D. Morrison, Revs. Pure Appl. Chem., 5, 22(1955); (c) J. D. Morrison, J. Appl. Phys., 28, 1409(1957).

10. (a) G. H. Wannier, Phys. Rev., 100, 1180(1956); (b) F. H. Dorman and J. D. Morrison, J. Chem. Phys., 31, 1320, 1335(1959); (c) Ibid., 34, 578, 1407(1961); (d) F. H. Dorman, J. D. Morrison, and A. J. C. Nicholson, Ibid., 32, 378(1960).

11. F. H. Dorman and J. D. Morrison, J. Chem. Phys., 35, 575(1961).

12. H. Hurzeler, M. G. Inghram, and J. D. Morrison, Ibid., 28, 76(1958).

13. J. Lennard-Jones and G. G. Hall, Trans. Faraday Soc., 48, 581(1952).

14. J. Berkowitz, H. Ehrhardt, and T. Tekaat, Z. Phys., 200, 69(1967).

15. F. W. McLafferty, T. Wachs, C. Lifshitz, G. Innorta, and P. Irving, J. Amer. Chem. Soc., 92, 6867(1970).

16. A. D. Baker, D. P. May, and D. W. Turner, J. Chem. Soc., B, 22(1968).

17. F. T. Deverse and A. B. King, J. Chem. Phys., 41, 38833(1964).

18. G. G. Meisels, C. T. Chen, B. G. Giessner, and R. H. Emmel, Ibid., 56, 793(1972).

19. E. Pettersson, E. Lindholm, Arkiv Fysik, 24, 49(1963).

20. (a) D. P. Stevenson, Radiation Res., 10, 610(1959); (b) H. Ehrhardt, F. Linder, and T. Tekaat, Advan. Mass. Spectrom., 4, 705(1968).

21. (a) A. B. King and F. A. Long, J. Chem. Phys., 29, 374(1958); (b) A. Kropf, E. M. Eyring, A. J. Wahrhaftig, and H. Eyring, Ibid., 32, 149(1960); (c) J. Collin, Bull. Soc. Roy. Sci. Liege, 7, 520(1970); (d) R. P. Buck and M. M. Bursey, Org. Mass. Spectrom., 3, 387(1970); (e) A. N. H. Yoe and D. H. Williams, Ibid., 5, 135(1971); (f) J. R. Gilbert and A. J. Stace, Ibid., 5, 1119(1971).

22. A. J. C. Nicholson, J. Chem. Phys., 29, 1313(1958).

23. (a) F. H. Dorman, J. Chem. Phys., 41, 2857(1964); (b) Ibid., 42, 65(1965); (c) Ibid., 43, 3507(1965).

24. (a) P. T. Smith, Phys. Rev., 36, 1293(1930); (b) R. H. Vaught, Ibid., 71, 93(1947); (c) E. M. Clarke, Can. J. Phys., 32, 764(1954); (d) E. O. Lawrence, Phys. Rev., 28, 947(1926); (e) W. B. Nottingham, Ibid., 55, 203(1939); (f) D. A. Hutchison, J. Chem. Phys., 24, 628(1956); (g) R. E. Fox, W. M. Hickam, T. Kjeldaas, and D. J. Grove, Phys. Rev., 84, 859(1951).

25. (a) H. D. Smyth , Proc. Roy. Soc. (London), A102, 283(1922); (b) L. G. Smith, Phys. Rev., 51, 263(1937); (c) T. Mariner and W. Bleakney, Ibid., 72, 807(1947).

26. (a) R. E. Honig, J. Chem. Phys., 16, 105(1948); (b) J. D. Morrison, Ibid., 19, 1305(1951); (c) F. R. Lossing, A. W. Tickner, and W. A. Bryce, Ibid., 19, 1254(1951); (d) V. H. Dibeler and R. M. Reese, J. Research Natl. Bur. Standards, 54, 127(1955).

27. (a) M. M. Bursey and F. W. McLafferty, J. Amer. Chem. Soc., 88, 529(1966); (b) Ibid., 4484(1966); (c) Ibid., 89, 1(1967); (d) M. M. Bursey and P. T. Kissinger, Org. Mass. Spectrom., 3, 305(1970).

28. M. M. Bursey, Org. Mass. Spectrom., 1, 31(1968).

29. H. Budzikiewicz, C. Djerassi, and D. H. Williams, "Mass Spectra of Organic Compounds," Holden-Day, San Francisco, California, 1967, Chapters 1 and 3.

30. L. P. Hammett, "Physical Organic Chemistry," McGraw-Hill, New York, N. Y., 1940, Chapter VII.

31. R. C. Cooks, I. Howe, and D. H. Williams, Org. Mass. Spectrom., 2, 137(1969).

32. B. Boone, R. K. Mitchum, and S. E. Scheppele, Int. J. Mass. Spectrom. Ion. Phys., 5, 21(1970).

33. F. W. McLafferty, in "Topics in Organic Mass Spectrometry," Vol. 8, A. L. Burlingame, ed., Wiley-Interscience, New York, N. Y., 1970, p. 223.

34. P. Natalis and J. L. Franklin, J. Phys. Chem., 69, 2943(1965).

35. J. H. Bowie, R. G. Cooks, G. E. Gream, and M. H. Laffer, Aust. J. Chem., 21, 1247(1968).

36. S. E. Scheppele, R. K. Mitchum, K. F. Kinneberg, G. G. Meisels, R. H. Emmel, in press.

37. F. H. Field and J. L. Franklin, "Electron Impact Phenomena and The Properties of Gaseous Ions," New York, N. Y., Academic Press, 1957.

38. G. G. Meisels, J. Y. Park, and B. G. Giessner, J. Amer. Chem. Soc., 42, 254(1970).

39. (a) Hiroshi Suzuki, " Electronic Absorption Spectra and Geometry of Organic Molecules," Academic Press, New York, N. Y., 1967, Chapter 21 and references cited therein; (b) K. Maruyama,

K. ono, and J. Osugi, Bull. Chem. Soc. Japan, 45, 847(1972); (c) H. Thompson, Trans. Faraday Soc., 36(1940); (d) C. Caldwell and R. LeFevre, J. Chem. Soc., 1614(1939); (e) I. Kneggs and K. Lonsdale, Nature London, 143, 1023(1939).

40. A. Foffani, S. Pignatano, B. Cantone, and F. Gasso, Z. Physik. Chem., 42, 221(1964).

41. R. I. Reed and J. C. D. Brand, Trans. Faraday Soc., 54, 478(1958).

42. K. Watanabe, J. Chem. Phys., 26, 542(1957).

43. J. W. Sidman, J. Amer. Chem. Soc., 78, 1527(1956).

44. W. A. Chupka, J. Chem. Phys., 54, 1936(1971).

45. R. G. Dromey and J. D. Morrison, Int. J. Mass. Spectrom Ion Phys., 4 475(1970).

46. R. G. Dormey, J. D. Morrison, and J. C. Traeger, Ibid., 6, 57(1971).

47. M. B. Wallenstein and M. Krauss, J. Chem. Phys., 34, 929(1961).

48. H. M. Grubb and S. Meyerson, in "Mass Spectrometry of Organic Ions," F. W. McLafferty, ed., Academic Press, New York, N. Y., 1963, Chapter 10.

49. A. G. Harrison, in "Topics in Organic Mass Spectrometry," Vol. 8, A. L. Burlinghame, ed., Wiley-Interscience, New York, N. Y., 1970, p. 121.

50. The compound preparation and SDIE correction was kindly performed by J. Drager and G. Prakash, Oklahoma State University.

51. A. Streitwieser, Jr., Progr. Phys. Org. Chem., 1, 1(1963).

52. A. G. Harrison, P. Kebarle, and F. P. Lossing, J. Amer. Chem. Soc., 83, 777(1961).

53. F. G. Grable and G. L. Kearns, J. Phys. Chem., 66, 436(1962).

54. A. Buchs, G. P. Rossetti, and B. P. Susz, Helv. Chim. Acta., 47, 1563(1964).

55. N. Einoff and B. Munson, Org. Mass. Spectrom, 2, 155(1973).

56. L. Fieser and M. Fieser, "Reagents for Organic Synthesis," John Wiley and Sons, Inc., New York, N. Y., 1967, p. 1159.

57. A. A. Riley and A. R. Gray, Org. Syn., Coll. Vol. II, 510(1943).

58. H. H. Hatt, A. Pilgrim, and W. J. Hurran, J. Chem. Soc., 93(1936).

59. C. D. Shacklett and H. A. Smith, J. Amer. Chem. Soc., 75, 2654 (1953).

60. J. H. Simmons and E. O. Rowler, Ibid., 65, 389(1943).

61. E. J. Eisenbraun, Org. Syn., 45, 28(1965).

62. I. Lalezari, M. Hatefi, M. A. Khoyi, N. Guiti, and F. Abtahi, J. Med. Chem., 14, 1138(1971).

63. K. Maruyama, K. Ono, and J. Osugi, Bull. Chem. Soc. Japan, 45, 847(1972).

64. IBM System 360 Scientific Subroutine Package, Version III, 1968; see also F. B. Hildebrand, "Introduction to Numerical Analysis," McGraw-Hill Book Co., Inc., New York, N. Y., 1956, p. 295.

65. A. G. Worthing and J. Geffner, "Treatment of Experimental Data," John Wiley and Sons, Inc., New York, N. Y., 1943, Chapter 9.

66. H. D. Springall and T. R. J. White, J. Chem. Soc., 2764(1954).

67. J. L. Franklin, J. Chem. Phys., 21, 2029(1953).

68. J. L. Franklin, J. G. Dillard, H. M. Rosenstock, J. T. Herron, K. Draxl, and F. H. Field, Nat. Stand. Ref. Data Ser., Nat. Bur. Stand., U. S., No. 26, 1969 and references cited therein.

69. R. K. Solly and S. W. Benson, J. Amer. Chem. Soc., 93, 1592(1971).

70. J. H. Beynon, "Mass Spectrometry and Its Applications to Organic Chemistry," Elsevier, Amsterdam, 1960, Chapter 8.

71. M. C. Hamming, "16th Annual Conference on Mass Spectrometry," American Society of Testing Materials, Committe E-14, Pittsburgh, Pa., 1968.

72. S. E. Scheppele, R. D. Grigsby, D. W. Whitaker, S. D. Hinds, K. F. Kinneberg, and R. K. Mitchum, Org. Mass. Spectrom.,

3, 571(1970).

73. (a) S. Goldschmidt and B. Acksteiner, Chem. Ber., 91, 503(1958);
(b) V. Sprio, Gazz. Chim. Ital., 85, 569(1955).

APPENDIXES

APPENDIX A

FIRST DERIVATIVE DATA

1 PHENYL-2-(4-METHYLPHENYL)-ETHAN-1,2-DIONE

MASS SPECTRUM NO. 2675 GLC OVEN TEMP. = 135

INTEGRATION TIME = 10 SEC. TRAP CURRENT = 20 A

MODULATION = 0.032 V RMS MODULATION FREQ. = 595 HZ

ACC. H.V. = 3.7 KV MULT. H.V. = 1.7 KV

SOURCE TEMP. = 230 DEG. C SEPERATOR TEMP. = 150 DEG. C

AVERAGED FIRST DERIVATIVE VALUES

EV	M/E 224	M/E 119	M/E 105	M/E 91	M/E 77	M/E 69
7.45	5.00	0.00	0.00	0.00	0.00	0.00
7.55	187.00	12.21	0.00	0.00	0.00	0.00
7.65	395.33	34.00	0.00	0.00	0.00	0.00
7.75	431.67	43.66	0.00	0.00	0.00	0.00
7.85	415.00	57.66	0.00	0.00	0.00	0.00
7.95	601.17	88.83	0.00	0.00	0.00	0.00
8.05	1078.60	115.00	0.00	0.00	0.00	0.00
8.15	1763.10	159.83	0.00	0.00	0.00	0.00
8.25	2242.20	207.66	0.00	0.00	0.00	0.00
8.35	3332.70	285.55	0.00	20.00	0.00	0.00
8.45	4487.20	437.16	0.00	54.67	0.00	0.00
8.55	6001.80	667.83	0.00	98.47	0.00	0.00
8.65	7797.30	912.16	81.38	115.47	0.00	0.00
8.75	9022.80	1300.50	134.84	169.87	0.00	0.00
8.85	11303.00	1750.80	206.84	191.34	0.00	0.00
8.95	14707.00	2684.80	192.17	233.00	0.00	0.00
9.05	15389.00	3692.70	179.87	239.47	0.00	0.00
9.15	18463.00	4920.80	252.34	338.07	0.00	0.00
9.25	22176.00	6333.80	301.50	368.47	0.00	0.00
9.35	23547.00	7597.00	421.00	440.27	0.00	0.00
9.45	24663.00	9996.50	416.67	478.00	0.00	0.00
9.55	26097.00	11797.00	539.00	457.27	0.00	0.00
9.65	28965.00	14219.00	682.84	522.87	0.00	0.00

9.75	31454.00	16183.00	738.34	456.00	0.00	0.00
9.85	31844.00	18666.00	923.00	519.07	0.00	0.00
9.95	34459.00	21282.00	995.67	428.50	0.00	0.00
10.05	35975.00	23697.00	1128.50	445.27	0.00	0.00
10.15	37491.00	27072.00	1411.60	545.27	0.00	0.00
10.25	38495.00	30116.00	1606.80	487.67	0.00	0.00
10.35	41726.00	32554.00	1923.80	403.27	0.00	0.00
10.45	44656.00	36519.00	2090.30	434.67	0.00	0.00
10.55	45976.00	38402.00	2291.80	464.87	0.00	0.00
10.65	46181.00	41032.00	2613.30	443.67	0.00	0.00
10.75	51265.00	43307.00	2714.60	452.47	0.00	0.00
10.85	54132.00	45882.00	3158.30	577.07	0.00	0.00
10.95	56369.00	48278.00	3692.20	570.67	0.00	0.00
11.05	59451.00	50385.00	3925.50	469.07	0.00	30.20
11.15	58856.00	51631.00	4205.80	449.47	0.00	140.60
11.25	61294.00	52576.00	4636.00	522.27	0.00	8.92
11.35	61439.00	54375.00	5174.00	594.07	0.00	378.80
11.45	66382.00	55473.00	5681.30	591.67	0.00	790.10
11.55	67049.00	56787.00	6062.80	607.67	0.00	499.20
11.65	68117.00	58522.00	6438.00	626.27	0.00	111.30
11.75	65339.00	59570.00	6958.30	617.67	0.00	361.30
11.85	69512.00	60715.00	7404.50	592.27	0.00	621.70
11.95	69462.00	62408.00	7865.30	709.67	0.00	741.60
12.05	68703.00	62330.00	8472.70	652.27	0.00	771.80
12.15	71579.00	63569.00	9107.80	805.87	50.66	954.70
12.25	67273.00	64027.00	9392.50	798.84	173.66	1296.40
12.35	69775.00	66555.00	9742.80	846.84	102.66	1307.00
12.45	71225.00	66502.00	10458.00	914.50	163.83	806.30
12.55	71225.00	66089.00	10860.00	952.27	188.83	308.40
12.65	71225.00	67925.00	11474.00	1123.30	126.83	989.70
12.75	71225.00	68950.00	11850.00	1150.30	278.63	1205.40
12.85	71225.00	69750.00	12141.00	1362.50	197.58	877.40
12.95	71225.00	70023.00	12839.00	1482.30	319.03	160.70
13.05	71225.00	69908.00	13103.00	1729.90	339.03	587.00
13.15	71225.00	70314.00	13853.00	1898.70	378.83	561.10
13.25	71225.00	69524.00	14279.00	2055.50	498.33	1226.60
13.35	71225.00	70703.00	14479.00	2422.90	439.33	1369.30
13.45	71225.00	71452.00	14727.00	2774.30	577.50	2821.70
13.55	71225.00	72230.00	15870.00	3189.70	666.83	3320.90
13.65	71225.00	72085.00	14968.00	3446.70	848.66	3152.10
13.75	0.00	71910.00	16129.00	3819.30	933.00	4364.70
13.85	0.00	73167.00	16455.00	4424.20	1135.50	5884.10
13.95	0.00	73363.00	16767.00	4580.10	1216.70	5738.70
14.05	0.00	73363.00	17788.00	5397.50	1377.00	7184.50
14.15	0.00	73363.00	17541.00	5897.10	1425.80	7099.00
14.25	0.00	73363.00	17861.00	6393.30	1671.80	9459.90
14.35	0.00	73363.00	18631.00	7316.90	2040.30	11853.00
14.45	0.00	73363.00	18417.00	7801.10	2395.70	12195.00
14.55	0.00	73363.00	18419.00	8627.10	2590.80	12754.00
14.65	0.00	73363.00	19868.00	9178.50	2921.40	16001.00

14.75	0.00	73363.00	20050.00	9640.90	3176.60	15364.00
14.85	0.00	73363.00	20074.00	10381.00	3525.80	18028.00
14.95	0.00	73363.00	20168.00	10868.00	3432.80	21255.00
15.05	0.00	0.00	20701.00	11939.00	4449.70	19306.00
15.15	0.00	0.00	20768.00	12739.00	4930.80	19936.00
15.25	0.00	0.00	21462.00	13009.00	4945.50	20862.00
15.35	0.00	0.00	21361.00	13835.00	5677.50	21586.00
15.45	0.00	0.00	21408.00	13850.00	5895.60	27829.00
15.55	0.00	0.00	22215.00	15104.00	6268.60	25950.00
15.65	0.00	0.00	21918.00	15821.00	6728.40	28502.00
15.75	0.00	0.00	22612.00	16118.00	7236.00	29650.00
15.85	0.00	0.00	22019.00	17894.00	7493.20	35790.00
15.95	0.00	0.00	24355.00	17771.00	8434.20	32285.00
16.05	0.00	0.00	23744.00	18974.00	8749.00	36981.00
16.15	0.00	0.00	23790.00	19863.00	8830.70	35598.00
16.25	0.00	0.00	24131.00	20325.00	10108.00	35024.00
16.35	0.00	0.00	24131.00	21278.00	10673.00	40426.00
16.45	0.00	0.00	24131.00	21798.00	11420.00	38739.00
16.55	0.00	0.00	24131.00	22166.00	12235.00	43723.00
16.65	0.00	0.00	24131.00	23140.00	12182.00	41718.00
16.75	0.00	0.00	24131.00	23508.00	12615.00	45749.00
16.85	0.00	0.00	24131.00	23807.00	13422.00	40756.00
16.95	0.00	0.00	24131.00	24471.00	14624.00	48809.00
17.05	0.00	0.00	24131.00	25641.00	14224.00	48002.00
17.15	0.00	0.00	24131.00	25431.00	15597.00	50944.00
17.25	0.00	0.00	24131.00	26172.00	15615.00	57347.00
17.35	0.00	0.00	24131.00	27687.00	16948.00	51249.00
17.45	0.00	0.00	24131.00	27502.00	17657.00	53655.00
17.55	0.00	0.00	0.00	28417.00	18608.00	53655.00
17.65	0.00	0.00	0.00	29136.00	18154.00	53655.00
17.75	0.00	0.00	0.00	27853.00	19240.00	53655.00
17.85	0.00	0.00	0.00	28914.00	20104.00	53655.00
17.95	0.00	0.00	0.00	28287.00	21302.00	53655.00
18.05	0.00	0.00	0.00	29150.00	21743.00	53655.00
18.15	0.00	0.00	0.00	30520.00	22860.00	53655.00
18.25	0.00	0.00	0.00	30520.00	23401.00	53655.00

PHENYL-2-(4-METHYLPHENYL)-ETHAN-1,2-DIONE

MASS SPECTRUM NO. 2429 GLC OVEN TEMP. = 135

INTEGRATION TIME = 1 SEC. TRAP CURRENT = 20 A

MODULATION = 0.032 V RMS MODULATION FREQ. = 620 HZ

ACC. H.V. = 3.7 KV MULT. H.V. = 1.7 KV

SOURCE TEMP. = 310 DEG. C SEPERATOR TEMP. = 150 DEG. C

AVERAGED FIRST DERIVATIVE VALUES

EV	M/E 224	M/E 119	M/E 105	M/E 91	M/E 77
7.05	0.00	0.00	0.00	0.00	0.00
7.15	0.00	0.00	0.00	0.00	0.00
7.25	0.00	0.00	0.00	0.00	0.00
7.35	0.00	0.00	0.00	0.00	0.00
7.45	0.00	0.00	0.00	0.00	0.00
7.55	0.00	0.00	0.00	0.00	0.00
7.65	0.00	0.00	0.00	0.00	0.00
7.75	0.00	0.00	0.00	0.00	0.00
7.85	12.63	0.00	0.00	0.00	0.00
7.95	26.00	0.00	0.00	0.00	0.00
8.05	46.18	0.00	0.00	0.00	0.00
8 15	74.76	0.00	0.00	0.00	0.00
8.25	113.40	0.00	0.00	0.00	0.00
8.35	154.58	0.00	0.00	0.00	0.00
8.45	195.84	0.00	0.00	0.00	0.00
8.55	317.70	0.00	0.00	0.00	0.00
8.65	389.46	0.00	0.00	0.00	0.00
8.75	521.22	0.00	0.00	0.00	0.00
8.85	593.16	0.00	0.00	0.00	0.00
8.95	698.85	8.88	0.00	0.00	0.00
9.05	807.62	14.00	0.00	0.00	0.00
9.15	890.91	18.00	0.00	0.00	0.00
9.25	1048.20	25.71	0.00	0.00	0.00

9.35	1138.50	36.93	0.00	0.00	0.00
9.45	1237.40	53.18	0.00	0.00	0.00
9.55	1318.40	73.71	0.00	0.00	0.00
9.65	1339.60	108.15	6.44	0.00	0.00
9.75	1384.50	158.00	8.73	0.00	0.00
9.85	1447.40	210.00	13.22	0.00	0.00
9.95	1509.90	269.25	20.47	0.00	0.00
10.05	1538.40	392.08	27.90	0.00	0.00
10.15	1720.10	497.19	35.94	0.00	0.00
10.25	1744.70	590.36	50.00	0.00	0.00
10.35	1727.50	718.94	55.80	1.50	0.00
10.45	1799.60	877.00	80.27	8.00	0.00
10.55	1875.20	986.82	96.81	14.50	0.00
10.65	1904.10	1133.80	116.94	21.00	0.00
10.75	1949.80	1283.90	130.78	27.50	0.00
10.85	1961.80	1425.90	147.88	34.10	0.00
10.95	1992.80	1585.00	182.63	40.80	0.00
11.05	2026.90	1755.40	200.69	47.30	0.00
11.15	1941.80	1883.00	217.80	53.80	0.00
11.25	2248.90	2007.10	234.25	60.20	0.00
11.35	2348.50	2117.10	276.13	67.00	0.00
11.45	2245.60	2297.00	294.04	73.40	0.00
11.55	2325.80	2346.70	322.75	80.00	0.00
11.65	2199.70	2501.80	348.56	86.50	0.00
11.75	2444.10	2606.00	395.65	108.70	0.00
11.85	2452.50	2655.20	413.88	121.80	66.33
11.95	2478.40	2793.50	472.88	130.00	224.66
12.05	2496.10	3047.80	489.94	135.00	334.83
12.15	2428.00	3202.20	527.67	137.60	278.50
12.25	2578.20	3327.40	556.45	138.50	208.33
12.35	2533.80	3417.00	602.50	165.77	228.66
12.45	2479.90	3549.50	655.33	224.10	322.33
12.55	2578.90	3689.40	681.06	257.20	325.83
12.65	2490.40	3874.80	740.00	265.80	396.66
12.75	2932.90	3933.80	841.88	298.80	255.66
12.85	2760.80	4099.80	846.33	382.50	386.00
12.95	2688.30	4289.60	869.66	421.60	492.66
13.05	2778.00	4339.50	962.53	527.40	691.00
13.15	2790.40	4519.70	1056.60	576.69	617.66
13.25	2755.80	4658.40	1091.80	680.13	884.33
13.35	2755.80	4933.20	1084.20	710.53	882.33
13.45	2755.80	4962.20	1182.30	816.80	988.16
13.55	2755.80	5077.20	1295.40	938.83	979.00
13.65	2755.80	5243.20	1236.90	1058.70	1349.60
13.75	2755.80	5255.00	1305.60	1183.40	1908.80
13.85	2755.80	5261.00	1421.50	1385.20	1706.00
13.95	2755.80	5413.30	1471.50	1527.40	1870.50
14.05	2755.80	5659.80	1615.90	1673.90	2418.70
14.15	2755.80	5645.90	1612.60	1822.50	2593.70
14.25	2755.80	5724.10	1669.70	2044.30	2849.80

14.35	0.00	5907.90	1709.10	2192.10	2864.20
14.45	0.00	5894.10	1752.40	2365.80	3429.20
14.55	0.00	6020.10	1877.60	2547.50	3903.20
14.65	0.00	6175.40	1880.70	2820.70	4125.30
14.75	0.00	6224.90	1974.60	3018.30	4903.50
14.85	0.00	6368.60	2022.90	3232.90	5152.30
14.95	0.00	6441.30	2051.70	3538.40	5724.80
15.05	0.00	6500.90	2162.30	3582.10	5936.30
15.15	0.00	6583.20	2211.10	3842.80	6635.00
15.25	0.00	6548.20	2221.90	4154.80	7288.00
15.35	0.00	6559.50	2329.10	4370.20	7311.50
15.45	0.00	6563.90	2377.10	4479.80	8211.00
15.55	0.00	6563.90	2548.20	4726.60	9176.20
15.65	0.00	6563.90	2500.40	4935.10	9712.70
15.75	0.00	6563.90	2490.10	5155.70	9951.70
15.85	0.00	6563.90	2648.60	5296.80	10281.00
15.95	0.00	6563.90	2712.80	5468.70	11188.00
16.05	0.00	6563.90	2706.20	5833.90	11771.00
16.15	0.00	6563.90	2746.10	5963.40	12176.00
16.25	0.00	0.00	2880.50	6246.10	12329.00
16.35	0.00	0.00	2932.90	6286.30	13543.00
16.45	0.00	0.00	2897.50	6481.30	14862.00
16.55	0.00	0.00	2864.10	6680.70	14872.00
16.65	0.00	0.00	3067.00	7018.50	16175.00
16.75	0.00	0.00	2865.00	7142.40	16099.00
16.85	0.00	0.00	3019.00	7350.00	17276.00
16.95	0.00	0.00	3077.70	7945.60	17751.00
17.05	0.00	0.00	3200.00	8072.50	18106.00
17.15	0.00	0.00	3125.00	8369.20	18634.00
17.25	0.00	0.00	3250.00	8487.60	20635.00
17.35	0.00	0.00	3310.00	8662.60	21270.00
17.45	0.00	0.00	3355.00	8715.90	21946.00
17.55	0.00	0.00	3140.00	9384.40	23504.00
17.65	0.00	0.00	3450.00	9650.60	22242.00
17.75	0.00	0.00	3480.00	9424.30	24407.00
17.85	0.00	0.00	3515.00	9402.30	25283.00
17.95	0.00	0.00	3550.00	9610.00	25794.00
18.05	0.00	0.00	3650.00	9809.00	26445.00
18.15	0.00	0.00	3605.00	9960.00	26480.00
18.25	0.00	0.00	3630.00	10125.00	28523.00
18.35	0.00	0.00	3645.00	10340.00	28648.00
18.45	0.00	0.00	3650.00	10686.00	28654.00
18.55	0.00	0.00	3665.00	10920.00	30501.00
18.65	0.00	0.00	3670.00	11080.00	30928.00
18.75	0.00	0.00	3670.00	11190.00	32392.00
18.85	0.00	0.00	3670.00	11290.00	31192.00
18.95	0.00	0.00	3670.00	11290.00	32832.00
19.05	0.00	0.00	3670.00	11290.00	32203.00
19.15	0.00	0.00	3670.00	11290.00	32909.00
19.25	0.00	0.00	3670.00	11290.00	33407.00

19.35	0.00	0.00	3670.00	11290.00	35113.00
19.45	0.00	0.00	3670.00	11290.00	33006.00
19.55	0.00	0.00	3670.00	11290.00	37492.00
19.65	0.00	0.00	3670.00	11290.00	35818.00
19.75	0.00	0.00	3670.00	11290.00	36984.00
19.85	0.00	0.00	3670.00	11290.00	34866.00
19.95	0.00	0.00	0.00	11290.00	35311.00
20.05	0.00	0.00	0.00	11290.00	36946.00
20.15	0.00	0.00	0.00	0.00	36667.00
20.25	0.00	0.00	0.00	0.00	37536.00
20.35	0.00	0.00	0.00	0.00	35978.00
20.45	0.00	0.00	0.00	0.00	36231.00
20.55	0.00	0.00	0.00	0.00	36231.00
20.65	0.00	0.00	0.00	0.00	36231.00
20.75	0.00	0.00	0.00	0.00	36231.00
20.85	0.00	0.00	0.00	0.00	36231.00
20.95	0.00	0.00	0.00	0.00	36231.00
21.05	0.00	0.00	0.00	0.00	36231.00
21.15	0.00	0.00	0.00	0.00	36231.00
21.25	0.00	0.00	0.00	0.00	36231.00
21.35	0.00	0.00	0.00	0.00	36231.00

1-PHENYL-2-(4-METHOXYPHENYL)-ETHAN-1,2-DIONE

MASS SPECTRUM NO. 2813 GLC OVEN TEMP. = 152

INTEGRATION TIME = 10 SEC. TRAP CURRENT = 20 A

MODULATION = 0.032 V RMS MODULATION FREQ. = 595 HZ

ACC. H.V. = 3.7 KV MULT. H.V. = 1.7 KV

SOURCE TEMP. = 250 DEG. C SEPERATOR TEMP. = 155 DEG. C

AVERAGED FIRST DERIVATIVE VALUES

EV	M/E 240	M/E 135	M/E 107	M/E 105	M/E 77
6.55	0.00	0.00	0.00	0.00	0.00
6.65	0.00	0.00	0.00	0.00	0.00
6.75	0.00	0.00	0.00	0.00	0.00
6.85	0.00	0.00	0.00	0.00	0.00
6.95	0.00	0.00	0.00	0.00	0.00
7.05	0.00	0.00	0.00	0.00	0.00
7.15	0.00	0.00	0.00	0.00	0.00
7.25	0.00	0.00	0.00	0.00	0.00
7.35	0.00	0.00	0.00	0.00	0.00
7.45	0.00	0.00	0.00	0.00	0.00
7.55	0.00	0.00	0.00	0.00	0.00
7.65	58.07	13.66	0.00	0.00	0.00
7.75	237.07	24.66	0.00	0.00	0.00
7.85	516.57	31.33	0.00	0.00	0.00
7.95	703.57	47.83	0.00	0.00	0.00
8.05	1151.20	56.83	0.00	0.00	0.00
8.15	2040.50	84.00	0.00	0.00	0.00
8.25	2784.70	127.66	0.00	0.00	0.00
8.35	3662.90	198.66	0.00	0.00	0.00
8.45	5340.60	285.66	0.00	0.00	0.00
8.55	6712.20	423.66	0.00	0.00	0.00
8.65	9971.10	613.00	0.00	0.00	0.00
8.75	12278.00	890.83	0.00	0.00	0.00

8.85	13765.00	1196.90	0.00	0.00	0.00
8.95	16584.00	1642.00	0.00	0.00	0.00
9.05	19316.00	2097.80	0.00	0.00	0.00
9.15	20498.00	2632.70	0.00	0.00	0.00
9.25	23500.00	3282.00	0.00	0.00	0.00
9.35	24847.00	3840.70	0.00	0.00	0.00
9.45	26138.00	4580.80	0.00	114.51	0.00
9.55	31433.00	5387.50	8.71	160.22	0.00
9.65	31280.00	6401.50	41.64	329.55	0.00
9.75	35692.00	7234.30	83.82	302.39	0.00
9.85	35011.00	9390.80	85.72	327.79	0.00
9.95	35579.00	9430.60	147.98	608.22	0.00
10.05	36547.00	10516.00	128.44	585.39	0.00
10.15	38990.00	11708.00	148.98	633.55	0.00
10.25	41776.00	12697.00	254.15	756.72	0.00
10.35	41449.00	14068.00	201.98	1133.20	26.03
10.45	44055.00	15143.00	239.48	1452.10	94.86
10.55	44681.00	16595.00	304.98	1432.10	114.69
10.65	47333.00	17740.00	376.32	1719.90	109.69
10.75	47025.00	19147.00	352.32	2260.90	59.36
10.85	50959.00	20382.00	355.98	2118.40	124.19
10.95	50236.00	21652.00	351.82	2698.60	157.86
11.05	51006.00	23017.00	411.86	2867.20	116.19
11.15	53264.00	24583.00	540.98	3786.40	275.69
11.25	51513.00	26355.00	656.48	3744.90	160.86
11.35	54176.00	28103.00	581.32	4600.40	211.53
11.45	57177.00	29192.00	504.48	5146.70	308.69
11.55	58740.00	30606.00	709.15	5857.10	390.86
11.65	58458.00	31950.00	672.65	6033.10	281.36
11.75	58748.00	33049.00	661.90	7738.60	380.36
11.85	63484.00	34105.00	768.72	8020.20	337.69
11.95	66884.00	35120.00	726.98	8069.20	406.29
12.05	61686.00	35928.00	700.58	10194.00	350.86
12.15	63623.00	37102.00	872.98	11826.00	426.36
12.25	67138.00	37911.00	718.15	12073.00	344.26
12.35	61573.00	38345.00	824.82	12125.00	348.53
12.45	63623.00	38885.00	750.15	13171.00	312.53
12.55	63623.00	39543.00	748.32	13920.00	389.86
12.65	63623.00	40034.00	846.32	15187.00	334.53
12.75	63623.00	41140.00	845.00	15321.00	324.36
12.85	63623.00	41740.00	1051.20	16760.00	273.36
12.95	63623.00	42527.00	1389.80	19486.00	453.69
13.05	63623.00	42743.00	1092.00	18686.00	480.86
13.15	0.00	43366.00	1307.20	19680.00	303.53
13.25	0.00	44315.00	1327.20	20617.00	273.61
13.35	0.00	44431.00	1811.60	22729.00	340.03
13.45	0.00	45091.00	1576.30	21830.00	259.06
13.55	0.00	46264.00	2092.00	25010.00	420.15
13.65	0.00	46798.00	2139.80	26754.00	348.19
13.75	0.00	47560.00	2648.30	26277.00	271.53

13.85	0.00	47372.00	2882.50	26703.00	533.24
13.95	0.00	48100.00	3440.20	29969.00	499.53
14.05	0.00	48354.00	4214.00	29000.00	425.53
14.15	0.00	49481.00	4488.70	33898.00	497.53
14.25	0.00	49840.00	5091.00	34839.00	568.15
14.35	0.00	51039.00	5859.70	34025.00	642.86
14.45	0.00	50638.00	6676.80	35714.00	843.53
14.55	0.00	51463.00	7318.80	37265.00	853.69
14.65	0.00	51132.00	8018.70	40377.00	958.53
14.75	0.00	51463.00	9104.20	39511.00	1163.40
14.85	0.00	51903.00	9837.20	42654.00	1374.20
14.95	0.00	51463.00	10855.00	41621.00	1823.00
15.05	0.00	51463.00	12116.00	42700.00	2138.50
15.15	0.00	51463.00	13085.00	43990.00	2214.20
15.25	0.00	51463.00	13780.00	47482.00	2503.70
15.35	0.00	0.00	15435.00	45958.00	2785.70
15.45	0.00	0.00	15750.00	48207.00	3305.70
15.55	0.00	0.00	17202.00	47344.00	3574.70
15.65	0.00	0.00	17564.00	48714.00	4091.00
15.75	0.00	0.00	18930.00	50130.00	4863.20
15.85	0.00	0.00	19665.00	47038.00	5442.50
15.95	0.00	0.00	20309.00	49337.00	5976.40
16.05	0.00	0.00	21718.00	49659.00	6500.50
16.15	0.00	0.00	20970.00	53143.00	7498.20
16.25	0.00	0.00	23015.00	52474.00	8227.00
16.35	0.00	0.00	23629.00	50027.00	9045.90
16.45	0.00	0.00	24652.00	52641.00	9614.40
16.55	0.00	0.00	25176.00	53939.00	10595.00
16.65	0.00	0.00	26415.00	53597.00	11261.00
16.75	0.00	0.00	26296.00	53415.00	12057.00
16.85	0.00	0.00	26067.00	55215.00	13626.00
16.95	0.00	0.00	26704.00	55199.00	14483.00
17.05	0.00	0.00	27787.00	55688.00	16182.00
17.15	0.00	0.00	29047.00	55688.00	16856.00
17.25	0.00	0.00	29013.00	55688.00	17648.00
17.35	0.00	0.00	30001.00	55688.00	18912.00
17.45	0.00	0.00	29160.00	55688.00	20596.00
17.55	0.00	0.00	29254.00	55688.00	20733.00
17.65	0.00	0.00	29905.00	55688.00	22084.00
17.75	0.00	0.00	29905.00	55688.00	23516.00
17.85	0.00	0.00	29905.00	0.00	24439.00
17.95	0.00	0.00	29905.00	0.00	25089.00
18.05	0.00	0.00	29905.00	0.00	25452.00
18.15	0.00	0.00	29905.00	0.00	28157.00
18.25	0.00	0.00	29905.00	0.00	28498.00
18.35	0.00	0.00	29905.00	0.00	29973.00
18.45	0.00	0.00	29905.00	0.00	31770.00
18.55	0.00	0.00	29905.00	0.00	31021.00
18.65	0.00	0.00	29905.00	0.00	32391.00
18.75	0.00	0.00	0.00	0.00	32845.00

18.85	0.00	0.00	0.00	0.00	34877.00
18.95	0.00	0.00	0.00	0.00	35333.00
19.05	0.00	0.00	0.00	0.00	36460.00
19.15	0.00	0.00	0.00	0.00	37870.00
19.25	0.00	0.00	0.00	0.00	38526.00
19.35	0.00	0.00	0.00	0.00	40325.00
19.45	0.00	0.00	0.00	0.00	41706.00
19.55	0.00	0.00	0.00	0.00	42551.00
19.65	0.00	0.00	0.00	0.00	43291.00
19.75	0.00	0.00	0.00	0.00	43765.00
19.85	0.00	0.00	0.00	0.00	45030.00
19.95	0.00	0.00	0.00	0.00	44817.00
20.05	0.00	0.00	0.00	0.00	45500.00
20.15	0.00	0.00	0.00	0.00	46810.00
20.25	0.00	0.00	0.00	0.00	47443.00
20.35	0.00	0.00	0.00	0.00	47002.00
20.45	0.00	0.00	0.00	0.00	48013.00
20.55	0.00	0.00	0.00	0.00	47620.00
20.65	0.00	0.00	0.00	0.00	51108.00
20.75	0.00	0.00	0.00	0.00	48900.00
20.85	0.00	0.00	0.00	0.00	48410.00
20.95	0.00	0.00	0.00	0.00	51178.00
21.05	0.00	0.00	0.00	0.00	51477.00
21.15	0.00	0.00	0.00	0.00	51158.00
21.25	0.00	0.00	0.00	0.00	52004.00
21.35	0.00	0.00	0.00	0.00	52004.00
21.45	0.00	0.00	0.00	0.00	52004.00
21.55	0.00	0.00	0.00	0.00	52004.00
21.65	0.00	0.00	0.00	0.00	52004.00
21.75	0.00	0.00	0.00	0.00	52004.00
21.85	0.00	0.00	0.00	0.00	52004.00
21.95	0.00	0.00	0.00	0.00	52004.00
22.05	0.00	0.00	0.00	0.00	52004.00

1-PHENYL-2-(4-METHOXYPHENYL)-ETHAN-1,2-DIONE

MASS SPECTRUM NO. 2890 GLC OVEN TEMP. = 155

INTEGRATION TIME = 10 SEC. TRAP CURRENT = 20 A

MODULATION = 0.030 V RMS MODULATION FREQ. = 595 HZ

ACC. H.V. = 3.7 KV MULT. H.V. = 1.7 KV

SOURCE TEMP. = 310 DEG. C SEPERATOR TEMP. = 162 DEG. C

AVERAGED FIRST DERIVATIVE VALUES

EV	M/E 240	M/E 135	M/E 107	M/E 105	M/E 77
6.55	0.00	0.00	0.00	0.00	0.00
6.65	0.00	0.00	0.00	0.00	0.00
6.75	0.00	0.00	0.00	0.00	0.00
6.85	0.00	0.00	0.00	0.00	0.00
6.95	0.00	0.00	0.00	0.00	0.00
7.05	0.00	0.00	0.00	0.00	0.00
7.15	145.30	0.00	0.00	0.00	0.00
7.25	290.60	34.67	0.00	0.00	0.00
7.35	435.90	71.67	0.00	0.00	0.00
7.45	581.30	56.17	0.00	0.00	0.00
7.55	726.62	70.17	0.00	0.00	0.00
7.65	871.95	82.17	0.00	0.00	0.00
7.75	1017.30	108.34	0.00	0.00	0.00
7.85	1162.60	142.34	0.00	0.00	0.00
7.95	1418.60	212.34	0.00	0.00	0.00
8.05	1728.30	376.34	0.00	0.00	0.00
8.15	2482.50	517.00	0.00	0.00	0.00
8.25	2155.80	715.00	0.00	0.00	0.00
8.35	3962.10	1015.70	0.00	0.00	0.00
8.45	4560.60	1327.70	0.00	0.00	0.00
8.55	6720.10	1677.70	0.00	0.00	0.00
8.65	5638.60	2114.00	0.00	0.00	0.00
8.75	7069.80	2491.20	0.00	0.00	0.00

8.85	7155.80	2620.70	0.00	0.00	0.00
8.95	7240.00	3612.80	26.84	129.96	0.00
9.05	8958.10	4314.50	66.34	88.50	0.00
9.15	8570.80	5147.00	153.00	169.00	0.00
9.25	10140.00	6191.30	37.34	106.34	0.00
9.35	8023.00	7501.30	205.84	501.34	0.00
9.45	12514.00	8531.50	161.84	170.00	0.00
9.55	10853.00	9452.20	141.67	443.34	0.00
9.65	11262.00	10505.00	183.84	584.84	0.00
9.75	11420.00	11962.00	294.67	708.50	0.00
9.85	13804.00	13173.00	204.00	964.17	0.00
9.95	17048.00	14102.00	495.00	880.50	0.00
10.05	13628.00	15093.00	398.00	1217.20	0.00
10.15	13812.00	16331.00	262.50	1292.70	0.00
10.25	14919.00	17569.00	568.50	1559.50	0.00
10.35	15985.00	18833.00	655.34	1912.80	0.00
10.45	18135.00	19728.00	371.00	2123.00	0.00
10.55	17425.00	21252.00	670.84	2323.70	0.00
10.65	18123.00	22279.00	435.50	2876.20	0.00
10.75	18068.00	23081.00	423.67	2679.20	0.00
10.85	20463.00	24917.00	698.34	2739.80	0.00
10.95	20075.00	26023.00	557.34	3272.80	0.00
11.05	23288.00	27602.00	381.17	3686.70	0.00
11.15	23660.00	28978.00	712.50	4188.00	0.00
11.25	21308.00	30788.00	613.50	4339.80	0.00
11.35	22690.00	32044.00	684.50	5201.70	0.00
11.45	19796.00	33116.00	730.67	5613.50	0.00
11.55	23404.00	35098.00	765.67	6302.70	0.00
11.65	20963.00	35938.00	947.00	6052.20	0.00
11.75	22664.00	37607.00	1236.20	7109.80	0.00
11.85	21287.00	39879.00	992.00	7388.20	0.00
11.95	23296.00	40961.00	974.17	7368.50	0.00
12.05	20349.00	41713.00	926.17	9218.30	0.00
12.15	20073.00	43527.00	1332.20	9247.50	0.00
12.25	25120.00	44621.00	1127.70	9472.70	0.00
12.35	28353.00	46293.00	1505.30	10164.00	0.00
12.45	24384.00	47276.00	1528.20	10939.00	57.57
12.55	22405.00	48741.00	2101.30	12308.00	26.14
12.65	27388.00	50663.00	2471.00	13562.00	88.77
12.75	29538.00	51360.00	2786.00	13157.00	120.57
12.85	25359.00	53766.00	3643.00	14853.00	141.07
12.95	26048.00	54867.00	3519.50	14359.00	101.86
13.05	30202.00	55936.00	3712.00	16452.00	202.57
13.15	25849.00	56942.00	4951.30	17005.00	203.71
13.25	26486.00	58033.00	5143.00	18068.00	210.57
13.35	30202.00	59706.00	5644.20	17973.00	252.57
13.45	30202.00	60346.00	7381.80	19573.00	341.14
13.55	30202.00	61750.00	7801.20	20246.00	425.57
13.65	30202.00	62793.00	8854.20	20364.00	502.90
13.75	30202.00	64138.00	9457.00	21754.00	395.74

13.85	30202.00	64631.00	10562.00	21335.00	661.07
13.95	30202.00	65693.00	12386.00	21691.00	889.75
14.05	30202.00	65531.00	14532.00	23691.00	854.40
14.15	30202.00	66786.00	15623.00	24980.00	1125.20
14.25	0.00	66968.00	16936.00	23986.00	1305.40
14.35	0.00	67231.00	17670.00	25366.00	1388.00
14.45	0.00	66992.00	18774.00	25499.00	1511.90
14.55	0.00	67231.00	21933.00	26580.00	1856.90
14.65	0.00	67231.00	21906.00	25929.00	2121.70
14.75	0.00	67231.00	23760.00	26649.00	2348.70
14.85	0.00	67231.00	25132.00	29587.00	2728.40
14.95	0.00	67231.00	27186.00	28781.00	3179.20
15.05	0.00	67231.00	27672.00	29606.00	3214.70
15.15	0.00	67231.00	29233.00	29317.00	3912.50
15.25	0.00	67231.00	31228.00	30163.00	4388.60
15.35	0.00	67231.00	32462.00	29641.00	4503.40
15.45	0.00	67231.00	32577.00	30081.00	5004.60
15.55	0.00	67231.00	33577.00	30452.00	5663.50
15.65	0.00	67231.00	34331.00	30996.00	5960.10
15.75	0.00	0.00	36212.00	32791.00	6577.90
15.85	0.00	0.00	36450.00	31339.00	7317.60
15.95	0.00	0.00	38715.00	30849.00	7623.60
16.05	0.00	0.00	39820.00	32197.00	8497.40
16.15	0.00	0.00	39214.00	32595.00	9208.10
16.25	0.00	0.00	41928.00	35494.00	9909.60
16.35	0.00	0.00	42672.00	32873.00	10725.00
16.45	0.00	0.00	44611.00	32778.00	10585.00
16.55	0.00	0.00	45633.00	35881.00	11627.00
16.65	0.00	0.00	44347.00	34066.00	12598.00
16.75	0.00	0.00	48498.00	34492.00	13484.00
16.85	0.00	0.00	50416.00	35466.00	13711.00
16.95	0.00	0.00	48382.00	35844.00	14373.00
17.05	0.00	0.00	50072.00	34472.00	14903.00
17.15	0.00	0.00	53100.00	36669.00	15580.00
17.25	0.00	0.00	49828.00	34280.00	16653.00
17.35	0.00	0.00	48795.00	36629.00	17437.00
17.45	0.00	0.00	51672.00	36629.00	17697.00
17.55	0.00	0.00	50432.00	36629.00	18395.00
17.65	0.00	0.00	53148.00	36629.00	18325.00
17.75	0.00	0.00	53869.00	36629.00	20125.00
17.85	0.00	0.00	54418.00	36629.00	20262.00
17.95	0.00	0.00	54418.00	36629.00	21869.00
18.05	0.00	0.00	50795.00	36629.00	21643.00
18.15	0.00	0.00	54418.00	36629.00	22153.00
18.25	0.00	0.00	53284.00	36629.00	22498.00
18.35	0.00	0.00	54418.00	36629.00	24046.00
18.45	0.00	0.00	54418.00	36629.00	23988.00
18.55	0.00	0.00	54418.00	0.00	23365.00
18.65	0.00	0.00	54418.00	0.00	24848.00
18.75	0.00	0.00	54418.00	0.00	25327.00

18.85	0.00	0.00	54418.00	0.00	25625.00
18.95	0.00	0.00	54418.00	0.00	26026.00
19.05	0.00	0.00	54418.00	0.00	26499.00
19.15	0.00	0.00	54418.00	0.00	27931.00
19.25	0.00	0.00	54418.00	0.00	27725.00
19.35	0.00	0.00	54418.00	0.00	27907.00
19.45	0.00	0.00	54418.00	0.00	28042.00
19.55	0.00	0.00	54418.00	0.00	27273.00
19.65	0.00	0.00	0.00	0.00	28715.00
19.75	0.00	0.00	0.00	0.00	26714.00
19.85	0.00	0.00	0.00	0.00	28832.00
19.95	0.00	0.00	0.00	0.00	27963.00
20.05	0.00	0.00	0.00	0.00	28811.00
20.15	0.00	0.00	0.00	0.00	28787.00
20.25	0.00	0.00	0.00	0.00	28776.00
20.35	0.00	0.00	0.00	0.00	28380.00
20.45	0.00	0.00	0.00	0.00	29360.00
20.55	0.00	0.00	0.00	0.00	28508.00
20.65	0.00	0.00	0.00	0.00	29287.00
20.75	0.00	0.00	0.00	0.00	29499.00
20.85	0.00	0.00	0.00	0.00	29083.00
20.95	0.00	0.00	0.00	0.00	30129.00
21.05	0.00	0.00	0.00	0.00	28999.00
21.15	0.00	0.00	0.00	0.00	29354.00
21.25	0.00	0.00	0.00	0.00	30170.00
21.35	0.00	0.00	0.00	0.00	30170.00
21.45	0.00	0.00	0.00	0.00	30170.00
21.55	0.00	0.00	0.00	0.00	30170.00
21.65	0.00	0.00	0.00	0.00	30170.00
21.75	0.00	0.00	0.00	0.00	30170.00
21.85	0.00	0.00	0.00	0.00	30170.00
21.95	0.00	0.00	0.00	0.00	30170.00

PHENYL-2-(3-TRIFLOROMETHYL)-ETHAN-1,2-DIONE

MASS SPECTRUM NO. 2908 GLC OVEN TEMP. = 113

INTEGRATION TIME = 10 SEC. TRAP CURRENT = 20 A

MODULATION = 0.032 V RMS MODULATION FREQ. = 595 HZ

ACC. H.V. = 3.7 KV MULT. H.V. = 1.7 KV

SOURCE TEMP. = 250 DEG. C SEPERATOR TEMP. = 150 DEG. C

AVERAGED FIRST DERIVATIVE VALUES

EV	M/E 278	M/E 259	M/E 173	M/E 105	M/E 145	M/E 77
7.80	-317.90	0.00	0.00	0.00	0.00	0.00
7.90	-236.20	0.00	0.00	0.00	0.00	0.00
8.00	-127.40	0.00	0.00	0.00	0.00	0.00
8.10	155.33	0.00	0.00	0.00	0.00	0.00
8.20	161.17	0.00	0.00	8.17	0.00	0.00
8.30	136.17	0.00	0.00	31.84	0.00	0.00
8.40	271.83	0.00	0.00	34.03	0.00	0.00
8.50	699.50	0.00	0.00	54.00	0.00	0.00
8.60	708.07	0.00	0.00	72.31	0.00	0.00
8.70	1250.80	0.00	0.00	101.74	0.00	0.00
8.80	1529.20	0.00	0.00	164.30	0.00	0.00
8.90	2526.60	0.00	0.00	252.80	0.00	0.00
9.00	2791.20	0.00	0.00	308.67	0.00	0.00
9.10	3228.80	0.00	0.00	521.00	0.00	0.00
9.20	3483.70	0.00	0.00	690.17	0.00	0.00
9.30	5625.80	0.00	13.33	916.17	0.00	0.00
9.40	4822.70	0.00	58.83	1272.80	0.00	0.00
9.50	6418.60	0.00	81.00	1766.70	0.00	0.00
9.60	9377.60	0.00	93.33	2286.80	0.00	0.00
9.70	8349.10	0.00	119.33	3042.70	0.00	0.00
9.80	8795.50	0.00	122.00	4101.50	0.00	0.00
9.90	10790.00	0.00	145.00	5119.60	0.00	0.00
10.00	12736.00	0.00	176.00	6245.80	0.00	0.00

10.10	13222.00	0.00	568.67	7719.80	0.00	0.00
10.20	17225.00	0.00	178.50	9149.50	0.00	0.00
10.30	15313.00	0.00	585.17	10680.00	0.00	0.00
10.40	16616.00	0.00	749.00	12249.00	0.00	0.00
10.50	18191.00	0.00	651.33	14638.00	0.00	0.00
10.60	18525.00	0.00	757.83	16318.00	0.00	0.00
10.70	21924.00	0.00	1075.30	18712.00	0.00	0.00
10.80	25192.00	0.00	1260.30	21156.00	0.00	0.00
10.90	24560.00	0.00	1459.80	23644.00	0.00	0.00
11.00	25206.00	0.00	1330.50	25816.00	-17.17	0.00
11.10	25207.00	0.00	1912.30	28398.00	-6.17	0.00
11.20	29630.00	0.00	1819.20	30810.00	188.83	0.00
11.30	28745.00	0.00	2517.80	33413.00	68.83	0.00
11.40	29475.00	0.00	2632.30	36329.00	115.00	0.00
11.50	31338.00	0.00	2643.00	38959.00	251.67	0.00
11.60	34523.00	0.00	2848.50	41799.00	148.50	10.00
11.70	32731.00	0.00	3468.70	43316.00	143.67	87.54
11.80	41051.00	0.00	3969.40	45396.00	209.50	120.57
11.90	35526.00	0.00	3553.90	48256.00	183.17	125.38
12.00	38909.00	0.00	4418.80	49746.00	198.83	102.71
12.10	41104.00	0.00	4303.20	51271.00	406.17	129.21
12.20	43325.00	0.00	4946.40	53772.00	113.67	110.54
12.30	36555.00	0.00	5865.80	55185.00	516.67	74.21
12.40	44094.00	0.00	6509.50	56535.00	407.14	132.04
12.50	40205.00	0.00	7044.00	59454.00	389.67	196.54
12.60	44084.00	0.00	7664.60	61183.00	456.33	123.38
12.70	44964.00	0.00	7837.30	63357.00	392.50	145.71
12.80	44964.00	521.16	8372.70	65003.00	285.67	205.71
12.90	44964.00	546.03	9573.20	66163.00	437.00	225.54
13.00	44964.00	606.33	9832.80	68032.00	465.83	385.38
13.10	44964.00	764.73	11230.00	69386.00	650.17	489.88
13.20	44964.00	374.69	11701.00	72109.00	658.00	570.38
13.30	44964.00	989.80	11793.00	74000.00	587.33	755.21
13.40	44964.00	655.48	13121.00	75841.00	429.83	1035.70
13.50	44964.00	994.97	13599.00	77077.00	708.83	1237.20
13.60	44964.00	1285.10	15676.00	79864.00	425.00	1576.90
13.70	44964.00	1292.50	15763.00	80024.00	544.00	1794.70
13.80	44964.00	710.61	16954.00	83533.00	484.33	2115.20
13.90	44964.00	2199.10	17947.00	83863.00	710.67	2745.70
14.00	44964.00	2690.40	18189.00	84937.00	624.17	3230.70
14.10	44964.00	3315.70	19162.00	86261.00	756.00	3648.20
14.20	44964.00	3403.90	21608.00	87565.00	741.67	4484.00
14.30	44964.00	5364.60	20025.00	88934.00	899.00	5206.80
14.40	0.00	5507.70	23697.00	88934.00	820.00	5836.20
14.50	0.00	6794.40	23349.00	88934.00	854.33	6837.50
14.60	0.00	9544.20	25838.00	88935.00	1042.30	7410.00
14.70	0.00	10144.00	26658.00	88934.00	940.00	8483.00
14.80	0.00	13407.00	28545.00	88934.00	1420.00	9682.40
14.90	0.00	15150.00	27424.00	88934.00	1722.80	10397.00
15.00	0.00	6436.00	29627.00	88934.00	1545.80	11775.00

15.10	0.00	20827.00	31231.00	88934.00	2292.50	13086.00
15.20	0.00	22005.00	30073.00	88934.00	2123.80	13499.00
15.30	0.00	21684.00	33034.00	88934.00	2370.20	15006.00
15.40	0.00	21625.00	34404.00	0.00	2661.70	16281.00
15.50	0.00	26999.00	32562.00	0.00	2810.70	17515.00
15.60	0.00	30088.00	35202.00	0.00	3176.80	18431.00
15.70	0.00	30131.00	36984.00	0.00	3212.70	20493.00
15.80	0.00	31849.00	36687.00	0.00	3836.20	20912.00
15.90	0.00	34717.00	36335.00	0.00	3880.30	22087.00
16.00	0.00	35130.00	38639.00	0.00	4699.30	23413.00
16.10	0.00	37331.00	40567.00	0.00	4414.00	25095.00
16.20	0.00	35486.00	40641.00	0.00	5350.70	26381.00
16.30	0.00	33133.00	40717.00	0.00	5944.80	27375.00
16.40	0.00	39194.00	42317.00	0.00	5912.70	29555.00
16.50	0.00	41151.00	43236.00	0.00	7223.80	30574.00
16.60	0.00	39452.00	42276.00	0.00	6614.50	32262.00
16.70	0.00	40622.00	44810.00	0.00	8387.30	33826.00
16.80	0.00	44022.00	48410.00	0.00	8310.20	35072.00
16.90	0.00	43473.00	46434.00	0.00	8518.50	36485.00
17.00	0.00	41263.00	47602.00	0.00	9211.00	37678.00
17.10	0.00	41676.00	48130.00	0.00	9953.30	39022.00
17.20	0.00	44812.00	45916.00	0.00	9880.80	39808.00
17.30	0.00	47201.00	48759.00	0.00	10987.00	42025.00
17.40	0.00	45032.00	48432.00	0.00	11721.00	44578.00
17.50	0.00	48757.00	47597.00	0.00	12583.00	44774.00
17.60	0.00	44337.00	51141.00	0.00	13977.00	44573.00
17.70	0.00	46816.00	51047.00	0.00	14711.00	46632.00
17.80	0.00	46816.00	51016.00	0.00	15456.00	49249.00
17.90	0.00	46816.00	49361.00	0.00	15887.00	51447.00
18.00	0.00	46816.00	51480.00	0.00	16554.00	51342.00
18.10	0.00	46816.00	49026.00	0.00	17224.00	54111.00
18.20	0.00	46816.00	53195.00	0.00	18618.00	53712.00
18.30	0.00	46816.00	55452.00	0.00	19845.00	56915.00
18.40	0.00	46816.00	53874.00	0.00	20678.00	58021.00
18.50	0.00	46816.00	54952.00	0.00	23419.00	58011.00
18.60	0.00	46816.00	54608.00	0.00	23043.00	58920.00
18.70	0.00	0.00	55562.00	0.00	23837.00	61789.00
18.80	0.00	0.00	55562.00	0.00	24257.00	62529.00
18.90	0.00	0.00	55562.00	0.00	26291.00	62663.00
19.00	0.00	0.00	55562.00	0.00	26215.00	65726.00
19.10	0.00	0.00	55562.00	0.00	28002.00	65100.00
19.20	0.00	0.00	55562.00	0.00	28171.00	67401.00
19.30	0.00	0.00	55562.00	0.00	30694.00	67028.00
19.40	0.00	0.00	55562.00	0.00	31039.00	67310.00
19.50	0.00	0.00	55562.00	0.00	30780.00	71064.00
19.60	0.00	0.00	0.00	0.00	34385.00	69838.00
19.70	0.00	0.00	0.00	0.00	32759.00	71001.00
19.80	0.00	0.00	0.00	0.00	33242.00	71609.00
19.90	0.00	0.00	0.00	0.00	35893.00	74380.00
20.00	0.00	0.00	0.00	0.00	36474.00	75125.00

20.10	0.00	0.00	0.00	0.00	39247.00	75237.00
20.20	0.00	0.00	0.00	0.00	36247.00	74791.00
20.30	0.00	0.00	0.00	0.00	37665.00	76502.00
20.40	0.00	0.00	0.00	0.00	38124.00	77425.00
20.50	0.00	0.00	0.00	0.00	41361.00	76846.00
20.60	0.00	0.00	0.00	0.00	44208.00	77102.00
20.70	0.00	0.00	0.00	0.00	44293.00	79138.00
20.80	0.00	0.00	0.00	0.00	41463.00	79289.00
20.90	0.00	0.00	0.00	0.00	44771.00	79677.00
21.00	0.00	0.00	0.00	0.00	46413.00	79558.00
21.10	0.00	0.00	0.00	0.00	47593.00	80686.00
21.20	0.00	0.00	0.00	0.00	47843.00	81864.00
21.30	0.00	0.00	0.00	0.00	49485.00	82915.00
21.40	0.00	0.00	0.00	0.00	50543.00	81477.00
21.50	0.00	0.00	0.00	0.00	52088.00	84014.00
21.60	0.00	0.00	0.00	0.00	51818.00	85655.00
21.70	0.00	0.00	0.00	0.00	53117.00	87575.00
21.80	0.00	0.00	0.00	0.00	52906.00	84604.00
21.90	0.00	0.00	0.00	0.00	52330.00	85616.00
22.00	0.00	0.00	0.00	0.00	56040.00	85133.00
22.10	0.00	0.00	0.00	0.00	57112.00	85598.00
22.20	0.00	0.00	0.00	0.00	59510.00	85114.00
22.30	0.00	0.00	0.00	0.00	58630.00	85522.00
22.40	0.00	0.00	0.00	0.00	60342.00	85522.00
22.50	0.00	0.00	0.00	0.00	59371.00	85522.00
22.60	0.00	0.00	0.00	0.00	60494.00	85522.00
22.70	0.00	0.00	0.00	0.00	59857.00	85522.00
22.80	0.00	0.00	0.00	0.00	61969.00	85522.00
22.90	0.00	0.00	0.00	0.00	61393.00	85522.00
23.00	0.00	0.00	0.00	0.00	64074.00	85522.00

PHENYL-2-(3-TRIFLOROMETHYL)-ETHAN-1,2-DIONE

MASS SPECTRUM NO. 2909 GLC OVEN TEMP. = 113

INTEGRATION TIME = 10 SEC. TRAP CURRENT = 20 A

MODULATION = 0.032 V RMS MODULATION FREQ. = 595 HZ

ACC. H.V. = 3.7 KV MULT. H.V. = 1.7 KV

SOURCE TEMP. = 310 DEG. C SEPERATOR TEMP. = 150 DEG. C

AVERAGED FIRST DERIVATIVE VALUES

EV	M/E 278	M/E 259	M/E 173	M/E 105	M/E 145	M/E 77
7.20	0.00	0.00	0.00	0.00	0.00	0.00
7.30	0.00	0.00	0.00	0.00	0.00	0.00
7.40	0.00	0.00	0.00	0.00	0.00	0.00
7.50	0.00	0.00	0.00	0.00	0.00	0.00
7.60	204.00	0.00	0.00	0.00	0.00	0.00
7.70	720.00	0.00	0.00	0.35	0.00	0.00
7.80	37.43	0.00	0.00	0.78	0.00	0.00
7.90	361.00	0.00	0.00	1.85	0.00	0.00
8.00	583.57	0.00	0.00	2.78	0.00	0.00
8.10	1008.30	0.00	0.00	3.58	0.00	0.00
8.20	1363.60	0.00	0.00	5.93	0.00	0.00
8.30	1607.50	0.00	0.00	7.45	0.00	0.00
8.40	1616.70	0.00	0.00	11.41	0.00	0.00
8.50	1588.20	0.00	0.00	14.43	0.00	0.00
8.60	3116.60	0.00	0.00	22.88	0.00	0.00
8.70	3586.30	0.00	0.00	31.45	0.00	0.00
8.80	3255.70	0.00	0.00	46.60	0.00	0.00
8.90	4122.50	0.00	0.00	69.22	0.00	0.00
9.00	4834.00	0.00	0.00	100.03	0.00	0.00
9.10	4975.80	0.00	0.00	131.45	0.00	0.00
9.20	7101.30	0.00	10.70	186.13	0.00	0.00
9.30	6925.20	0.00	6.87	240.20	0.00	0.00
9.40	7342.70	0.00	68.20	303.83	0.00	0.00

9.50	9992.80	0.00	149.70	391.06	0.00	0.00
9.60	12144.00	0.00	141.30	502.86	0.00	0.00
9.70	11929.00	0.00	213.01	607.03	0.00	0.00
9.80	12451.00	0.00	427.20	737.67	0.00	0.00
9.90	13787.00	0.00	398.20	876.42	0.00	0.00
10.00	12747.00	0.00	277.70	1073.80	0.00	0.00
10.10	16199.00	0.00	533.04	1234.40	0.00	0.00
10.20	16023.00	0.00	669.20	1436.70	0.00	0.00
10.30	17597.00	0.00	608.04	1662.70	0.00	0.00
10.40	17762.00	0.00	939.20	1874.10	0.00	0.00
10.50	19004.00	0.00	853.04	2133.50	0.00	0.00
10.60	21348.00	0.00	1107.70	2395.70	0.00	0.00
10.70	20579.00	0.00	1363.90	2672.10	0.00	0.00
10.80	25945.00	0.00	1797.70	2929.40	230.79	0.00
10.90	26708.00	0.00	1896.30	3178.90	324.17	0.00
11.00	30233.00	0.00	2120.40	3401.90	277.00	0.00
11.10	30010.00	0.00	2519.00	3674.70	409.62	0.00
11.20	28969.00	0.00	2607.70	3978.10	415.46	0.00
11.30	30230.00	0.00	2888.40	4362.90	280.15	0.00
11.40	32238.00	0.00	3248.00	4617.60	440.96	24.67
11.50	31980.00	0.00	3859.90	4876.70	519.00	44.00
11.60	35718.00	0.00	4673.40	5244.20	396.00	20.50
11.70	36730.00	0.00	4930.50	5559.60	535.96	16.17
11.80	38417.00	0.00	4931.50	5808.60	367.60	49.17
11.90	34816.00	0.00	6496.30	6134.20	520.29	44.84
12.00	35325.00	0.00	6062.70	6254.60	762.79	51.00
12.10	35325.00	0.00	6223.90	6644.00	567.12	52.84
12.20	35325.00	0.00	6952.00	6936.50	729.62	85.17
12.30	35325.00	0.00	8741.90	7484.90	652.96	111.17
12.40	35325.00	0.00	8213.50	7746.80	834.62	146.00
12.50	35325.00	0.00	8765.00	8013.30	963.79	180.50
12.60	35325.00	673.34	10747.00	8267.40	839.29	187.17
12.70	35325.00	1010.30	11343.00	8530.10	765.46	248.00
12.80	35325.00	1423.50	11393.00	8831.60	826.96	356.67
12.90	35325.00	574.17	12499.00	9074.10	888.12	389.67
13.00	35325.00	765.84	13848.00	9267.60	975.29	543.17
13.10	0.00	795.17	15348.00	9677.80	854.62	654.34
13.20	0.00	1110.70	16691.00	9771.90	1059.70	757.00
13.30	0.00	830.50	18119.00	10246.00	1073.20	860.50
13.40	0.00	965.50	18470.00	10556.00	1408.60	1040.50
13.50	0.00	1038.70	20092.00	10723.00	1229.20	1271.00
13.60	0.00	1092.70	21647.00	10925.00	1249.90	1544.80
13.70	0.00	1668.00	22427.00	11141.00	1273.30	1732.70
13.80	0.00	1367.30	23276.00	11385.00	1617.60	2033.20
13.90	0.00	2240.00	25223.00	11266.00	1506.70	2338.80
14.00	0.00	3521.00	28196.00	11779.00	1990.10	2613.80
14.10	0.00	3282.80	29429.00	11781.00	1942.10	3025.70
14.20	0.00	4773.00	29501.00	11938.00	2084.60	3308.20
14.30	0.00	4585.50	31238.00	11905.00	2180.50	3738.20
14.40	0.00	7427.20	33404.00	11692.00	2676.80	4240.70

14.50	0.00	7418.00	35523.00	12143.00	3072.30	4664.00
14.60	0.00	10055.00	34805.00	12263.00	2868.50	5051.30
14.70	0.00	12288.00	36398.00	12080.00	3411.60	5444.00
14.80	0.00	13644.00	38545.00	12243.00	2991.80	5799.50
14.90	0.00	16039.00	41231.00	12243.00	4038.20	6411.50
15.00	0.00	17552.00	40680.00	12243.00	4531.20	6887.30
15.10	0.00	20524.00	42893.00	12243.00	4821.90	7477.50
15.20	0.00	21471.00	43125.00	12243.00	5738.70	8016.00
15.30	0.00	23178.00	46592.00	12243.00	5706.80	8707.00
15.40	0.00	24585.00	49648.00	12243.00	6758.00	8990.80
15.50	0.00	23779.00	46492.00	12243.00	6683.10	9393.50
15.60	0.00	28194.00	49492.00	12243.00	8040.60	10104.00
15.70	0.00	27740.00	50411.00	12243.00	8412.60	10639.00
15.80	0.00	33692.00	50139.00	12243.00	8453.60	10945.00
15.90	0.00	30605.00	55059.00	0.00	10129.00	11609.00
16.00	0.00	32571.00	55973.00	0.00	8991.60	12148.00
16.10	0.00	32897.00	54688.00	0.00	10672.00	12623.00
16.20	0.00	34637.00	56710.00	0.00	11913.00	13410.00
16.30	0.00	36035.00	58400.00	0.00	11196.00	13628.00
16.40	0.00	33264.00	58831.00	0.00	12867.00	14021.00
16.50	0.00	40865.00	59240.00	0.00	13869.00	14423.00
16.60	0.00	37490.00	60847.00	0.00	15178.00	15294.00
16.70	0.00	37811.00	61492.00	0.00	16585.00	15884.00
16.80	0.00	38681.00	62409.00	0.00	18454.00	15798.00
16.90	0.00	38409.00	64132.00	0.00	18505.00	16527.00
17.00	0.00	38307.00	67852.00	0.00	19908.00	17434.00
17.10	0.00	39708.00	66362.00	0.00	21420.00	17408.00
17.20	0.00	41159.00	65971.00	0.00	21519.00	17990.00
17.30	0.00	43499.00	68467.00	0.00	22534.00	18311.00
17.40	0.00	40155.00	66734.00	0.00	24592.00	18879.00
17.50	0.00	45530.00	70038.00	0.00	24486.00	19006.00
17.60	0.00	45511.00	67594.00	0.00	26772.00	19502.00
17.70	0.00	41562.00	67008.00	0.00	27388.00	19776.00
17.80	0.00	40533.00	66979.00	0.00	27801.00	20229.00
17.90	0.00	43694.00	70591.00	0.00	29817.00	20692.00
18.00	0.00	46454.00	72867.00	0.00	30572.00	20544.00
18.10	0.00	45454.00	71666.00	0.00	32389.00	21183.00
18.20	0.00	51462.00	72372.00	0.00	35107.00	21224.00
18.30	0.00	42468.00	70182.00	0.00	35561.00	21389.00
18.40	0.00	49022.00	72871.00	0.00	37143.00	21470.00
18.50	0.00	51294.00	72871.00	0.00	39258.00	22507.00
18.60	0.00	48562.00	72871.00	0.00	38232.00	22430.00
18.70	0.00	48562.00	72871.00	0.00	38331.00	22637.00
18.80	0.00	48562.00	72871.00	0.00	39449.00	22574.00
18.90	0.00	48562.00	72871.00	0.00	41677.00	23319.00
19.00	0.00	48562.00	72871.00	0.00	42316.00	23234.00
19.10	0.00	48562.00	72871.00	0.00	44249.00	23353.00
19.20	0.00	48562.00	72871.00	0.00	44642.00	24648.00
19.30	0.00	48562.00	72871.00	0.00	48880.00	23952.00
19.40	0.00	48562.00	0.00	0.00	47111.00	24001.00

19.50	0.00	0.00	0.00	0.00	50303.00	24307.00
19.60	0.00	0.00	0.00	0.00	52951.00	24600.00
19.70	0.00	0.00	0.00	0.00	49983.00	24720.00
19.80	0.00	0.00	0.00	0.00	52968.00	25090.00
19.90	0.00	0.00	0.00	0.00	50692.00	24607.00
20.00	0.00	0.00	0.00	0.00	54166.00	24817.00
20.10	0.00	0.00	0.00	0.00	53249.00	24782.00
20.20	0.00	0.00	0.00	0.00	57561.00	25092.00
20.30	0.00	0.00	0.00	0.00	57949.00	25092.00
20.40	0.00	0.00	0.00	0.00	57473.00	25092.00
20.50	0.00	0.00	0.00	0.00	60727.00	25092.00
20.60	0.00	0.00	0.00	0.00	58897.00	25092.00
20.70	0.00	0.00	0.00	0.00	59658.00	25092.00
20.80	0.00	0.00	0.00	0.00	61399.00	25092.00

1,2-DIPHENYLETHAN-1,2-DIONE

MASS SPECTRUM NO. 2865 GLC OVEN TEMP. = 125

INTEGRATION TIME = 10 SEC. TRAP CURRENT = 20 A

MODULATION = 0.032 V RMS MODULATION FREQ. = 595 HZ

ACC. H.V. = 3.7 KV MULT. H.V. = 1.7 KV

SOURCE TEMP. = 250 DEG. C SEPERATOR TEMP. = 150 DEG. C

AVERAGED FIRST DERIVATIVE VALUES

EV	M/E 210	M/E 105	M/E 77
7.15	0.00	0.00	0.00
7.25	0.00	0.00	0.00
7.35	0.00	0.00	0.00
7.45	175.30	0.00	0.00
7.55	204.00	19.20	0.00
7.65	230.20	27.60	0.00
7.75	644.50	35.60	0.00
7.85	752.00	57.20	0.00
7.95	967.30	85.40	0.00
8.05	1357.70	115.40	0.00
8.15	2170.20	176.20	0.00
8.25	3302.00	257.20	0.00
8.35	4253.00	376.20	0.00
8.45	6208.70	530.00	0.00
8.55	7884.80	744.00	0.00
8.65	10131.00	1092.00	0.00
8.75	12251.00	1495.60	0.00
8.85	14458.00	2062.80	0.00
8.95	16921.00	2730.60	0.00
9.05	18562.00	3520.20	0.00
9.15	20557.00	4420.10	0.00
9.25	21493.00	5418.90	0.00
9.35	24187.00	6546.90	0.00

9.45	26317.00	7683.30	0.00
9.55	27006.00	8813.80	0.00
9.65	29617.00	10030.00	0.00
9.75	29591.00	11178.00	0.00
9.85	32577.00	12420.00	0.00
9.95	32767.00	14044.00	0.00
10.05	34921.00	15071.00	0.00
10.15	37458.00	16648.00	0.00
10.25	39163.00	17970.00	0.00
10.35	41637.00	19266.00	0.00
10.45	41740.00	20641.00	0.00
10.55	43307.00	22346.00	0.00
10.65	44974.00	23964.00	0.00
10.75	49206.00	25714.00	0.00
10.85	52318.00	27095.00	0.00
10.95	55143.00	28920.00	0.00
11.05	55236.00	30016.00	0.00
11.15	58568.00	31983.00	0.00
11.25	59126.00	33437.00	0.00
11.35	60844.00	35059.00	0.00
11.45	64689.00	36609.00	0.00
11.55	64141.00	38677.00	20.60
11.65	68292.00	40665.00	17.60
11.75	68173.00	42398.00	38.30
11.85	71364.00	44952.00	14.40
11.95	73405.00	47066.00	68.80
12.05	73290.00	48606.00	49.90
12.15	73948.00	50363.00	69.00
12.25	75388.00	52200.00	129.00
12.35	75557.00	53966.00	146.40
12.45	77986.00	55822.00	130.90
12.55	78072.00	56821.00	181.80
12.65	80200.00	58421.00	284.60
12.75	83838.00	60243.00	384.60
12.85	76871.00	61596.00	451.60
12.95	82886.00	63140.00	625.90
13.05	83535.00	64449.00	791.40
13.15	83672.00	65403.00	950.40
13.25	83672.00	67002.00	1315.60
13.35	83672.00	68313.00	1671.80
13.45	83672.00	69427.00	1937.60
13.55	83672.00	69089.00	2275.40
13.65	83672.00	69810.00	2763.80
13.75	0.00	69809.00	3445.80
13.85	0.00	71234.00	3890.60
13.95	0.00	71367.00	4448.30
14.05	0.00	72280.00	5238.10
14.15	0.00	72340.00	5880.90
14.25	0.00	72398.00	6736.70
14.35	0.00	72498.00	7433.20

14.45	0.00	73102.00	8470.60
14.55	0.00	73033.00	9347.60
14.65	0.00	73761.00	10148.00
14.75	0.00	72831.00	11102.00
14.85	0.00	72831.00	12016.00
14.95	0.00	72831.00	13290.00
15.05	0.00	72831.00	14010.00
15.15	0.00	72831.00	15049.00
15.25	0.00	72831.00	15862.00
15.35	0.00	72831.00	16756.00
15.45	0.00	72831.00	17763.00
15.55	0.00	72831.00	18674.00
15.65	0.00	72831.00	20114.00
15.75	0.00	72831.00	20815.00
15.85	0.00	72831.00	22158.00
15.95	0.00	72831.00	23165.00
16.05	0.00	0.00	24735.00
16.15	0.00	0.00	25238.00
16.25	0.00	0.00	25980.00
16.35	0.00	0.00	27462.00
16.45	0.00	0.00	28203.00
16.55	0.00	0.00	29984.00
16.65	0.00	0.00	30466.00
16.75	0.00	0.00	31069.00
16.85	0.00	0.00	32391.00
16.95	0.00	0.00	33031.00
17.05	0.00	0.00	34469.00
17.15	0.00	0.00	35316.00
17.25	0.00	0.00	36681.00
17.35	0.00	0.00	37353.00
17.45	0.00	0.00	38023.00
17.55	0.00	0.00	38580.00
17.65	0.00	0.00	39292.00
17.75	0.00	0.00	40949.00
17.85	0.00	0.00	41682.00
17.95	0.00	0.00	42318.00
18.05	0.00	0.00	43359.00
18.15	0.00	0.00	44073.00
18.25	0.00	0.00	44684.00
18.35	0.00	0.00	44880.00
18.45	0.00	0.00	46737.00
18.55	0.00	0.00	46202.00
18.65	0.00	0.00	48687.00
18.75	0.00	0.00	48872.00
18.85	0.00	0.00	48994.00
18.95	0.00	0.00	49652.00
19.05	0.00	0.00	50399.00
19.15	0.00	0.00	51448.00
19.25	0.00	0.00	51449.00
19.35	0.00	0.00	51172.00

19.45	0.00	0.00	52195.00
19.55	0.00	0.00	52032.00
19.65	0.00	0.00	53351.00
19.75	0.00	0.00	53886.00
19.85	0.00	0.00	52105.00
19.95	0.00	0.00	52819.00
20.05	0.00	0.00	53660.00
20.15	0.00	0.00	53875.00
20.25	0.00	0.00	53755.00
20.35	0.00	0.00	52057.00
20.45	0.00	0.00	53880.00
20.55	0.00	0.00	53412.00
20.65	0.00	0.00	53412.00
20.75	0.00	0.00	53412.00
20.85	0.00	0.00	53412.00
20.95	0.00	0.00	53412.00
21.05	0.00	0.00	53412.00

1-PHENYL-2-(PHENYL-D5)-ETHAN-1,2-DIONE

MASS SPECTRUM NO. 2906 GLC OVEN TEMP. = 123

INTEGRATION TIME = 10 SEC. TRAP CURRENT = 20 A

MODULATION = 0.030 V RMS MODULATION FREQ. = 595 HZ

ACC. H.V. = 3.7 KV MULT. H.V. = 1.7 KV

SOURCE TEMP. = 250 DEG. C SEPERATOR TEMP. = 155 DEG. C

AVERAGED FIRST DERIVATIVE VALUES

EV	M/E 215	M/E 110	M/E 105	M/E 82	M/E 77
7.50	0.00	0.00	0.00	0.00	0.00
7.60	0.00	0.00	0.00	0.00	0.00
7.70	0.00	0.00	0.00	0.00	0.00
7.80	0.00	0.00	0.00	0.00	0.00
7.90	0.00	0.00	0.00	0.00	0.00
8.00	32.64	12.57	16.83	0.00	0.00
8.10	18.67	24.57	28.83	0.00	0.00
8.20	81.83	33.83	32.83	0.00	0.00
8.30	219.83	39.00	43.50	0.00	0.00
8.40	484.50	66.00	65.67	0.00	0.00
8.50	728.33	60.17	99.67	0.00	0.00
8.60	989.50	117.00	148.00	0.00	0.00
8.70	1487.50	152.00	215.67	0.00	0.00
8.80	2014.50	278.83	320.86	0.00	0.00
8.90	2380.80	406.50	431.83	0.00	0.00
9.00	2855.50	572.00	592.00	0.00	0.00
9.10	3693.50	790.67	897.50	0.00	0.00
9.20	4367.50	1198.10	1224.80	0.00	0.00
9.30	5353.00	1717.30	1666.50	0.00	0.00
9.40	6805.50	2111.80	2160.80	0.00	0.00
9.50	7293.80	2743.20	2705.30	0.00	0.00
9.60	8366.80	3321.30	3343.20	0.00	0.00
9.70	7720.50	4152.70	4000.20	0.00	0.00

9.80	8567.00	5084.00	4968.00	0.00	0.00
9.90	9056.30	6022.80	5982.00	0.00	0.00
10.00	10046.00	7099.20	6923.50	0.00	2.90
10.10	10732.00	8064.70	8005.10	30.04	30.24
10.20	12477.00	9122.00	8964.60	239.86	46.74
10.30	13466.00	10256.00	9939.30	228.15	14.71
10.40	14608.00	11369.00	11208.00	224.92	25.00
10.50	16517.00	12577.00	12352.00	433.43	44.14
10.60	16787.00	13961.00	13648.00	407.58	76.07
10.70	16781.00	14958.00	14704.00	275.58	85.57
10.80	17499.00	15895.00	15738.00	468.67	27.14
10.90	18977.00	16940.00	16910.00	411.46	42.71
11.00	19774.00	18296.00	18323.00	804.58	27.45
11.10	21262.00	19597.00	19976.00	737.29	46.57
11.20	21869.00	20821.00	20754.00	637.86	56.43
11.30	22786.00	21875.00	21957.00	974.79	47.43
11.40	23942.00	23842.00	23302.00	907.58	7.43
11.50	24773.00	24304.00	24627.00	809.72	6.28
11.60	24377.00	25504.00	26314.00	952.79	95.71
11.70	25077.00	27249.00	27174.00	1316.60	110.00
11.80	28121.00	28759.00	28586.00	1406.10	52.28
11.90	26999.00	29420.00	29552.00	1313.30	26.71
12.00	27545.00	30602.00	31368.00	1505.50	72.14
12.10	28314.00	31698.00	32612.00	1859.90	43.86
12.20	28971.00	34184.00	34047.00	1788.50	58.71
12.30	28391.00	34520.00	35472.00	1770.50	58.57
12.40	29896.00	35698.00	36775.00	1687.10	64.28
12.50	28680.00	38002.00	37514.00	1674.70	99.14
12.60	30262.00	39106.00	38862.00	2082.90	117.57
12.70	29933.00	40423.00	40585.00	2704.00	225.14
12.80	31031.00	41332.00	42008.00	2895.20	210.71
12.90	32029.00	42105.00	43563.00	2035.80	265.14
13.00	31554.00	44058.00	43937.00	3138.60	309.00
13.10	32382.00	45052.00	45811.00	2748.80	367.14
13.20	33589.00	46529.00	47582.00	2995.30	502.00
13.30	35136.00	47202.00	48360.00	3314.30	637.00
13.40	32886.00	47886.00	49142.00	3752.50	745.86
13.50	32224.00	48453.00	49510.00	4652.80	914.14
13.60	33564.00	49866.00	49952.00	5112.10	1105.70
13.70	32836.00	50028.00	51439.00	5351.50	1310.60
13.80	32145.00	52023.00	51830.00	5781.30	1626.60
13.90	33524.00	52558.00	52189.00	6281.70	1948.30
14.00	33524.00	52472.00	53427.00	8153.60	2265.10
14.10	33524.00	52731.00	53677.00	7643.90	2478.60
14.20	33524.00	53252.00	55212.00	9373.40	2884.60
14.30	33524.00	53870.00	54465.00	11468.00	3257.10
14.40	33524.00	55146.00	55083.00	11922.00	3676.90
14.50	33524.00	54615.00	55438.00	12847.00	4115.60
14.60	33524.00	54758.00	55701.00	13923.00	4574.90
14.70	33524.00	55205.00	55924.00	14966.00	5130.40

14.80	0.00	55205.00	55924.00	17345.00	5833.90
14.90	0.00	55205.00	55924.00	17475.00	6172.40
15.00	0.00	55205.00	55924.00	19310.00	6998.60
15.10	0.00	55205.00	55924.00	21278.00	7171.90
15.20	0.00	55205.00	55924.00	23466.00	8279.70
15.30	0.00	0.00	0.00	22761.00	8980.20
15.40	0.00	0.00	0.00	24194.00	9108.20
15.50	0.00	0.00	0.00	26948.00	9995.70
15.60	0.00	0.00	0.00	28836.00	10246.00
15.70	0.00	0.00	0.00	29736.00	10722.00
15.80	0.00	0.00	0.00	31474.00	12012.00
15.90	0.00	0.00	0.00	33095.00	12790.00
16.00	0.00	0.00	0.00	35755.00	13387.00
16.10	0.00	0.00	0.00	37579.00	14101.00
16.20	0.00	0.00	0.00	39935.00	14349.00
16.30	0.00	0.00	0.00	39070.00	15555.00
16.40	0.00	0.00	0.00	42084.00	15798.00
16.50	0.00	0.00	0.00	42378.00	16131.00
16.60	0.00	0.00	0.00	45512.00	17415.00
16.70	0.00	0.00	0.00	48098.00	18405.00
16.80	0.00	0.00	0.00	49476.00	18229.00
16.90	0.00	0.00	0.00	51946.00	20049.00
17.00	0.00	0.00	0.00	52959.00	20652.00
17.10	0.00	0.00	0.00	54738.00	20744.00
17.20	0.00	0.00	0.00	55505.00	21281.00
17.30	0.00	0.00	0.00	58518.00	21832.00
17.40	0.00	0.00	0.00	58854.00	22192.00
17.50	0.00	0.00	0.00	59465.00	22608.00
17.60	0.00	0.00	0.00	61788.00	23516.00
17.70	0.00	0.00	0.00	66455.00	24208.00
17.80	0.00	0.00	0.00	68761.00	24660.00
17.90	0.00	0.00	0.00	70103.00	25878.00
18.00	0.00	0.00	0.00	70520.00	26338.00
18.10	0.00	0.00	0.00	72902.00	26622.00
18.20	0.00	0.00	0.00	71636.00	27497.00
18.30	0.00	0.00	0.00	76395.00	28271.00
18.40	0.00	0.00	0.00	73243.00	28497.00
18.50	0.00	0.00	0.00	78191.00	30292.00
18.60	0.00	0.00	0.00	79039.00	28187.00
18.70	0.00	0.00	0.00	79689.00	29805.00
18.80	0.00	0.00	0.00	79879.00	30206.00
18.90	0.00	0.00	0.00	81090.00	30759.00
19.00	0.00	0.00	0.00	81795.00	31375.00
19.10	0.00	0.00	0.00	84891.00	31322.00
19.20	0.00	0.00	0.00	84891.00	31461.00
19.30	0.00	0.00	0.00	84891.00	32760.00
19.40	0.00	0.00	0.00	84891.00	33028.00
19.50	0.00	0.00	0.00	84891.00	34823.00
19.60	0.00	0.00	0.00	84891.00	32978.00
19.70	0.00	0.00	0.00	84891.00	32483.00
19.80	0.00	0.00	0.00	84891.00	33860.00
19.90	0.00	0.00	0.00	84891.00	33328.00
20.00	0.00	0.00	0.00	0.00	33323.00
20.10	0.00	0.00	0.00	0.00	33383.00
20.20	0.00	0.00	0.00	0.00	33383.00
20.30	0.00	0.00	0.00	0.00	33383.00
20.40	0.00	0.00	0.00	0.00	33383.00
20.50	0.00	0.00	0.00	0.00	33383.00
20.60	0.00	0.00	0.00	0.00	33383.00
20.70	0.00	0.00	0.00	0.00	33383.00
20.80	0.00	0.00	0.00	0.00	33383.00
20.90	0.00	0.00	0.00	0.00	33383.00

APPENDIX B

NUMERICAL TREATMENT OF dI/dE DATA

APPENDIX B

NUMERICAL TREATMENT OF dI/dE DATA

The experimental dI/dE values for each ion were numerically smoothed twice using subroutine SE-15.[64] For each ion the d^2I/dE^2 value at the i-th voltage V_i was computed, using the doubly smoothed dI/dE values $y(ds)_{i+k}$, where $k = \pm 1, \pm 2$, and ± 3, Equation 24 where h equals the energy interval 0.100 eV.

$$F''(V_i) = \frac{1}{h}\{ \frac{[3\ y(ds)_{i+1} - y(ds)_{i-1}\ ]}{4} - 3[\ \frac{y(ds_{i+2} - y(ds)_{i-2}]}{20} + \frac{[y(ds)_{i+3} - y(ds)_{i-3}\ ]}{60} \} \tag{24}$$

Equation 24 can be derived by differentiating the polynomial of degree six which is fitted to seven consecutive points and solving for the coefficients in Equation 25. The $F''(V_i)$ values were then smoothed once to obtain the SDIE curves.

$$F''(V_i) = A\ [\ \frac{y(ds)_{i+1} - y(ds)_{i-1}]}{2h} - B[\ \frac{y(ds)_{i+2} - y(ds)_{i-2}\ ]}{4h} + C\ [\ \frac{y(ds)_{i+3} - y(ds)_{i-3}\ ]}{6h} \tag{25}$$

The standard deviation in dI/dE was calculated at three energies for each ion investigated in the spectrum of I, II, III, IV, and V. The predicted per cent deviation in dI/dE may be computed from Equation 26 by dividing by the dI/dE value.

$$\sigma_{sn} = I \left\{ \left\{ \frac{\kappa \eta R_b \lambda \omega_e^2}{\omega_m^2 + \omega_e^2 T_i} \right\} \left\{ \frac{1 + \sigma_m^2}{\eta^2} \right\} \left\{ \frac{1 - RC}{T_i} + \frac{RC}{T_i} \exp^{-(T_i/RC)} \right\} \right\} \quad (26)$$

Values of the quantities used in equation 26 are $\kappa = 1.030$, $R_b = 1.1 \times 10^8$ ohms, $\lambda = 1.5921 \times 10^{-19}$C, $\omega_e/2\pi = 660\ Hz$, $\omega_m/2\pi = 600 Hz$, $(1 + \sigma_m^2/\eta^2) = 1.92$, η = experimental multiplier gain, (T_i) = integration time, RC = lock-in-amplifer time constant, and I is the integrated dI/dE value.

The standard deviation in d^2I/dE^2 values for each ion was computed in the following manner. Let y_i and $y(s)_i$ represent the experimental and once smoothed dI/dE values for a given ion at the i-th eV. The smoothing routine performs a moving five-point average. The $y(s)_i$ values are given in terms of the y_i values by Equation 27. Except for the end point regions the coefficients in Equation 27 have the value 1/5.

$$y(s)_i = a_1 y_{i-2} + a_2 y_{i-1} + a_3 y_i + a_4 y_{i+1} + a_5 y_{i+2} \quad (27)$$

Zeros values were added below onset and the average maximum was extended to eliminate the end-point effects in SE-15. The $y(ds)_i$ are obtained from $y(ds)_i$ by application of Equation 27 to $y(s)_i$. Clearly, the

$y(ds)_i$ can be expressed in terms of the y_i. The expression so obtained is given in Equation 28. Thus two five-point smoothes of dI/dE are equivalent to one nine-point smooth where the coefficients of the latter are determined by those of the former.

$$y(ds)_i = \sum_{k=-4}^{k=+4} b_k y_{i+k}$$

where

$$b_k = \frac{5 - |k|}{25}, \quad k = 0, \pm 1, \ldots . \pm 4 \tag{28}$$

Similary, the $y(ds)_i$ in Equation 24 can be expressed in terms of the y_i. The desired function $F''(V_i)$ can be obtained by convoluting the coefficients of Equation 28 into those Equation 27. An antisymmetric set of fifteen coefficients is obtained whose values are

$-C_{-7} = C_7 = 1/1500$, $-C_{-6} = C_6 = 7/1500$, $-C_{-5} = C_5 = 30/1500$, $-C_{-4} = C_4 = 67/1500$, $-C_{-3} = C_3 = 59/1500$, $-C_{-2} - C_2 = 58/100$, $-C_{-1} = C_1 = 74/1500$, $C_0 = 0$. Therefore d^2I/dE^2 at the i-th eV is formally given by Equation 29. The contribution to $\underline{\sigma}^2$ in $F''(V_i)$ from the i + j value of dI/dE is $C_j^2 \, \underline{\sigma}_{i+j}^2 / k^2 .^{65}$ The contribution is $(1/k^2) \sum_{j=-7}^{j=+7} C_j^2 \underline{\sigma}_{i+j}^2$. For ease of calculation the standard deviation in dI/dE assumed constant over the range of dI/dE values required to calculate d^2I/dE^2 value. The contribution to $\underline{\sigma}^2$ due to the uncertainty in the energy interval h is given by evaluation of $\left[F''(V_i)/\partial h\right]^2 \underline{\sigma}_h^2$. Owing to possible variations in the mean electron energy resulting from variations in the filament temperature the uncertainty in h was increased from 0.003

to 0.005 eV. The standard deviation in d^2I/dE^2 is thus given by Equation 30 , where $\underline{\sigma}(y_i)$ is the per cent standard deviation in dI/dE.

$$F''(V_i) = \frac{1}{h} \left[F''(V_i)\ \underline{\sigma}_h^2 + 0.015787 \left[\frac{\underline{\sigma}(y_i) y_i}{100} \right]^2 \right]^{1/2} \qquad (30)$$

The data in the following tables were computed from Equations 26 and 30. To obtain the ion current at the lock-in amplifier input the integrated first derivative values must be multiplied by $M/\sqrt{2}$ times the frequency response of the electron multiplier, where M is the RMS modulation. For the instrumental arrangement used the frequency response was 0.74 and the RMS modulation was 0.032 volt. All calculations using either ion intensity or derivative values were converted from counts per unit time to volts input to the lock-in amplifier.

1-PHENYL-2-(4-METHYLPHENYL)-ETHAN-1,2-DIONE, I.S. TEMP. = 230 DEG. C

ION	EV	FD	% SIGMA FD	SD	% SIGMA SD
224	7.85	319.65	11.47	3955.80	5.13
224	9.05	11863.00	2.68	21934.00	5.32
224	11.15	55554.00	2.22	16992.00	10.42
119	9.05	3064.70	1.32	15166.00	5.01
119	10.05	21545.00	0.68	28182.00	5.04
119	12.05	61682.00	0.70	8871.80	7.88
105	9.95	916.37	3.57	1987.30	5.41
105	11.65	6053.60	1.87	4818.60	5.81
105	15.05	20353.00	1.70	2558.30	17.72
91	13.05	1546.40	5.05	2693.20	6.19
91	15.75	15776.00	1.46	7744.50	6.25
91	17.55	27558.00	1.38	2939.10	17.06
77	14.25	1587.30	6.14	2728.30	6.72
77	17.25	15417.00	2.88	6754.20	9.66
77	20.35	34885.00	2.66	3710.90	31.80

1-PHENYL-2-(4-METHYLPHENYL)-ETHAN-1,2-DIONE, I.S. TEMP. = 310 DEG. C

ION	EV	FD	% SIGMA FD	SD	% SIGMA SD
224	8.65	389.46	4.43	902.08	5.55
224	11.25	2248.90	4.16	599.73	20.21
224	12.85	2760.80	4.80	235.26	71.02
119	9.55	986.82	1.10	1369.00	5.10
119	11.55	3689.40	0.97	1340.90	6.01
119	13.55	6020.10	1.01	922.33	9.67
105	9.85	147.88	5.40	208.91	6.93
105	12.05	962.53	3.24	580.43	8.40
105	16.55	3139.60	3.10	476.10	26.16
91	13.05	421.60	5.62	632.99	6.86
91	15.05	3538.40	2.22	2153.70	6.79
91	18.05	11267.00	1.77	1327.20	19.55
77	14.05	1870.50	6.00	2417.40	7.68
77	17.05	17751.00	2.73	7019.90	10.00
77	19.55	33006.00	2.72	5153.90	22.44

1-PHENYL-2-(4-METHOXYPHENYL)-ETHAN-1,2-DIONE, I.S. TEMP. = 250 DEG. C

ION	EV	FD	% SIGMA FD	SD	% SIGMA SD
240	8.05	1595.90	10.47	6629.90	5.92
240	9.15	20895.00	4.17	22085.00	7.04
240	11.55	57898.00	4.72	14335.00	24.49
135	9.35	3365.20	1.49	6483.10	5.09
135	11.25	24782.00	0.88	14616.00	5.34
135	13.35	44165.00	0.97	6202.00	10.05
107	13.15	1246.70	14.60	1138.40	20.71
107	15.25	13035.00	3.79	9996.70	7.97
107	16.55	24402.00	3.44	7181.60	15.53
105	11.05	2746.80	6.72	3734.70	7.97
105	14.25	32269.00	3.31	13853.00	10.91
105	15.85	48833.00	3.35	4939.10	41.91
77	15.05	1757.30	7.21	2543.90	8.01
77	17.05	14651.00	2.47	10768.00	6.54
77	20.65	48556.00	2.20	4853.90	28.08

1-PHENYL-2-(4-METHOXYPHENYL)-ETHAN-1,2-DIONE, I.S. TEMP. = 310 DEG. C

ION	EV	FD	% SIGMA FD	SD	% SIGMA SD
240	7.85	1295.90	26.33	2668.50	16.83
240	8.35	3892.60	15.50	7057.70	11.85
240	10.75	19148.00	12.99	7869.10	40.02
135	8.95	3112.70	2.83	6060.30	5.32
135	11.35	30469.00	1.56	14401.00	6.49
135	13.75	62546.00	1.50	9813.60	13.02
107	13.15	4212.10	11.27	5403.90	12.12
107	14.75	22288.00	5.27	14306.00	11.46
107	17.15	49804.00	5.20	4933.80	66.14
105	10.85	2809.10	11.73	2662.70	16.34
105	13.05	15210.00	7.07	8065.40	17.49
105	15.35	29730.00	7.02	3215.50	81.71
77	14.35	1275.60	9.66	1768.80	10.08
77	17.05	14414.00	4.43	6604.90	13.13
77	18.95	25623.00	4.39	5010.00	28.62

1-PHENYL-2-(3-TRIFLOROMETHYL)-ETHAN-1,2-DIONE, I.S. TEMP. = 250 DEG. C

ION	EV	FD	% SIGMA FD	SD	% SIGMA SD
278	9.10	3453.30	14.64	6597.60	10.85
278	10.80	23116.00	9.15	14737.00	18.72
278	12.10	39879.00	8.97	8517.70	53.02
259	14.00	2172.90	20.18	4949.60	12.20
259	15.00	15231.00	7.80	19629.00	9.10
259	16.50	38236.00	7.62	9534.60	38.71
173	11.30	2047.10	12.16	2332.20	14.31
173	14.50	22978.00	5.61	12294.00	14.09
173	17.20	45118.00	5.26	10422.00	29.03
105	9.80	3273.50	2.37	8277.80	5.14
105	11.40	33685.00	1.15	26910.00	5.32
105	13.80	81121.00	1.20	15903.00	9.17
145	15.00	1594.20	20.33	1989.00	21.08
145	18.00	16085.00	6.97	7905.80	18.50
145	23.00	62737.00	5.57	9423.90	46.83
77	13.80	1951.10	6.91	3614.50	6.85
77	17.80	47549.00	2.82	15073.00	12.25
77	20.50	77011.00	3.02	5226.80	56.06

1-PHENYL-2-(3-TRIFLOROMETHYL)-ETHAN-1,2-DIONE, I.S. TEMP. = 310 DEG. C

ION	EV	FD	% SIGMA FD	SD	% SIGMA SD
278	8.60	2744.30	2.12	4696.60	5.24
278	9.50	9703.10	1.45	11458.00	5.23
278	11.40	32280.00	1.18	17778.00	5.68
259	13.50	1040.20	35.23	1162.20	39.93
259	14.90	13978.00	8.32	18706.00	9.27
259	18.00	44420.00	9.70	6607.80	82.11
173	11.80	6289.30	8.19	4419.10	15.47
173	13.80	27238.00	4.88	15660.00	11.77
173	16.80	65419.00	4.56	7315.00	51.45
105	9.50	3670.80	2.34	8196.70	5.17
105	12.30	66098.00	1.06	30668.00	5.76
105	13.80	101412.00	1.08	18053.00	9.14
145	14.90	3650.00	11.65	3530.10	15.94
145	16.80	16525.00	6.26	12228.00	11.74
145	21.20	64299.00	5.14	7496.90	55.60
77	13.20	662.10	6.38	1226.30	6.61
77	15.30	8006.50	2.75	5330.90	7.21
77	18.70	22371.00	2.79	2414.20	32.81

1,2-DIPHENYLETHAN-1,2-DIONE ,I.S. TEMP. = 250 DEG. C

ION	EV	FD	% SIGMA FD	SD	% SIGMA SD
210	7.65	423.46	2.89	5308.50	5.01
210	8.55	8329.40	1.62	20035.00	5.07
210	11.15	57641.00	1.33	18536.00	7.20
105	8.45	665.89	2.74	5073.50	5.02
105	11.45	36844.00	0.80	19387.00	5.35
105	13.45	68314.00	0.79	5349.90	13.62
77	12.90	3988.10	0.86	2510.50	5.29
77	15.50	17797.00	1.92	10722.00	6.41
77	18.40	45300.00	1.85	7250.30	15.33

1-PHENYL-2-(PHENYL-D5)-ETHAN-1,2-DIONE, I.S. TEMP. = 250 DEG. C

ION	EV	FD	% SIGMA FD	SD	% SIGMA SD
215	8.50	850.73	11.18	2978.20	6.41
215	10.20	12395.00	5.94	11191.00	9.66
215	12.30	28860.00	5.98	3284.90	66.23
110	9.40	1792.30	3.17	4697.70	5.23
110	12.10	30866.00	1.60	12795.00	6.97
110	13.70	49698.00	1.61	8329.60	13.06
105	9.40	2295.80	2.97	5364.60	5.25
105	12.10	32633.00	1.57	13350.00	6.95
105	13.70	51103.00	1.61	7224.60	15.14
82	13.90	6122.90	10.75	6608.70	13.48
82	15.80	30034.00	5.30	17473.00	12.49
82	18.60	77074.00	4.61	12714.00	35.47
77	13.90	4632.40	5.12	7598.90	6.35
77	15.80	31021.00	2.76	18906.00	7.57
77	18.60	80613.00	2.56	11538.00	22.99

APPENDIX C

THERMODYNAMICS OF FRAGMENTATION

APPENDIX C

THERMODYNAMICS OF FRAGMENTATION

The deviations in the calculated data for I, II, and III were computed[65] assuming, unless uncertainties were specifically given, either an arbitrary five per cent error or the average deviation in each quantity used in the calculation.

1-(Methylphenyl)-2-phenylethane-1,2-dione (I)

The ΔH_f(I) was estimated as follows: The ΔH_f of IV is -21.8 kcal/mole.[66] The group equivalents[67] value for ΔH_f of 4-methylbenzaldehyde (-10.5 kcal/mole),[68] and the group equivalents value for ΔH_f of 4-methylbenzophenone (3.3 kcal/mole)[68] compared to the experimental ΔH_f for benzophenone (12.5 kcal/mole)[68], yield values of -10.5 and -9.2 kcal/mole respectively for $\Delta\Delta H_f$ for replacement of a para hydrogen by methyl. These results together with the value of ΔH_f(IV) (-21.8 kcal/mole) give estimates for ΔH_f(I) of -31.0 and -32.3 kcal/mole. The group equivalents value for ΔH_f(I) is -28.3 kcal/mole. The three values give an average of -30.54 ± 1.48 kcal/mole for ΔH_f(I).

The experimental ionization potential of IV of 8.86 ± 0.14 eV and the ΔH_f(IV) gives via Equation 31 a value of 183.5 ± 3.6 for ΔH_f(IVa)

which is in good agreement with a previously reported value of 180 kcal/mole.[34]

$$\Delta H_f(IVa) = IP(IV)/23.06 + \Delta H_f(IV) \qquad (31)$$

The $\Delta\Delta H_f$ for replacement of a p-hydrogen by methyl was estimated to be $-14.50 \pm .72$ kcal/mole from ΔH_f of the molecular ions of 4-methylbenzophenone (214 kcal/mole) and benzophenone (228 kcal/mole) and 4-methylbenzaldehyde (194 kcal/mole) and benzaldehyde (209 kcal/mole).[68] The ΔH_f of Ia was then estimated to be 168.0 ± 3.7 kcal/mole and the ionization potential of I calculated to be 8.61 ± 0.17 eV.

Equation 32a is applicable to the formation of Ic via C-1--C-2 bond rupture. Taking a recent value of 26.1 ± 2.0 kcal/mole for ΔH_f

$$AP(Ic) = \{\Delta H_f(Ic) + \Delta H_f(C_7H_5O) - \Delta H_f(I)\}/23.06 \qquad (32a)$$

of the benzoyl radical[69] and a value of 167.7 ± 3.2 kcal/mole for ΔH_f of Ic, vide post, leads to a value of 9.73 ± 0.18 eV for the appearance potential of Ic. Equation 32b is valid for formation of Ic via two-bond rupture. Values[68] of 72.0 and 26.42 kcal/mole for ΔH_f of

$$AP(Ic) = \{\Delta H_f(Ic) + \Delta H_f(C_6H_5) + \Delta H_f(CO) - \Delta H_f(I)\}/23.06 \qquad (32b)$$

C_6H_5 and CO lead to a value of 10.58 ± 0.23 eV for the appearance potential of Ic. The $\Delta H_f(Ic)$, i.e., 167.7 ± 3.2 kcal/mole, was calculated from $\Delta H_f(Ib)$, vide post, with the assumption that $\Delta\Delta H_f$ between Ic and Ib equals -14.5 kcal/mole.

The appearance potentials for formation of Ib via one- and two-bond-rupture mechanisms were calculated using Equations 33 and 34 respectively. The appearance potential of the benzoyl ion in the

$$AP(Ib) = \{\Delta H_f(Ib) + \Delta H_f(C_8H_7O) - \Delta H_f(I)\}/23.06 \quad (33)$$

$$AP(Ib) = \{\Delta H_f(Ib) + \Delta H_f(C_7H_7) + \Delta H_f(CO) - \Delta H_f(I)\}/23.06 \quad (34)$$

mass spectrum of I was found to be 9.98 ± 0.12 eV and leads to a ΔH_f (Ib) of 182.2 ± 3.1 kcal/mole. These values are close to the previously reported values of 9.7 eV and 186 kcal/mole.[34] The $\Delta H_f(C_8H_7O)$ was estimated to be 18.2 ± 2.0 kcal/mole from the ΔH_f of the benzoyl radical and the difference (7.9 kcal/mole) in the heats of formation of the 4-methylbenzyl and benzyl radicals.[68] Likewise it was necessary to use the value -7.9 kcal/mole and ΔH_f of the C_6H_5 radical (72 kcal/mole) to estimate the heat of formation of the 4-methylphenyl radical (64.1 ± 3.6 kcal/mole). Equations 33 and 34 lead to values of 10.02 ± 0.17 and 10.86 ± 0.22 eV respectively for the appearance potential of Ib.

The appearance potential of Ie from Ic was calculated using equation 35. Values of 232 kcal/mole from the ionization-dissociation of toluene[68] and 209 kcal/mole from the ionization of cycloheptatrienyl radical[68] for the ΔH_f(Ie) lead to values of 11.37 ± 0.47 eV for the appearance potential of Ie.

$$AP(Ie) = \{\Delta H_f(Ie) + \Delta H_f(C_7H_5O) + \Delta H_f(CO) - \Delta H_f(I)\}/23.06 \quad (35)$$

Equation 36 is applicable to the formation of Id from Ib. A value of 299 kcal/mole is obtained for ΔH_f of the C_6H_5 ions in the mass

$$AP(Id) - \{\Delta H_f(Id) + \Delta H_f(C_8H_7O) + \Delta H_f(CO) - \Delta H_f(I)\}/23.06 \quad (36)$$

spectra of benzaldehyde and acetophenone.[34] Thus a value of 13.95 ± 0.66 eV is calculated for the appearance potential of Id.

1-(4-Methylphenyl)-2-phenylethane-1,2-dione (II)

The ΔH_f of II was estimated from the ΔH_f(IV) and the difference in the ΔH_f of 4-methoxyacetophenone (-57.0 kcal/mole) and acetophenone (-23.0 kcal/mole), 4-methoxybenzophenone (-23.9 kcal/mole) and benzophenone (+12.5 kcal/mole), and 4-methoxybenzaldehyde (-48.1 kcal/mole) and benzaldehyde (-10.5 kcal/mole).[68] The ΔH_f(IV) combined with these differences yields an average value of -57.8 ± 1.21 kcal/mole, which is in good agreement with the value of -55.52 kcal/mole calculated by group equivalents method.

The ΔH_f of IIa was estimated from the ΔH_f of IVa and $\Delta\Delta H_f$ between the molecular ions of 4-methoxyacetophenone (142 kcal/mole) and acetophenone (191 kcal/mole), 4-methoxybenzaldehyde (150 kcal/mole) and benzaldehyde (209 kcal/mole), 4-methoxybenzophenone (178 kcal/mole) and benzophenone (228 kcal/mole), and the 4-methoxybenzyl cation (160 kcal/mole) and the benzyl cation (216 kcal/mole) produced from their corresponding radicals.[68] The average $\Delta\Delta H_f$ together with ΔH_f(IV) give an average value of 129.01 ± 2.25 for ΔH_f(IIa). From the

ΔH_f of II and the ΔH_f of IIa the ionization potential of II is calculated to be 8.10 ± 0.11 eV.

Equation 37 is valid for the calculation of the appearance potential of IIc via C-1--C-2 bond rupture. A value of 26.1 ± 2.0 kcal/mole

$$AP(IIc) = \{\Delta H_f(IIc) + \Delta H_f(C_7H_5O) - \Delta H_f(II)\}/23.06 \quad (37)$$

for $\Delta H_f(C_7H_5O)$ and 128.7 ± 2.0 kcal/mole for $\Delta H_f(IIc)$ yields a value of 9.22 ± 0.14 kcal/mole for the appearance potential of IIc. Equation 38 applies to the formation of IIc via a two-bond-rupture mechanism.

$$AP(IIc) = \{\Delta H_f(IIc) + \Delta H_f(C_6H_5) + \Delta H_f(CO) - \Delta H_f(II)\}/23.06 \quad (38)$$

Values of 72.0 and 26.42 kcal/mole for ΔH_f of C_6H_5 and CO lead to a value of 10.07 ± 0.20 kcal/mole for A.P.(IIc). The ΔH_f of IIc was estimated from $\Delta H_f(C_7H_5O^+)$ (182.2 ± 3.1 kcal/mole) and the $\Delta\Delta H_f$ between a para-methoxy group and hydrogen as calculated IIa.

The appearance potentials for formation of IIb via one- and two-bond-rupture mechanisms were calculated using Equations 39 and 40 respectively. The $\Delta H_f(C_8H_7O_2)$ was estimated to be -8.4 ± 2.6 kcal/mole from the $\Delta H_f(C_7H_5O)$ and the $\Delta\Delta H_f$ between the 4-methoxybenzyl radical (3.0 kcal/mole) and the benzyl radical (37.5 kcal/mole).[68] Likewise the $\Delta H_f(C_6H_5)$ of 72 ± 3.6 kcal/mole and the $\Delta H_f(C_7H_7O)$ of

$$AP(IIb) = \{\Delta H_f(IIb) + \Delta H_f(C_8H_7O_2) - \Delta H_f(II)\}/23.06 \quad (39)$$

$$AP(IIb) = \{\Delta H_f(IIb) + \Delta H_f(C_7H_7O) + \Delta H_f(CO) - \Delta H_f(II)\}/23.06 \quad (40)$$

37.5 ± 4.0 kcal/mole. Equations 39 and 40 lead to values of 10.05 ± 0.18 and 19.89 ± 0.23 eV respectively for the appearance potential of IIb.

Equation 41 describes the calculation of the appearance potential of IIe. The ΔH_f(IIe) was estimated from the $\Delta H_f(C_6H_5^+)$[68] (299 ± 14.9 kcal/mole) and the ΔH_f(IV) for p-methoxy substitution of hydrogen used

$$AP(IIe) = \{\Delta H_f(IIe) + \Delta H_f(C_7H_5O) + \Delta H_f(CO) - \Delta H_f(II)\}/23.07 \quad (41)$$

in the calculation of ΔH_f of II. The average value determined from the above is 245.5 ± 7.6 kcal/mole and yields a value of 13.14 ± 0.35 eV for the appearance potential of IIe.

The formation of IId proceeds via two pathways, one consisting of loss of CO from IIb while the other involves loss of the elements of formaldehyde from IIe. The appearance potentials leading to these pathways are given by Equations 42 and 43. Equation yields a value of 13.96 ± 0.66 eV for the appearance potentials of IId while Equation 43, using a value of -28.0 ± 1.4 kcal/mole for $\Delta H_f(CH_2O)$[68], gives a value of 14.25 ± 0.66 eV for the appearance potential of IId.

$$AP(IId) = \{\Delta H_f(IId) + \Delta H_f(C_8H_7O_2) + \Delta H_f(CO) - \Delta H_f(II)\}/23.06 \quad (42)$$

$$AP(IId) = \{\Delta H_f(IId) + \Delta H_f(C_7H_5O) + \Delta H_f(CO) + \Delta H_f(CH_2O) - \Delta H_f(II)\}/23.06 \quad (43)$$

1-(3-trifluoromethylphenyl)-2-phenylethane-1,2-dione (III)

The ΔH_f(III) was estimated from both the group equivalence value of III of -154.7 kcal/mole and from the ΔH_f(IV) (-21.8 kcal/mole) plus the ΔH_f of benzene (19.8 kcal/mole) and benzotrifluoride (-138.87 kcal/mole)[68] yielding ΔH_f(III) of -180.47 kcal/mole. These two estimates give an average value of ΔH_f(III) of -163.29 $\pm$ 11.66 kcal/mole.

The ΔH_f(IIIa) was estimated from the ΔH_f of IV and the $\Delta\Delta H_f$ (-149.0 kcal/mole) between the benzotrifluoride molecular ion (84 kcal/mole) and the benzene molecular ion (233 kcal/mole). The $\Delta\Delta H_f$ calculated from the group equivalents method gives -135.2 kcal/mole. The average of these two values of $\Delta\Delta H_f$ when combined with the ΔH_f of IV gives an average value of ΔH_f(IIa) of 40.41 $\pm$ 7.8 kcal/mole. The difference in this result and the ΔH_f(IIIa) gives an ionization potential of 8.83 $\pm$ 0.61 eV for IIIa.

The $\Delta H_f(CF_3C_7H_4O)$ and $(CF_3C_6H_4)$ were estimated from the group equivalence value of ΔH_f of -135.2 kcal/mole for substitution of a trifluoromethyl group for a hydrogen and from the experimental ΔH_f calculated from benzene and benzotrifluoride. The average ΔH_f of -146.4 $\pm$ 12.2 kcal/mole when combined with the $\Delta H_f(C_7H_5O)$ and (C_6H_5) yield values for $\Delta H_f(CF_3C_7H_4O)$ and $(CF_3C_6H_4)$ of -120.3 $\pm$

12.4 kcal/mole and -74.4 $\pm$ 12.7 kcal/mole respectively.

The ΔH_f of IIc and IIIe were estimated from average $\Delta\Delta H_f$ for replacement of hydrogen by a trifluoromethyl group (-142.1 kcal/mole) as in IIa and the ΔH_f of the m/e 105 and 77 ions. These values yield 40.24 $\pm$ 7.56 kcal/mole for ΔH_f(IIc) and 156.9 $\pm$ 16.5 kcal/mole for ΔH_f(IIIc).

Equations 44 and 45 are appropriate for the calculation of the appearance potentials of IIIb and IIIc resulting from C-1--C-2 bond rupture in IIIa. Using 26.1 $\pm$ 2.0 kcal/mole for $\Delta H_f(C_7H_5O)$[69] and 182.2 $\pm$ 3.1 kcal/mole for ΔH_f(IIIb), Equations 44 and 45 yield values for the appearance potentials of IIIb and IIIc of 9.77 $\pm$ 0.75 eV and 9.96 $\pm$ 0.60 eV respectively.

$$AP(IIIb) = \{\Delta H_f(IIIb) + \Delta H_f(CF_3C_7H_4O) - \Delta H_f(III)\}/23.06 \quad (44)$$

$$AP(IIIc) = \{\Delta H_f(IIIc) + \Delta H_f(C_7H_5O) - \Delta H_f(III)\}/23.06 \quad (45)$$

The appearance potentials of IIIb and IIIc assuming a two-bond-rupture mechanism are calculated from Equations 46 and 47. Using a value of 73.0 $\pm$ 3.6 kcal/mole for $\Delta H_f(C_6H_5)$,[68] Equations 46 and 47 yield values of 10.61 $\pm$ 0.76 eV and 10.80 $\pm$ 0.63 eV for ΔH_f of IIIb and IIIc respectively.

$$AP(IIIb) = \{\Delta H_f(IIIb) + \Delta H_f(CF_3C_6H_4) + \Delta H_f(CO) - \Delta H_f(III)\}/23.06 \quad (46)$$

$$AP(IIIc) = \{\Delta H_f(IIIc) + \Delta H_f(C_6H_5) + \Delta H_f(CO) - \Delta H_f(III)\}/23.06 \quad (47)$$

The appearance potentials of IIId and IIIe were calculated from Equations 48 and 49 using a value of 299.0 ± 17.9 kcal/mole for $\Delta H_f(IIId)$

$$AP(IIId) = \{\Delta H_f(IIId) + \Delta H_f(CF_3C_7H_4O) + \Delta H_f(CO) - \Delta H_f(III)\}/23.06 \quad (48)$$

$$AP(IIIe) = \{\Delta H_f(IIIe) + \Delta H_f(C_7H_5O) + \Delta H_f(CO) - \Delta H_f(III)\}/23.06 \quad (49)$$

and 26.1 ± 2.0 kcal/mole for $\Delta H_f(CO)$,[68] and the previously described values for the other quantities. Equations 48 and 49 yield values of 13.68 ± 0.98 eV and 13.87 ± 0.88 eV for the appearance potentials of IIId and IIIe respectively.

APPENDIX D

COMPUTER PROGRAM FOR THE PROCESSING OF LOW RESOLUTION MASS SPECTRAL DATA

APPENDIX D

COMPUTER PROGRAM FOR THE PROCESSING OF LOW RESOLUTION MASS SPECTRAL DATA

A computer program (HACP) was written to facilitate the routine reduction of low resolution mass spectra.[32] The program will correct ion intensities for naturally occurring heavy isotopes of carbon, hydrogen, nitrogen, and oxygen.[70] The following discussion details the programs usage and utility for both heavy isotope corrections and data reduction.

The program, written in Fortran IV, contains 311 source cards with maximum utilization of 168 K bytes of core in the compile step and 128 K bytes of core in the execution step. Up to ten spectra (j) can be averaged. The maximum number of m/e values and their corresponding intensities is 500 per spectrum.

A logic flow diagram is shown in Figure 56. Each m/e value and the corresponding intensity in the j spectra are assigned array positions m(i) and PT(i,j) respectively. The program is separated into subroutines, each of which is outlined below:

a) Subroutine INIT sets the initial array values to zero.

b) Subroutine READ performs all input operations.

c) Subroutine CORREC corrects spectra for naturally occurring ^{13}C, ^{2}H, ^{15}N, and ^{18}O.

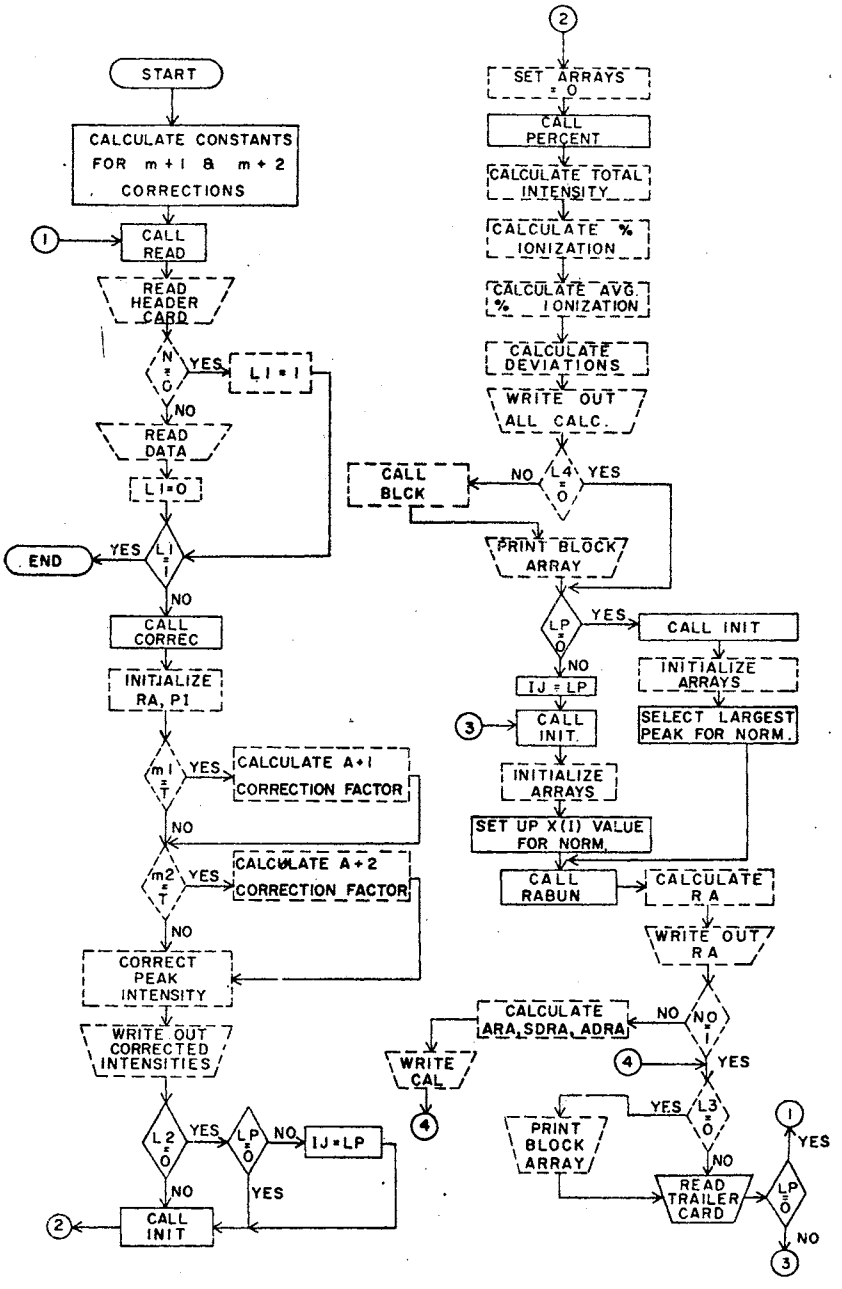

Figure 56. Logic flow diagram - solid figures represent flow through main program, dashed figures represent flow through subroutines.

d) Subroutine PERCNT calculates the per cent ionization for each of the j spectra. If j > 1 the average per cent ionization and the associated average and standard deviations are calculated.

e) Subroutine RABUN normalizes each of the j spectra. If j >1 the average relative abundance and the associated standard and average deviations are calculated. The subroutine can select the base peak for normalization.

f) Subroutine BLCK prints the per cent ionizations or relative abundances, average values if j > 1, in the form of a rectangular array of width 14 m/e values beginning with m/e 3.[71]

The following is a detailed description for the compilation of a data deck. The header card, first card, contains the integer number of data cards in columns 1-3, the integer number of spectra in columns 6-7, and any identifying comments in columns 9-72. Additional information may be entered on cards two and three if desired; all comments will appear on the computer output. The fourth card is a control card which controls subroutine implementation. The control card has seven entries, Table XXI. The data card(s) contain eight entries, Table XXII. The last card, trailer card, of the set has two entries. The first entry, column 4, corresponds to entry one of the control card. If zero, the next data set will be read but if a m(i) value (array position), the previous data set will be normalized to the ion intensity corresponding to this array position. The second entry, column 7, corresponds to the second entry in the control card. All other control functions during this operation are implemented by the control card. The program terminates normally when entry one of the header card is zero.

TABLE XXI

CONTROL OF SUBROUTINE IMPLEMENTATION

Entry	Value	Type[a]	Column	Function
1	0	I	4	Spectrum normalized with respect to most intense ion.
	m(i)	I	4	Spectrum normalized with respect to m/e value corresponding to this array position.
2	0	I	7	Percent ionization is not calculated.
	1	I	7	Percent ionization is calculated.
3	0	I	10	Heavy atom correction subroutine is not called.
	1	I	10	Heavy atom correction subroutine is called.
4	0	I	13	Relative abundance is not printed in form of block array.
	1	I	13	Relative abundance is printed in form of block array.[b]
5	0	I	16	Percent ionization is not printed in form of block array.
	1	I	16	Percent ionization is printed in form of block array.[b]
6	0	I	17-19	Block array printing is deleted.
	Highest m/e value	I	17-19	Regulates length of block array, if 4 and/or 5 are 1.
7[c]	I.D. number	FP	20-24	Places identification number at the lower left of the bar graph.
	0.	FP	20-24	Plot is deleted.

a) Integer or floating point, b) If j>1 average values printed, c) Applies only to HACP/BG.

TABLE XXII

FORMAT FOR DATA CARD(S)

Entry	Column(s)	Type[a]	Value of Entry
1	1-3	I	m/e value.
2	4-9, ···, 58-63	F	The peak intensity in arbitrary units, up to 10 entries.
3	65-66	I	Number of carbons in elemental composition.
4	68-69	I	Number of hydrogens in elemental composition.
5	71-72	I	Number of nitrogens in elemental composition.
6	74-75	I	Number of oxygens in elemental composition.
7	79	A	A T in column 79 results in the correction of the intensity at m/e(A) for heavy isotope contributions from m/e(A-1).[b,c]
8	80	A	A T in column 80 results in the correction of the intensity of m/e(A) of the heavy atom contribution from m/e(A-2).[b,d]

a) Integer, floating or alphanumeric.

b) If no heavy atom corrections are made columns 65-80 are blank.

c) It is necessary to have an elemental composition for m/e(A-1).

d) It is necessary to have an elemental composition for m/e(A-2).

Program HACP/BG, heavy atom computer program with bar graph generation, consists of HACP modified by subroutine BARPLT. Subroutine BARPLT plots the experimental or corrected mass spectra in bar graph form. The computer software must include and be compatible with the basic Calcomp software. Subroutine BARPLT may be called from HACP/BG by entry seven on the control card, Table XXI. If BARPLT is not called the program will do the same numerical operations as HACP.

APPENDIX E

OTHER SYNTHESIS

APPENDIX E

Synthesis of 2-Phenylacetophenone-2',3',4',5',6'-d_5

Phenylacetaldehyde (7.6 g, 0.6 mole) dissolved in 50 ml. of ether (distilled from lithium aluminum hydride) was added dropwise to phenylmagnesium bromide-d_5 which was prepared from bromobenzene-d_5[72] (10.5 g, 0.65 mole) and magnesium turnings (1.6 g, 0.65 mole) in 25 ml. of anhydrous ether. The reaction mixture was hydrolyzed by pouring it onto 50 g of crushed ice followed by the addition of 20 ml. of 2.2 M sulphuric acid. The crude 1-(phenyl-d_5)-2-phenylethanol was extracted with ether and the combined ether extracts were neutralized (5% Na_2CO_3), dried ($MgSO_4$), and filtered. Removal of the ether under reduced pressure yielded a yellow oil (10.2 g). Column chromatography (2.5 cm x 75 cm, 60-200 mesh silica gel, 50:50 $CCl_4/CHCl_3$) gave 1.22 g of 1-(phenyl-d_5)-2-phenylethanol. Oxidation[61] of this material at 0° followed by sublimation (55°@ 0.25 mm) gave 0.78 g, 7.5% . of 2-phenylacetophenone-2',3',4',5',6'-d_5, m.p. 52.7° - 53.5°.

Synthesis of 2-Phenylacetophenone-2-d_2

2-Phenylacetophenone (10.0 g, 0.051 mole) and deuterium oxide in p-dioxane (distilled from lithium aluminum hydride) containing a small

amount of dried potassium carbonate were refluxed for nine hours. The solution was then concentrated under reduced pressure, ether was added, and the aqueous phase extracted with ether. The ether extracts were combined, dried ($MgSO_4$), and filtered, and the ether removed under reduced pressure. This exchange and workup was repeated five times, monitoring the percentage deuterium incorporation (see Table XXIII), in each exchange by NMR. Purification by sublimation at 50° and 0.25 mm gave 6.5 g (65.2%) of 2-phenylacetophenone-2-$\underline{d}_2$, m.p. 54.6°- 55.1°.

TABLE XXIII

PERCENTAGE OF DEUTERIUM INCORPORATION IN 2-PHENYLACETOPHENONE

Exchange Number	Molar Excess D_2O	Incorporation of D %
1	2	92.
2	4	92.
3	6	97.
4	10	94.
5	3	97.2

Synthesis of 2-(Phenyl-$\underline{d}_5$)ethanol

Ethylene oxide (21.0 g, 0.478 mole) dissolved in 100 ml. anhydrous ether was added dropwise to phenylmagnesium bromide-$\underline{d}_5$ which

was prepared from 5.0 g (0.208 mole) of magnesium turnings and 26.4 g (0.163 mole) of bromobenzene-$\underline{d}_5$ in 25 ml. of anhydrous ether at 0° over a period of one hour. The reaction mixture was hydrolyzed with a saturated ammonium chloride solution. The ether layer was separated, washed (staurated with NaCl solution), dride ($MgSO_4$), filtered, and concentrated under reduced pressure. Distillation of the crude product (b.p. 58° - 59° @ 0.48 mm) yielded 15.85 g, 78 per cent of 2-(phenyl-$\underline{d}_5$)ethanol.

Synthesis of 2-(Phenyl-$\underline{d}_5$)acetophenone

Diphenylcadmium was prepared from phenylmagnesium bromide (prepared from bromobenzene (11.4 g, 0.073 mole) dissolved in anhydrous ether and 2.5 g (0.103 mole) magnesium turnings suspended in ether) and 6.8 g (0.037 mole) of anhydrous cadmium chloride. The ether was distilled out of the reaction flask and an equivalent volume of anhydrous benzene (distilled from sodium) added. Phenyl-$\underline{d}_5$-acetyl chloride (5.8 g, 0.0364 mole) dissolved in 20 ml. anhydrous benzene was added dropwise over a period of one hour. The reaction mixture was hydrolyzed with a saturated Rochelle salt solution (sodium potassium tartrate). The organic layer was separated and the aqueous layer extracted with ether. The benzene layer and the ether extracts were combined and neutralized (5% Na_2CO_3), dried ($MgSO_4$), filtered, and concentrated under reduced pressure. Recrystallization twice from methanol-Skelly F solvent gave 1.90 g, (26%) of 2-(phenyl-$\underline{d}_5$)-acetophenone, m.p. 54.2° - 55°.

Synthesis of 2-Phenylacetophenone Azine

2-Phenylacetophenone (0.5 g, 0.0026 mole, Eastman Kodak Co.) and ninety-five per cent hydrazine hydrate (0.075 g, 0.00125 mole) were refluxed 50 ml. absolute ethanol containing two drops of glacial acetic acid for 3.5 hours. Filtration followed by recrystallization once from ethanol yielded 0.10 g (38%) of the azine, m.p. 159.9° - 160.6° (lit. 161°, 164°).[73]

Synthesis of 2-(Phenyl-$\underline{d}_5$)acetophenone Azine

2-(Phenyl-$\underline{d}_5$)acetophenone (1.38 g, 0.0068 mole) was converted to the azine by the above procedure. Recrystallization twice from acetone gave 0.083 g (61%) of azine, m.p. 163.8° - 164.6°.

Synthesis of 2-Phenylacetophenone-$\underline{2}',\underline{3}',\underline{4}',\underline{5}',\underline{6}'$-$\underline{d}_5$ Azine

2-Phenylacetophenone-$\underline{2}',\underline{3}',\underline{4}',\underline{5}',\underline{6}'$-$\underline{d}_5$ (0.68 g, 0.0034 mole) was converted to the azine by the above procedure. Recrystallization twice from ethanol-acetone (80:20) gave 0.15 g (22%) of 2-phenylacetophenone-$\underline{2}',\underline{3}',\underline{4}',\underline{5}',\underline{6}'$-$\underline{d}_5$ azine, m.p. 163.6° - 164.6°.

Synthesis of 1,2-Diphenylethanol-$\underline{2}$-$\underline{d}_2$

2-Phenylacetophenone-$\underline{2}$-$\underline{d}_2$ (1.5 g, 0.00765 mole) dissolved in 15 ml. of anhydrous ether was added dropwise to a stirred suspension of lithium aluminum hydride (0.145 g, 0.0038 mole) in 15 ml. anhydrous

ether at 0 over a period of 0.5 hour. The reaction mixture was warmed to 25 and stirred for two hours followed by hydrolysis with a saturated Rochelle satl solution (sodium potassium tartrate). The ether layer was separated and the aqueous layer extracted with ether. The combined ether extracts were washed with water, dried ($MgSO_4$), filtered, and concentrated under reduced pressure. Sublimation at 50° and 0.125 mm yielded 1.45 g (93.8%) of 1,2-diphenylethanol-2-d_2, m.p. 66° -67°.

Synthesis of 2-Phenylacetophenone-2,2-d_2 Azine

2-Phenylacetophenone-2,2-d_2 (1.0 g, .00505 mole) and hydrazine hydrate-d_6 (0.1412 g, .0027 mole, Merck Sharpe and Dohme) were refluxed in 15 ml. glacid acetic acid-O-d for forty-five minutes. The resultant yellow crystalline suspension was filtered and the solid washed with deuterium oxide. Recrystallization twice from acetone yielded 0.0635 g (64%) of 2-phenylacetophenone-2,2-d_2 azine, m.p. 163.1° - 164°.

Synthesis of 1-Phenyl-2-(phenyl-d_5)-ethanol

2-(phenyl-d_5)acetophenone (0.52 g, 0.0026 mole) was converted to the corresponding alcohol by the previous procedure. Recrystallization from ethanol-water solvent yielded 0.33 g (63%) of 2-(phenyl-d_5)-ethanol, m.p.66° - 66.5°.

Synthesis of the Trimethylsilyl (TMS) Ethers

Trimethylsilyl derivatives of 1-(phenyl-$\underline{d}_5$)-2-phenylethanol, 1-phenyl-2-(phenyl-$\underline{d}_5$)entanol, and 1,2-diphenylethanol-$\underline{2}$-$\underline{d}_2$ were prepared by reacting 2 mg of the alcohol with trimethylsilylimidazole (Applied Science TMSIM - 1805) for five minutes. The reaction product was purfied, by preparative GLC (0.25" x 20' , 5% SE-30 on 100/120 Chromosorb-W @ 200°) and immediately sealed in a capillary tube.

Mass Spectral Determination of the %D

Spectra were recorded using the LKB 9000 and the CEC 21-110B mass spectrometers. Spectra taken with the CEC 21-110B instrument were obtained with an all-glass probe at 130°. The source temperature was 160° and the trap current was 75 μA. Low-voltage spectra were recorded with the repeller plates near the block potential. Spectra taken with the LKB were obtained using either the direct probe or the all-glass heated-inlet system. The ion source temperature was 250° and the trap current 65 μA. Low-voltage spectra were recorded with the extraction plates near the block potential.

All spectra were corrected for natural abundance[32] ^{13}C, ^{2}H, and ^{15}N using an IBM 360-65 computer. The molecular ion region of the low-voltage spectra taken on the LKB and the CEC yield an average atom %D of 99.422 $\pm$ 0.036 for 2-phenylacetophenone-$\underline{2}'$,$\underline{3}'$,$\underline{4}'$,$\underline{5}'$,$\underline{6}$,-$\underline{d}_5$ azine and 99.256 $\pm$ 0.014 for 2-(phenyl-$\underline{d}_5$)-acetophenone azine. The values are in

reasonable agreement with the %D label found in 1-(phenyl-$\underline{d}_5$)-2-phenylethanol TMS ether (98.99 atom %D) and 1-phenyl-2-(phenyl-$\underline{d}_5$)ethanol TMS ether (99.15 atom %D).

The %D label determined from the M-93 region of 2-phenylacetophenone-$\underline{2},\underline{2}$-$\underline{d}_2$ azine was found to vary with ion source temperature. A plot of the ratio of $\underline{m}/\underline{e}$ 298/299 versus ion source temperature is presented in Figure 57. The calculated %D also showed considerable day-to-day variation under the same operating conditions. The TMS ether of 1,2-diphenylethanol-$\underline{2}$-$\underline{d}_2$ contained 97.43 atom %D by MS analysis, which is in reasonable agreement with the NMR result.

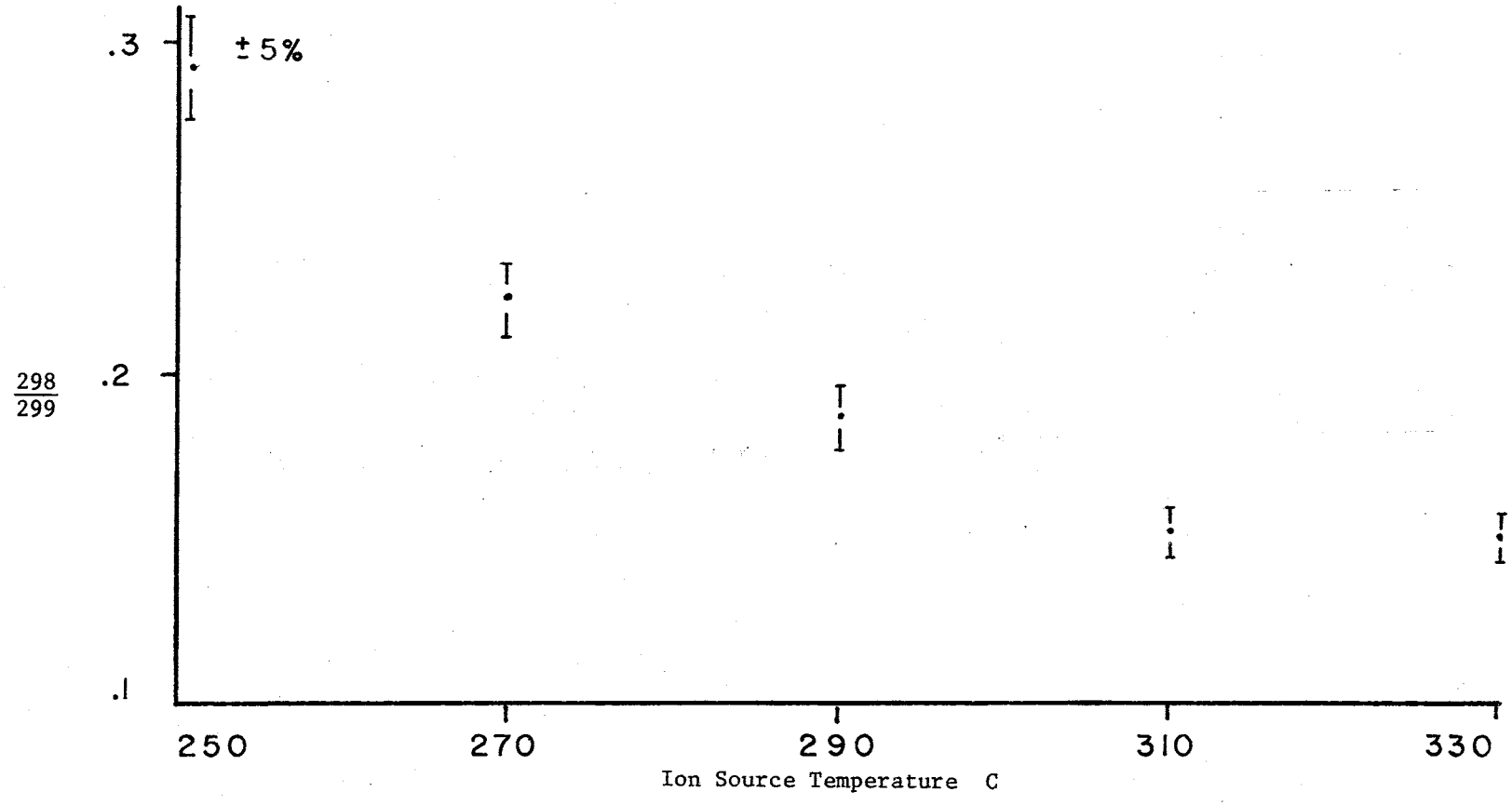

Figure 57. Temperature dependance of the m/e 298/m/e 299 ratio in 2-phenylacetophenone-d_2 azine

VITA

Ronald Kem Mitchum

Candidate for the Degree of

Doctor of Philosophy

Thesis: MECHANISM OF ELECTRON IMPACT INDUCED DECOMPOSITION OF MONOSUBSTITUTED 1,2-DIPHENYLEHTANE-1,2-DIONES

Major Field: Chemistry

Biographical:

Personal Data: Born in Elk City, Oklahoma, on December 2, 1946, the son of Emmett B. and Regina Mitchum. Married Doris Jane Romans on August 26, 1965 and a son, Christopher Scott was born in 1970.

Education: Graduated from Canute Public High School, Canute, Oklahoma, in 1965; received Bachelor of Science degree from Southwestern State College, Weatherford, Oklahoma, with a major in Chemistry, in May, 1968; completed requirements for Doctor of Philosophy degree July, 1973.

Professional Experience: Graduate Teaching Assistant, Oklahoma State University, 1968-1970; NSF Trainee, 1970-1972; member of Phi Lambda Upsilon.